Pass on knowledge from me even if it is only one verse.

“Prophet Muhammad (saw)”

It’s not easy to raise children nowadays
Nowadays life is a fast paced race
Jungle and maze decide your race
It is our will which satisfies
It never doubts, it never tries
So it all comes down to patience
Integrity and patience lead you through qualifications

“dedicated to Madar and Baba”

Table of Contents

Chapter one **7**
1. Introduction 7
1.1 Polymers, from prehistory till now 7
1.2 Conjugated polymers; a solution to Global Warming: 9
1.3 Synthetic approaches towards Conjugated polymers: 20
1.4 Applications 31
1.5 Aim and outline of the thesis 43
1.6 References 47
Chapter two **57**
2. Synthetic Approaches Towards Quinoxaline Core – Monomer Synthesis 57
2.1 Introduction 57
2.2 The Immino-oxime monomer synthesis toward the dithiocarbamate quinoxaline monomer 6 63
2.3 The Benzothiadiazole monomer synthesis toward the dithiocarbamate quinoxaline monomer 6 73
2.4 Conclusion 91
2.5 Experimental section 93
2.6 References 104
Chapter Three **108**
3. Exploring the Dithiocarbamate Route as an Entry Toward Plain Quinoxaline Phenylene 108
3.1 Introduction 108
3.2 Polymerisation 116
3.3 Characterisation 126
*3.*4 *p*-Quinodimethane formation; observation of the potential intermediate. 135
3.5 Conclusion 146
3.6 Experimental section 147
3.7 References 151

Chapter Four **154**
4. Different Approaches to Introduce Side Chains; Soluble Derivatives of Poly (*para*-Quinoxaline Vinylene) PQV 154
4.1 Introduction 154
4.2 Introduction of side chains; synthesis towards soluble derivatives of PQV 159
4.3 Conclusion 169
4.4 Experimental section 170
4.5 References 183
Chapter Five **187**
5. Physical Characterisation and Device Towards Organic Solar Cells 187
5.1 Introduction 187
5.2 Photoluminescence (PL) and Electron Pulsed Resonance (EPR) 188
5.3 Solar cell device and Atomic Forse Microscopy (AFM) 193
5.4 Conclusion 197
5.5 Experimental section 199
5.6 References 202
Chapter Six **205**
6. Summary 205
6.1 Introduction 205
6.2 Synthetic approaches towards Quinoxaline Core – Monomer synthesis 205
6.3 Exploring Polymerisation towards Plain PQV 207
6.4 Different approaches to introduce side chains; soluble derivatives of PQV 209
6.5 Physical characterisation and device towards Solar Cells 211
6.6 References 213
Samenvatting **215**
List of abbreviations **219**
List of publications **223**
Acknowledgement **225**

Chapter one

1. Introduction

1.1 Polymers, from prehistory till now

Polymers (plastics) have been with us since the beginning of time. The word *plastic* is originally derived from the Greek and Latin, meaning to mold, shape or to form. The word *polymer* comes from the Greek word Polumerẽs. “Polu” means poly or many and “meros” means part (many parts).[1] Starting from the Prehistoric time, polymers can be divided into three groups:[2]

1- Natural Polymers
2- Semi-synthetic polymers
3- Fully-synthetic polymers

The era of “Classical polymers” started with the discovery of natural polymers. Among the natural polymers are the polysaccharide cellulose based on glucose as a monomer (e.g. cotton, flax and papyrus), polypeptides based on amino acids as a monomer of (e.g. wool, silk, leather, horn), polyisoprene from plants in the Amazon area (e.g. rubber, Figure 1.1) and dyes and other high molecular hydrocarbons based on petroleum from Middle East to China. The use of these polymers dates back to 5000 years ago up till the first part of the nineteenth century. In the second part of the nineteenth century semi-synthetic polymers were prepared. Among them the most famous one are (a) Ebonite, (b) Celluloid and (c) Galalith (Figure 1.1). Ebonite prepared by vulcanising the natural rubber, was discovered by Charles Goodyear in 1839. Celluloid (the first thermoplastic) was obtained from nitrocellulose and camphor in 1870 and Galalith, which was discovered by Adolph Spitteler and Wilhelm Krische in 1889, was prepared from milk protein casein.[3]

The oldest recorded fully-synthetic polymer was Bakelite (Figure 1.1), which was prepared and patented by Leo Hendrik Baekeland in 1907. Bakelite was used as nonconductive and heat-resistant electrical insulator in radio and telephone casings. With this the era of “Processing Classical Polymers” started. It was not until 1920, when Staudinger together with the American chemist Carothers published a paper entitled “Uber Polymerization” that this paper initiated a decade of intense research and presented to the world the development of modern “Polymer Science”.

Figure 1.1: (left to right) natural rubber, semi-synthetic Galalith and a fully-synthetic Bakelite phone

Since then, polymer materials can be subdivided as belonging to four generations.[4] The first generation polymers brought to the market dates back to before 1950s. They are simple plastics like poly (vinyl-chloride) or PVC (1927) used for plumping pipes and bottles, polystyrene (1930) used for videocassettes, polyamides or nylon (1938) used for ropes and clothes, low-density polyethylene (1941) and many more. The second generation of polymer materials emerged between 1950-1965. The advantage of this group compared to the first generation polymers was that they had high-density, higher mechanical strength and higher softening temperature. These characteristics made them suitable for use as construction materials, fibres and films. Among them are high-density polyethylenes, polycarbonates, linear polyesters and many more. Between 1965 and 1976 was the third generation polymers was brought to the market. They were characterized by more complex chemical structures, had higher molecular strengths, higher softening temperature and high chemical resistance. Kevlar® (1971) belongs to this

generation of polymers, which can be used in bullet proof vests and fire proof garments for fire fighters.

the past it was considered laughable to imagine plastics as conductive polymers. Thanks to the discovery by Hideki Shirakawa, Alan G. MacDiarmid and Alan J. Heeger (Figure 1.2) in 1977, conducting polymers - the forth generation polymers - are playing a very important role ever since.[5]

Figure 1.2: (from left to right) Hideki Shirakawa, Alan G. MacDiarmid and Alan J. Heeger, the three Noble Prize winners in the field of the conjugated polymers

1.2 Conjugated polymers; a solution to Global Warming:

1.2.1 Conjugated polymers and their doping properties

In 1977, the three scientists - Hideki Shirakawa, Alan G. MacDiarmid and Alan J. Heeger – observed 10^9 times more conductivity by oxidising polyacetylene (PA) with chlorine, bromine or iodine vapour.[5] The 'doped' form of PA had a conductivity of 10 Siemens per meter (S m^{-1}). As a comparison, Teflon has a conductivity of 10^{-16} S m^{-1} while silver and copper has a conductivity of 10^8 S m^{-1} (Figure 1.3). Therefore, the three scientists were rewarded with The Nobel Prize in Chemistry in the year 2000 entitled "for the discovery and development of electrically conductive

polymers". Due to their breakthrough the era of electronically conducting materials based on conjugated polymers – organic semiconductors - has started. At the beginning the semiconductors were prepared by doping the polymers. On one hand, this helped us understand the mechanisms of the electrical transport and methods for the synthesis of these primary conductive materials. On the other hand, there were only few applications due to the poor processability and environmental stability of these primary conductive materials.[6] However, during the last two decennia, due to better synthesis methods and processing technology the properties of these conductive polymers have improved enormously. Because of these improvements the conjugated materials are being prepared with better purity and solubility leading to better active materials. An extended study on the polymerisation chemistry towards the different classes of polymers is presented in several papers and books.[7-9]

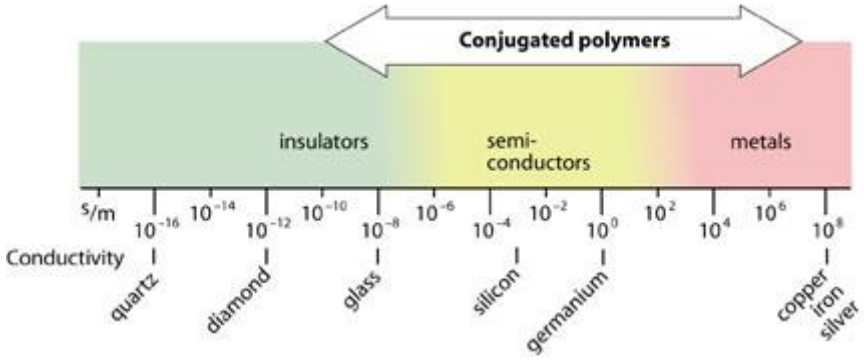

Figure 1.3: Conductivity of some materials in Siemens per meter (S m^{-1})

Nowadays there is also a large interest in preparing new conjugated polymers with further optimised and even more improved solubility, optical and electronic properties and even more improved solubility. These active materials – organic semiconductors – are being used in biosensors[10-12], organic field effect transistors (OFETs)[13-16], polymer light-emitting diodes (PLED's)[17, 18], photovoltaic cells[19-26], flat-panel displays[27], photodiodes[23, 28], electronic noses[29-31], polymer batteries[32-34], lasers[35-40], smart windows[41-46], light-emitting electrochemical cells (LECs)[47-52] and organic solar cells[23, 28, 53-55].

An overview of molecular structures of some conjugated polymers is presented in Figure 1.4.

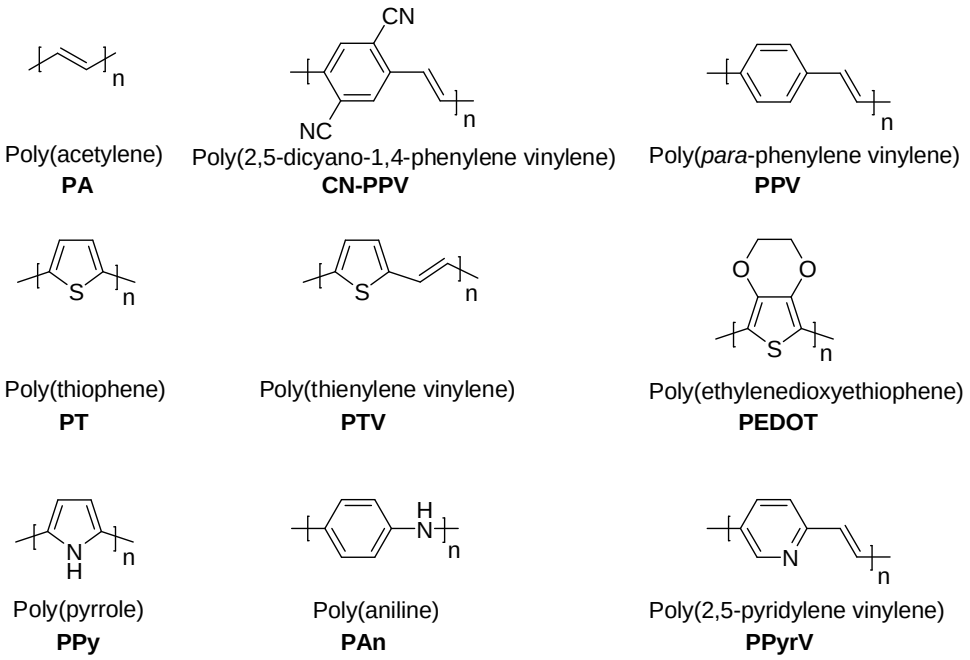

Poly(acetylene) **PA**

Poly(2,5-dicyano-1,4-phenylene vinylene) **CN-PPV**

Poly(*para*-phenylene vinylene) **PPV**

Poly(thiophene) **PT**

Poly(thienylene vinylene) **PTV**

Poly(ethylenedioxyethiophene) **PEDOT**

Poly(pyrrole) **PPy**

Poly(aniline) **PAn**

Poly(2,5-pyridylene vinylene) **PPyrV**

Figure 1.4: Overview of some conjugated polymers.

A common characteristic between all the conjugated polymers is their extended π-conjugated system, which exists of adjacent carbon atoms alternating with single (σ) bonds and double (σ and π) bonds in their backbone. The σ bonds are formed by three equivalent triangular sp^2 hybridised orbital (Figure 1.5). Hereby, the fourth orbital – the two p_z orbital - that are out-of-plane, overlap with each other resulting in a π bond. The π-electrons are not tightly attached – delocalised - so they become mobile along the conjugated polymer chain.

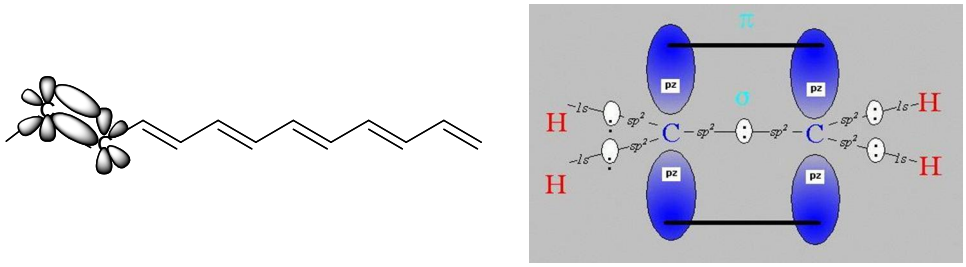

Figure 1.5: (left) trans poly(acethylene) and (right) example of a sp^2 hybridised orbital and p_z orbital.

It has to be pointed out that conjugation is not the only condition for the polymer material to become conductive. In addition, the polymer must have a partially empty valence band (VB) or a partially filled conduction band (CB). Therefore the polymer needs to be injected with charge carriers i.e. electrons and holes (Figure 1.6). A hole is a position where an electron is missing. This hole can be filled with an electron from neighbouring position, which leads to the formation of a new hole. Eventually, this allows charge carriers to migrate over a long distance. These charge carriers can be generated by many processes like *electrical simulation*, *photo excitation* or *chemical doping*. In the case of chemical doping, the process is generally reversible at low doping level. Hereby, the polymer chain can either be oxidised by removing an electron (oxidation or p-doping) and becoming positively charged or the polymer chain can be reduced by adding an electron (reduction or n-doping) and becoming negatively charged.[56] A hopping mechanism, whether it is intrachain hopping (between conjugated parts of the same chain) or interchain hopping (between conjugated parts of different chains) is widely accepted as the mechanism for charge transport in conjugated polymers.

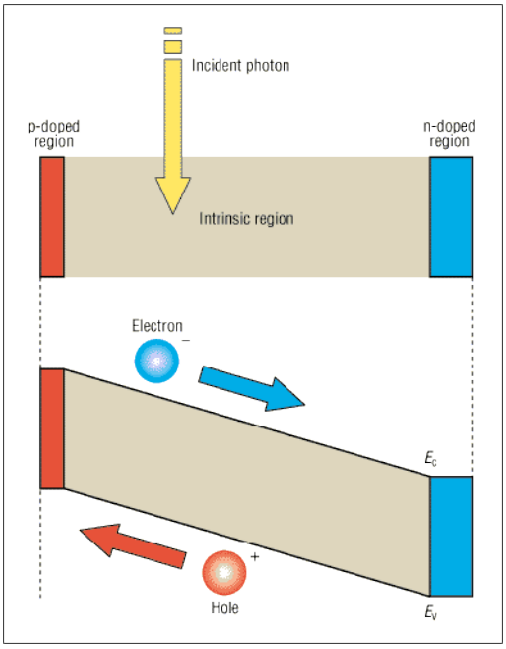

Figure 1.6: Charge injection in a conjugated polymer; A photon knocks an electron from the valence band and into the conduction band and two charge carriers are formed. The hole in the valence band and the electron in the conduction band.

The electronic properties of a polymer material are mainly determined by their electronic structure. The best way to describe the electronic structure of a conjugated system is with the help of the molecular orbital theory. According to the molecular orbital theory the mentioned overlap of the p_z orbitals yields lower energy bonding (π) and higher energy anti-bonding (π^*) molecular orbitals.[57, 58] It is also accepted that from N atomic orbitals, N molecular orbitals can be formed. When many molecular orbitals (N) are packed together the π orbitals form the valance band (VB) and the π^* orbitals form the conduction band (CB), where each of them cover a range of energies. The gap – the energy difference – between the highest occupied molecular orbital (HOMO) and the lowest unoccupied molecular orbital (LUMO) is called the band gap (Eg). The occurance of a band gap was predicted by Rudolf Peierls in 1956, years before the synthesis of the first conjugated polymer.[59] Tuning the size of this band gap allow to modify the electronic and optical properties of the material. The excistence of such band gap leads to the

semoconductive properties of conjugated polymers. Depending on the synthesis of the desired chemical structure the band gap of conjugated polymers can vary between 0.5 till 4 eV while the band gap for a metal is zero and the band gap for an insulator is more than 4 eV (Figure 1.7). Among the conjugated polymers, low band gap polymers (LBG) are identified as an important subclass of conjugated polymers (Eg < 2 eV). Due to this small band gap the low band gap polymer can have a higher intrinsic conductivity and possibly a higher charge carrier mobility leading to devices with better performance. As a result the LBG will absorb light close to the near infrared instead of the visible area of the light spectrum and in this way it will become transparent upon doping.[60, 61]

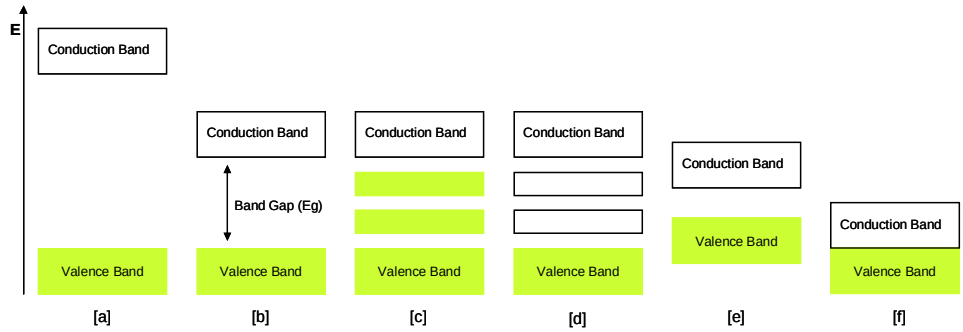

Figure 1.7: [a] band model of insulators, [b] band model of a conventional conjugated polymer, [c] band model of an n-doped conjugated polymer, [d] band model of a p-doped conjugated polymer, [e] band model of a low band gap polymer, [e] band model of metals.

1.2.2 Conjugated polymers and their electronic properties

Su, Schrieffer and Heeger (SSH) were the first scientists who formulated the SSH Hamiltonian and with this they calculated the first electronic structure of a conjugated polymer.[62, 63] According to their theory conjugated polymers can be divided into two classes of electronic structures:

I. Conjugated polymers with a degenerate ground state, *trans*-polyacethylene,

II. Conjugated polymers with a non-degenerate ground state, *cis*-polyacethylene with all the other conjugated polymers (e.g. poly(*para*-phenylene) PPP, PPV etc.).

In Figure 1.8 the potential energy is presented as a function of the bond length alternation ΔE_r (defined here simply as the difference in length between a single bond and the next double bond) for conjugated polymers with a degenerate ground state and with a non-degenerate ground state. As it can be seen, in the degenerate ground state of the conjugated polymers the change in the bond length alternation leads to similar structures (left, A and B) with the same energy. While in the non-degenerate ground state of the conjugated polymers the bond length alternation leads to two different structures (right, aromatic and quinoide) with two different energies. In this case it is important to notice that the aromatic form of PPP has the lowest ground state energy and the quinoide form of PPP has the highest ground state energy.

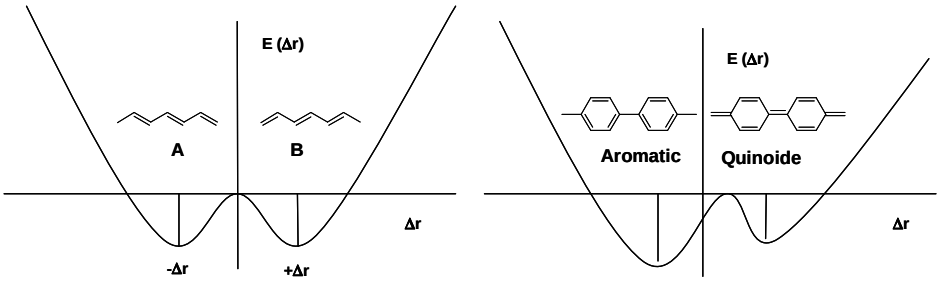

Figure 1.8: potential energy as a function of the bond length alternation for the two classes of conjugated polymers; (left) conjugated polymers with a degenerate ground state, *trans*-polyacethylene and (right) conjugated polymers with a non-degenerate ground state, poly(*para*-phenylene) PPP.

As it was mentioned before, conjugated polymers with a degenerate ground state will have the same ground state energy when the single and double bonds are interchanging in the polymer. During this interchange in the conjugated system, there is a possibility for a defect (soliton) to occur during the process of bond alternation. The solitons are quasi particles with one new electronic state in the

middle of the band gap (Eg). This state can be single occupied (neutral soliton = free radical), double occupied (negative soliton = carbon) or empty (positive soliton = carbocation), Figure 1.9.

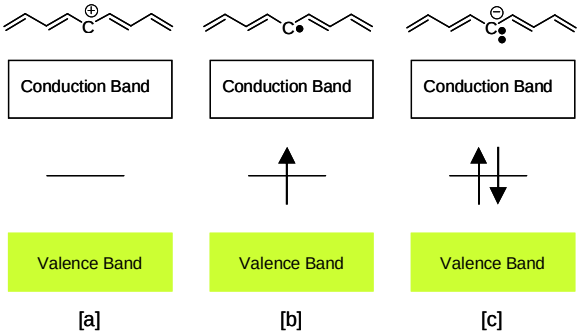

Figure 1.9: Energy diagram for the three type of solitons in generate ground state conjugated polymer; [a] positive soliton, [b] neutral soliton and [c] negative soliton.

When structural relaxation takes place at the backbone of a conjugated polymer with a non-degenerate ground state, two new electronic states appears in the band gap (Eg). In this case the quasi particles are consisting of excitons (neutral), polarons (one charge) and bipolarons (double charge), Figure 1.10. Polarons (radical cations or radical anions) with their two electronic transitions (high energy HE and low energy LE) have an open shell structure (Figure 1.10, [a] and [c]), therefore they can be observed by electron spin resonance (ESR). On the other hand, bipolarons (carbodications or carbodianions) with their one electronic transition have closed shell structure, therefore they can not be observed by ESR (Figure 1.10 [b] and [d]).

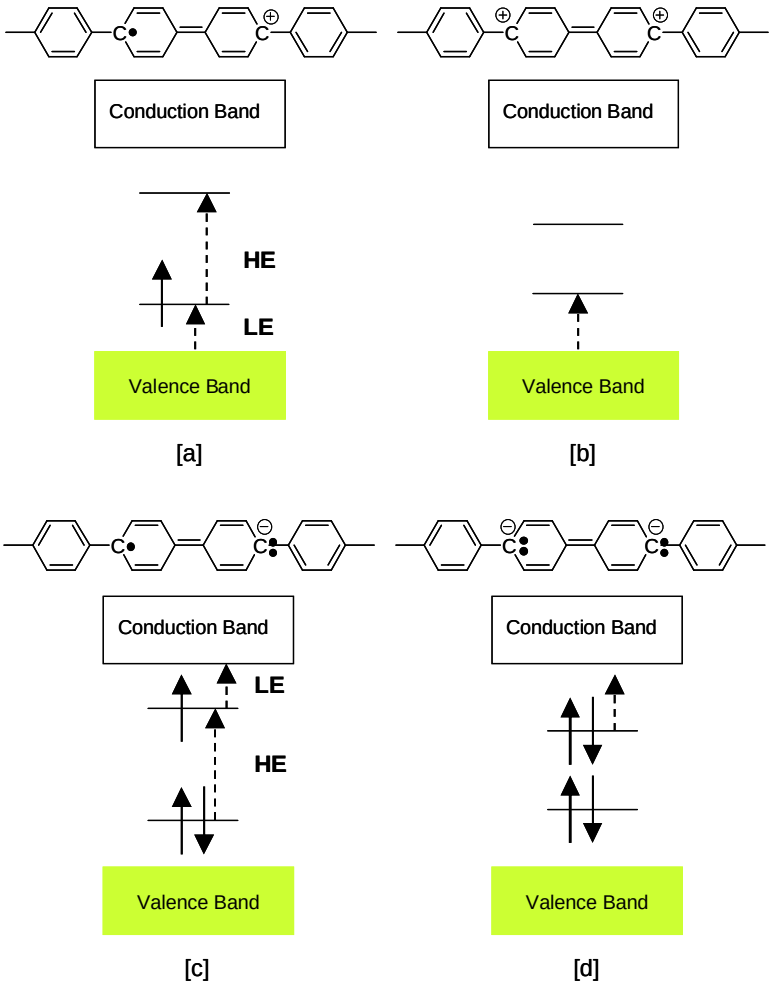

Figure 1.10: Energy diagram and allowed optical transitions for the non-generated ground state conjugated polymer; [a] positive polaron, [b] positive bipolaron, [c] negative polaron and [d] negative bipolaron.

1.2.3 Conjugated polymers and their optical absorption properties

As it was mentioned before, tuning the size of the band gap (Eg) determines the electronic and optical properties of a semi-conducting material – conjugated polymer. There are different ways that can be applied to obtain the value of the band gap Eg:

I. Prediction by theoretical calculation (VEH)
II. Experimental determination (CV and UV-Vis)

A method which is widely known for predicting the band structure of a conjugated polymer is the Valence Effective Hamiltonian (VEH) pseudo potential technique. Another method, which gives a straightforward and rapid estimation of the band gap energy of a conjugated polymer, is the experimental determination by electrochemistry such as cyclic voltammetry (CV) and ultraviolet-visible spectroscopy (UV-Vis).

UV-Vis is also a good method for determining the optical absorption properties of conjugated polymers. Optical properties are usually related to the interaction of a material with electromagnetic radiation in the frequency range from infrared (IR) to ultravioled (UV).[64] It is well known that conjugated polymers are semiconductors with a band gap Eg ranging from 0.5 to 4 eV and most of them are interacting with visible light. When light with sufficient energy is absorbed by the material an electron is promoted or excited from the valence band (VB) into the conduction band (CB) creating an exciton (electron-hole pair), Figure 1.11, left).

The lowest energy (light with the highest wavelength) necessary to excite an electron is equal to the Eg which is exciting an electron from HOMO into the LUMO. A decrease of the Eg results in a red shift of the absorption spectrum. The exciton can eventually decay to the ground state radiatively (*i.e.* photoluminescence) or non-radiatively. The Eg can be determined by taking the tangent on the low energetic side of the UV-Vis spectrum (Figure 1.11, right). The intersection of this tangent together with the abscissa gives a value for the band gap (optical band gap).

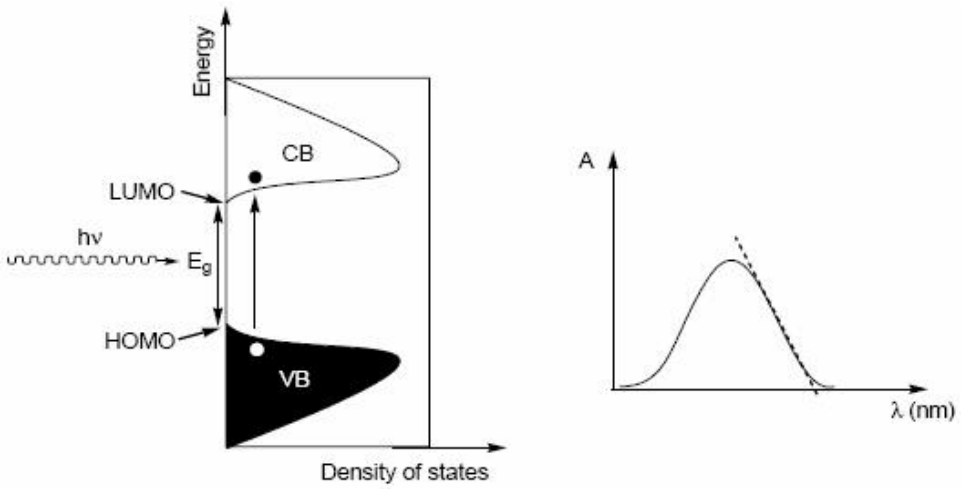

Figure 1.11: Density of states band structure (left); corresponding absorption spectrum (right).

In an UV-Vis spectrum, the absorbance is plotted as a function of the wavelength. Therfore, it is imporntant to convert the nanometer scale into electron-volt using the equation of Planck:

$$E = h\nu = \frac{hc}{\lambda} \quad \Rightarrow \quad E\,(eV) = \frac{1240.8}{\lambda\,(nm)}$$

In this equation (left), E is the energy (in J), h is the Planck constant (6.626 10-34 Js), c is the speed of light (3 10^8 ms^{-1}), $\nu$is the frequency (in s^{-1} or Hz) and $\lambda$is the wavelength (in m). Knowing that 1 eV equals 1.602 10-19 J, a simple conversion equation is the result (right).

It is clear now that the band gap of a conjugated polymer not only influences the electronic properties but also determines the optical properties such as absorbance (colour), electroluminescence (conversion of electrical energy into light) and photoluminescence (conversion of UV-light into visible light).

Concerning bang gap engineering, Roncali did some excellent work on revealing the relationship between the structure and the band gap of polyaromatic conjugated systems. According to him the value of the band gap Eg varies depending on different parameters and can be controlled to a certain extent by molecular design.[7] In this way the band gap can be described as the sum of five contributions: the energy related to the bond length alternation ($E^{\Delta r}$), the mean deviation from planarity (E^{θ}), the aromatic resonance energy (E^{res}), the inductive or mesomeric electronic effects of substituents (E^{sub}) and the intermolecular or interchain coupling in the solid state (E^{int}). In Figure 1.12 the different parameters for determining the band gap of a conjugated polymer are depicted with polythiophene as the representative molecule.

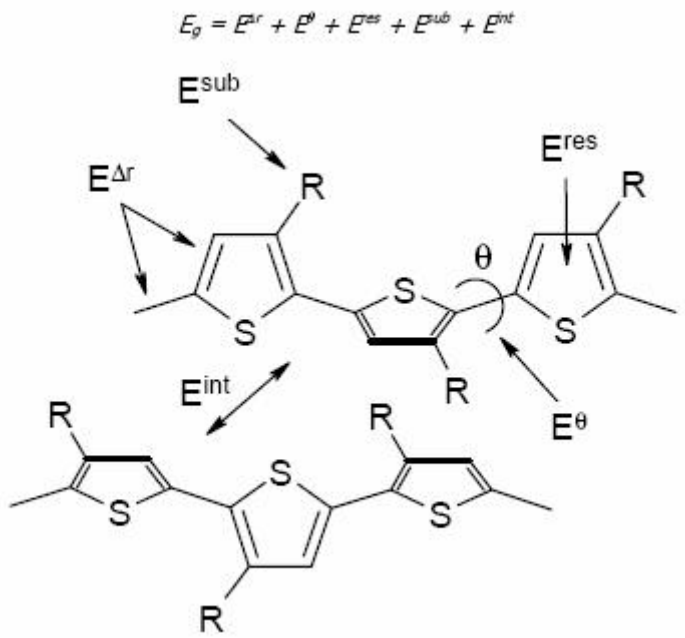

Figure 1.12: Parameters determining the band gap of conjugated polymers.

1.3 Synthetic approaches towards Conjugated polymers:

In 1990, Jeremy Burroughes, Richard Friend and Donald Bradley discovered that if they put a voltage over a PPV film, a yellow-green light was emitting.[65] Since then

within the family of conjugated polymers enormous research is being done on PPV type materials.

Fundamentally, there are two major approaches towards the synthesis of PPVs:

I. oxidative or reductive coupling

II. precursor route

Among the first approach is the direct synthesis of PPV where the double bond (the ethylene linkage between the aromatic cores) is generated *in situ*. This type of synthesis takes place through the step-growth polycondensation reactions, such as Wittig[66], McMurray[67] and Knoevenagel condensation[68] reactions. Another possibility to prepare PPVs is the palladium catalysed cross-coupling reactions, such as Heck reactions[69, 70], Stille reactions[71, 72], Suziki reactions[73] and Sonogashira reactions[74]. Also a direct way is the electrochemically polymerisation[75, 76] of different type of monomer compounds. Unfortunately, all the mentioned synthetic routes lead to insoluble and infusible materials with low molecular weight (oligomers).[77-83]

This problem makes the conjugated polymers less interesting for application. A solution to this problem is the synthesis of conjugated polymers with long flexible alkyl or alkoxy side chains. Poly(2-methoxy-5,2'-ethylhexyloxy-1,4-phenylene vinylene) MEH-PPV[84] and poly(2-methoxy-5-(3,7-dimethyloctyloxy)-1,4-phenylene vinylene) MDMO-PPV[85] are examples of soluble PPV derivatives in their conjugated form, Figure 1.13.

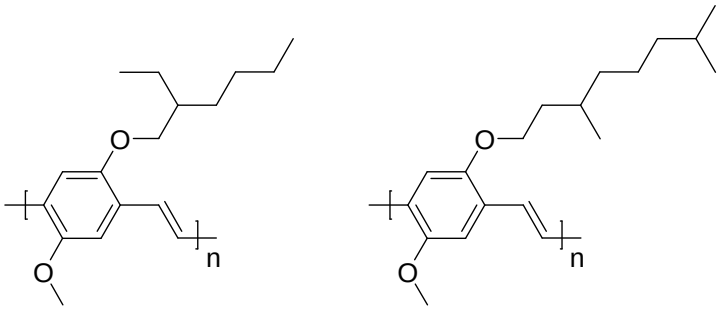

MEH-PPV **MDMO-PPV**

Figure 1.13: Chemical structures of Poly(2-methoxy-5,2'-ethylhexyloxy-1,4-phenylene vinylene) MEH-PPV and poly(2-methoxy-5-(3,7-dimethyloctyloxy)-1,4-phenylene vinylene) MDMO-PPV

However, this approach can not always be applied at any time, especially not for complex functionalised materials. Another solution is the approach to conjugates polymers via a precursor route. Since this thesis only deals with the second approach, the precursor route, only this approach will be discussed in here.

1.3.1 The precursor approach towards conjugated polymers

Another solution to processable conjugated polymers, in this case PPVs and their derivatives, is the approach via precursor route. For this approach the conjugated polymer is synthesised via a soluble intermediate – soluble precursor polymer – that can be casted into thin film before solid state conversion to the insoluble conjugated polymer. Soluble polymers are essential for processable polymers and their application in devices. All precursor routes towards PPVs are based on the same kind of chemistry, Scheme 1.1.

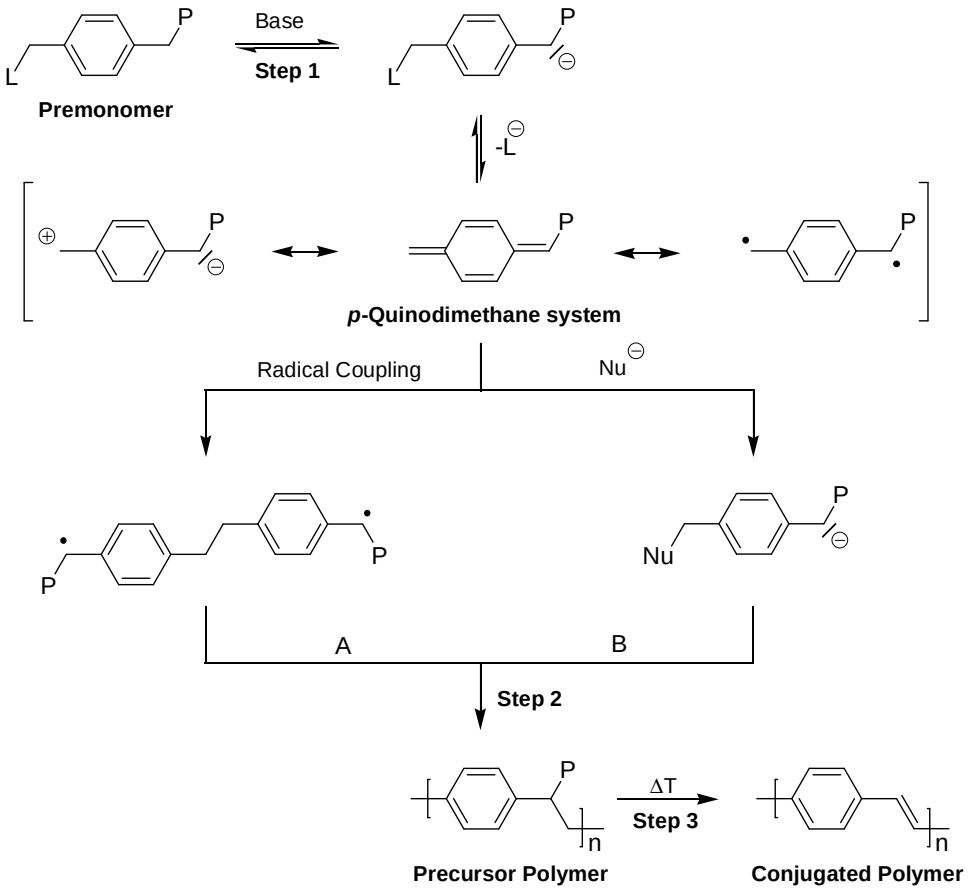

Scheme 1.1: General reaction scheme of the precursor routes towards PPV

The difference between the precursor routes towards PPV derivatives is in the substituents on their premonomer, i.e. the leaving group (L) and polarizer (P) and the polymerisation conditions (base, solvent, reaction temperature and time). The task of the leaving group (L) is to be an atom or a functional group with good leaving group capacities. This way the actual monomer – the *p*-quinodimethane system – will be formed efficiently upon elimination of the premonomer. The polarizer, which should be an atom or a functional group, has four tasks. The first task of the polarizer is to polarize the *p*-quinodimethane system in such a way that the propagation occurs only via consecutive head to tail additions and the undesired head to head and tail to tail additions should be kept to an absolute minimum. A second task of the polarizer is the generation of soluble precursor

polymers and that preferentially in common organic solvents that are being used for processing techniques such as spincoating. An important task of the polarizer is its ability for thermal elimination from the precursor polymer to the conjugated polymer. A final task of the polarizer is to avoid the formation of harmful elimination products during the elimination, which can hamper an efficient device performance. An overview of the specific polarizer and leaving group is presented in Table 1.1. It has to be noticed that all the precursor routes (except sulphinyl precursor route) have in common that they use a symmetrically substituted premonomer.

As it can be seen in Scheme 1.1, the premonomer reacts with a base and deprotonation occurs leading to an anion. Step 1 is proceeding via the base induced 1,6-elimination of the leaving group on the anion leading to the *in situ* formation of the actual monomer - the *p*-quinodimethane system.[86, 87] This *p*-quinodimethane system can be represented both under its diamagnetic and paramagnetic resonance form. The polymerisation of the highly reactive *p*-quinodimethane system to the precursor polymer occurs spontaneously. This can either occur via a radical chain polymerisation or by an anionic chain polymerisation, depending on the monomer and the polymerisation conditions.[88, 89] A lot of research has been done on the mechanism of the polymerisation. There are indications that the anionic polymerisation leads to low molecular weight material.[90] The radical polymerisation leads to high molecular weight material.[91-94] However, discussions about the mechanism are still ongoing and beyond the scope of this work.

Precursor Routes	Leaving Group (L)	Polariser (P)
Dehalogenation (Gilch)	Cl or Br	Cl or Br
Sulphonium (Wessling-Zimmerman)	$^{+}SR_2X^{-}$	$^{+}SR_2X^{-}$
Sulphinyl	Cl or Br	S(O)R
Xanthate	SC(S)OR	SC(S)OR
Dithiocarbamate	$SC(S)NR_2$	$SC(S)NR_2$

Table 1.1: Overview of the specific polarizer and leaving group for various precursor routes

1.3.2 The Dehalogenation Precursor Route

The dehalogenation precursor route, also called the Gilch route, was first investigated by Gilch and Wheelwright, Scheme 1.2. They polymerised the symmetrical α,α'-dichloro-p-xylene monomer **1** to PPV by treating it with a large excess of the base, potassium *tertiair* butoxide (K*t*BuO), dissolved in benzene.[95] Hereby premature basic elimination occurred leading to insoluble PPV fragments. Later, to avoid this problem and obtain a soluble precursor polymer, the modification to one equivalent of the base was used leading to chlorine precursor polymer **2**.[96]

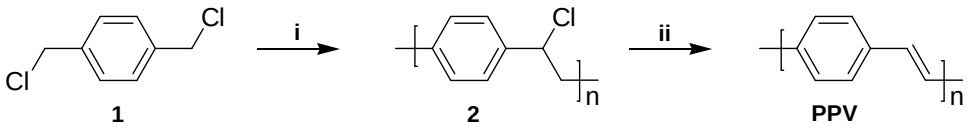

Scheme 1.2: The Gilch route, reaction conditions: i: 1 equivalent K*t*BuO, THF or 1,4-dioxane, RT; ii: 10 equivalent K*t*BuO, THF or 1,4.dioxane, reflux.

The mechanism of this polymerisation is related to sulphonium precursor route.[97, 98] However, this precursor polymer is on one hand not soluble in most common organic solvents (e.g. chloroform, THF) and on the other hand not very stable.[99-101] The Gilch route is widely used to synthesise soluble conjugated polymers and the conversion of the chlorine precursor polymer towards PPV can be achieved, *in situ* in solution, either by a thermal treatment at 300°C for 1 hour or by the addition of an excess amount of base. In industry, the Gilch route is an efficient method to synthesise soluble high molecular weight conjugated polymers such as MEH-PPV and MDMO-PPV (Figure 1.13). In literature, no real distinction is made between the direct route (excess amount of base) and the precursor route (one equivalent of base) towards PPV, it is always presented as the Gilch route.

1.3.3 The Sulphonium Precursor Route

The Sulphonium Precursor Route, also called as the Wessling route, towards PPV was discovered and patented by Wessling and Zimmerman in 1968.[102,103] Among the precursor routes, the Wessling route became one of the most studied precursor

routes towards PPV. The mechanism of the polymerisation is a multi-step process which is described in Scheme 1.3.[103, 104]

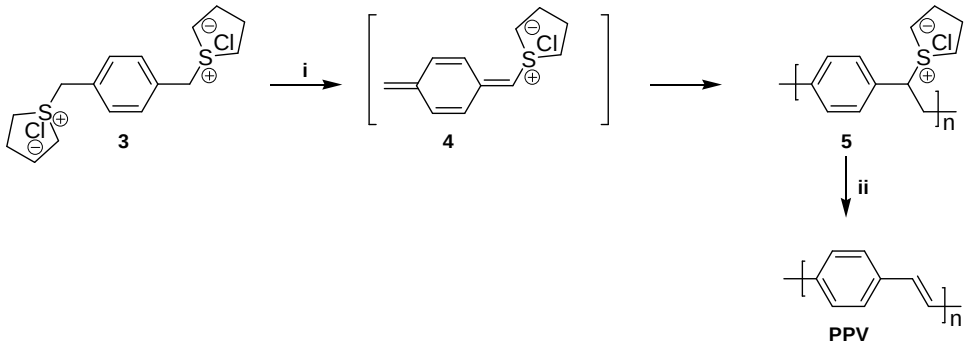

Scheme 1.3: The Sulphonium Precursor Route, reaction conditions: i: NaOH, MeOH/H_2O or Bu_4NOH, MeOH, 0°C, 1h, 20-90%; ii: 160-300°C, 12h.

In order to avoid partial base-induced elimination, the symmetrical bissulphonium salt **3** is treated with slightly less than one equivalent of base at 0°C leading to the ionic precursor polymer **5**. Although both linear and cyclic thioethers can be used, still the latter is favoured due to some side reactions occurring during the thermal elimination to the conjugated structure **PPV**.[105] In general often polar protic solvents are used as the solvent for the polymerisation and the yields vary between 20 and 90% depending on the reaction conditions.[105,106] Important to note is that the monomoer concentration is very crusial for this polymerisation route. High monomer concentration (0.2 M) not only leads to high polymerisation yields but it also leads to an insoluble gel-like polymer. Reduction of the monomer concentration proved to be efficient leading to soluble precursor polymer (0.5 M). However, hereby the yield drops to around 55%. The conversion of the precursor polymer to the conjugated structure **PPV** takes place by a thermal treatment between 160 and 300°C for a sufficient long time.[107]

Despite the fact that there are many different PPV derivatives which have been synthesised via this precursor route[108], there is also a disadvantage attached to this route – the formation of the instable precursor polymers. Due to the good leaving group capacities and their sensitivity for nucleofiles the sulphonium group can undergo all kind of side reactions during polymerisation leading to gel

formation, premature elimination, solvent substitution and irriversible sp3 defects in the polymer backbone or a combination of all. Moreover, electron poor aromatic systems (nitro or cyano substituents) or monomer with an extended aromatic systems are extremely difficult to synthesise via Wessling route.

1.3.4 The Sulphinyl Precursor Route

In order to overcome the problems mentioned above, the Sulphinyl precursor route was discovered which, unlike other precursor routes, starts with the asymmetric premonomer **6**.[109-111] On one hand, there is a good leaving group needed to produce an effcient *p*-quinodimethane system. On the other hand, a bad leaving group is needed in order to produce stable precursor polymer. Therefore, the only solution was the synthesis of an asymmetric monomer. This procedure was developed in our lab with halogen atoms as a good leaving group and a sulphinyl group as the polarizer, Scheme 1.4.

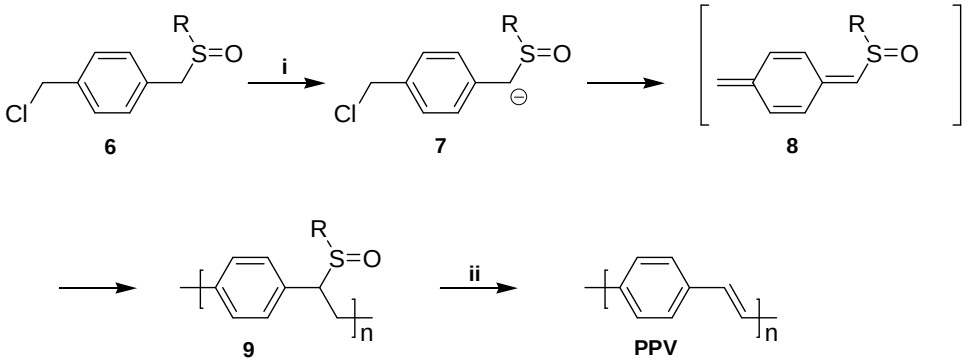

Scheme 1.4: The Sulphinyl Precursor Route, Reaction conditions: i: Na*t*BuO, solvent; ii: 100-150°C, vacume.

Addition of a base (1 till 1.3 equivalent) leads to selective deprotonation on the side of the sulphinyl group and the formation of the actual monomer, *p*-quinodimethane system **8**. The monomer polymerises at once to the stable soluble precursor polymer **9**. This precursor polymer can eventually be converted to PPV by thermal elimination at low temperature (70 - 100°C).[112]

1.3.5 The Xanthate Precursor Route

The Xanthate Precursor Route was developed as a modification of the sulphonium precursor route in an attempt to overcome the disadvantages mentioned before, Scheme 1.5.[113] A symmetrical bisxanthate monomer **10** is polymerised with K*t*BuO as the base in dry THF at 0°C. Although there is no evidence presented, the polymerisation is proposed to proceed via the *p*-quinodimethane system **11**.

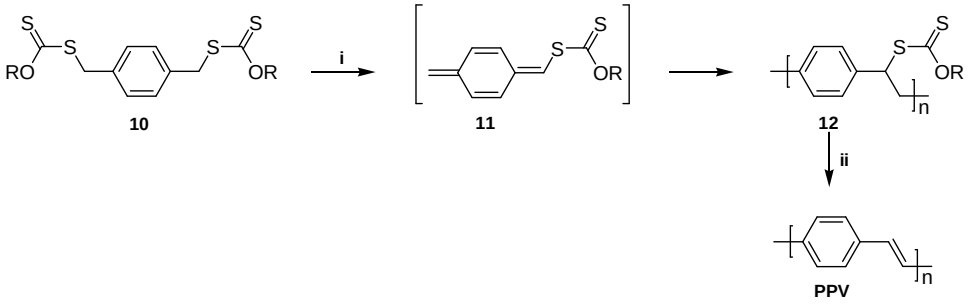

Scheme 1.5: The Xanthate precursor route, Reaction conditions: i: K*t*BuO, THF, 0°C; ii: 160-250°C, inert atmosphere.

During the polymerisation, cis- and trans-precursor polymers **12** are formed. At higher temperatures the cis-precursor polymers can be completely converted to the thermodynamically stable trans-precursor polymers.[114] Polymerisation at low temperature results in reasonable yields with high molecular weight. Hereby, the precursor polymers are stable at room temperature and soluble in common organic solvents. The precursor polymer can eventually be converted to PPV by thermal elimination (160 - 250°C).

An important advantage is the higher electroluminescence efficiency of the material. Using this precursor route the efficiency of a single layer LED device, ITO / PPV / Al was 0.22% compared to earlier value of 0.01%. It was proved that this higher efficiency was due to the absence of hydrogen chloride during elimination.[115] Although there are some advantaged attached to this route still there is a limited publication record to be found.

1.3.6 The Dithiocarbamate Precursor Route

In 2003 Henckens and coworkers reported on a new precursor route, the dithiocarbamate precursor route. They used this route for the synthesis of Poly(Thienylene Vinylene) (PTV) and its derivatives.[116] Using this route low polydispersity index could be obtained and they could exclude the disadvantages attached to earlier mentioned precursor routes. Namely, side chain reactions, gel formation, premature elimination and limited solubility of the precursor polymers. The dithiocarbamate precursor route is the precursor route used in this work.

Monomer synthesis

The monomer synthesis for the dithiocarbamate precursor route is more straightforward than the synthesis of the monomers for the sulphinyl precursor route. In the case of electron-rich starting products towards the synthesis of the monomer, this route is superior compared to all the other precursor routes mentioned before. Therefore, the versatility is broad toward the synthesis of other conjugated polymers. The synthesis of the dithiocarbamate monomer is similar to the synthesis of the bisxanthate monomer **10**, Scheme 1.6.[117] The bisdithiocarbamate monomer **13** can be obtained by nucleophilic substitution of sodium diethyldithiocarbamate trihydrate to α,α'-dichloro-*p*-xylene **1** or to bissulphonium salt **3** in diethyl ether or ethanol at room temeprature.

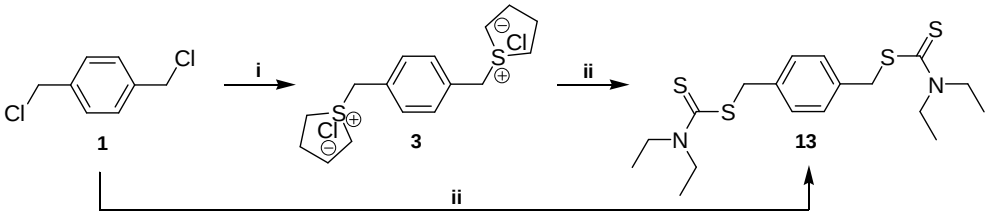

Scheme 1.6: Synthesis of the dithiocarbamate monomer: i: THT; ii: $NaSC(S)NEt_2 \cdot 3H_2O$, solvent, RT.

Polymerisation

The polymerisation of the premonomer **13** was carried out with lithium diisopropyl amide (LDA) or lithium hexamethyl diisopropyl amide (LHMDS) as the base in dried THF as the solvent and with a monomer concentration of 0.2 M, Scheme 1.7.

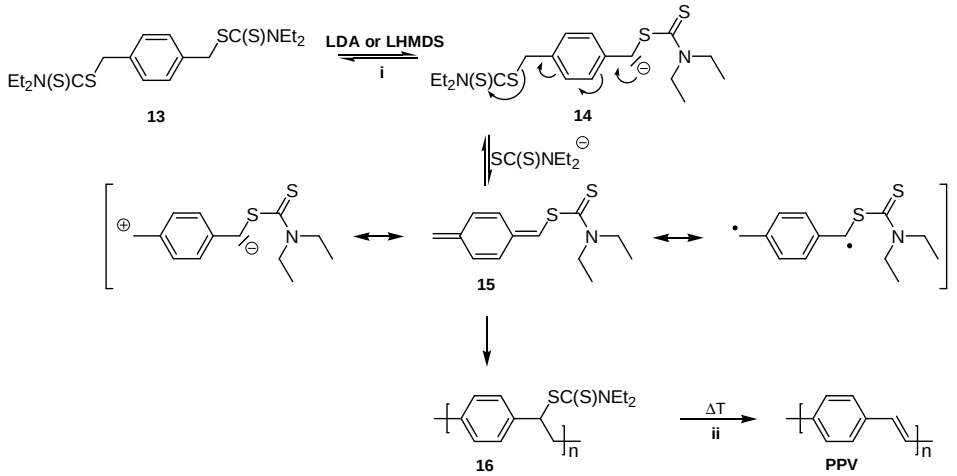

Scheme 1.7: The dithiocarbamate precursor route, reaction conditions: i: LDA or LHMDS, dry THF, 90 minutes; ii: thermal elimination.

Hereby, the premonomer **13** reacts with LDA or LHMDS and deprotonation occurs leading to the anion **14**. 1,6-elimination of the leaving group (one dithiocarbamate group) on **14** leads to the *in situ* formation of the actual monomer - the *p*-quinodimethane system **15**. The polymerisation of the highly reactive *p*-quinodimethane system to the precursor polymer **16** occurs spontaneously. This can either occur via a radical chain polymerisation or by an anionic chain polymerisation, depending on the monomer and the polymerisation conditions. The polymerisations are typically terminated after 90 minutes reaction by pouring the reaction mixture into ice water by which the precursor polymer precipitates. The aqueous solution was neutralised using dilute hydrogen chloride (1M). After extraction with chloroform the combined organic layers were concentrated in vacuo. The crude polymer was dissolved in small amount of chloroform and precipitated in methanol, collected and dried. The residual fraction is also concentrated in vacuo and analysed. Reasonable molecular weights were observed with low polydispersities.[118] Since this route is quite recently discovered,

arguments about the mechanism are still ongoing and beyond the scope of this work. The dithiocarbamate precursor route opens a wide range of possibilities to prepare materials for device application. This way, the disadvantages mentioned before, can be limited and a wide range of conjugated polymers can be synthesised that were otherwise not possible via other routes, e.g. electron poor materials like poly(quinoxaline vinylene).

Conversion to the conjugated structure

The last step in the polymerisation is the thermal elimination of the polarizer (the dithiocarbamate group) on the soluble precursor polymer **16** to yield the double bond leading to the insoluble conjugated structure **PPV**. Hereby, the precursor polymer **16** was spin coated from a $CHCl_3$ solution (10 mg/mL) onto NaCl disks at 500 rpm or quartz disks at 700 rpm, respectively. Subsequently, the disks were placed in a thermo cell. A dynamic heating rate of 2°C/min up to 350°C under continuous flow of nitrogen was used for the conversion process using *in situ* UV-Vis and *in situ* FT-IR spectroscopy.

1.4 Applications

1.4.1 Application of conjugated polymers for electronic devices

Nowadays plants are unable to absorb the huge amount of extra carbon dioxide that is released in the earth's atmosphere mainly by burning of fossil fuel. As a result, this adds to the greenhouse effect which leads to the increase of the global mean surface temperature.[119,120] As the concern for global warming is increasing every year, the general public becomes more and more aware of the limitations one is facing concerning the stability of future supply of today's main energy sources (i.e. oil, coal, gas, uranium) and their long-term effects on the natural balance on our planet. Therefore, we are urged to develop renewable energy sources.

Fortunately, we have renewable energy sources which neither run out nor have any significant harmful effects on the environment. Harvesting energy directly from the sunlight using photovoltaic (PV) technology is being widely recognized as an essential component of future global energy production. Provided that PV devices can be made truly economically competitive with fossil fuels and other emerging renewable energy technologies, large scale manufacturing of these devices offers a sustainable energy source which can supply a significant fraction of our daily energy needs.

Semi-conducting polymers (conjugated polymers) draw a lot of interest the last few decades. They can be used as active layer in biosensors[10-12], organic field effect transistors (OFETs)[13-16], polymer light-emitting diodes (PLED's)[17, 18], photovoltaic cells[19-26], flat-panel displays[27], photodiodes23, 28, electronic noses[29-31], polymer batteries[32-34], lasers[35-40], smart windows[41-46], light-emitting electrochemical cells (LECs)[47-52] and organic solar cells[23, 28, 53-55]. Organic semiconductors have many advantages, such as low cost synthesis and ease of processing for device application. It is hoped that one day conventional processing steps such as roll-to-roll processing and doctor-blade techniques can be used to make large-area, inexpensive very thin organic solar cells on flexible substrates. It is proposed that such flexible solar cells could be used in different ways, from handheld devices to commercial power production.

1.4.2 Organic versus Inorganic Solar cells

In 1839, a Frenchman, Henri Becquerel was the first scientist that investigated the photovoltaic effect and discovered that an electric current could be produced by shining light onto certain chemical solutions. Selenium was the first solid material in which the photovoltaic effect was observed in 1877. This material was used for many years for light meters, which only required a very small amount of power. In 1905 and 1930 subsequently, Einstein and Schottky provided a deeper understanding of the scientific principles of these materials.

The extensive study on solar cells started in the 1950s when in 1954 Chapin, Pearson and Fuller at Bell Laboratories developed the first inorganic (crystalline silicon) p-n junction solar cell, which had an efficiency of 6%.[121] From 1958 this solar cell was used in specialised applications such as orbiting space satellites. Over the years, solar cells have been made from many other semiconductor materials with various device configurations such as amorphous thin-film structures, single crystal, polycrystalline, ribbon, sliver, etc. single-crystal, polycrystalline, and amorphous.[122] Since the discovery of solar cells, the efficiency has reached 24% for crystalline Si solar cells[123]. Although, today they account for 95% of the photovoltaic devices[124], one of the major obstacles for implementation for larg-scale power generation is the large production costs due to the high material consumption of high grade Si as a basis for this technology. This is preventing them from producing cost effectively. However, to prevent these problems, solar cells based on organic materials (e.g. conjugated polymeric materials) are extensively studied as an alternative during the last few years.

The first investigation on organic photovoltaic cell dates back to 1959, when Kallmann and Pope observed a photovoltaic effect in a single crystal of anthracene when sandwiched between two identical electrodes and illuminated from one side. The cell exhibited a photovoltage of 200 mV with an extremely low efficiency.[125] During the years many efforts were done to study the mechanism and improve efficiency of organic solar cells. A major breakthrough in the cell performance came in 1986 when Tang discovered that much higher efficiencies (about 1%) are attainable when bringing an electron donor and an electron acceptor together in one cell[126]. This concept of heterojunction is the heart of all three currently existing types of organic photovoltaic cells: dye-sensitized solar cells[127], planar organic semiconductor cells[126, 128] and high surface area, or bulk heterojunction cells[23,129].
Also Gregg and co-workers (1989 and 2003) did a lot of research on the mechanism of organic solar cells, especially studying the difference between inorganic (conventional) solar cells and organic solar cells.[130-132] According to Gregg in inorganic solar cells the electrons and holes are generated together in the bulk of the material and they are not tightly bound to each other. The free charge carriers are separated from each other by the built-in electric field of the device and

travel to their respective electrode where they are transported out of the semi-conducting material (Figure 1.14, left). Conventional devices are based on so-called minority carrier materials meaning the *diffusion* in the built-in electric field creates the photovoltaic current.

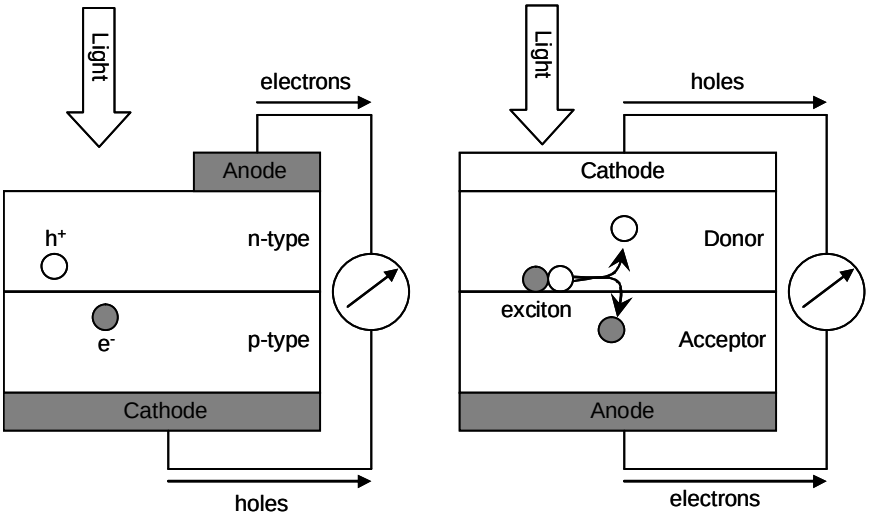

Figure 1.14: Schematic diagram of an inorganic p-n junction solar cell (left) and an organic solar heterojunction solar cell (right).

In contrast, in organic solar cells, the charge carriers are tightly bound to eachother in the form of excitons and they only dissociate at the interface. In the case of heterojunction they dissociate at the interface between donor and acceptor organic materials. Organic materials are so-called majority carriers materials because holes exist primarily in one phase (the donor phase), electrons exist primarily in the other phase (the acceptor phase), and their *movements* to the opposite electrodes result directly in current flow (Figure 1.14, right).

1.4.3 Organic solar cells and their photovoltaic principle

Parker introduced the metal-insulator-metal (MIM) tunnel diode with metal electrodes of asymmetrical work function.[133] This MIM device is one of the most widely used **single layer** organic semiconductor device (e.g. LED). The asymmetry of the work function results in an electric field that facilitates transport of separated

charge carriers toward the respective contacts. The resulted electric field is mainly not sufficient to break up the photogenerated exciton. Therefore, the exciton diffuses within the organic layer until it reaches a contact where it may be broken up to supply separate charges, or recombine, Figure 1.15. As exciton diffusion lengths are short, 1-10 nm for organic materials[134], only those excitons generated in a small region within <10 nm from the contact contribute to the photocurrent. Single layer solar cells based on PPV delivered power conversion efficiencies of less than 0.1 % under white light illumination[135].

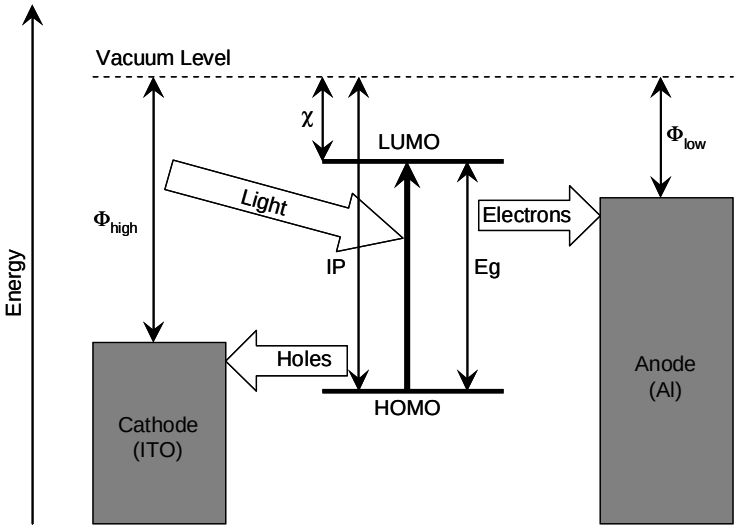

Figure 1.15: Schematic diagram of the band structure of a single layer organic solar cell having only one material in the active layer and different types of metal electrodes.

In 1986, Tang achieved the next breakthrough in the field of organic solar cells by introducing the **bilayer heterojunction** device[126] (Figure 1.16). The device which was prepared from phthalocyanine and a tetracarboxylic derivative was placed between the electrodes and resulted in a power conversion efficiency of 0.95 %. Sariciftci and co-workers investigated the use of conjugated polymers in this two layer devices. They prepared solar cells by evaporating C_{60} on top of a spin-cast poly(2-methoxy-5-(-2'-ethyl-hexyloxy)-1,4-phenylene vinylene) (MEH-PPV)[136]. Hereby, the MEH-PPV was used to absorb visible light and transport holes to the ITO electrode following exciton dissociation at the interface. The C_{60}, with an

electron affinity of about 0.7 eV larger than the conjugated polymer was used to accept electrons and transport them to the aluminium electrode. Devices with efficiencies from 0.1 % up to 1.9 % were achieved[134, 137].

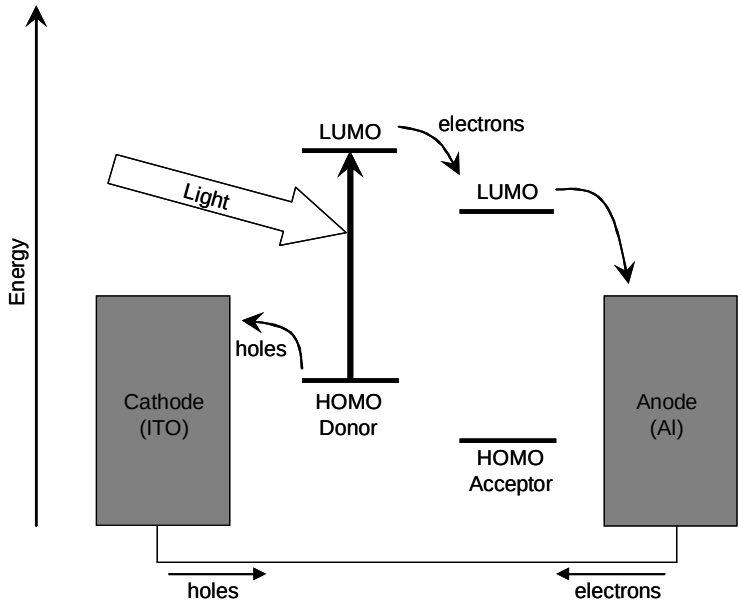

Figure 1.16: Schematic diagram of the band structure of a (bulk/ bilayer) heterojunction organic solar cell: The active layer contains a donor and an acceptor. The electrons are short-circuited, which equalizes their work functions.

Since, in organic solar cells, exciton dissociation process only occurs at the donor/ acceptor interface. Hereby, the exciton diffusion lengths are small (1-10 nm)[138] and this limits the effective light-harvesting layer. Therefore, controlling the structure of the active layer (morphology) is crucial to obtain efficient devices. For most organic semiconductors the film thickness should be more than 100 nm in order to absorb enough light. The interesting part is that on one hand ticker film layers increase light absorption and on the other hand this results in only a small fraction of the exctions reaching the interface and dissociating. Attempts have been made by scientists to maximise/ optimise the interface between the phases. In 1995 Yu and co-workers published theirs results on a solar cell, where an electron donating material (MEH-PPV) and an electron accepting material (C_{60}) were blended together in the active layer – **bulk heterojunction** – resulting in the increase of the

interface. Hereby, they obtained a monochromatic conversion efficiency of 2.9 %[55]. Since then a lot of research have been done on this type of solar cells, but the performance remained relative low due to the lack of suitable donor polymers[139-142]. A better morphology of the active layer was obtained after an additional annealing step for P3HT:PCBM- bulk heterojunction solar cells with an efficiency of 5 %[26]. Possible alternatives may be realised by substituting the fullerene acceptor material by a polymeric acceptor material. Possibly this may lead to an even better control on morphology and device characteristics. Therefore, more research needs to be done towards suitable acceptor polymers in order to make a real all-polymer solar cell. Figure 1.17 depics a bulk heterojunction device. The difference between a bilayer heterojunction and a bulk heterojunction is depicted as well

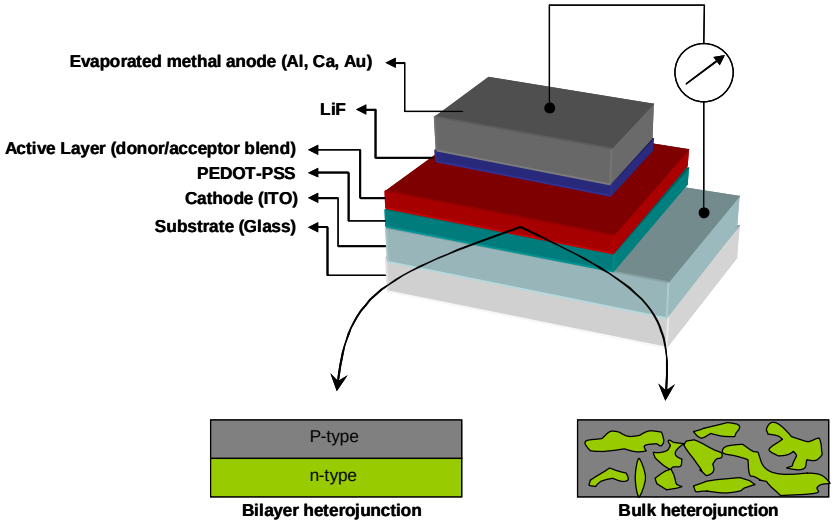

Figure 1.17: Diagram of a bulk heterojunction device. The difference between a bilayer heterojunction and a bulk heterojunction is depicted as well.

Concerning the conventional – inorganic – solar cell, the light enters from the anode side while the anode itself consists of a grid of conductive material. On the other hand, the organic solar cell consists of at least four distinct layers, not counting the substrate, which may be glass or some flexible, transparent polymer. On top of this substrate is laid a 100-200 nm thick layer of transparent cathode, indium thin oxide (ITO) electrode. Between the cathode and the active layer is a 100 nm thick layer of the conductive polymer mixture poly(3,4-

ethylenedioxythiophene)/poly(styrenesulfonate) (PEDOT-PSS) applied. The PEDOT-PSS layer has several functions. It serves as a hole transporter and exciton blocker, it smoothens out the ITO surface, it seals the active layer from oxygen and it keeps cathode material from diffusing into the active layer. Further, on top of the PEDOT-PSS, is deposited the active layer. This photoactive layer is either applied by spin-coating or by thermal evaporation. This layer is responsible for light absorption, exciton generation/ dissociation, and charge carrier diffusion. The active layer consists of a heterjunction device made up of a donor and an acceptor material. On top of the active layer is deposited the anode made of aluminium, but it can also be calcium, silver or gold. Furthermore, a very thin layer of lithium fluoride (LiF) (5-10 Å) is usually placed between the active layer and the anode. It seems that LiF does not react chemically, but serves as a protective layer – guarantee for good ohmic contact.

In an organic photovoltaic cell three processes occur during the conversion of solar energy into electrical energy: (1) Absorption of light; (2) charge transfer and separation of the opposite charges and (3) charge transport and the collection at the electrodes[143].

Figure 1.18 depicts the schematic drawing of the working principle of an organic solar cell. Here it can be seen that when light is absorbed an electron is promoted from the highest occupied molecular orbital (HOMO) to the lowest unoccupied molecular orbital (LUMO) forming an exciton. In the case of bulk heterojunction solar cells this process needs to be followed by exciton dissociation which leads to charge generation.

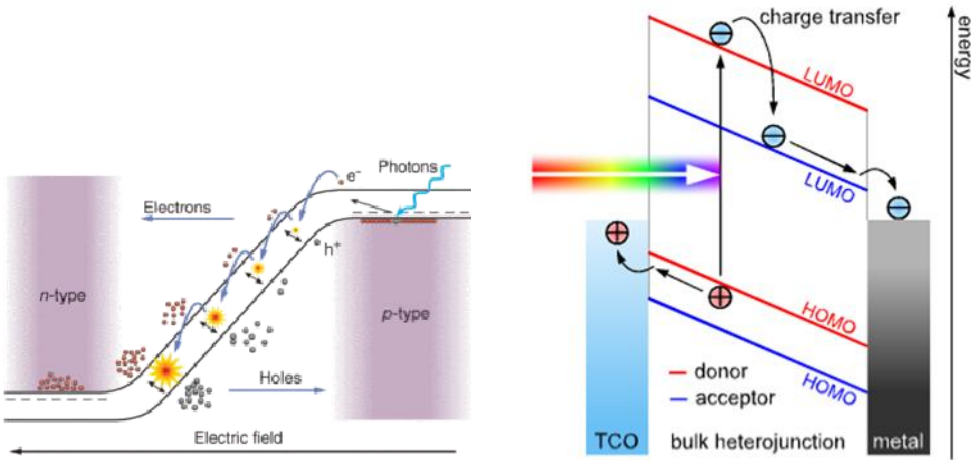

Figure 1.18: schematic drawing of the working principle of an organic solar cell

This is one of the key steps in the conversion of solar light into electrical energy. In most organic solar cells, charges are created by photoinduced electron transfer where an electron is transferred from an electron donor (a p-type semiconductor) to an electron acceptor (an n-type semiconductor). Moreover two important notes need to be taken in account:

1) The energy of the absorbed photon must be used for generation of the charge-separated state and must not be lost via competitive processes like fluorescence, non-radiative decay, internal conversion or intersystem crossing.
2) The charge-separated state must be stabilised, in order to let the photogenerated charges migrate to one of the electrodes.

1.4.4 Characterisation of solar cells

Much terminology surrounds photovoltaic devices. Therefore, it is important to define some terms and discuss them in the context of organic solar cells. First of all it is important to review what happens in a solar cell in the dark and upon exposure to illumination. A graph of current (**I**) versus voltage (**V**) is a common way to illustrate the properties of solar cells. In the dark, the **I**-**V** curve passes through the

origin with no potential, no current flows. But then the device is exposed to light, the **I-V** curve shifts downward, as illustrated in Figure 1.19.

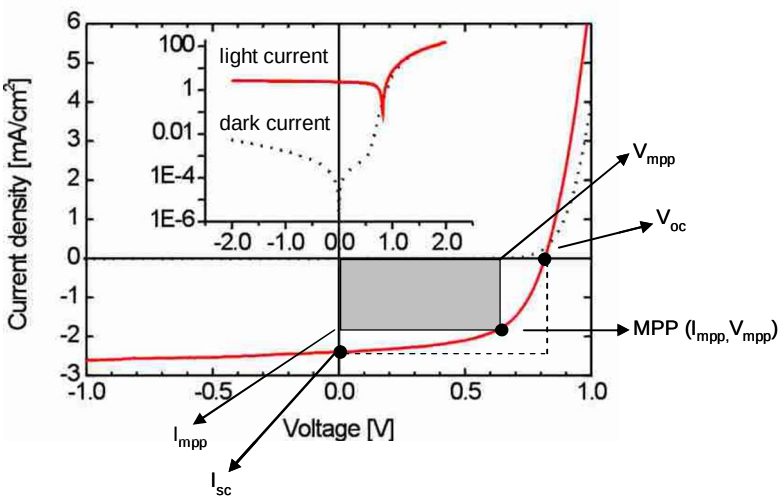

Figure 1.19: Logarithmic (up) and linear (down) current *versus* voltage (I-U) curves for photovoltaic devices. The figure shows how the devices characteristics change from dark (dotted line) upon illumination (solid line). Key points are also indicated.

Air Mass (AM) – Is a measure of how much atmosphere sunlight must travel through to reach the earth's surface. This is denoted as "AM(χ)", where χ is the inverse of the cosine of the zenith angle of the sun. A typical value for solar cell measurements is AM 1.5, which means that the sun is at an angle of 48°. Air mass describes the spectrum of radiation, but not its intensity. For solar cell purposes, the intensity is commonly fixed at 100 W/cm^2.

Concerning the reproducibly characterisation of solar cells, *standard test conditions* had been carried out for conventional inorganic solar cells. Later, this was adapted for the organic solar cells.

These test conditions are based on a spectral distribution, reflecting the emission spectrum of the sun measured on a clear sunny day with a radiant intensity of 1000 W/m^2 that is received on a tilted plane surface with an angle of incidence of 48.2°. This spectrum that also counts for a model atmosphere containing specified

concentrations of, e.g., water vapour, carbon dioxide, and aerosol is referred to as an “Air Mass 1.5 Global” (AM1.5G, IEC 904-3) spectrum, Figure 1.20. These standard test conditions also include a measuring temperature of 25 °C.

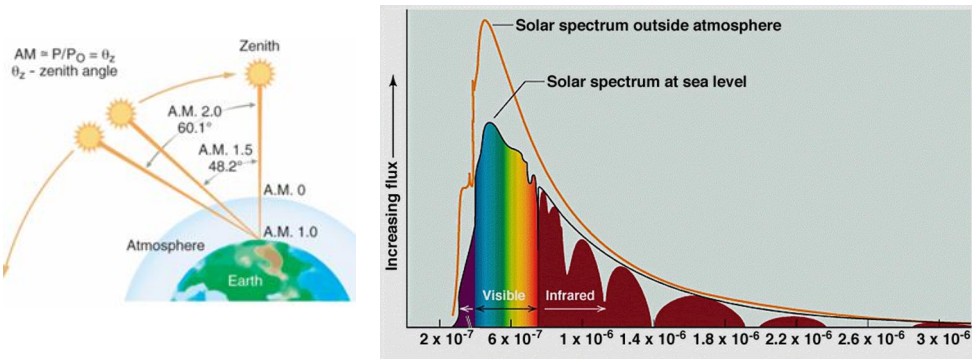

Figure 1.20: Definition of AM0, AM1.0 and AM1.5 solar spectra (left) and the corresponding AM
1.5 spectrum (right).

Open-Circuit Voltage (V_{oc}) – Is the maximum possible voltage across a photovoltaic cell; the voltage across the cell in sunlight when no current is flowing, Figure 1.9.

Short-Circuit Current (I_{sc}) – This is the current that flows through an illuminated solar cell when there is no external resistance (i.e. when the electrodes are simply connected or short-circuited). The short-circuit current is the maximum current that a device is able to produce. Under an external load, the current will always be less than I_{sc}, Figure 1.19.

Maximum Power Point (I_{mpp}, V_{mpp}) – Is the point (I_{mpp}, V_{mpp}) on the **I–V** curve where the maximum power is produced. Power (**P**) is the product of current and voltage (**P = I·V**) and is illustrated in the Figure 1.19 as the area of the rectangle formed between a point on the I–V curve and the axes. The maximum power point is the point on the **I–V** curve where the area of the resulting rectangle is largest.

Fill Factor (FF) – Is the ratio of a photovoltaic cell’s actual maximum power output to its theoretical power output if both current and voltage were at their maxima., I_{sc}

and V_{oc}, respectively. This is a key quantity used to measure cell performance. It is a measure of the "squareness" of the **I–V** curve, Figure 1.19. The fill factor is mainly influenced by the series resistance and shunting resistance. For a good fill factor, first of all the shunt resistance of a photovoltaic device has to be very high in order to prevent leakage currents. Second, the series resistance has to be very low, which then is reflected by a sharp rise in the forward current. For polymer-fullerene solar cells fill factors as high as 0.6 have been determined. The formula for fill factor in terms of the above quantities is:

$$FF = \frac{I_{mpp} V_{mpp}}{I_{sc} V_{oc}}$$

Power Conversion Efficiency (PCE or η_e) – Is the ratio of power output to power input. In other words, PCE measures the amount of power produced by a solar cell relative to the power available in the incident solar radiation (P_{in}). P_{in} here is the sum over all wavelengths and is generally fixed at 100 W/cm^2 when solar simulators are used. This is the most general way to define the efficiency. The formula for PCE, in terms of quantities defined above, is:

$$\eta_e = \frac{I_{mpp} V_{mpp}}{P_{in}} = \frac{I_{sc} V_{oc} FF}{P_{in}}$$

Quantum Efficiency (QE) – Is the efficiency of a device as a function of the energy or wavelength of the incident radiation. For a particular wavelength, it specifically relates the number of charge carriers collected to the number of photons shining on the device. QE can be reported in two ways: internal QE and external QE.

External Quantum Efficiency – Is the type of quantum efficiency that includes losses by reflection and transmission. External quantum efficiency is also called IPCE (Incident Photon to Current Efficiency).

Internal Quantum Efficiency – Is the type of quantum efficiency that factors out losses due to reflection and transmission of photons such that it considers

processes only involving absorbed photons. By accounting for transmission and reflection processes, external Quantum Efficiency can be transformed into internal Quantum Efficiency.

The nanomorphology of donor/acceptor composite is known to have an important influence for the device efficiency[144]. The conditions for the film preparation (e.g. the choice of solvent) are crucial for the domain size in the interpenetrating network. On the one hand, a large interface between the donor/acceptor phases is desired for efficient charge separation. The domain size should be not larger than the exciton diffusion length (approximately 10 nm for most conjugated polymers). On the other hand, interpenetrating paths of the individual phases are required for the charge transport to the electrodes. It is also expected that a larger interface increase recombination of charge carriers. The blend morphology is investigated by several techniques like atomic force microscope[145], transmission electron microscope[146,147], scanning electron microscopy[145], photoluminescence[145] and near field optical microscope. It is generally found that smaller domain sizes lead to higher efficient devices in the case of solution cast processes.

In a recent publication Scharber an co-workers describe some design rules for electron donor materials. Based on his model the ideal material parameters for a conjugated polymer-PCBM device were determined. He claims that the efficiency of a solar cell can be predicted solely as a function of the band gap and the LUMO level of the donor. So besides a reduction of the band gap, new donor materials must be designed to optimize the LUMO as this parameter dominantly drives the solar cell efficiency[148].

1.5 Aim and outline of the thesis

The evidence of global warming continues to build-up the last few years. Therefore, we will have to find a way to produce electricity without the release of carbon dioxide and other greenhouse gasses which is caused by the use of non-renewable and polluting fossil fuels. Wind power is already a significant source of energy in many parts of the world. It can supply 10 percent of the world's electricity

within two decades. An efficient and marvellous idea is to catch the Sun's radiant light energy and convert it into electrical energy. It's nothing new of course. Nature has been capturing the energy in light for millions of years. Each leaf is a form of solar cell, producing energy for plants and trees to grow in a chemical process known as Photosynthesis. In this case, by inserting solar panels in several areas, light or the sun's energy is transferred to electricity by Photovoltaic solar cells. This renewable energy source will neither run out nor have any significant harmful effects on our environment. Solar power has been growing in a global capacity by 33 percent annually and it has been widely recognized as an essential component of future global energy production. Greenpeace and industry research shows that with some government support, the solar industry could supply electricity to over 2 billion people globally in the next 20 years. By 2040 solar photovoltaics would become cost competitive with traditional fossil fuels if the production of photovoltaic panels was increased to 500 megawatts a year leading to a supply nearly 25 percent of global electricity demand. Direct conversion of sunlight into electricity by photovoltaic cells is known for many years and efficiencies of 24 % energy conversion of the terrestrial sunlight have been obtained. Unfortunately, the costs for material consumption and production of these materials are very high; therefore thin film photovoltaic devices can be a solution to these high costs. In general most of the materials, which are used in thin film photovoltaic devices, are inorganic semiconductors. These inorganic semiconductors need high temperature operations for their production, which leads to difficulties in handling and high production costs.

In order to avoid the problems mentioned in this chapter, organic semiconductors, can be promising materials for photovoltaic solar cell devices. The last few years, in particular, conjugated polymers with their extended π-conjugated system gained interest as alternative semiconductor materials. There is alot of industrial interest for devices like organic field effect transistors (OFETs), polymer light-emitting diodes (PLED's), photovoltaic cells, light-emitting electrochemical cells (LECs) and

organic solar cells. Many advantages are attached to organic semiconductors for organic solar cells compared to their conventional inorganic counterparts. Since processing from solution is possible, this offers an easy way for device fabrication and cheap production costs. Therefore, the properties of organic semiconductor can be tuned for the desired application of devices. These devices can be made flexible and semi-transparent with light weight and different coloured materials. Further, the photovoltaic solar cells can be easily integrated into other devices. In order to apply these semiconductive materials for the application in solar cells, material properties like good environmental stability, broad and intense absorption spectra and high charge carrier mobility are needed.

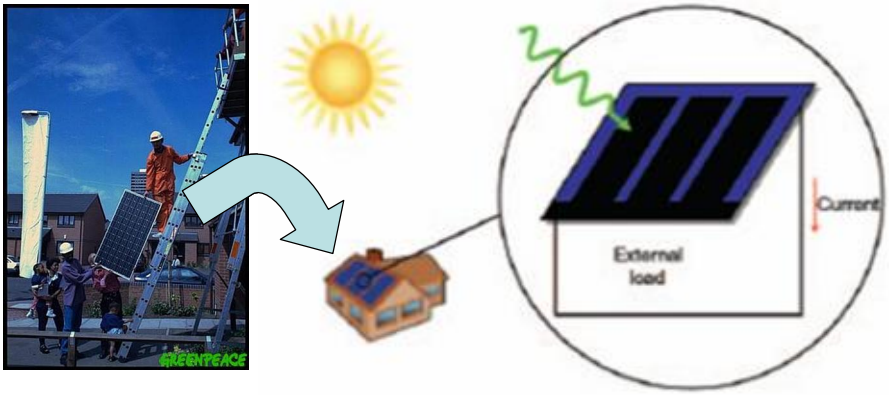

The aim of the research done in this dissertation is the synthesis and characterisation of conjugated polymers, in particular Quinoxaline based conjugated polymers towards solar cells. There are two major approaches towards conjugated polymers: the direct synthesis via oxidative or reductive coupling and the indirect synthesis via the precursor route approach. In this approach a soluble non conjugated polymer is converted into its insoluble conjugated form. In this dissertation the second approach, the precursor route, is being used for the preparation of the polymers. The synthesis of the diphenyl quinoxaline monomer, which is carried out via the Immino-oxime cyclisation route and the Benzothiadiazole route, will be discussed in **chapter two**. The polymerisation of the plain diphenyl quinoxaline monomer will be discussed in **chapter three**, which is a good candidate for organic solar cell application. An effort was made to

introduce different side chains - soluble derivatives - of diphenyl quinoxaline units for photovoltaic application, which will be discussed in **chapter four**. Finally, in **chapter five**, the results on the physical characterisation of PQV and device towards Solar Cells will be presented followed by some outlook and perspective in **chapter six**.

1.6 References

1. L. Breban, "Synthesis and characterisation of Poly(arylene vinylene) derivatives with potential for high induced molecular order", *Dissertation*, Hasselt University, **2007**

2. E. Nies, "Polymers; General Introduction & Definitions", *Catholic University of Leuven*, manuscript

3. E. Goethals, "Inleiding tot de polymeer wetenschappen", *University of Ghent*, **1993**, Cursus

4. B. Rånby, W. R. Salaneck and I. Lundstrom, "The Interconnection of Chemical and Electronic Structure", The Interconnection of Chemical and Electronic Structure, *Oxford University Press*, Oxford, **1993**, 15-26

5. H. Shirakawa, E. J. Louis, A. G. MacDiarmid, C. K. Chiang and A. H. Heeger, *J. Chem. Soc. Chem. Comm.*, **1977**, 578

6. B. L. Groenendaal, F. Jonas, D. Freitag, H. Pielartzik and J. R. Reynolds, "Poly(3,4-ethylenedioxythiophene) and its derivatives: Past, present, and future", *Advanced Materials*, 12, (7), **2000**, 481-494

7. J. Roncali, "Synthetic principles for bandgap control in linear pi-conjugated systems", *Chemical Reviews*, 97, (1), **1997**, 173-205

8. R. Kiebooms, R. Menon and K. Lee, "Handbook of advanced electronic and photonic materials and devices", *Academic Press*, **2001**, vol. 8

9. J. Rodriguez, H. J. Grande and T. F. Othero, "Handbook of organic conductive molecules and polymers", *John Wiley & Sons*, New York, **1997**, vol. 2

10. P. S. Heeger and A. J. Heeger, *PNAS*, 96, (22), **1999**, 12219

11. M. Gerard, A. Chaubey and B. D. Malhotra, *Biosensors & Bioelectronics*, 17, **2002**, 345

12. P. Cooreman, R. Thoelen, J. Manca, M. v. d. Ven, V. Vermeeren, L. Michiels, M. Ameloot and P. Wagner, *Biosensors & Bioelectronics*, 20, **2005**, 2151

13. A. R. Brown, A. Pomp, C. M. Hart and D. M. d. Leeuw, *Science*, 270, **1995**, 972

14. C. D. D. Dimitrakopoulos and P. R. L. Malenfant, *Advanced Materials*, 14, **2002**, 99

15. C. Reese, M. Roberts and M. L. Bao, *Materialstoday*, **2004**, 20

16. L. L. Chua, J. Zaumseil, J. F. Chang, E. C. W. Ou, P. K. H. Ho, H. Sirringhaus and R. H. Friend, "General observation of n-type field-effect behaviour in organic semiconductors", *Nature*, 434, (7030), **2005**, 194-199

17. D. D. C. Bradley, *Synthetic Metals*, 54, **1993**, 401

18. A. Kraft, A. C. Grimsdale and A. B. Holmes, "Electroluminescent conjugated polymers - Seeing polymers in a new light", *Angewandte Chemie-International Edition*, 37, (4), **1998**, 402-428

19. H. Hoppe and N. S. Sariciftci, "Organic Solar cells: An overview", *Journal of Materials Research*, 19, (7), **2004**, 1924

20. H. Spanggaard and F. C. Krebs, "A brief history of the development of organic and polymeric photovoltaics", *Solar Energy Materials and Solar Cells*, 83, (2-3), **2004**, 125

21. N. S. Sariciftci, L. Smilowitz, A. J. Heeger and F. Wudl, *Science*, 258, **1992**, 1474

22. D. Meissner, *Photon*, **1999**,

23. C. J. Brabec, N. S. Sariciftci and J. C. Hummelen, "Plastic solar cells", *Advanced Functional Materials*, 11, (1), **2001**, 15-26

24. J. Johnson, *C & EN*, **2004**, 25

25. G. Dennler and N. S. Sariciftci, *Proceedings of IEEE*, 93, (8), **2005**, 1429

26. M. Reyes-Reyes, K. Kim and D. L. Carroll, "High-efficiency photovoltaic devices based on annealed poly(3-hexylthiophene) and 1-(3-methoxycarbonyl)-propyl-1-phenyl-(6,6)C-61 blends", *Applied Physical Letters*, 87, (8), **2005**, 083506

27. B. Geffroy, P. L. Roy and C. Prat, "Organic light-emitting diode (OLED) technology: materials, devices and display technologies", *Polymers International*, 55, (6), **2006**, 572

28. J. J. M. Halls, C. A. Walsh, N. C. Greenham, E. A. Marseglia and R. H. Friend, *Nature*, 376, **1995**, 498

29. D. Vangeneugden, R. Kiebooms, P. Adriaensens, D. Vanderzande, J. Gelan, J. Desmet and G. Huyberechts, *Acta Polymers*, 49, **1998**, 687

30. J. Gruber, E. K. C. Yoshikawa, Y. Bao and H. Geise, *e-Polymers*, no. 014, **2004**, 1

31. L. O. Péres and J. Gruber, *Materials Science & Engineering C*, **2006**, in press

32. P. Nigrey, D. MacInnes, D. Nairns, A. G. MacDiarmid and A. J. Heeger, *Electrochemical Society*, 128, (8), **1981**, 1651

33. A. Wirsén, "Electroactive Polymer Materials", *Technomic publishing AG*, Switzerland, **1987**,

34. J. Miller, *Advanced Materials*, 5, (9), **1993**, 671

35. F. Hide, M. Diaz-Garcia, D. Schwartz, M. Anderson and Q. Pie, *Science*, 273, **1996**, 1833

36. M. Diaz-Garcia, F. Hide, B. J. Schwartz, M. R. Anderson and Q. Pei, *Synthetic Metals*, 84, **1997**, 455

37. N. Tessler, F. R. Denton and R. H. Friend, *Nature*, 382, **1996**, 695

38. B. J. Schwartz, M. Diaz-Garcia, F. Hide, M. Anderson and Q. Pei, *Polymer Preprints*, 38, **1997**, 325

39. N. Tessler, *Advanced Materials*, 11, **1999**, 363

40. M. McGehee and A. J. Heeger, *Advanced Materials*, 12, **2000**, 1655

41. W. A. Gazotti, G. Casalbore-Miceli, A. Geri and M.-A. D. Paoli, *Advanced Materials*, 10, (60), **1998**,

42. M. G. Kanatzidis, *C & EN*, 3, **1990**, 36

43. R. Wisnieff, *Nature*, 394, **1998**, 225

44. A. A. Argun, P.-H. A. C. Thompson, I. Schwendeman, C. L. Gaupp, J. Hwang, N. P. Pinto, D. B. Tanner, A. G. MacDiarmid and J. R. Reynolds, *Chemical Materials*, 16, **2004**, 4401

45. S. Sindhu, K. N. Rao, S. Ahuja, A. Kumar and E. S. R. Gopal, *Materials Science & Engineering: B*, 1-2, **2006**, 39

46. S. Roth, "One-Dimensional Metals", One-Dimensional Metals, *Weinheim VCH*, **1995**, 209

47. Y. Yang and Q. Pei, *Journal of Applied Physics*, 81, **1997**, 3294

48. Y. Yang and Q. Pei, *Polymer Preprints*, 38, **1997**, 335

49. L. Holzer, F. P. Wenzl, S. Tasch, G. Leising and B. Winkler, *Applied Physics Letters*, 75, **1999**, 2014

50. L. Holzer, B. Winkler, F. P. Wenzl, S. Tasch and L. Dai, *Synthetic Metals*, 100, **1999**, 71

51. D. J. Dick, A. J. Heeger, Y. Yang and Q. Pei, *Advanced Materials*, 8, **1996**, 895

52. Q. B. Pei, G. Yu, C. Zhang, Y. Yang and A. J. Heeger, "Polymer Light-Emitting Electrochemical-Cells", *Science*, 269, (5227), **1995**, 1086-1088

53. S. E. Shaheen, C. J. Brabec, N. S. Sariciftci, F. Padinger, T. Fromherz and J. C. Hummelen, "2.5% efficient organic plastic solar cells", *Applied Physics Letters*, 78, (6), **2001**, 841-843

54. F. Padinger, R. S. Rittberger and N. S. Sariciftci, "Effects of postproduction treatment on plastic solar cells", *Advanced Functional Materials*, 13, (1), **2003**, 85-88

55. G. Yu, J. Gao, J. C. Hummelen, F. Wudl and A. J. Heeger, "Polymer Photovoltaic Cells - Enhanced Efficiencies Via a Network of Internal Donor - Acceptor Heterojunctions", *Science*, 270, (5243), **1995**, 1789

56. J.-L. Brédas and G. B. Street, *Acc. Chemical Review*, 18, **1985**, 309

57. D. F. Shriver, P. W. Atkins and C. H. Langford, "Inorganic Chemistry - second edition", *Oxford University Press*, **1994**, 91

58. G. O. Spessard and G. L. Miessler, "Organometallic Chemistry", *Prentice Hall*, New Jersey, **1997**,

59. R. E. Peierls, "Quantum Theory of Solids", *Oxford, Clarendon Press*, London, **1956**,

60. H. S. Nalwa and K. Kaeriyama, "Handbook of Organic Conductive Molecules and Polymers", *John Wiley & Sons*, Chichester, **1997**, 296

61. A. Henckens, "Synthesis, characterisation and application in electronic devices of low band gap materials based on thiophene derivatives", *Dissertation*, Hasselt University, **2003**

62. W. P. Su, J. R. Schrieffer and A. J. Heeger, *Physical Review Letters*, 42, **1979**, 1698

63. W. P. Su, J. R. Schrieffer and A. J. Heeger, *Journal of Physical Review B*, 22, **1980**, 2099

64. M. Rohatgi, "Fundamentals of photochemistry", *Wiley Eastern Ltd.*, New Delhi, **1978**,

65. J. H. Burroughes, D. D. C. Bradley, A. R. Brown, R. N. Marks, K. Mackay, R. H. Friend and P. L. Burn, *Nature*, 347, **1990**, 539

66. R. N. McDonald and T. W. Cambell, *Journal of American Chemical Society*, 82, **1960**, 4669

67. M. Rehahn and A. D. Schlüter, *Makromol. Chem. Rapid. Commun.*, 11, **1990**, 375

68. E. G. J. Staring, R. C. J. Demandt, D. Braun, G. L. J. Rikken, Y. A. R. R. Kessener, A. H. J. Venhuizen, M. M. F. Knippenberg and M. Bouwmans, *Synthetic Metals*, 71, **1995**, 2179

69. A. Greiner and W. Heitz, *Macromol. Chem. Rapid Commun.*, 9, **1988**, 581

70. R. F. Heck, *Org. Reactions*, 27, **1982**, 345

71. F. Babudri, S. R. Cieco, G. M. Farinola, F. Naso, A. Bolognesi and W. Porzio, *Macromol. Rapid Commun.*, 17, **1996**, 905-911

72. Z. Bao, W. K. Chan and L. Yu, *Journal of American Chemical Society*, 117, **1995**, 12426

73. F. Koch and W. Heitz, *Macromol. Chem. Phys.*, 198, **1997**, 1531-1544

74. M. J. Edelmann, J. M. Raimundo, N. F. Utesch, F. Diederich, C. Boudon, J. P. Gisselbrecht and M. Gross, "Dramatically enhanced fluorescence of heteroaromatic chromophores upon insertion as spacers into oligo(triacetylene)s", *Helvetica Chimica Acta*, 85, (7), **2002**, 2195-2213

75. H. Nishihara, M. Tateishi, K. Aramaki, T. Oshawa and O. Kimura, *Chem. Letters*, **1987**, 539

76. W. P. Chang, W. T. Wang and P. W. Lin, *Polymer*, 37, **1996**, 1513

77. W. Heitz, W. Brügging, L. Freund, M. Gailberger, A. Greiner, H. Jung, U. Kampschulte, N. Niesser, F. Osan, H. W. Schmidt and M. Wicker, *Macromol. Chem.*, 189, **1988**, 119-127

78. H. Martelock, A. Greiner and W. Heitz, *Macromol. Chem.*, 192, **1991**, 967-979

79. A. Greiner, H. Martelock, A. Noll, N. Siegfried and W. Heitz, *Polymer*, 32, (10), **1991**, 1857-1861

80. M. Remmers, M. Schultze and G. Wagner, *Macromol. Rapid Communication*, 17, **1996**, 239-252

81. A. W. Cooke and K. B. Wagener, *Macromolecules*, 24, **1990**, 1404

82. M. Rehahn and A.-D. Schlüter, *Chem. Letters*, 11, **1987**, 375

83. M. Hanack, J. L. Segura and H. S. Spreitzer, *Advanced Materials*, 8, **1996**, 663

84. F. Wudl and G. Sardanov, *US Patent 5*, 189, **1993**, 136

85. H. Becker, H. Spreitzer, W. Kreuder, E. Kluge, H. Schenk, I. Parker and Y. Cao, *Advanced Materials*, 12, (1), **2000**, 42

86. A. Issaris, D. Vanderzande, P. A. Adriaensens and J. Gelan, *Macromolecules*, 31, (14), **1988**, 4426

87. B. R. Cho, Y. K. Kim and M. S. Han, *Macromolecules*, 31, **1998**, 2098

88. L. Hontis, M. V. D. Borght, D. Vanderzande and J. Gelan, *Polymer*, 40, **1999**, 6615

89. A. Issaris, D. Vanderzande and J. Gelan, *Polymer*, 38, (1), **1997**, 2571

90. D. J. M. Vanderzande, L. Hontis, A. Palmaerts, D. V. D. Berghe, J. Wouters, L. Lutsen and T. J. Cleij, "Block-type architectures for Poly(p-Phenylene Vinylene) derivatives: A reality or an illusion", *Proceedings of SPIE*, 5937, **2005**, 116-125

91. L. Hontis, L. Lutsen, D. Vanderzande and J. Gelan, *Snythetic Metals*, 119, **2001**, 135

92. L. Hontis, V. Vrindts, D. Vanderzande and L. Lutsen, "Verification of radical and anionic polymerization mechanisms in the sulfinyl and the Gilch route", *Macromolecules*, 36, (9), **2003**, 3035-3044

93. J. Wiesecke and M. Rehahn, *Angewandte Chemie International Edition*, 42, (5), **2003**, 567

94. J. Wiesecke and M. Rehahn, *Polymer Preprints*, 45, (1), **2004**, 174

95. H. G. Gilch and W. L. Wheelwright, *Journal of Polyner Science*, 4, **1966**, 1337

96. W. J. Swatos and B. Gordon, *Polmer Preprints*, 31, (1), **1990**, 505

97. B. R. Hsieh, Y. Yu, E. W. Forsythe, G. M. Schaaf and W. A. Feld, *Journal of the American Chemical Society*, 120, **1998**, 231

98. B. R. Hsieh, W. C. Wan, Y. Yu, Y. Gao, T. E. Goodwin, S. A. Gonzales and W. A. Feld, *Macromolecules*, 31, **1998**, 651

99. D. Braun, E. G. J. Starin, R. C. J. E. Demandt, G. L. J. Rikken, Y. A. R. R. Kessener and A. H. J. Venhuizen, *Synthetic Metals*, 55-57, **1993**, 914

100. B. R. Hsieh and W. A. Field, *Polymer Preprints*, 34, **1993**, 410

101. G. J. Sarnecki, P. L. Burn, A. Kraft, R. H. Friend and A. B. Holmes, *Synthetic Metals*, 44-57, **1993**, 914

102. R. A. Wessling and R. G. Zimmerman, *US Patent*, 3401152, **1969**,

103. R. A. Wessling, *Journal of Polymer Science Polymer Symp.*, 72, **1985**, 55

104. F. R. I. Denton, P. M. Lahti and F. E. Karasz, *Journal of Polymer Science Part a-Polymer Chemistry*, 30, **1992**, 2223

105. R. W. Lenz, C.-C. Ham, J. Strenger-Smith and F. E. Karasz, *Journal of Polymer Science Polymer Chemistry*, 26, **1988**, 3241

106. R. Garay and R. W. Lenz, *Macromolecular Chem. Suppl.*, 15, **1989**, 1

107. R. O. Garay, U. Baier, C. Bubeck and K. Mullen, *Advanced Materials*, 5, **1993**, 561

108. R. Garay and F. E. Karasz, *Chem. Mater.*, 3, **1991**, 941

109. F. Louwet, D. Vanderzande and J. Gelan, *Synthetic Metals*, 52, **1992**, 125

110. F. Louwet, D. Vanderzande and J. Gelan, "A General Synthetic Route to High-Molecular-Weight Poly(P-Xylylene)-Derivatives - a New Route to Poly(P-Phenylene Vinylene)", *Synthetic Metals*, 69, (1-3), **1995**, 509-510

111. F. Louwet, D. Vanderzande, J. Gelan and J. Mullens, "A New Synthetic Route to a Soluble High-Molecular-Weight Precursor for Poly(P-Phenylenevinylene) Derivatives", *Macromolecules*, 28, (4), **1995**, 1330-1331

112. E. Kesters, L. Lutsen, D. Vanderzande, J. Gelan, T. P. Nguyen and P. Molinié, *Thin Solid Films*, 120, **2002**, 404

113. S. Son, A. Dodabalapur, A. J. Lovinger and M. E. Galvin, "Luminescence Enhancement by the Introduction of Disorder into Poly(P-Phenylene Vinylene)", *Science*, 269, (5222), **1995**, 376-378

114. J. Wouters, "Anionische en Radicalaire mechanismen in de Polymerisatie van MDMO-PPV", *Pre-PhD dissertation*, Hasselt University, **2006**

115. S. C. Lo, A. K. Sheridan, I. D. W. Samuel and P. L. Burn, "Comparison of the electronic properties of poly[2-(2 '-ethylhexyloxy)-1,4-phenylenevinylene] prepared by different precursor polymer routes", *Journal of Materials Chemistry*, 9, (9), **1999**, 2165-2170

116. A. Henckens, K. Colladet, S. Fourier, T. J. Cleij, L. Lutsen, J. Gelan and D. Vanderzande, "Synthesis of 3,4-diphenyl-substituted poly(thienylene vinylene) low-band-gap polymers via the dithiocarbamate route", *Macromolecules*, 38, (1), **2005**, 19-26

117. A. Henckens, I. Duyssens, L. Lutsen, D. Vanderzande and T. J. Cleij, "Synthesis of poly(p-phenylene vinylene) and derivatives via a new precursor route, the dithiocarbamate route", *Polymer*, 47, (1), **2006**, 123-131

118. E. Kesters, S. Gillissen, F. Motmans, L. Lutsen and D. Vanderzande, "Polymerization behavior of xanthate-containing monomers toward PPV precursor

polymers: Study of the elimination behavior of precursor polymers and oligomers with in-situ FT-IR and UV-Vis analytical techniques", *Macromolecules*, 35, (21), **2002**, 7902-7910

119. "Intergovernmental Panel on Climate Changes (IPCC)", *Third assessment report - climate changes 2001*, Web site: www.meto.gov.uk,

120. "United Nations Environment Programme (UNEP)", *Global environment outlook (GEO year book 2004/5)*, Web site: www.unep.org/geo/yearbook,

121. D. M. Chapin, C. S. Fuller and G. L. Pearson, *Journal of Applied Physics*, 25, **1954**, 676

122. R. W. Miles, K. M. Hynes and I. Forbes, "Photovoltaic solar cells: An overview of state-of-the- art cell development and environmental issues", *Prog. Cryst. Growth*, 51, (1-3), **2005**, 1

123. M. A. Green, K. Emery and D. L. K. e. al., "Solar cell efficiency tables (version 28)", *Prog. Photovoltaics*, 14, (5), **2006**, 455

124. A. Goetzberger, C. Hebling and H. W. Schock, "Photovoltaic materials history, status and outlook", *Materials Science & Engineering R-Reports*, 40, (1), **2003**, 1

125. H. Kallmann and M. Pope, "Photovoltaic effect in organic crystals", *Journal of Chemical Physics Review B*, 30, **1959**, 585

126. C. W. Tang, "Two-layer organic photovoltaic cell", *Applied Physics Letters*, 48, **1986**, 183

127. M. Grätzel, "Photoelectrochemical cells", *Nature*, 414, **2001**, 338

128. P. Peumans, V. Bulovic and S. R. Forrest, "Efficient photon harvesting at high optical in-tensities in ultrathin organic double-heterostructure photovoltaic diodes", *Applied Physics Letters*, 76, **2000**, 2650

129. S. E. Shaheen, R. Radspinner, N. Peyghambarian and G. E. Jabbour, "Fabrication of bulk
heterojunction plastic solar cells by screen printing", *Applied Physics Letters*, 79, **2001**, 2996

130. B. A. Gregg and M. C. Hanna, "Comparing organic to inorganic photovoltaic cells: theory, experiment, and simulation", *Journal of Applied Physical*, 93, (6), **2003**, 3605-3614

131. B. A. Gregg, "Excitonic solar cells", *Journal of Physical Chemistry B*, 107, (20), **2003**, 4688-4698

132. B. A. Gregg, M. A. Fox and A. J. Bard, "2,3,7,8,12,13,17,18-octakis (beta-hydroxyethyl)porphyrin (octaethanolporphyrin) and its liquid-crystalline derivatives - synthesis and characterization", *Journal of American Chemical Society*, 111, (8), **1989**, 3024-3029

133. I. D. Parker, *Journal of Applied Physics*, 75, **1994**, 1656

134. J. J. M. Halls, K. Pichler and R. H. Friend, "Exciton diffusion and dissociation in a poly(p-phenylenevinylene)/C-60 heterojunction photovoltaic cell", *Applied Physical Letters*, 68, (22), **1996**, 3120

135. S. Karg, W. Riess and M. Meier, "Characterization of Light-Emitting-Diodes and Solar Cells Based on Poly-Phenylene-Vinylene", *Synthetic Metals*, 57, (1), **1993**, 4186

136. N. S. Sariciftci, D. Braun and C. Zhang, "Semiconducting Polymer Buckminsterfullerene Heterojunctions - Diodes, Photodiodes, and Photovoltaic Cells", *Applied Physical Letters*, 62, (6), **1993**, 585

137. W. Greens, T. Aernouts and J. Poortmans, "Organic co-evaporated films of PPV-pentamer and C-60: model systems for donor/acceptor polymer blends", *Thin Solid Films*, 403, **2002**, 438

138. S. Glenis, G. Tourillon and F. Garnier, *Thin Solid Films*, 139, (3), **1986**, 221

139. F. L. Zhang, M. Jonforsen and D. M. Johansson, "Photodiodes and solar cells based on the n-type polymer poly(pyridopyrazine vinylene) as electron acceptor", *Synthetic Metals*, 138, (3), **2003**, 555

140. H. J. Snaith, A. C. Arias and A. C. Morteani, "Charge generation kinetics and transport mechanisms in blended polyfluorene photovoltaic devices", *Nano Letters*, 2, (12), **2002**, 1353

141. J. J. M. Halls, J. Cornil and D. A. d. Santos, "Charge- and energy transfer processes at polymer/polymer interfaces: A joint experimental and theoretical study", *Physics Review B*, 60, (8), **1999**, 5721

142. A. J. Breeze, Z. Schleisinger and S. A. Carter, "Improving power effciencies in polymer - polymer blend photvoltaics", *Solar Energy Materials and Solar Cells*, 83, (2-3), **2004**, 263

143. C. J. Brabec, V. Dyakonov and J. Parisi, "Organic Photovoltaics, concepts and realization", *Springer-Verlag*, Berlin, **2003**,

144. P. Peumans, S. Uchida and S. Forrest, *Nature*, 425, **2003**, 158

145. H. Hoppe, M. Niggemann, C. Winder, J. Kraut, R. Hiesgen, A. Hinsch, D. Meissner and N. S. Sariciftci, "Nanoscale morphology of conjugated polymer/fullerene-based bulk-heterojunction solar cells", *Advanced Functional Materials*, 14, (10), **2004**, 1005-1011

146. J. K. v. Duren, J. Loos, F. Morrissey, C. M. Leewis, K. P. H. Kivits, L. J. v. Ijzendoorn, M. T. Rispens, J. C. Hummelen and R. A. J. Janssen, *Advanded Functional Materials*, 12, **2002**, 665

147. T. Martens, J. D'Haen, T. Munters, Z. Beelen, L. Goris, J. Manca, M. D'Olieslaeger, D. Vanderzande, L. D. Schepper and R. Andriessen, *Synthetic Metals*, 138, **2003**, 243

148. M. C. Scharber, D. Mühlbacher, M. Koppe, P. Denk, C. Waldauf, A. J. Heeger and C. J. Brabec, *Advanced Functional Materials*, 18, (6), **2006**, 789

Chapter two

2. Synthetic Approaches Towards Quinoxaline Core – Monomer Synthesis

2.1 Introduction

Quinoxaline derivatives are very important nitrogen-containing heterocycles and have been widely used in several applications: in pharmaceuticals[1], as part of various antibiotics and they are active against various transportable tumors[2,3], in dyes[4], as DNA cleaning agents[5, 6], as efficient electroluminescent materials[7] and in organic semiconductors[8, 9].

In the past decades many efforts were made to prepare Quinoxaline and their derivatives. However, they have not found wide-spread use primarily due to the high cost of the tetraamines and tetraketones used in their synthesis[10]. In fact, tetraketones are not commercially available. Moreover, the thermally stable polymers are prepared by Friedlander Reaction run in an undesirable solvent (e.g. *m*-cresol), Scheme 2.8. The mechanism involved is the double polycondensation of mentioned tetraketones with tetraamines producing a condensed heterocyclic repeat unit, known as a polyquinoxaline, Scheme 2.9.

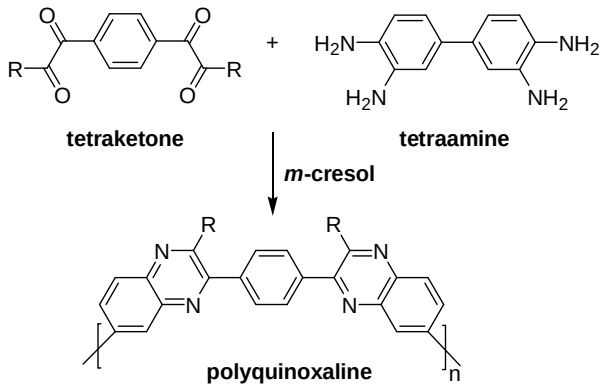

Scheme 2.8: Thermally Stable Polymers via the Friedlander Reaction

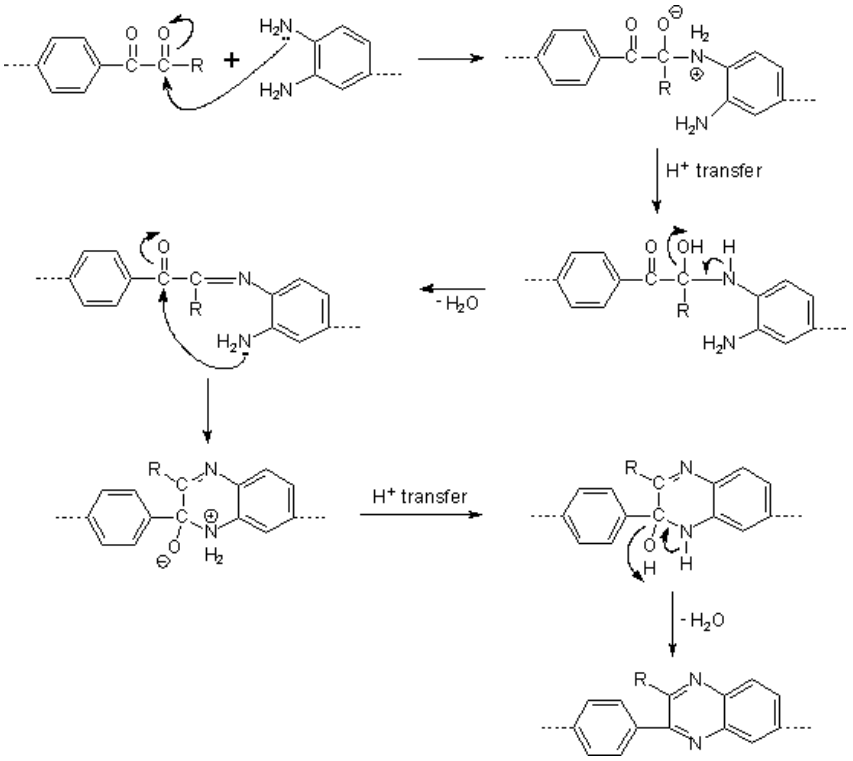

Scheme 2.9: Reaction mechanism for the synthesis of polyquinoxaline via Friedlander Reaction.

In 1989, Harris and Korleski were the first ones that synthesised the self-polymerisable monomer mixture of 2-(4-hydroxyphenyl)-3-phenyl-6-

fluoroquinoxaline and 3-(4-hydroxyphenyl)-2-phenyl-6-fluoroquinoxaline in an overall yield of 11% using a four-step synthetic route[11]. They started with a mixed benzoin condensation of benzaldehyde and anisaldehyde to afford 4-methoxybenzoin, which was oxidised to 4-methoxybenzil. This intermediate was demethylated with hydrogen bromide to 4-hydroxybenzil, which was condensed with 1,2-diamino-4-fluorobenzene leading to the monomer mixture. Later, in order to improve the overal yield in the Korleski route, 4-hydroxybenzil was synthesised using the Friedel-Crafts acylation. Thus, 4-(phenylacetyl)anisole was obtained in greater than 60% yield from the reaction of phenylacetyl chloride and anisole in carbon disulfide in the presence of aluminium chloride. 4-(Phenylacetyl)anisole was oxidised to 4-methoxybenzil with copper(II)bromide in dimethylsulfoxide and ethyl acetate. The remainder of the reaction sequence was the same as mentioned in Scheme 2.10.

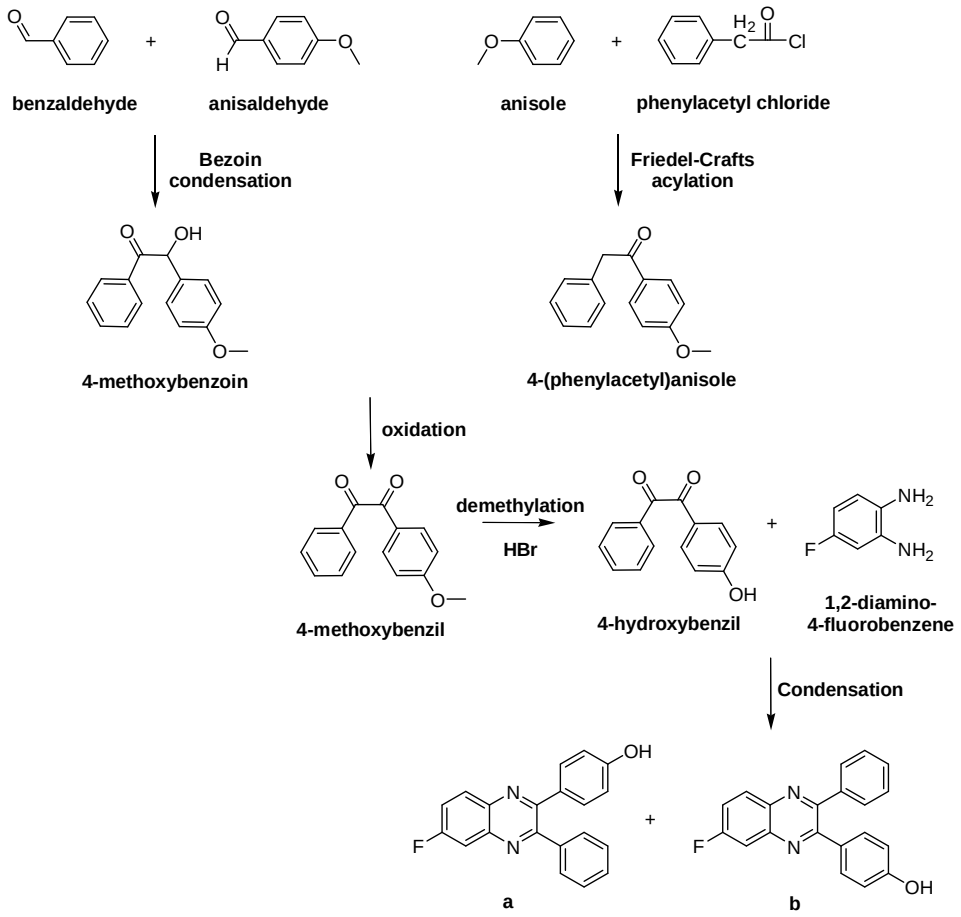

Scheme 2.10: Phenylquinoxaline synthesis by Benzoin condensation and Friedel-Crafts acylation; (**a**) 2-(4-hydroxyphenyl)-3-phenyl-6-fluoroquinoxaline and (**b**) 3-(4-hydroxyphenyl)-2-phenyl-6-fluoroquinoxaline.

The overall yield of this route was three times that of the previous route[12]. It was found out that when 1,2-diamino-4-fluorobenzene is sublimed under reduced pressure immediately prior to use, 91% yield of monomer mixture of 2-(4-hydroxyphenyl)-3-phenyl-6-fluoroquinoxaline (**a**) and 3-(4-hydroxyphenyl)-2-phenyl-6-fluoroquinoxaline (**b**) can be obtained.

Robinson and Taylor demonstrated the conversion of various α-hydroxyketones to quinoxalines via palladium-catalysed aerobic oxidation followed by *in situ* trapping

with phenylenediamines, Scheme 2.11. The isolated yields of this series of quinoxalines were in the range of 66 - 91%[13].

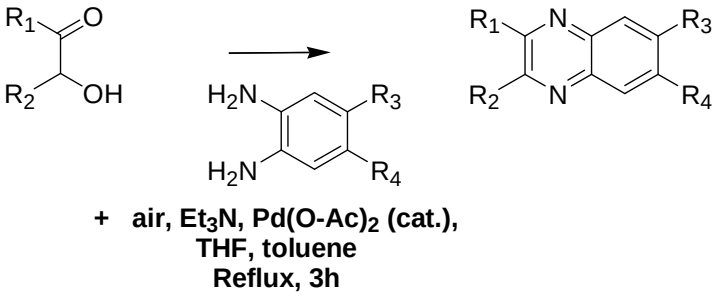

Scheme 2.11: Quinoxaline synthesis by Aerobic Oxidation

In 2004, Lisheng Mao and co-workers published the synthesis and electrochemical properties of the symmetrical and unsymmetrical 2,3-disubstituted Quinoxalines by palladium catalysed Suzuki-Miyaura coupling reactions - 2,3-dichloroquinoxaline - in the presence of various boronic acids (Scheme 2.12)[14]. Hereby quinoxaline yields in the range of 65 to 96% were obtained.

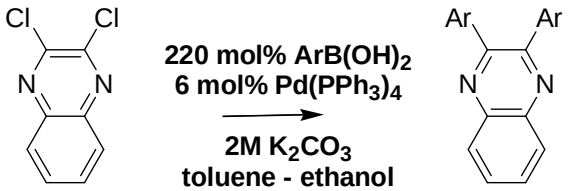

Scheme 2.12: Synthesis of symmetrical 2,3-disubstituted quinoxalines by $Ph(PPh_3)_4$-catalysed coupling of 2,3-dichloroquinoxaline with Boronic acids.

An interesting entry from oxalyl chloride to quinoxalines was made by Ji and Lee which they published in 2005, Scheme 2.13. Hereby, they demonstrated the synthesis of quinoxalines by the condensation between 1,2-phenylenediamines and 1,2-diketo compounds, which are available by the cross-coupling reactions of oxalyl chloride with mixed copper-magnesium reagents or by the direct acylation of pyrrole with oxalyl chloride with yields as high as 96%[15].

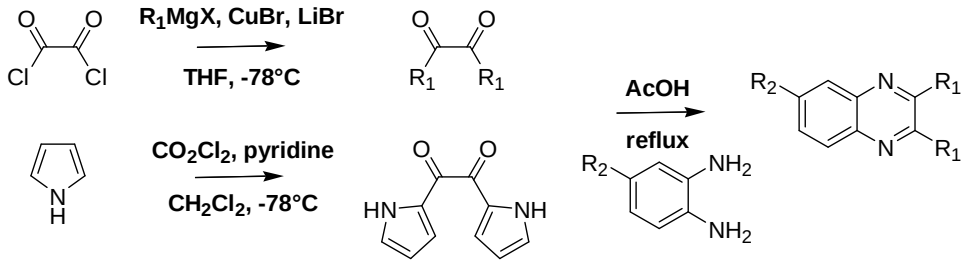

Scheme 2.13: Quinoxaline synthesis; a facile entry from Oxalyl Chloride

Further, quinoxaline derivatives can also be obtained by bismuth-catalysed oxidative coupling of epoxides and ene-1,2-diamines with yields in the range of 53 to 71%[16].

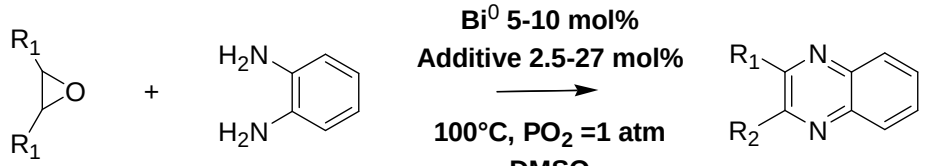

Additive = $Cu(OTf)_2$, TfOH

Scheme 2.14: Synthesis of 2,3-disubstituted Quinoxaline derivatives from epoxides and phenylene diamine.

Since many of these reactions leads to the formation of undesired side products, lack of regioselectivity and hard purification, two improved synthetic routes are presented in this chapter that can be suitable candidates for the synthesis of Quinoxaline derivatives.

In this chapter, the synthesis of the diphenyl quinoxaline monomer will be discussed which after polymerisation (chapter three) can be used as an interesting candidate for photovoltaic application. An effort was made to synthesise Quinoxaline monomer via the Immino-oxime cyclisation route and the Benzothiadiazole route. Also some modification of the mentioned routes will be discussed. All the synthesised intermediary and final compounds were analysed by ^{1}H-NMR, ^{13}C-NMR, GC-MS and IR.

2.2 The Immino-oxime monomer synthesis toward the dithiocarbamate quinoxaline monomer 6

In order to avoid the problems mentioned above (e.g. lack of regioselectivity and hard purification) the cyclisation of functionalised 1-N-4-aryl-1,4-diaza-1,3-dienes is one of the most promising in therms of regiochemistry and generality. The first work on cyclisation of these materials was done by Hamish McNab and co-workers in 1982. It involved radical cyclisation of α-arylimino phenylhydrazones of α-dicarbonyl compounds to quinoxalines, which employed vigorous conditions (gas-phase thermolysis) and was plagued by low yields and other practical disadvantages[17]. Another early example is the photocyclisation of acetate and benzoate esters of the α-phenylimino oxime of benzyl, which was rather limited in scope and suffered from low yields[18]. The cyclisation route involved in this chapter is the oxidative cyclisation of benzyl α-arylimino oxime to diphenyl Quinoxaline with their promising regioselectivity and good yields[19, 20].

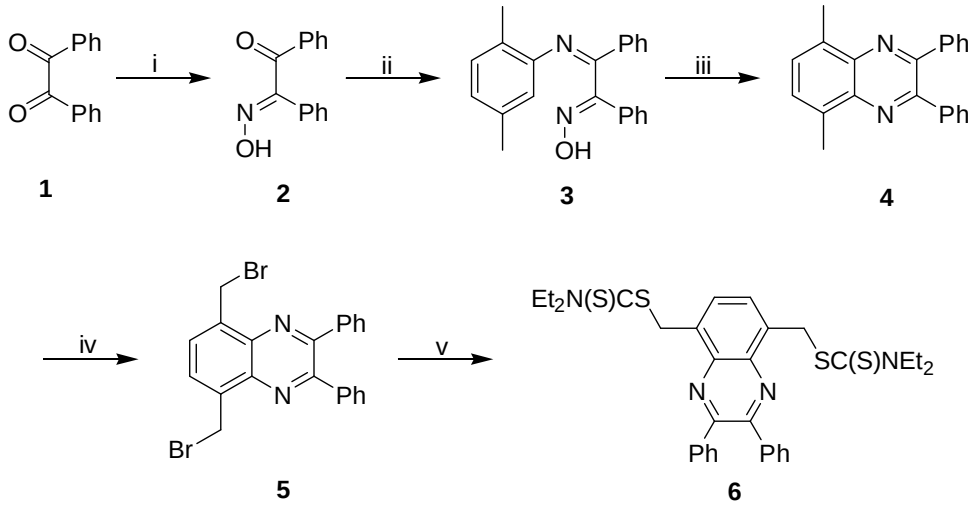

Scheme 2.15: The dithiocarbamate monomer **6** synthesis via the immino-oxime cyclisation route: i) H_2N-OH.HCl, NaOH, 0°C, EtOH/ H_2O, RT, 2h; ii) aniline, *p*-TsOH, inert atmosphere, 140°C, 72h; iii) Ac_2O, 140°C, 6h, H_2O, 0°C, 2h; iv) NBS, BPO, CCl_4, inert atmosphere, illumination, 93°C, 24h; v) $NaSC(S)NEt_2.3H_2O$, ether or ethanol, RT, 2h.

The commercially available benzil **1** was dissolved in ethanol and a concentrated solution of hydroxylamine hydrochloride in water was added. To the reaction mixture was added drop-wise a cold solution of sodium hydroxide in water for 15 min. The reaction mixture was stirred for 2 hours at room temperature. Then, the mixture was diluted with water and filtered off. The solid (unreacted substrate) was recovered and washed with a little water. The filtrate was acidified with glacial acetic acid and stirred for 0.5 hour. The formed solid was filtered off, dried to dryness and crystallised from ethanol, then by toluene to afford **2** as yellowish crystals.

The mechanism involved for the synthesis of **2** is the condensation of **1** with hydroxylamine hydrochloride[21]. First the hydroxylamine adds to the diketone to form an unstable intermediate similar to a hemiacetal, Scheme 2.16. Notice that it is the more nucleophilic nitrogen atom, and not the oxygen atom, of the hydroxylamine that adds to the carbonyl group. Like hemiacetals, the intermediate is unstable and can decompose by loss of water leading to the oxime product 2 in 72% yield.

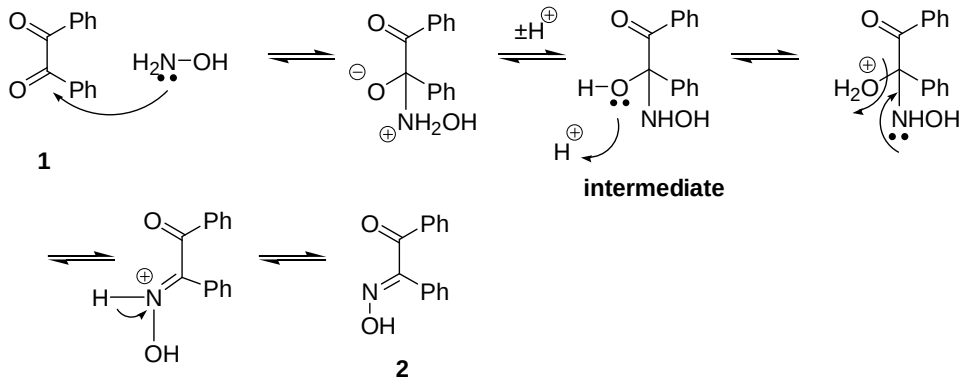

Scheme 2.16: Mechanism for the preparation of α-benzil monooxime **2**

For the synthesis of 2-[(2,5-dimethylphenyl)imino]-1,2-diphenyl-etanone oxime **3** (i.e. an imine), the mechanism involved is the condensation of **2** with dimethylaniline (**amine**) which is similar to the one for oxime formation, scheme 2.3. It is known that imines are the nitrogen analogues of carbonyl compounds and

the formation of imines require acid catalysis[21]. Without the acid catalysis (in this case, the *p*-toluenesulphonic acid), the reaction is very slow, though in some cases it may still take place (for example oximes, **2**) but it will form much faster with it. It is important to note that acid is not needed for the addition step in the mechanism (the rate-determing-step **RDS**), but it is needed for the elimination of water later on in the reaction. Imine formation is the fastest at about pH 4-6. At lower pH, too much amine will be protonated and the rate of the first step will be slow. At higher pH the proton concentration is too low to allow protonation of the OH leaving group in the dehydration step.

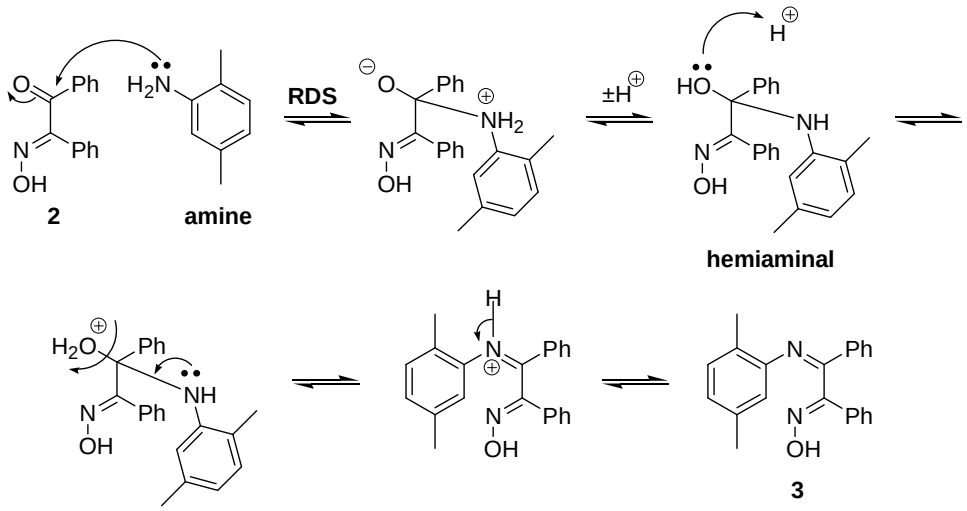

Scheme 2.17: Mechanism for the preparation of 2-[(2,5-dimethylphenyl)imino]-1,2-diphenyl-ethanone oxime **3**

Concerning the apparatus used for the synthesis of **3**, a modification needs to be made. When the reaction is carried out in a regular reaction flask, the equilibrium can not be stimulated towards the required product. In order to remove the water formed during the reaction and in this way to stimulate the equilibrium towards the required product. The flask used for the reaction mixture was equipped with an additional attachment, i.e. a Dean-Stark attachment (Figure 2.21, right). Unfortunately also this apparatus was not helpful to produce the required product.

Another option was the use of a Soxhlet filled with a drying agent (e.g. calcium chloride), (Figure 2.21, left).

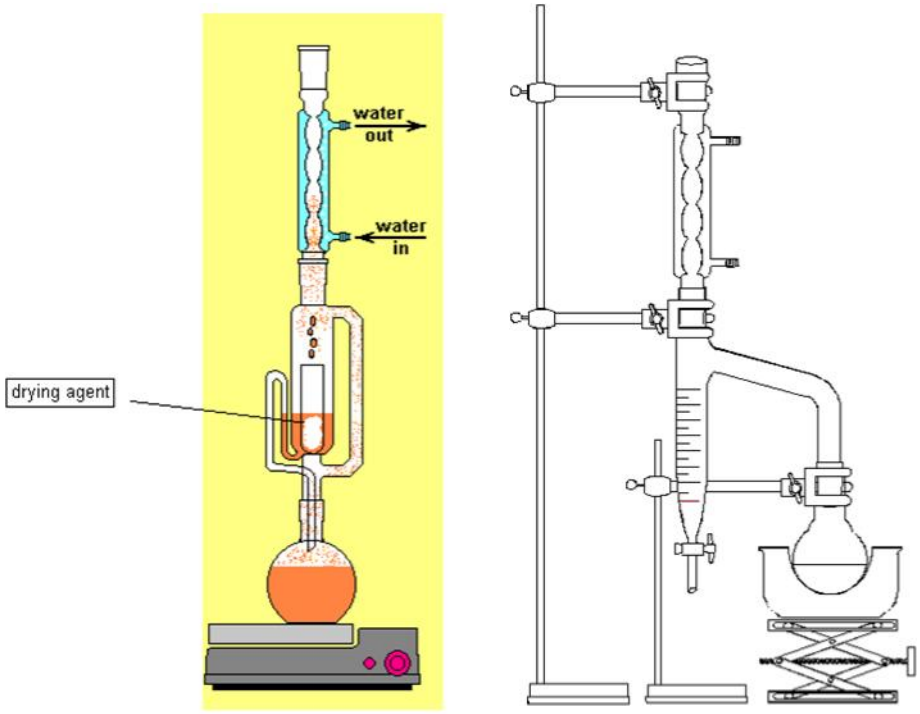

Figure 2.21: Soxhlet filled with drying agent (left) and Dean-Stark attachment (right)

Taking use of the above mentioned Soxhlet filled with calcium chloride attached to the reaction flask, the commercially available dimethylaniline, *p*-toluenesulphonic acid and **2** were dissolved in toluene. The reaction mixture was stirred and refluxed for 72 hours under an inert atmosphere. The solvent was removed under reduced pressure. The oil was purified by column chromatography then the fractions were dissolved in CH_2Cl_2 and extracted with diluted hydrochloric acid. After filtration and evaporation to dryness **3** was obtained in good yield (86%).

To a round-bottomed flask equipped with a reflux condenser, a magnetic stirring bar and a heating mantel was added **3** dissolved in acetic anhydride. The reaction mixture was stirred and refluxed for 6 hours. The cool mixture was poured to cold

water and stirred for two hours. The formed sticky crude product was filtered off, washed with water and dried under vacuum overnight to afford **4** in 92% yield.

The product in this step can be obtained by oxidative cyclisation of benzil α-arylimino oxime **3** to 2,3-diphenyl-quinoxaline **4** as it can be depicted in Scheme 2.18.

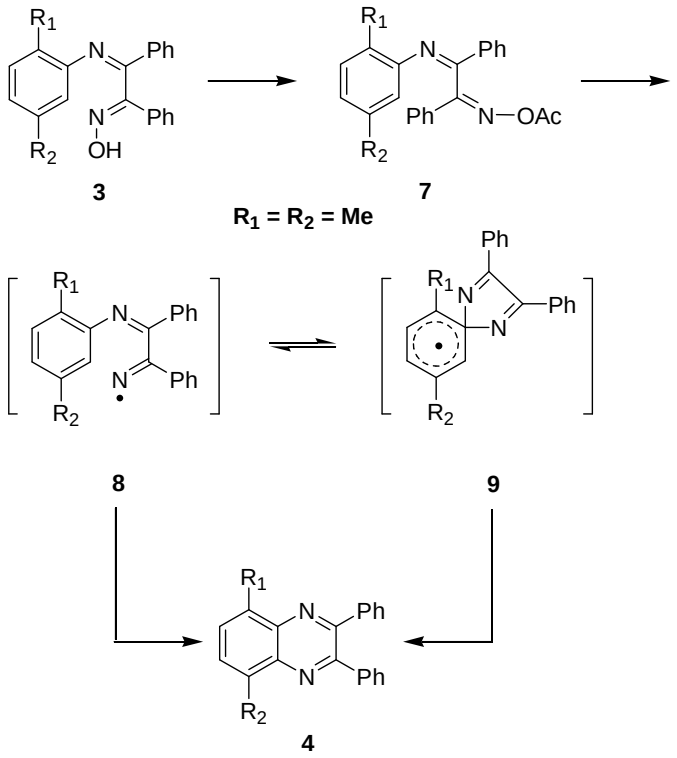

Scheme 2.18: Mechanism for the preparation of 5,8-dimethyl-2,3-diphenylquinoxaline **4** by homolytic aromatic substitution

According to the results obtained for other analogues of quinoxalines by Xekoukoulotakis and co-workers, the cyclisation of the α-arylimino oxime **3** to 2,3-diphenyl-quinoxaline **4** in acetic anhydride, is in accordance with a homolytic aromatic substitution by a iminyl radical **8**. It proceeds after an initial acetylation step via the iminyl radical **8** and the spirodienyl radical **9**.[20] An alternative

mechanism that could be proposed is a classical non-radical route – electrophylic aromatic substitution, Scheme 2.19.

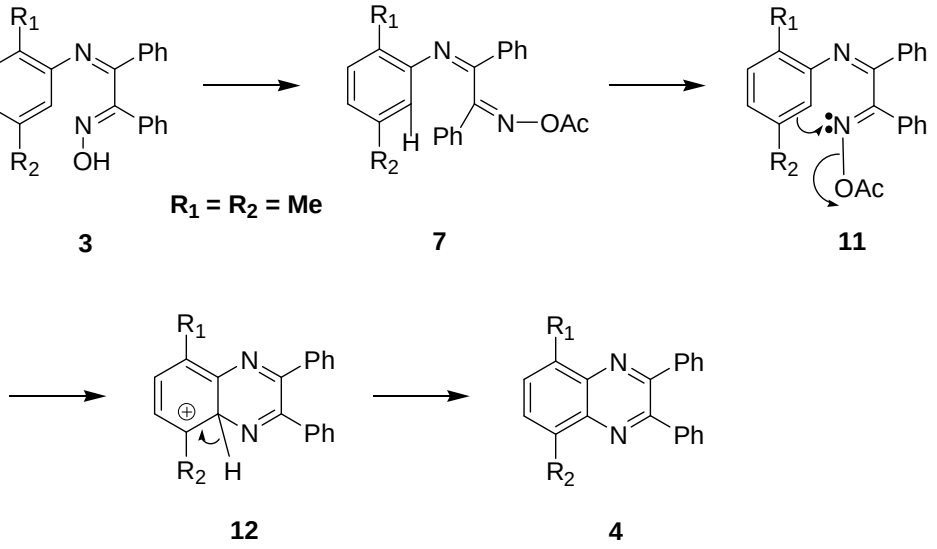

Scheme 2.19: Mechanism for the preparation of 5,8-dimethyl-2,3-diphenylquinoxaline **4** by electrophylic aromatic substitution

However, it should be mentioned that from the experiments in our hand no arguments were found for either of the mechanisms.

Indeed according to literature, when symmetrical α-arylimino oximes are used (R_1 = R_2), the *ortho* substituted product is often dominant and the mechanism is in accordance with intermolecular homolytic aromatic substitution by iminyl radicals[22]. Moreover, when the substituents are attached at $\mathbf{C_3}$ and $\mathbf{C_4}$, two different products(**A** and **B**) can be obtained with **A** as the predominant product, Scheme 2.20 [17, 20]. However, in our case, the α-arylimino oxime **3** is symmetric (R_1 = R_2) and they are positioned at $\mathbf{C_3}$ and $\mathbf{C_6}$, therefore the only available position for the reaction to take place is the *ortho* position ($\mathbf{C_2}$) and the only possible product is the diphenyl Quinoxaline **4**, Scheme 2.18.

Unfortunately the reaction turned out to be irreproducible. Instead of the diphenyl Quinoxaline product **4**, the stable ester intermediate **7** can be formed and not

converted to the final product. The presence of the intermediate **7** was confirmed by the ^{1}H-NMR analysis. As comparison the ^{1}H-NMR spectra of **4** and **7** are subsequently depicted in Figure 2.22 and Figure 2.23.

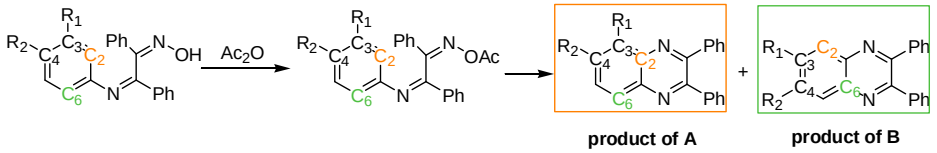

Scheme 2.20: Mechanistic explanation for the *ortho* substituted cyclisation product

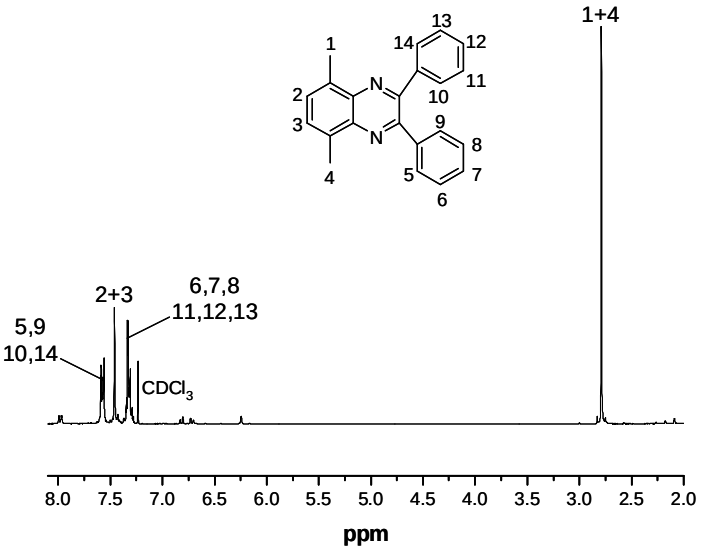

Figure 2.22: ^{1}H-NMR spectrum of 4 in $CDCl_3$

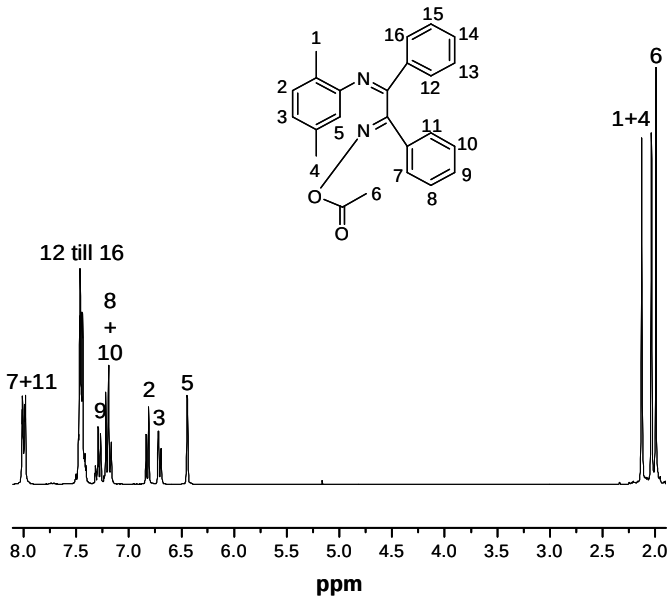

Figure 2.23: ^{1}H-NMR spectrum of 7 in $CDCl_3$

In order to avoid this problem, different solvents (acetic anhydride, chlorobezene, toluene) and/ or different additional solvents (HCl, conc. or acetic acid) were used. In some of the experiments there was also a catalyst (*p*-toluenesulphonic acid or zinc chloride) used. In case the reaction works and the crude compound is purified, quite high yields in good purity can be obtained. The reaction can be completed by monitoring it by TLC. All the experiments were performed using different reaction times and different temperatures. Also some experiments were done with these intermediates to succeed in converting them to the final product **4**. Although many steps were undertaken, we could not resolve the problems concerning the irreproducibility.

To a round-bottomed flask equipped with a magnetic stirring bar and a heating mantel was added **4** and N-bromosuccinimide (**NBS**) dissolved in CCl_4. A small amount of benzoylperoxide (**BPO**) was added as the initiator. The reaction mixture was stirred and refluxed at 93°C under an inert atmosphere and illuminated by a lamp of 200 Watt overnight. After almost 24h the reaction was stopped, the

succinimide filtered off and washed with $CHCl_3$. The filtrate was left in the fridge overnight. The solid part was filtered off and both (solid and liquid) parts were analysed by TLC. The solvent of the liquid part was distilled under reduced pressure and the residue was purified by column chromatography. After crystallisation and drying under vacuum the pure product **5** was obtained in rather low yield (20%).

The mechanism involved is the selective radical bromination – benzylic substitution of H by Br. There are relatively few ways of functionalising an unfunctionalised centre, but radical benzylic bromination is one of these. Just as tertiary radicals are more stable than primary ones, so benzylic radicals are even more stable than tertiary ones. In case bromine is used as the reagent, the disadvantage is the competing side reaction where dibromination or tribromination can take place. In order to avoid this side reaction, it is better not to use bromine but a compound that releases molecular bromine slowly during the reaction - NBS. The starting material **4** undergoes benzylic bromination when it is treated with NBS in CCl_4 in the presence of peroxides (BPO) or light, Scheme 2.21. The reaction is *initiated* by the formation of a small amount of Br· (possibly by dissociation of the N-Br bond of the NBS). In the *first chain-propagating* step, the bromine atom abstracts one of the benzylic hydrogen atoms forming a benzyl radical **13**. In the *second chain-propagating* step the benzyl radical **13** reacts with a molecule of bromine. This step results in the formation of a molecule of benzyl bromide and a bromine atom. The bromine atom then brings about a repetition of the first chain-propagating step yielding product **5**.

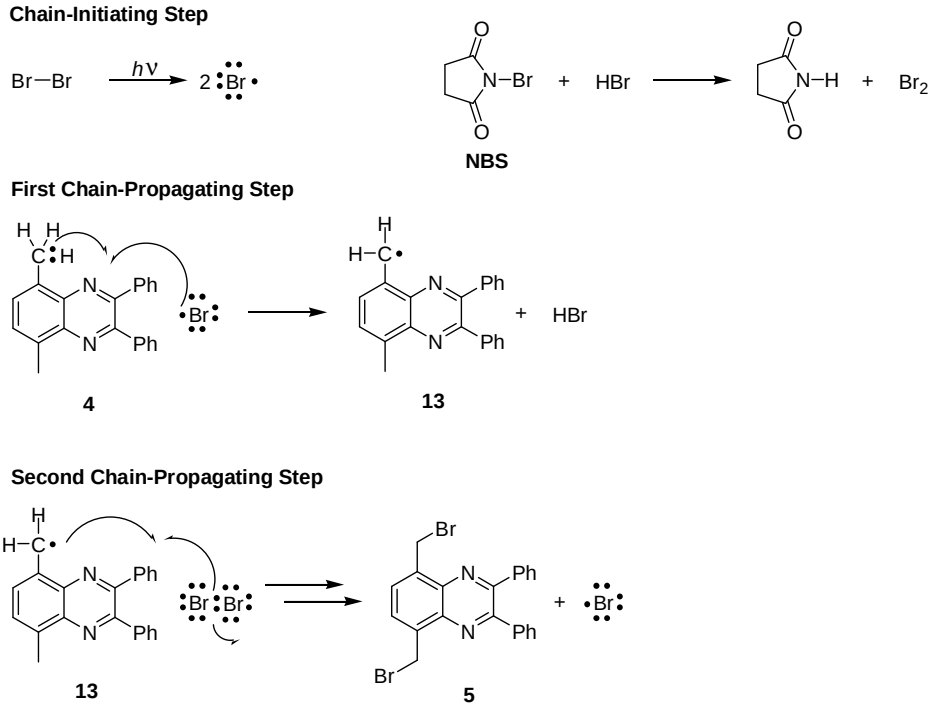

Scheme 2.21: Mechanism for the preparation of 1,4-bis(bromomethyl)-2,3-diphenylquinoxaline

To a round bottomed flask equipped with a magnetic stirring bar was added **5** and sodium-diethyldithiocarbamate-trihydrate dissolved in diethyl ether. The reaction mixture was stirred at room temperature and monitored by TLC. The reaction was stopped by the addition of water and extracted with diethyl ether then dried over $MgSO_4$. After filtration and evaporation an effort was made to recrystallise the crude product, which failed.

In case the reaction works, this reaction involves nucleophilic substitution of **5** with sodium-diethyldithiocarbamate-trihydrate, Scheme 2.22. Hereby, the negatively charged sulphur attacks the CH_2 group leading to the replacement of the bromine ion and the formation of the desired the dithiocarbamate quinoxaline monomer **6**.

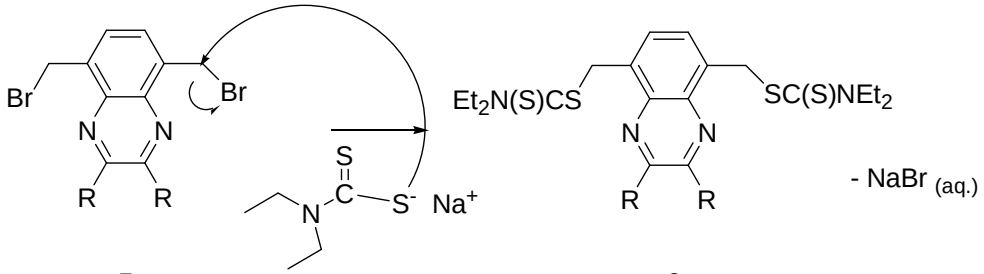

5 **6**

Scheme 2.22: Mechanism for the preparation of the dithiocarbamate Quinoxaline monomer **6**

Although the dithiocarbamate quinoxaline monomer **6** can be obtained via said reaction sequence, we decided to abandon this approach for two reasons:

- The lack of reproducibility of the cyclisation to product **4**.
- Low yield of the brominated product **5**.

2.3 The Benzothiadiazole monomer synthesis toward the dithiocarbamate quinoxaline monomer 6

In order to avoid the problems concerning the cyclisation of α-arylimino oxime (hard purification, low yields and irreproducibility) another route was needed to prepare the dithiocarbamate quinoxaline monomer **6**. A route which is easy to carry out and which leads to high yields with good purity of the intermediary products is the Benzothiadiazole route[23, 24].

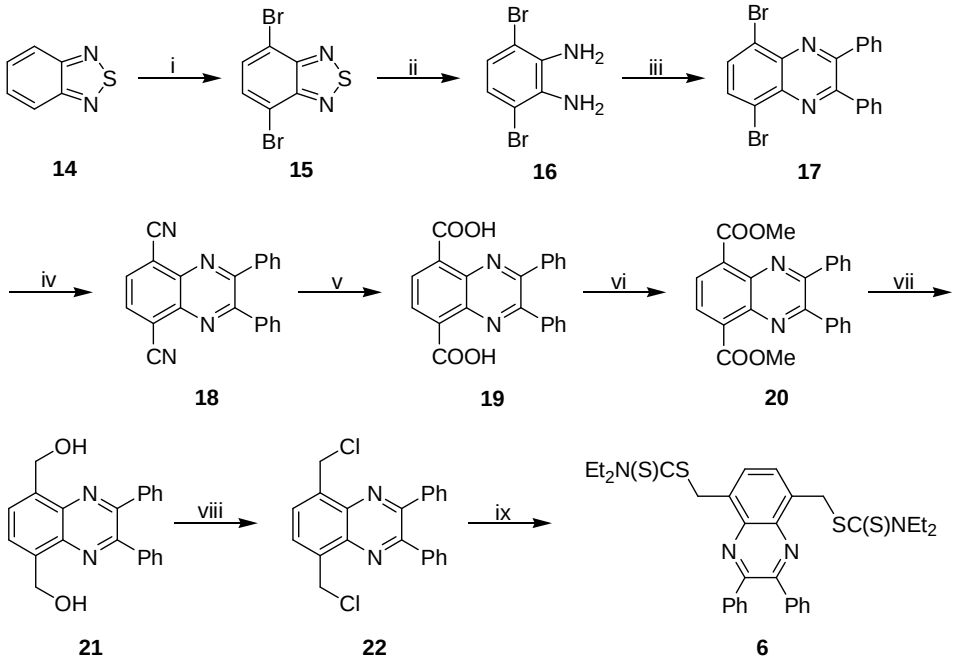

Scheme 2.23: The dithiocarbamate quinoxaline monomer **6** synthesis via the Benzothiadiazole route: i) Br_2, HBr, 130°C, 5h, RT, 20h; ii) $NaBH_4$, EtOH, 5h, 0°C, RT, 20h, inert atmosphere; iii) Benzil, EtOH, ΔT, 27h; iv) CuCN, DMF, 164°C, 4h, $FeCl_3$, HCl, H_2O, 65°C, 0.5h; v) NaOH (10%), H_2O, EtOH, 110°C, 24h, HCl; vi) MeOH, H_2SO_4 (1%), inert atmosphere, 80°C, 20h; vii) $NaBH_4$, EtOH, inert atmosphere, refluxed, 5h, NH_4Cl, RT, 24h; viii) $SOCl_2$, RT, 24h; ix) $NaSC(S)NEt_2$, diethyl ether, 72h.

The dibrominated product **15** was prepared by bromination of commercially available 2,1,3-benzothiadiazole **14**. To the commercially available **14** was added HBr (48%) and the reaction mixture was stirred and refluxed at 130°C. To the refluxing mixture was added drop wise the elemental bromine in excess during 5 hours. After subsequently 2.5 hours, 4 hours, 4.5 hours was an additionally amount of HBr added to facilitate the stirring. After cooling overnight and carefully filtration the product was washed with a large amount of water and dried under vacuum to obtain **15** as brown crystals in 100% yield[24, 25].

It is expected that the reaction follows the mechanism of electrophilic aromatic substitution. In such case the observed regioselectivity is surprising. Due to the electron withdrawing character of the two nitrogen atoms, the electrons from the benzene ring are moving towards the nitrogen atoms. On the other hand the sulphur atom acts as an electron donor. This causes the four carbon atoms of the benzene ring to become negatively charged, Scheme 2.24. However, the two carbon atoms attached to the thiadiazole ring (**C1** and **C4**) are more negatively charged than the carbon atoms (**C2** and **C3**). Therefore, the electrophilic aromatic substitution with the partially positive charged Br (δ^+) may preferentially take place at the position one and four (**C1** and **C4**). The electrophilic aromatic substitution starts with an attack of the positive bromine ion Br (δ^+) on benzene to form an *arenium ion* **23**. Since aromatisation is in favour, the areium ion transfers a proton to the negatively charged bromine ion Br^- and after a second electrophilic substitution the desired product **15** is obtained.

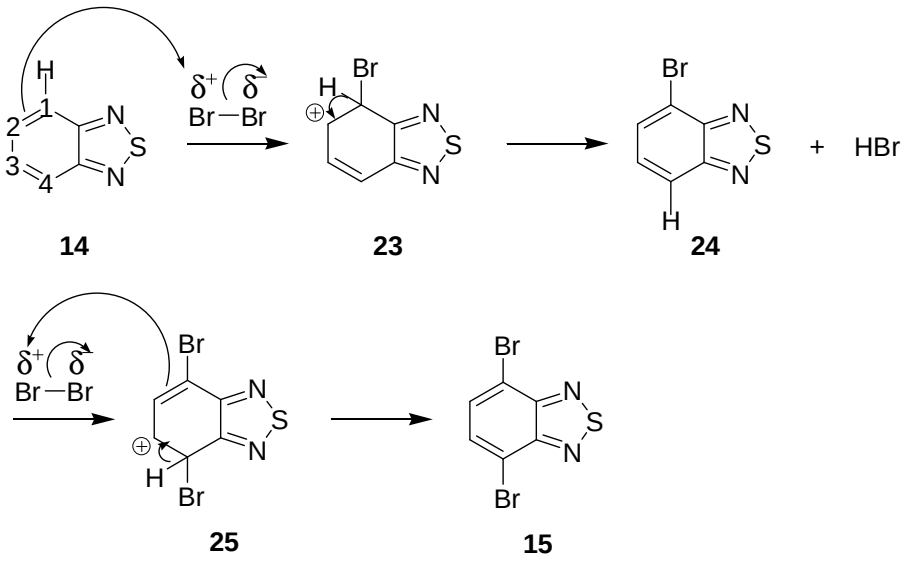

Scheme 2.24: Mechanism for the synthesis of 4,7-dibromo-benzo[1,2,5]thiadiazole **15**.

To **15** suspended in absolute ethanol and cooled to 0°C $NaBH_4$ was added in small portions during 5 hours. The reaction mixture was continued stirring at room

temperature for 20 hours. The solvent was evaporated and the reaction mixture was dissolved in an amount of water. After extraction with diethyl ether, the combined organic layers were dried over Na_2SO_4. Filtration and evaporation of the solvent gave **16** as pale brown product in good yield (93%)[24, 26].

The reduction of **15** to **16** takes place with the reducing agent $NaBH_4$. The hydride ion attacks the nitrogen from the ring, Scheme 2.25. Since the benzene structure is easy to regenerate the breaking of the π-system costs less energy and it is easy to carry out. In this process the second nitrogen atom is protonated by the solvent. Then, as sulphur is not part of the aromatic system anymore, a reduction takes place on sulphur causing the breaking of the N-S bond. These steps are repeated until all hydrogen atoms attached to boron have been transformed leading to the evolution of H_2S and the formation of the desired product **16**.

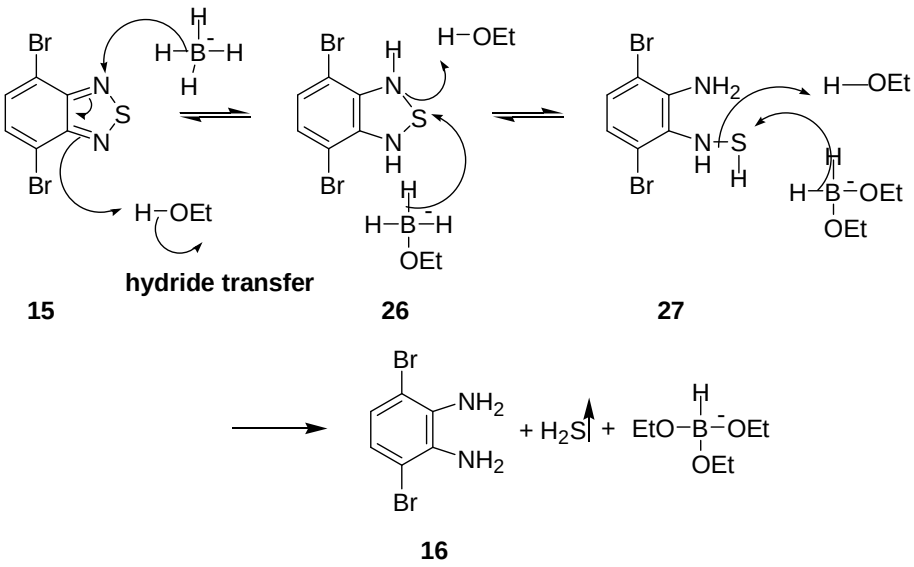

Scheme 2.25: Mechanism for the synthesis of 3,6-dibromo-benzene-1,2-diamine **16**.

16 and **1** were dissolved in absolute ethanol and the reaction mixture was stirred at reflux temperature for 48 hours. After completion of the reaction, the reaction mixture was cooled to ambient temperature overnight. Then, the precipitate was

filtered off, washed with cold ethanol and air-dried to afford **17** as pure milk-coffee coloured product in 79% yield[24, 26, 27].

Product **17** was obtained by condensation of 1,2-diamine **16** with 1,2-dicarbonyl **1**. The partially negative charged nitrogen atom attacks on the carbonyl group leading to the breaking of the double bond between the carbon and oxygen atoms, Scheme 2.26. Then, a proton is shifted from the nitrogen atom to the oxygen due to an internal acid-base reaction. This reaction is repeated until no proton is left on the nitrogen atoms. Finally, the electron pair from the nitrogen forms a double bond between the nitrogen atom and carbon leading to the formation of water and the desired product **17**.

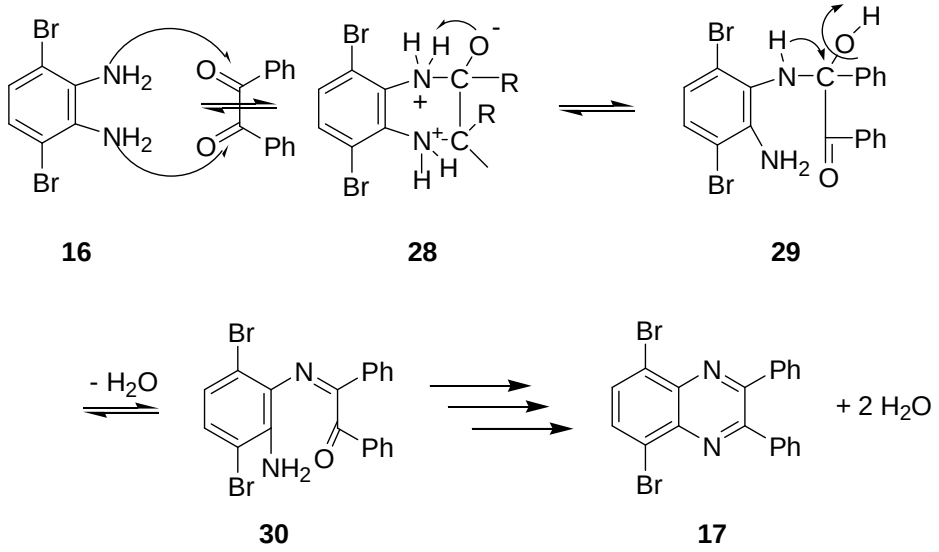

Scheme 2.26: Mechanism for the synthesis of 5,8-dibromo-2,3-diphenyl-quinoxaline **17**.

Since chemical reactions are very time and reagent consuming one is trying to find a way in using cheap reagents, shortening the reaction time and improving productivity. Therefore, a modification of the procedure was carried out for the synthesis of diphenyl quinoxaline product **17** from 1,2-diamine **16** and 1,2-dicarbonyl **1**. Instead of carrying out the condensation at reflux temperature for 48

hours, the reaction was carried in the presence of a small amount of iodine. The method of iodine catalysed synthesis of diphenyl Quinoxaline is very simple, efficient, clean and without any other side products[28, 29]. In the absence of iodine, the reaction takes more than 24 hours to complete. In the optimised reaction condition, 1,2-diamine **16** and 1,2-dicarbonyl **1** in ethanol were mixed with iodine (10 mol %) and stirred at room temperature for 15 minutes. After completion of the reaction, a simple work up affords the product in excellent yield. The role of iodine is not clearly known, but it can act as a mild Lewis acid. Possibly iodine plays a complex role in accelerating the dehydrative steps and thus promotes the formation of products[28, 29].

In the next step, in a flask **17** and CuCN were dissolved in DMF. The reaction mixture was stirred and refluxed under an inert atmosphere at 164°C for 4 hours. After the reaction mixture was cooled down, it was poured into a solution of $FeCl_3$, concentrated HCl and water and stirred at 65°C for 30 minutes. The aqueous solution was extracted with $CHCl_3$ and the organic layer washed with HCl (1:1) and 15% NaOH (aq.). To neutralise the combined organic layers they were washed twice with H_2O. They were also washed with NaCl (sat.) and finally dried over $MgSO_4$. After filtration and evaporation the yellow coloured product **18** was obtained in 91% yield[24, 30, 31].

Product **18** was obtained by nucleophilic substitution with a cyanide ion. First of all, an intermediary complex is formed between cyanide, cupper bromide and the starting material (in Scheme 2.27 bromobenzene is taken as an example). An important step is the disintegration of the complex, which is carried out with an aqueous solution of iron (III) chloride and hydrochloric acid.

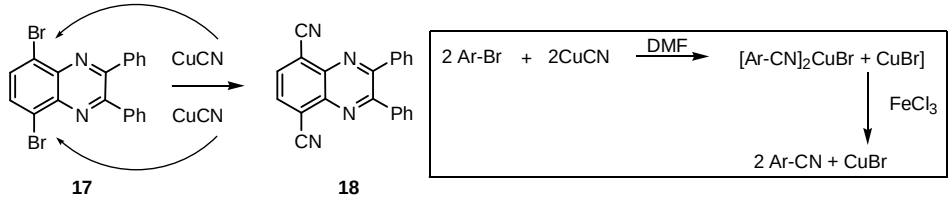

17 **18**

Scheme 2.27: Mechanism for the synthesis of 2,3-diphenyl-quinoxaline-5,8-dicarbonitrile **18**.

To **18** suspended in NaOH (10%) was added absolute ethanol and the mixture was heated overnight (100°C). After completion of the reaction the condenser was detached and the solution was refluxed for a few minutes in the open flask to remove dissolved ammonia and some of the ethanol. The suspension was cooled and filtered. To the filtrate hydrochloric acid (conc.) was added until the precipitation of the product was complete. The crude yellow coloured product was filtered off and it was dried. Finally, crystallisation from hot toluene resulted in the formation of pale brown crystals **19** in 95% yield[24, 26, 31].

This reaction is carried out by the base-promoted hydrolysis of **18**. An acid-catalysed hydrolysis is excluded due to a possible protonation of the nitrogen atoms in the aromatic ring. The hydroxide ion attacks the nitrile carbon atom leading to the breaking of the triple bond, Scheme 2.28. The negatively charged nitrogen accepts a proton from water followed by *tautomerisation*. Then, the hydroxide ion attacks the acyl carbon of the amide, which involves a nucleophilic substitution leading to the formation of the dianion **33**. Finally, by displacement of the amide ion and proton transfer leading to ammonia the desired product **19** is formed.

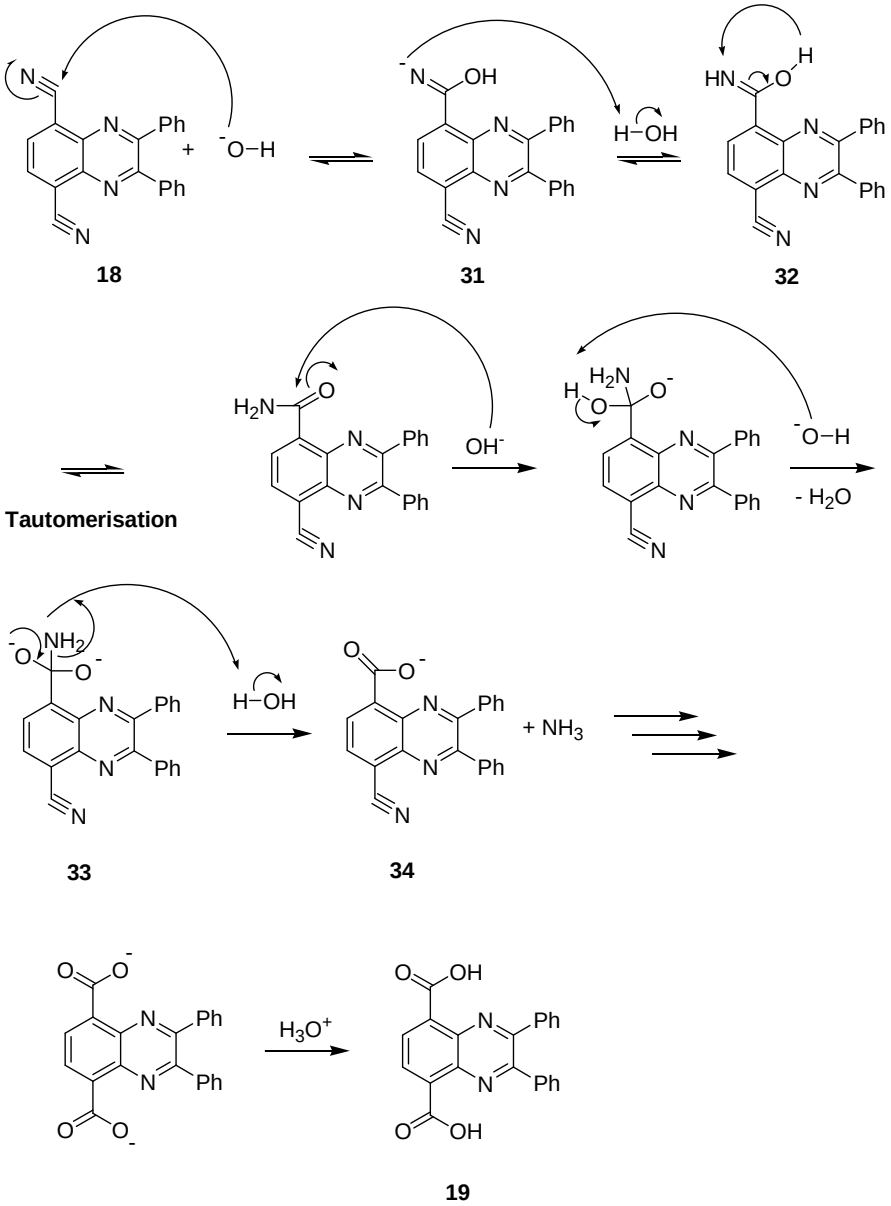

Scheme 2.28: Mechanism for the synthesis of 2,3-diphenyl-quinoxaline-5,8-dicarboxylic acid **19**.

The starting material **19** was added to a mixture of MeOH and H_2SO_4 (70%) and refluxed at 80°C under inert conditions overnight. After completion of the reaction, the condenser was detached and the reaction mixture was cooled. The reaction

mixture was extracted with CH_2Cl_2 and the combined organic layers were washed with water and dried over $MgSO_4$. After filtration and evaporation **20** was obtained as yellow oil (81%)[24, 32].

The mechanism involved is acid-catalysed esterification of **19**. They proceed very slowly in the absence of strong acids, but they reach equilibrium within a matter of a few hours when an acid and an alcohol are refluxed with a small amount of concentrated sulphuric acid or hydrogen chloride. In this case the carboxylic acid **19** is used with methanol and sulphuric acid, Scheme 2.29. First of all, the carboxylic acid accepts a proton from the strong acid catalyst. Then, the alcohol attacks the protonated carbonyl group to give a tetrahedral intermediate. Further, a proton is lost at one oxygen atom and gained at another. Loss of a molecule of water gives a protonated ester. Finally, transfer of a proton to a base is leading to the desired ester **20**.

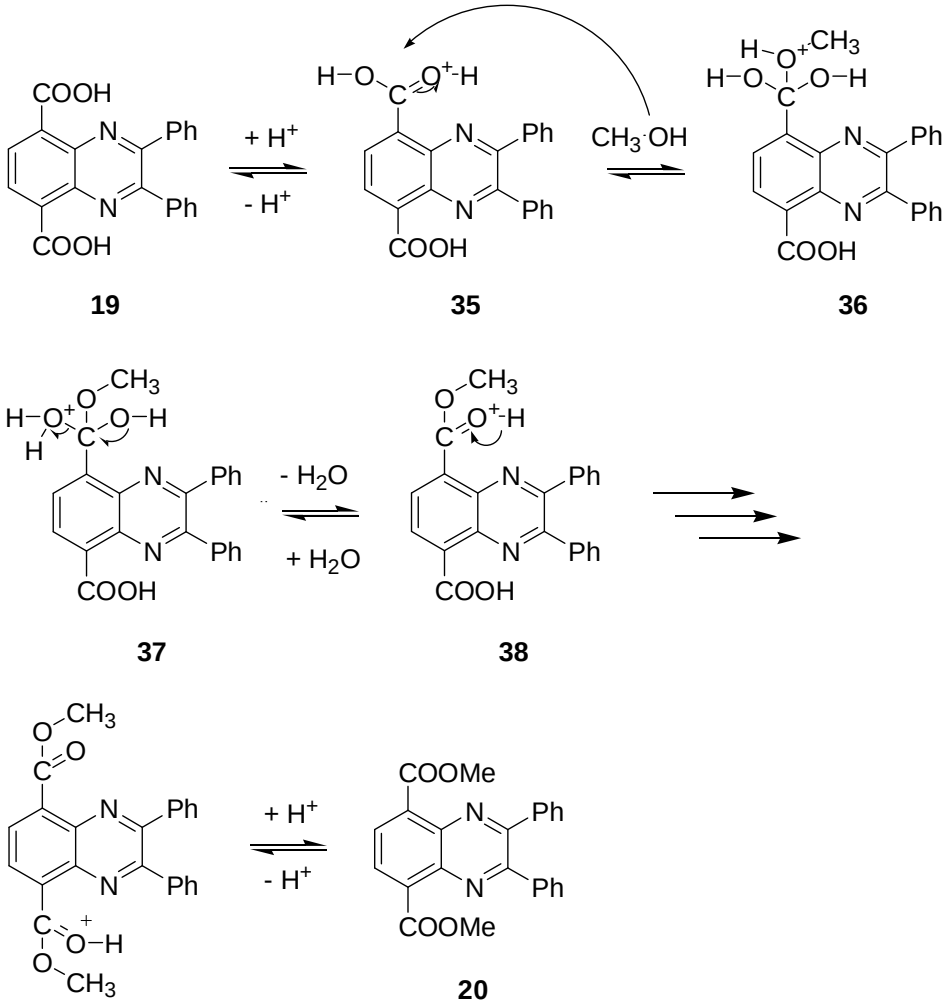

Scheme 2.29: Mechanism for the synthesis of 2,3-diphenyl-quinoxaline-5,8-dicarboxylic acid dimethyl ester **20**.

To the diester **20** suspended in absolute ethanol was added $NaBH_4$ in one portion. The reaction mixture was refluxed under inert atmosphere for 5 hours. After cooling down a saturated NH_4Cl solution was added and the solution was stirred overnight. The solvent was evaporated and the precipitated solids were dissolved by addition of the necessary minimum amount of water. The resulting solution was extracted with ethyl acetate and the combined organic layers were dried over $MgSO_4$. After filtration and evaporation the crude brown foam **21** that was obtained was used in the next step without further purification[24, 33, 34].

The diester **20** is reduced by the less powerful reducing agent sodium borohydride $NaBH_4$. The key step in the reduction of a carbonyl compound is the transfer of a *hydride ion* from boron to the carbonyl carbon leading to the alkoxide ion **39**. In this transfer the hydride acts as a *nucleophile*. The mechanism for the reduction of **20** by sodium borohydride is illustrated in Scheme 2.30. The steps are repeated until all hydrogen atoms attached to boron have been transferred and the desired product **21** is formed.

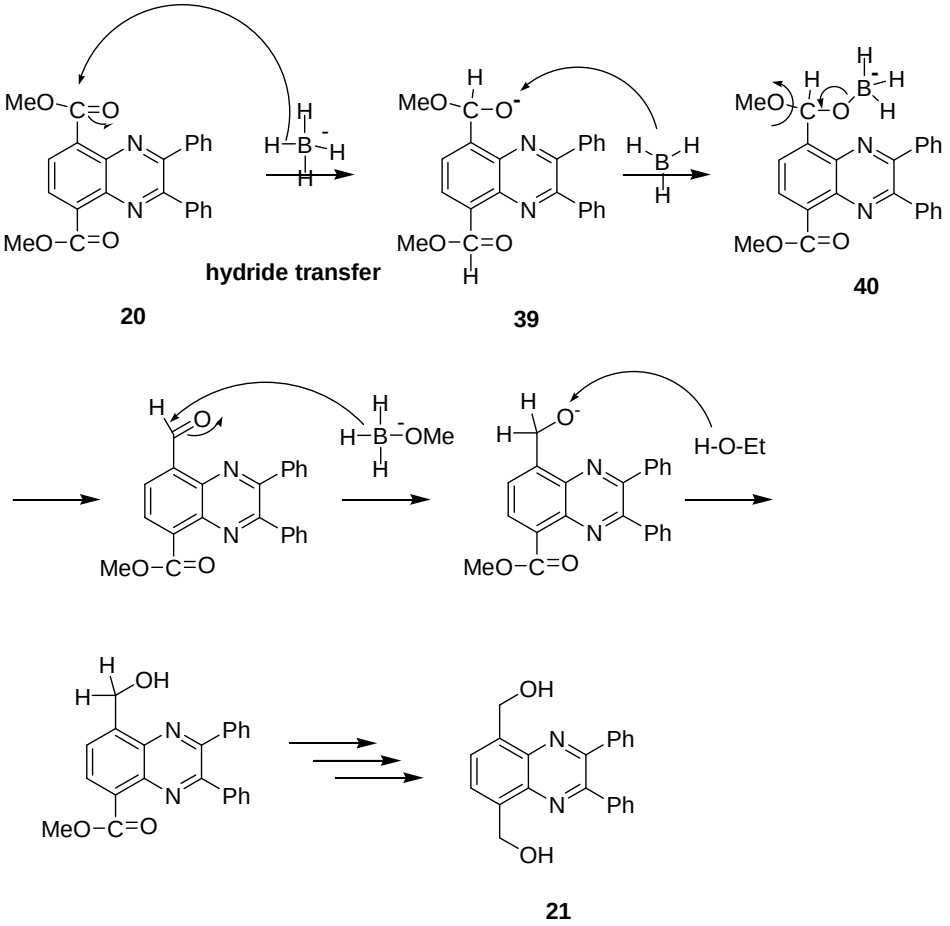

Scheme 2.30: Mechanism for the synthesis of (8-Hydroxymethyl-2,3-diphenyl-quinoxalin-5-yl)-methanol **21**.

An amount of **21** was dissolved in thionyl chloride and the reaction mixture was stirred under inert atmosphere for 3 days and monitored by TLC. After completion the reaction mixture was cooled to room temperature and very slowly pH was brought to 7 by saturated $NaHCO_3$. After neutralising the reaction mixture it was extracted with CH_2Cl_2 and the combined organic layers were washed with water and dried over $MgSO_4$. After filtration and evaporation the dark red coloured compound **22** that was obtained was used in the next step without further purification[33, 35, 36].

The reaction mechanism involves initial formation of the alkyl chlorosulfite **41**, Scheme 2.31. Then a chlorine ion can bring about an S_N2 displacement of a very good leaving group, $ClSO_2^-$, which by decomposing (to the gas SO_2 and Cl^- ion), helps drive the reaction to completion.

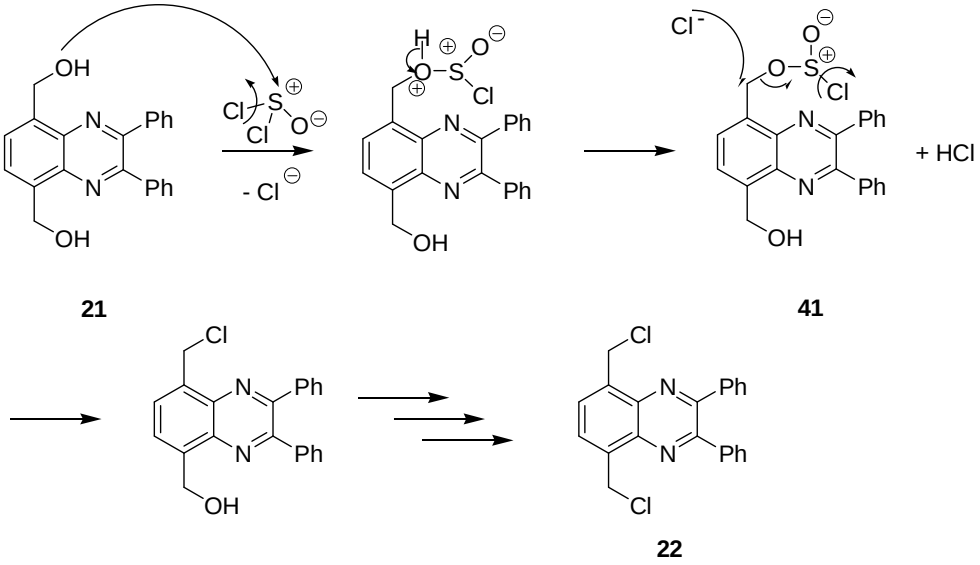

Scheme 2.31: Mechanism for the synthesis of 5,8-bis-chloromethyl-2,3-diphenyl-quinoxaline **22**.

2.3.1 Alternative routes towards chlorination of the dithiocarbamate quinoxaline monomer 6

Since there were many problems at the stage of chlorination of the diol **21** leading to very impure dichloro **22**, an alternative procedure was needed in order not to waste the expensive intermediary materials and improve the synthetic route, Scheme 2.32. The experiments were carried out with 8-hydroxymethyl quinoline **47** and hydroxymethyl pyridine **49**. The intermediary product **47** was prepared by the reduction of commercially available quinoline-8-carbaldehyde **46** according to the procedure described for the synthesis of **21**. As the reaction procedure for the synthesis of products **48** and **50** respectively starting from the compounds **49** and **47** respectively are the same, for the comparison of the parameters and analysis results only the preparation of **50** will be described further.

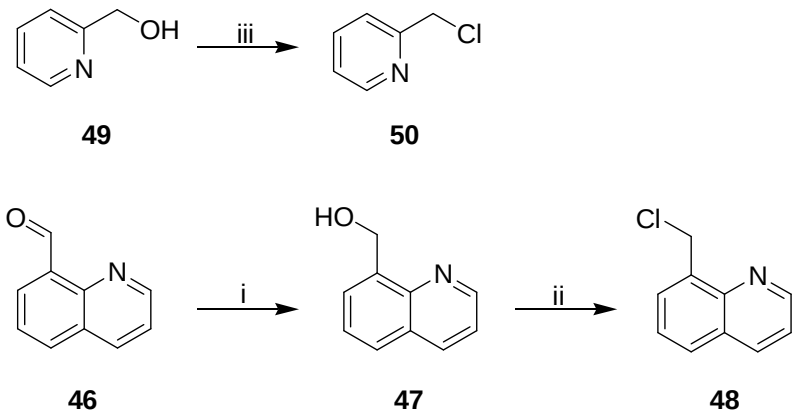

Scheme 2.32: Alternative routes towards chlorination of the dithiocarbamate quinoxaline monomer **6**: i) reduction, EtOH, $NaBH_4$; ii) and iii) $SOCl_2$

In a one-necked round-bottomed flask equipped with a magnetic stirring bar and a heating mantel was added **49** dissolved in thionyl chloride. The reaction mixture was stirred under inert atmosphere at ambient temperature for 24 hours. After completion it was cooled to ambient temperature and neutralised by saturated $NaHCO_3$. Extraction and drying yielded **50** in good yield.

Several attempts were made to carry out the synthesis of **50** from **49**. The experiments were carried out in different solvents and at different reaction conditions. From the experiments it can be noticed that thionyl chloride in combination with pyridine in THF under inert atmosphere led to the formation of many side products leading to impure product. When thionyl chloride dissolved in THF under inert atmosphere was used only a small concentration of the product was formed. Surprisingly, the best results were obtained when the reaction took place without pyridine and without THF. Using at room temperature only thionyl chloride as the reagent and as the solvent leads to the formation of pure product. As a comparison ^{1}H-NMR spectra of subsequently the impure product and the pure product are depicted in Figure 2.24 and Figure 2.25.

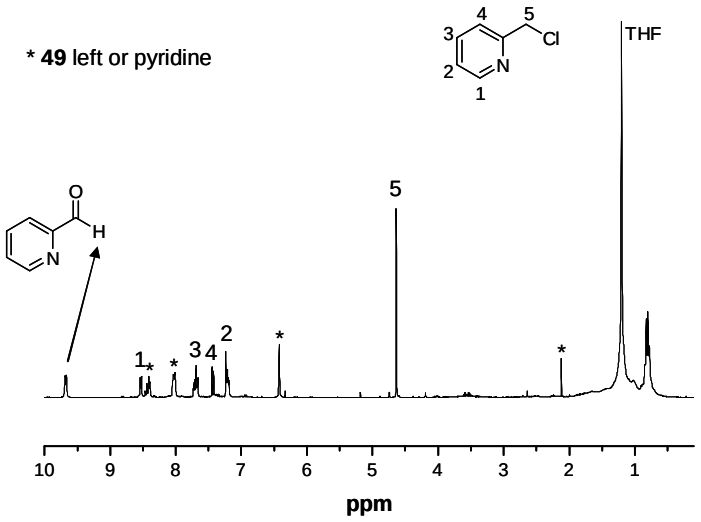

Figure 2.24: ^{1}H-NMR spectrum of impure 50 in $CDCl_3$

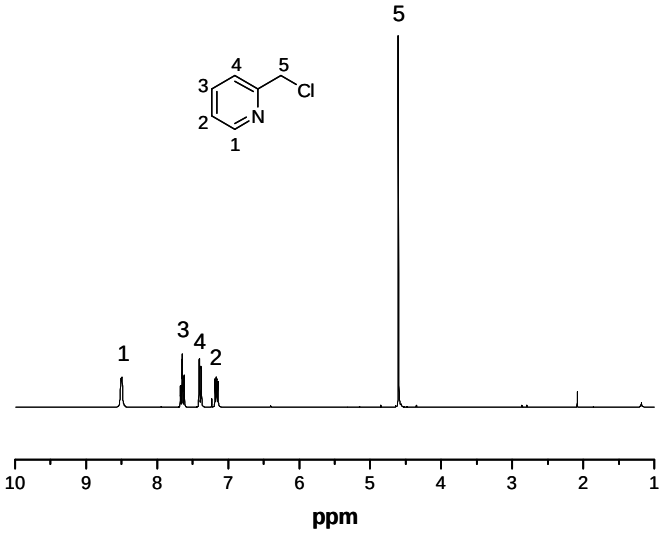

Figure 2.25: ^{1}H-NMR spectrum of pure 50 in $CDCl_3$

Also comparable results were obtained for the synthesis of **48** from **47** using the same reaction parameters. Therefore, as the experiments with 8-hydroxymethyl quinoline **47** and hydroxymethyl pyridine **49** delivered promising results, the dichloro **22** was prepared according to this procedure and used in the next step without further purification.

A mixture of **22** and sodium diethyldithiocarbamate trihydrate in diethyl ether was stirred at ambient temperature and monitored by TLC. After completion of the reaction the reaction mixture was quenched with water, extracted with diethyl ether and the combined organic layers were dried over $MgSO_4$. After filtration and evaporation of the solvent the milk coloured compound was purified by column chromatography. The fractions were collected and crystallised to obtain **6** as yellow crystals[37].

Also this reaction involves nucleophilic substitution of **22** with sodium-diethyldithiocarbamate-trihydrate, Scheme 2.33. Hereby, the negatively charged

sulphur attacks the CH_2 group leading to the leaving of the chlorine ion and the formation of the desired the dithiocarbamate quinoxaline monomer **6**.

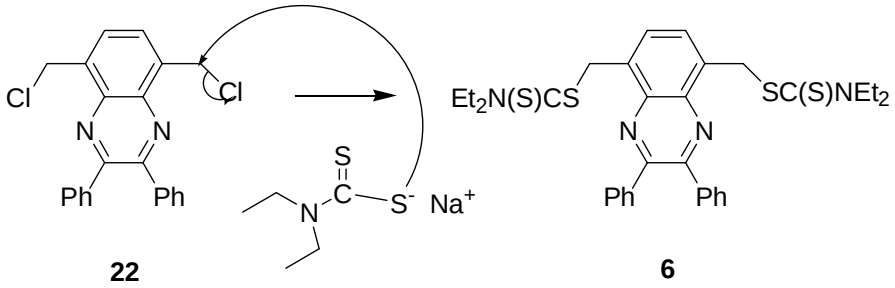

Scheme 2.33: Mechanism for the synthesis of the dithiocarbamate Quinoxaline monomer **6**.

2.3.2 Alternative routes towards the dithiocarbamate quinoxaline monomer 6

Since there are many steps towards the synthesis of the dithiocarbamate quinoxaline monomer **6** via the Immino-oxime cyclisation route (chapter 2.1.1) and the Benzothiadiazole route (chapter 2.2.1), efforts have been made to find some alternative routes in order to improve the efficiency of the synthesis route.

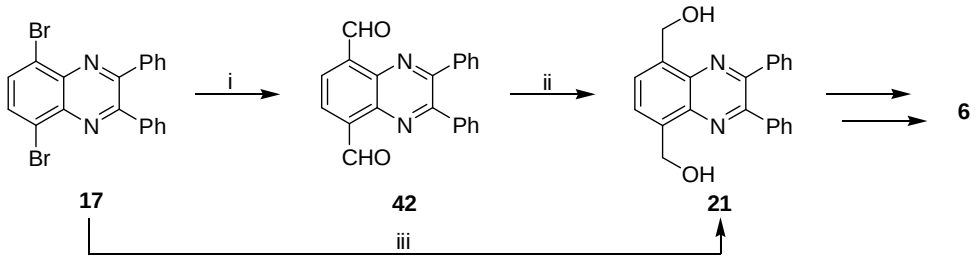

Scheme 2.34: Alternative routes towards the dithiocarbamate quinoxaline monomer **6** synthesis: i) THF, 1.6M *n*-BuLi, –78°C, formylpiperidine, N_2, 12h; ii) reduction, EtOH, $NaBH_4$; iii) THF, *t*-BuLi, –78°C, paraformaldehyde, 4h.

Inspired by the extensive work of David Hawkins and co-workers on the synthesis of thienothiophenes, we tried out the double annelation process shown in Scheme

2.34 [38]. The aim of this experiment was to make an effort in order to improve the synthesis procedure towards quinoxalines and their derivatives. Hereby the four step procedure from the intermediary products **17** to **21** (Scheme 2.23) can be replaced by the simple two step procedure of **17** to **21** via **42**, Scheme 2.34. To a three-necked round bottomed flask **17** was dissolved in THF. *n*-BuLi was added with syringe to the solution from above and stirred at –78°C for 30 minutes. Hereby N_2 was bubbled through the solution. Then, the solution was quenched with formylpiperidine, and thereafter the mixture was stirred for 12 hours at 25°C. For the work up 30 ml of HCl 2M was added and extracted with $CHCl_3$. After drying, the crude product was purified by column chromatography, followed by crystallisation to yield **42** as brown crystals.

The reduction of **42** to **21** was carried out in two different ways and with two different reducing agents. First method: to a dry 50 ml three-necked round-bottomed flask equipped with a magnetic stirring bar and an ice bath was added lithium aluminium hydride $LiAlH_4$ dissolved in dry THF. The reaction mixture was cooled to 0°C and stirred under nitrogen atmosphere. The dialdehyde **42** was added as a solid via a solid dropping funnel. After the addition is complete, the reaction mixture was refluxed at 75°C for 1.5 hours. The reaction mixture was cooled to 0°C in an ice bath and quenched by sequentially cautious addition of water, aqueous 10% NaOH solution and water. After extraction with diethyl ether and drying, the crude compound was purified by column chromatography. The use of the strong reducing agent $LiAlH_4$ for the reduction of the dialdehyde **42** to the diol **21** was not successful due to the formation of the major side product **44**, Scheme 2.35. This was deduced from the ^{1}H-NMR spectrum which showed a typical absorption from such methyl groups at 2.16 ppm. **44** was most probably formed because of the over reduction of **42**. $LiAlH_4$ is a too strong reducing agent in this case. A method which can be more effective is selective reduction of aldehyde with sodium borohydride in ethanol[39].

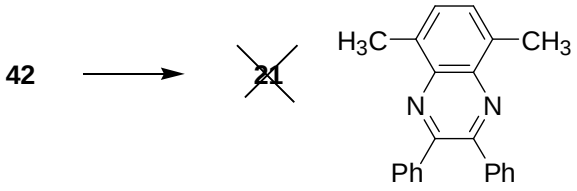

Scheme 2.35: The side products formed during the reduction of dialdehyde **42** to diol **21**.

Second method: to a 50 ml three-necked round-bottomed flask equipped with a condenser was added **42** dissolved in ethanol. To this was added $NaBH_4$ and the reaction mixture was stirred at room temperature for 1 hour 15 minutes. After completion of the reaction the mixture was filtered through a pad of celite and the filtrate was concentrated under reduced pressure to obtain the crude compound, which could not be identified as **21**.

Several attempts were made to carry out the synthesis of **21** from **17**. In a three-necked round-bottomed flask equipped with a magnetic stirring bar and continuous nitrogen flow **17** was suspended in dry THF and cooled to –78°C. *t*-BuLi was added to the suspension during 15 minutes and stirred for 2 hours. Paraformaldehyde in THF was added *slowly* to the reaction mixture using a solid dropping funnel and stirred for 4 hours. After warming up to room temperature water was added and stirred for 20 minutes. The suspension was filtered, washed subsequently with water, methanol and aceton. The reaction mixture so obtained showed on TLC to be quite complex and was not further analysed.

2.3.3 Alternative routes from nitrile 18 towards ester 43

Two different procedures were used in order to improve the route towards the synthesis of our the dithiocarbamate quinoxaline monomer **6**, Scheme 2.36.[40, 41] First method: to a round-bottomed flask equipped with a magnetic stirring bar and a heating mantel were added **18**, ethanol and H_2SO_4 and refluxed during 22 hours under an inert atmosphere. After cooling to room temperature the reaction mixture was poured to ice-cold water. The organic layer was separated and washed with

Na_2CO_3 solution and dried over $MgSO_4$. After filtration and evaporation of the solvent, the crude compound was concentrated under reduced pressure.

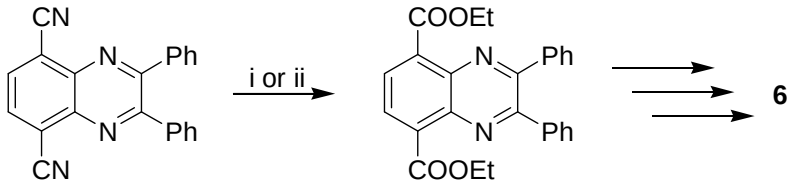

18 **43**

Scheme 2.36: alternative routes towards the dithiocarbamate quinoxaline monomer **6** synthesis: i) H_2SO_4, EtOH, ΔT, 22h, N_2; ii) EtOH, chlorotrimethylsilane, 50°C, 4h, N_2.

Second method: to a round-bottomed flask equipped with a magnetic stirring bar and a heating mantel were sequentially added **18**, ethanol and chlorotrimethylsilane and heated at 50°C for 4 hours under an inert atmosphere. After being cooled down to room temperature, water was added to the mixture and followed by the addition of Na_2CO_3 and CH_2Cl_2. After filtration, the residue was washed with CH_2Cl_2 and the filtrate was dried over $MgSO_4$ and concentrated at low pressure. Then the crude compound was dried under reduced pressure in the desiccator overnight.

Unfortunately, after many attempts to prepare the diester **43** from dicyano derivative **18** with either of the two methods, the starting product was recovered to a major extend.

2.4 Conclusion

In this chapter the main focus was directed development of the synthetic approaches towards the quinoxaline core, in particular the dithiocarbamate quinoxaline monomer synthesis. First efforts were made to prepare the dithiocarbamate quinoxaline monomer **6** via the Immino-oxime cyclisation route. As

it was known from the literature this procedure was the best known procedure and for this at first the procedure seemed promising but in our hands the cyclisation of α-arylimino oxime appeared irreproducible. Also the bromination to 1,4-bis(bromomethyl)-2,3-diphenylquinoxaline **5** was not efficient and productive which did not lead to the formation of the desired the dithiocarbamate quinoxaline monomer **6**.

Therefore, a better procedure was found to be the Benzothiadiazole route. Although, there are many steps attached to this route, still good yields and reproducible products were obtained. Many efforts were made to optimise the procedure and improve the yield and purity of the intermediary products for the mentioned route by:

- Applying modifications for the synthesis of 5,8-dibromo-2,3-diphenyl-quinoxaline **17** leading to high and pure product.
- Applying alternative routes to shorten the reaction time for the synthesis of **43** via **18** and for the synthesis of **21** via dialdehyde **42**.
- Applying alternative routes to improve the reaction rate of the chlorination step toward **22**.

Although the synthesis of 2,3-Diphenyl-quinoxaline-5,8-dicarbaldehyde **42** is promising, the reduction of this product to (8-Hydroxymethyl-2,3-diphenyl-quinoxalin-5-yl)-methanol **21** yielded in many impurity when the reaction was carried out with lithiumaluminium hydride $LiAlH_4$ as the reagent in THF.

However, when compound **20** was used and the reaction was carried out in ethanol with sodium borohydride as the reagent, high yield and good purity was obtained. At first, the chlorination towards 5,8-bis-chloromethyl-2,3-diphenyl-quinoxaline **22** was not very efficient and the use of an optimised procedure helped us to improve this route which afterwards was applied for the synthesis of our the dithiocarbamate quinoxaline monomer **6** in good yield. This dithiocarbamate quinoxaline monomer can be used for polymerisation via the dithiocarbamate route which will be discussed in the next chapter.

2.5 Experimental section

2.5.1 Materials

All solvents used in the synthesis were distilled before use. Tetrahydrofuran (THF) was refluxed under nitrogen with sodium metal and benzophenone until a blue colour persisted and was then distilled. All the commercially available products were purchased from Acros or Aldrich. Benzil **1**, 2,5-dimethylaniline, quinoline-8-carbaldehyde **46** and 2-hydroxymethyl pyridine **49** were purchased from Acros or Aldrich and used without further purification.

2.5.2 Characterisation

Nuclear magnetic resonance (NMR) spectra were recorded on a Varian Inova 300 spectrometer at 300 MHz for ^{1}H-NMR and at 75 MHz for ^{13}C-NMR using a 5 mm probe.

Gas chromatography/mass spectrometry (GC/MS) analyses were carried out with TSQ – 70 or Voyager mass spectrometers (Thermoquest); the capillary column was a Chrompack Cpsil5CB or Cpsil8CB.

Fourier Transform Infra Red spectroscopy (FT-IR) was performed on a Perkin Elmer Spectrum One FT-IR spectrometer (nominal resolution 4 cm-1, summation of 16 scans). Samples for the FT-IR characterisation were prepared by spin-coating the compounds from a chloroform solution (6 mg/ml) onto NaCl disks (diameter 25 mm and thickness 1 mm) at 500 rpm.

TLC analyses were made on Merck aluminium sheets, 20 x 20 cm, covered with silica gel 60 F254.

2.5.3 Synthesis

α-benzil monooxime (2)

To a three-necked round-bottomed flask equipped with a large magnetic stirring bar, an electronic thermometer and ice water bath, was added **1** (42 g, 0.2 mol), ethanol (18 ml) and a concentrated solution of hydroxylamine hydrochloride (17.5 g, 0.25 mol) in water (25 ml). To the reaction mixture was added drop wise a cold solution of sodium hydroxide (30 g) in water (120 ml) for 15 min. Then the reaction mixture was stirred for 2 hours at room temperature. The mixture was diluted with water (280 ml) and filtered off. The solid (unreacted substrate), was recovered (1.90 g) and was washed with a little bit of water. The filtrate was acidified with glacial acetic acid and stirred for 0.5 hour. The formed solid was filtered off, dried to dryness and crystallised from ethanol/ toluene mixture (Note). The yellowish crystals that were obtained were dried under vacuum (33.3 g, 74%). ^{1}H-NMR ($CDCl_3$): 7.98-7.93 (m, 2H), 7.65-7.54 (m, 2H), 7.53-7.48 (m, 1H), 7.47-7.39 (m, 2H), 7.38-7.30 (m, 3H), 2.08 (br s, 1H); FT-IR (NaCl, cm^{-1}): 3378, 3273, 1645, 1580, 1450; GC-MS: 225 (M^+), 194 (M^+- O-N), 178 (M^+- O-N-O), 166 (M^+- O-N=C-O), 152 (M^+- O-N=C-C=O), 77 (M^+- O-N=C-C-phenylion), 51 (C_4H^{3+}).

Note: There is strongly recommended to filter hot toluene solution through folded filter paper. Use 250 ml of toluene on 25 grams of substrate.

2-[(2,5-dimethylphenyl)imino]-1,2-diphenyl-etanone oxime (3)

To a round bottomed flask (500 ml) equipped with a Soxhlet (filled with $CaCl_2$), a magnetic stirring bar and a heating mantel was added **2** (24.54 g, 0.109 mol), 2,5-dimethylaniline (13.7 ml, 0.109 mol), *p*-toluenesulphonic acid (110 mg, cat.) and toluene (131 ml). The reaction mixture was stirred and refluxed for 72 hours under an inert atmosphere. The formed brown oil was left purified by column chromatography (hexane : EtOAc = 9:1). The pure fractions were collected and dried under vacuum (30.7 g, 86%). ^{1}H-NMR ($CDCl_3$): 8.10-8.07 (d, 4H), 7.53-7.41 (m, 4H), 7.27-7.14 (m, 2H), 6.83-6.72 (dd, 3H), 2.15-2.03 (s, 6H); GC-MS: 328 (M^+), 311 (M^+-OH), 297 (M^+-N-OH), 282 (M^+-N-OH-CH_3), 267 (M^+-N-OH-2CH_3),

192 (M^+-N-OH-2CH_3-Ph), 178 (M^+-N-OH-2CH_3-Ph-N), 165 (M^+-N-OH-2CH_3-Ph-N=C), 77 (M^+-N-OH-2CH_3-Ph-N=C-phenylion-C), 51 (C_4H^{3+}).

5,8-dimethyl-2,3-diphenylquinoxaline (4)

To a round-bottomed flask (100 ml) equipped with a reflux condenser, a magnetic stirring bar and a heating mantel was added **3** (1.20 g, 3.66 mmol) and acetic anhydride (25 ml). The reaction mixture was stirred and refluxed for 6 hours. The cooled mixture was poured to cold water (100 ml) and stirred for two hours. The formed product was filtered off, washed with water and dried under vacuum overnight (1.04 g, 92%). ^{1}H-NMR ($CDCl_3$): 7.64-7.61 (m, 4H), 7.48 (s, 2H), 7.38-7.32 (m, 6H), 2.83 (s, 6H); ^{13}C-NMR ($CDCl_3$): 140.22 (2C), 139.62 (2C), 134.83 (4C), 130.79-129.36 (6C), 128.64-128.05 (6C), 16.94 (2C).

1,4-bis(bromomethyl)-2,3-diphenylquinoxaline (5)

To a round-bottomed flask (250 ml) equipped with a magnetic stirring bar and a heating mantel was added **4** (5.01g, 0.016 mol) and NBS (5.66 g, 0.032 mol) dissolved in CCl_4 (115 ml). A small amount of BPO (37.80 mg) was added as the initiator. The reaction mixture was stirred and refluxed at 93°C under an inert atmosphere and illuminated by a lamp of 200 Watt overnight. After almost 24h the reaction was stopped, the succinimide filtered off and washed with $CHCl_3$ (2 x 25 ml). The filtrate was left in the fridge overnight. Next day, the solid part was filtered off (NBS) the liquid part was distilled under reduced pressure and purified by column chromatography (pure hexane then slowly CH_2CL_2). The fractions were collected and crystallised from $CHCl_3$. The pure product was dried under vacuum (1.54 g, 20%). ^{1}H-NMR ($CDCl_3$): 7.80 (s, 2H), 7.63-7.59 (t, 4H), 7.42-7.31 (m, 6H), 5.21 (s, 4H); GC-MS: 466/468 (M^+), 387 (M^+-Br), 307 (M^+-2Br), 293 (M^+-2Br-CH_2), 279 (M^+-2Br-2CH_2), 204 (M^+-2Br-2CH_2-C_6H_2), 176 (M^+-2Br-2CH_2-C_6H_2-2N), 154 (M^+-2Br-2CH_2-C_4H_2-2N=C), 77 (M^+-2Br-2CH_2-C_6H_2-2=C-phenylion), 51 (C_4H^{3+}).

The dithiocarbamate Quinoxaline monomer; Diethyl-dithiocarbamic acid 8-diethylthiocarbamoylsulfanylmethyl-2,3-diphenyl-quinoxalin-5-ylmethyl ester via the Immino-oxime cyclisation route (6)

To a round bottomed flask (50 ml) equipped with a magnetic stirring bar was added **5** (14.5 mg, 0.031 mol) in ether (10 ml). To this mixture Sodium diethyldithiocarbamate trihydrate (16.1 mg, 0.071 mol) was added and the mixture was stirred at room temperature for 2 hours. The reaction was stopped by adding water (10 ml). After extraction with diethyl ether and drying over $MgSO_4$, the compound was filtered and dried under vacuum leading to a crude mixture containing the product. Efforts toward purification failed.

The dithiocarbamate quinoxaline monomer; Diethyl-dithiocarbamic acid 8-diethylthiocarbamoylsulfanylmethyl-2,3-diphenyl-quinoxalin-5-ylmethyl ester via the Benzothiadiazole route (6)

A mixture of **22** (33 g, 0.087 mol) and sodium diethyldithiocarbamate trihydrate (196 g, 0.87 mol) in 680 mL of diethyl ether was stirred at ambient temperature and monitored by TLC. After completion of the reaction the reaction mixture was quenched with water, extracted with diethyl ether and the combined organic layers were dried over $MgSO_4$. After filtration and evaporation of the solvent the milk coloured compound was purified by column chromatography with *n*-hexane/ $CHCl_3$ = 9/1 as the solvent. The fractions were collected and crystallised from a mixture of *n*-hexane/ $CHCl_3$ = 7/3 to obtain yellow crystals (16.0 g, 30% yield). Mp: 168.8 °C; ^{1}H-NMR ($CDCl_3$): 7.91 (s, 2H), 7.61-7.58 (dt, 4H), 7.39-7.28 (m, 6H), 5.31-5.24 (t, 4H), 4.08-4,01 (q, 4H), 3,75-3.67 (q, 4H), 1,33-1.22 (m, 12H); ^{13}C-NMR ($CDCl_3$): 195.52 (2C), 151.96 (2C), 139.19 (2C), 136.64 (2C), 134.92 (2C), 129.84 (6C), 48.08 (6C), 41.30 (4C), 36.22 (2C), 12.34 (4C); FT-IR (NaCl, cm^{-1}): 1484, 1415, 1269, 1206.

4,7-dibromo-benzo[1,2,5]thiadiazole (15)

To 72 mL solution of HBr (48 volume %) 2,1,3-benzothiadiazole (50 g, 0.37 mol) **14** was added and the reaction mixture was stirred and refluxed at 130°C. To the refluxing mixture was added drop wise 58 mL of elemental bromine (1.14 mol) in excess during 5 hours. After subsequently 2.5 hours, 4 hours, 4.5 hours was

additionally added 50 mL of HBr to facilitate the stirring. After cooling overnight and carefully filtration the product was washed with a large amount of water and dried under vacuum to obtain brown crystals (106.7 g, 100% yield). Mp: 178,5 °C; ^{1}H-NMR ($CDCl_3$): 7.70 (s, 2H); ^{13}C-NMR ($CDCl_3$): 152.76 (2C), 132.19 (2C), 113.73 (2C); FT-IR (NaCl, cm^{-1}): 3072, 3043, 1274, 1079; GC-MS: 294/292 (M^+), 215/213 (M^+-Br), 134 (M^+-2Br), 101 (M^+-2Br-S), 51 ($C_4H_3^+$).

3,6-dibromo-benzene-1,2-diamine (16)

To **15** (10 g, 0.034 mol) suspended in 340 mL absolute ethanol and cooled to 0°C $NaBH_4$ (22.8 g, 0.60 mol) was added in small portions during 5 hours. The reaction mixture was continued stirring at room temperature for 20 hours. The solvent was evaporated and the reaction mixture was dissolved in 200 mL of water. After extraction with diethyl ether (5 x 100 mL), the combined organic layers were dried over Na_2SO_4. Filtration and evaporation of the solvent gave the pale brown product (8.40 g, 93% yield). Mp: 85,8-90 °C; ^{1}H-NMR ($CDCl_3$): 7.71 (s, 2H), 1.52 (s, 4H); ^{13}C-NMR ($CDCl_3$): 133,54 (2C), 123,08 (2C), 109,51 (2C); FT-IR (NaCl, cm^{-1}): 3080, 1570, 1451, 1068, 767; GC-MS: 264/266 (M^+), 183/185 (M^+-Br), 105 (M^+-2Br, Φ-C≡O^+), 78 (M^+-2Br –2NH_2), 77 (phenylion), 51 (C_4H^{3+}).

5,8-dibromo-2,3-diphenyl-quinoxaline (17)

Without Iodine: To a 250 ml round-bottomed flask equipped with a large magnetic stirring bar, a reflux condenser, a heating mantel and electronic thermometer was added **16** (9.97 g, 0.038 mol) and **1** (8.0 g, 0.038 mol) dissolved in ethanol (160 ml). The reaction mixture was stirred and refluxed for 48 hours. The reaction mixture was cooled to ambient temperature overnight. The precipitate was filtered off, washed with cold ethanol and air-dried. The product was obtained as milk-coffee coloured solid (13.1 g, 79% yield).

With Iodine: 1 g of **16** (0.0038 mol) and **1** (0.80 ml, 0.0038 mol) were dissolved in 10 mL absolute ethanol. To this was added iodine (10 mol %) and the reaction mixture was stirred at room temperature for 15 minutes. After completion of the reaction, the reaction mixture was poured onto crushed ice (100 mL) and stirred for 10-15 min. Then, the solid which separated was filtered, washed with aqueous

sodium thiosulfate solution (3 x 50 mL) to remove iodine and subsequently with water, and then dried under vacuum to afford the pure milk-coffee coloured product (1.72 g, 87% yield). Mp: 215.8 °C; ^{1}H-NMR ($CDCl_3$): 7.90 (s, 2H), 7,66-7.62 (2d, 4H), 7,39.7.31 (dd, 6H); GC-MS: 438/440 (M^+), 360 (M^+-Br), 279 (M^+-2Br), 207 (M^+-2Br-C_6H_2), 177 (M^+-2Br-C_6H_2-N_2), 154 (M^+-2Br-C_6H_2-2N=C), 77 (phenylion), 51 (C_4H^{3+}).

2,3-diphenyl-quinoxaline-5,8-dicarbonitrile (18)

In a flask **17** (9.28 g, 0.021 mol) and CuCN (4.33 g, 0.048 mol) were dissolved in 27 mL DMF. The reaction mixture was stirred and refluxed under an inert atmosphere at 164°C for 4 hours. After the reaction mixture was cooled down, it was poured into a solution of $FeCl_3$ (27 g), HCl (conc., 6.9 mL) and water (40.5 mL) and stirred at 65°C for 30 minutes. The aqueous solution was extracted with $CHCl_3$ (5 x 50 mL) and the organic layer washed with 30 mL HCl (1:1) and 30 mL 15% NaOH (aq.). To neutralise the combined organic layers they were washed twice with H_2O (100 mL). They were also washed with NaCl (sat., 100 mL) and finally dried over $MgSO_4$. After filtration and evaporation a yellow coloured product was obtained (6.46 g, 91% yield). Mp: 274,8-275,2 °C; ^{1}H-NMR ($CDCl_3$): 8.15 (s, 2H), 7.64 (d, 4H), 7.39 (q, 4H), 7.22 (s, 2H); ^{13}C-NMR ($CDCl_3$): 156,39 (2C), 140.10 (2C), 136.93 (2C), 133.92 (2C), 130.29 (4C), 130.09 (2C), 128.39 (4C), 117.05 (2C), 114.76 (2C); GC-MS: 332 (M^+), 305 (M^+-CN), 255 (M^+-CN-HCCCN), 77 (phenylion), 51 (C_4H^{3+}); FT-IR (NaCl, cm^{-1}): 2231, 1682, 1600, 1342, 1223.

2,3-diphenyl-quinoxaline-5,8-dicarboxylic acid (19)

To **18** (6.44 g, 0.019 mol) suspended in 140 mL NaOH (10%) was added absolute ethanol (70 mL) and heated overnight (100°C). After completion of the reaction the condenser was detached and the solution was refluxed for a few minutes in the open flask to remove dissolved ammonia and some of the ethanol. The suspension was cooled and filtered. To the filtrate hydrochloric acid (conc.) was added until the precipitation of the product was complete. The crude yellow coloured product was filtered off and it was dried. Finally, recrystallisation from hot toluene resulted to pale brown crystals (6.69 g, 95% yield). Mp: 266,6-267,1 °C; ^{1}H-NMR ($CDCl_3$): 8,94 (s, 2H), 7,45 (d, 4H), 7,24 (t, 4H), 7,15 (t, 2H); ^{13}C-NMR ($CDCl_3$): 164.07 ,

153.64, 138.14, 135.35, 131.11, 129.34, 128.66; GC-MS: 370 (M^+), 326 (M^+-COOH), 279 (M^+-2xCOOH), 251 (-CH_2=CH_2), 77 (phenylion); FT-IR (NaCl, cm^{-1}): 3024, 2676, 1739, 1587, 1448, 1351, 1280, 1225.

2,3-diphenyl-quinoxaline-5,8-dicarboxylic acid dimethyl ester (20)

24.8 g of **19** (0.067 mol) was added to a mixture of MeOH (250 mL) and H_2SO_4 (50 mL, 70%) and refluxed at 80°C under inert conditions overnight. After completion of the reaction, the condenser was detached and the reaction mixture was cooled. The reaction mixture was extracted with CH_2Cl_2 (3 x 50 mL). The combined organic layers were washed with water and dried over $MgSO_4$. After filtration and evaporation a yellow oil was obtained (21.3 g, 81% yield). Mp: 144,4-144,8 °C; ^{1}H-NMR ($CDCl_3$): 8.10 (s, 2H), 7.66 (d, 4H), 7.36 (m, 6H), 4.05 (s, 6H); ^{13}C-NMR ($CDCl_3$): 166.37 (2C), 152.91 (4C), 138.06 (2C), 133.45 (4C), 129.97 (2C), 129.64 (2C), 129.41 (2C), 128,2 (4C), 52.63 (2C); GC-MS: 398 (M^+), 383 (M^+-Me), 340 (-OMe), 279 (-COOMe), 105 (- Φ-C≡O^+), 77 (phenylion), 51 ($C_4H_3^+$); FT-IR (NaCl, cm^{-1}): 3058, 3024, 2951, 1733, 1282.

(8-Hydroxymethyl-2,3-diphenyl-quinoxalin-5-yl)-methanol (21)

To the diester **20** (5.43 g, 0.014 mo) suspended in 272 mL absolute ethanol was added $NaBH_4$ (11.5 g, 0.30 mol) in one portion. The reaction mixture was refluxed under inert atmosphere for 5 hours. After cooling down a saturated NH_4Cl solution (272 mL) was added and the solution was stirred overnight. The solvent was evaporated and the precipitated solids were dissolved by addition of the minimum amount of water necessary. The resulting solution was extracted with ethyl acetate (5 x 50 mL) and the combined organic layers were dried over $MgSO_4$. After filtration and evaporation the crude brown foam that was obtained was used in the next step without further purification. ^{1}H-NMR ($CDCl_3$): 7.55 (s, 2H), 7.46 (d, 4H), 7.30 (m, 6H), 5.18 (s, 4H); ^{13}C-NMR ($CDCl_3$): 151.68 (2C), 145,53 (2C), 138.40 (2C), 137.55 (2C), 129.64 (2C), 129.47 (2C), 128.97 (2C), 128.64 (2C), 128.31 (2C), 128.14 (2C), 62.54 (2C); GC-MS: 342 (M^+), 325 (M^+-OH), 311 (- CH_2), 295 (-OH), 284 (-CH_2), 178 (-$C_6H_4N_2$), 77 (phenylion), 51 ($C_4H_3^+$); FT-IR (NaCl, cm^{-1}): 3213, 1064.

Bis(hydroxymethyl)-2,3-diphenyl-quinoxaline (21)

Method A: To a dry 50 ml three-necked round-bottomed flask equipped with a magnetic stirring bar and an ice bath was added $LiAlH_4$ (0.16 g, 4.2 mmol) dissolved in dry THF (35 ml). The reaction mixture was cooled to 0°C and stirred under nitrogen atmosphere. The **42** (0.70 g, 2.1 mmol) was added as a solid *VERY SLOWLY* via a solid dropping funnel. After the addition is complete, the reaction mixture was refluxed at 75°C for 1.5 hours (colour turned to red wine). The reaction mixture was cooled to 0°C in an ice bath and quenched by sequentially cautious addition of water (2 ml), aqueous 10% NaOH solution (2 ml) and water (5 ml). The reaction mixture was held at 0°C under stirring for 30 minutes, and then it was allowed to warm to room temperature. The reaction mixture was filtered and washed on the filter with diethyl ether. The filtrate was extracted with diethyl ether (3 x 5 ml) and dried over $MgSO_4$. After filtration and evaporation the crude compound was analysed and this proved that the product was not formed.

Method B: To a 50 ml three-necked round-bottomed flask equipped with a condenser, was added the **42** (0.80 g, 2.4 mmol) dissolved in ethanol (36 ml). To this was added $NaBH_4$ (0.091 g, 2.4 mmol) and the reaction mixture was stirred at room temperature for 1 hour 15 minutes. The reaction progress was monitored by TLC. After completion of the reaction the mixture was filtered through a pad of celite and the filtrate was concentrated under reduced pressure to obtain a complex mixture which was not further analysed.

5,8-bis-chloromethyl-2,3-diphenyl-quinoxaline (22)

33.8 g of **21** (0.099 mol) was dissolved in thionyl chloride (350 mL, 4.82 mol). The reaction mixture was stirred under inert atmosphere for 3 days and monitored by TLC. After completion the reaction mixture was cooled to room temperature and v*ery slowly* pH was brought to 7 by saturated $NaHCO_3$. After neutralising the reaction mixture it was extracted with CH_2Cl_2 (3 x 50 mL) and the combined organic layers were washed with water and dried over $MgSO_4$. After filtration and evaporation the dark red coloured compound that was obtained was used in the next step without further purification. ^{1}H-NMR ($CDCl_3$): 7.87 (s, 2H), 7.63 (t, 4H), 7.38 (m, 6H), 5,34 (s, 4H); ^{13}C-NMR ($CDCl_3$): 152.49 (4C), 138,65 (2C), 136.18 (2C), 129.98 (2C), 129.63 (4C), 129.03 (2C), 128.11 (4C), 41,17 (2C).

2,3-Diphenyl-quinoxaline-5,8-dicarbaldehyde (42)

To a three-necked round bottomed flask (50ml) diBromophenyl quinoxaline (1 g, 0.0023 mol) was dissolved in THF (12.5 ml). *n*-BuLi (1.6M, 0.0050 mol, 3.1 ml) was added SLOWLY with syringe to the solution from above and stirred at –78°C for 30 minutes. Hereby N_2 was bubbled through the solution.

Then, the solution was quenched with formylpiperidine, and where after the mixture was stirred for 12 hours at 25°C. For the work up 30 ml of HCl 2M was added and a extraction with $CHCl_3$ (3 x 10 ml) was performed. The organic layer was dried over $MgSO_4$ and the solvent was evaporated. The crude product was purified by column chromatography (hexane: EtOAc = 9:1), followed by crystallisation from $CHCl_3$/ hexane) to yield brown crystals (0.70 g, 91%). ^{1}H-NMR ($CDCl_3$): 11.47 (s, 2H), 8.42 (s, 2H), 7.64-7.53 (m, 4H), 7.47-7.31 (m, 6H); GC-MS: 338 (M^+), 309 (M^+-CHO), 280 (M^+-2CHO), 254 (M^+-2CHO-CH=CH), 178 (M^+-2CHO-CH=CH-C_4N_2), 154 (M^+-2CHO-CH=CH-C_4-2N=C), 77 (phenylion), 51 ($C_4H_3^+$).

2,3-Diphenyl-quinoxaline-5,8-dicarboxylic acid diethyl ester (43)

Method A: To a round-bottomed flask equipped with a magnetic stirring bar and a heating mantel were added **18** (0.50 g, 1.51 mmol), ethanol (abs., 5 ml) and H_2SO_4 (conc., 0.32 ml) and refluxed during 22 hours under an inert atmosphere. After cooling to room temperature the reaction mixture was poured to ice-cold water (20 ml). The organic layer was saturated so CH_2Cl_2 added to get the organic layer. The organic layer was separated and washed with Na_2CO_3 solution (10%) and dried over $MgSO_4$. After filtration and evaporation of the solvent, the crude compound was concentrated under reduced pressure which was identified as the starting product.

Method B: To a round-bottomed flask equipped with a magnetic stirring bar and a heating mantel were sequentially added **18** (0.50 g, 1.51 mmol), ethanol (abs., 5 ml) and chlorotrimethylsilane (1.14 ml, 9.06 mmol) and heated at 50°C for 4 hours under an inert atmosphere. After being cooled down to the room temperature, water (2 ml) was added to the mixture and followed by the addition of Na_2CO_3 (0.33 g) and CH_2Cl_2 (10 ml). After filtration, the residue was washed with CH_2Cl_2 (10 ml) and the filtrate was dried over $MgSO_4$ and concentrated at low

pressure. Then the crude compound was dried under reduced pressure in the desiccator overnight and analysed as the starting product.

8-Hydroxymethyl quinoline (47)

To a 100 ml three-necked round-bottomed flask equipped with a magnetic stirring bar was added **46** (200 mg, 1.27 mmol) dissolved in ethanol (20 ml). $NaBH_4$ (48 mg, 1.27 mmol) and $(NH_4)_2CO_3$ (122 mg, 1.27 mmol) were added to this solution. The reaction mixture was stirred at room temperature for 4 minutes and monitored by TLC. After completion of the reaction the crude mixture was filtered through a pad of celite and the filtrate was concentrated under reduced pressure to give the pure yellow coloured product (202 mg, 100%). ^{1}H-NMR ($CDCl_3$): 8.82-8.80 (dd, 1H), 8.15-8.11 (dd, 1H), 7.72-7.68 (dd, 1H), 7.56-7.53 (d, 1H), 7.46-7.35 (m, 2H), 5.17 (s, 2H); ^{13}C-NMR ($CDCl_3$): 149.01 (1C), 146.98 (1C), 138.04 (1C), 136.77 (1C), 128.39 (1C), 127.69 (1C), 127.36 (1C), 126.38 (1C), 121.11, 64.39 (1C); GC-MS: 159 (M^+), 142 (M^+-OH), 128 (M^+-OH-CH_2), 102 (M^+-OH-CH_2-C_2H), 77 (M^+-OH-CH_2-C_2H-CH=CH), 63 (M^+-OH-CH_2-C_2H-CH=CH-N).

8-Chloromethyl-quinoline (48)

In a one-necked round-bottomed flask (100 ml) equipped with a magnetic stirring bar and a heating mantel was added **47** (0.28 g, 1.8 mmol) dissolved in thionyl chloride (2.8 ml). The reaction mixture was stirred under inert atmosphere at room temperature for 24 hours. After completion the reaction mixture was cooled to ambient temperature, *Very Slowly* pH was brought to 7 by saturated/ concentrated $KHCO_3$, extracted with CH_2Cl_2 (3 x 5 ml) and the combined organic layers were washed with water and dried over $MgSO_4$. After filtration and evaporation the product was obtained as pale brown crystals (014 g, 44%). ^{1}H-NMR ($CDCl_3$): 8.96-8.93 (dd, 1H), 8.13-8.09 (dd, 1H), 7.82-7.79 (d, 1H), 7.77-7.42 (d, 1H), 7.52-7.46 (t, 1H), 7.41-7-36 (q, 1H), 5.31 (s, 2H); ^{13}C-NMR ($CDCl_3$): 150.02 (1C), 145.70 (1C), 136.24 (1C), 135.46 (1C), 129.97 (1C), 128.62 (1C), 128.20 (1C), 126.19 (1C), 121.36, 42.37 (1C); GC-MS: 177/179 (M^+), 142 (M^+-Cl), 116 (M^+-Cl-CH_2-C), 90 (M^+-Cl-CH_2-C-HC=CH).

2-Chloromethyl-pyridine (50)

In a one-necked round-bottomed flask (100 ml) equipped with a magnetic stirring bar and a heating mantel was added **49** (0.50 ml, 5.20 mmol) dissolved in thionyl chloride (5 ml). The reaction mixture was stirred under inert atmosphere at room temperature for 24 hours. After completion the pH of the reaction mixture was brought *Very Slowly* to 7 by saturated $NaHCO_3$, extracted with CH_2Cl_2 (3 x 5 ml) and the combined organic layers were washed with water and dried over $MgSO_4$. After filtration and evaporation the red coloured product that was obtained was dried under vacuum (0.86 g, 84%). ^{1}H-NMR($CDCl_3$): 8.52-8.50 (d, 2H), 7.68-7.62 (dt, 1H), 7.41-7.38 (d, 1H), 7.19-7.14 (dt, 1H), 4.61 (s, 2H); ^{13}C-NMR; GC-MS: 127/129 (M^+), 92 (M^+-Cl), 78 (M^+-Cl-CH2), 65 (M^+-Cl-CH_2-CH), 51 M+-Cl-CH_2-CH-N).

2.6 References

1. J. Andres, Z. Belen, A. Ibnacio and M. Antonio, *Journal of Medical Chemistry*, 48, **2005**, 2019

2. C. Bailly, S. Echepare, F. Gago and M. Waring, *Anti-Cancer Drug Design*, 15, **1999**, 291

3. G. Sakata, K. Makino and Y. Kurasawa, *Heterocycles*, 27, **1988**, 2481-2515

4. E. D. Brock, D. M. Lewis, T. I. Yousaf and H. H. Harper, *The Procter and Gamble Company, USA*, WO 9951688, **1999**,

5. T. R. Kazunobu, O. Tomohiro and M. Shuichi, *Chemical Communications*, **2002**, 212

6. S. Louis, M. G. Marc, J. W. Jory and P. B. Joseph, *Journal of Organic Chemistry*, 68, **2003**, 4179

7. K. R. J. Thomas, V. Marappan, T. L. Jiann, C. Chang-Hao and T. Yu-ai, *Chemical Materials*, 17, **2005**, 1860

8. D. O'Brien, M. S. Weaver, D. G. Lidzey and D. D. C. Bradley, *Applied Physical Letters*, 69, **1996**, 881

9. S. Dailey, J. W. Feast, R. J. Peace, R. C. Raga, S. Till and E. L. Wood, "Synthesis and device characterisation of side-chain polymer electron transport materials for organic semiconductor applications", *Journal of Materials Chemistry*, 11, **2001**, 2238-2243

10. J. K. Stille, *Macromolecules*, 14, **1981**, 870

11. F. W. Harris and J. E. Korleski, *Polym. Mat. Sci. Eng. Proc.*, 61, **1989**, 870

12. B. S. Kim, J. E. Korleski, Y. Zhang, D. J. Klein and F. W. Harris, "Development of a new poly(phenylquinoxaline) for adhesive and composite applications", *Polymer*, 40, (16), **1999**, 4553-4562

13. R. S. Robinson and R. J. K. Taylor, *Synlett*, 6, **2005**, 1003-1005

14. L. Mao, H. Sakurai and T. Hirao, "Facile synthesis of 2,3-disubstituted quinoxalines by Suzuki-Miyaura coupling", *Synthesis-Stuttgart*, (15), **2004**, 2535-2539

15. J. Ji and K.-I. Lee, "A Facile Entry to Quinoxalines from Oxalyl Chloride", *Journal of the Korean Chemical Society*, 49, (2), **2005**, 150-154

16. S. Antoniotti and E. Dunach, "Direct and catalytic synthesis of quinoxaline derivatives from epoxides and ene-1,2-diamines", *Tetrahedron Letters*, 43, (22), **2002**, 3971-3973

17. H. McNab, "The Thermolysis of Polyazapentadienes .2. Formation of Quinoxalines from 5-Aryl-1-Phenyl-1,2,5-Triazapentadienes", *Journal of the Chemical Society-Perkin Transactions 1*, (8), **1982**, 1941-1945

18. D. Armesto, W. M. Horspool, M. Apoita, M. G. Gallego and A. Ramos, *Journal of Chemical Society Perkin Trans.*, 1, **1989**, 2035-2038

19. A. J. Maroulis, Domzatidou, K.C., Hadjiantoniou-Maroulis, C.P., "Synthesis of 2,3-Diphenylquinoxaline 1-Oxides by Oxidative Cyclization of Benzil a-Arylimino Oximes", *Synthesis*, **1998**, 1769-1772

20. N. P. Xekoukoulotakis, Hadjiantoniou-Maroulis, C.P., Maroulis, A.J., "Synthesis of quinoxalines by cyclization of alfa-arylimino oximes of alfa-dicarbonyl compounds", *Tetrahedron. Lett.*, 41,, **2000**, 10299-10302

21. J. Clayden, N. Greeves, S. Warren and P. Wothers, "Organic Chemistry", *Oxford University Press Inc.*, New York, **2001**,

22. R. D. Gandour, *Tetrahedron*, 36, **1980**, 1001-1009 and references therein

23. M. Jonforsen, "Synthesis and Characterisation of Conjugated Polymers with High Electron Affinity", *Ph.D. dissertation*, Chalmers University Of Technology, **2002**

24. M. J. Edelmann, J. M. Raimundo, N. F. Utesch, F. Diederich, C. Boudon, J. P. Gisselbrecht and M. Gross, "Dramatically enhanced fluorescence of heteroaromatic chromophores upon insertion as spacers into oligo(triacetylene)s", *Helvetica Chimica Acta*, 85, (7), **2002**, 2195-2213

25. W. Szczepankiewicz,"Scientific Report; Investigation of new routes for synthesis if new classes of polyphenylenevinylene and polyquinoxalinevinylene materials", *Scientific report,* Hasselt University, **2002**,

26. COVION,"3,6-dibromo-1,2-phenylenediamine", Covion Report, reference number AP 3053; G 865 L008, **2001**,

27. M. Jonforsen, T. Johansson, L. Spjuth, O. Inganas and M. R. Andersson, "Synthesis and characterization of poly(quinoxaline vinylene)s and poly(pyridopyrazine vinylene)s with phenyl substituted side-groups", *Synthetic Metals*, 131, (1-3), **2002**, 53-59

28. S. V. More, M. N. V. Sastry, C. C. Wang and C. F. Yao, "Molecular iodine: a powerful catalyst for the easy and efficient synthesis of quinoxalines", *Tetrahedron Letters*, 46, (37), **2005**, 6345-6348

29. R. S. Bhosale, S. R. Sarda, S. S. Ardhapure, W. N. Jadhav, S. R. Bhusare and R. P. Pawar, "An efficient protocol for the synthesis of quinoxaline derivatives at room temperature using molecular iodine as the catalyst", *Tetrahedron Letters*, 46, (42), **2005**, 7183-7186

30. G. Venugopal, "New Methods for the Synthesis of Substituted Nitriles", *http://etd1.library.duq.edu/theses/submitted/etd-06302003-144025/unrestricted/GudipatiThesis.pdf*, electronic, **03.05.2006**

31. Z. Olomi, "Synthese en Polymerisatie van Cyano-PPV", *Bachelor's dissertation*, UHasselt, **2001**

32. B. S. Furniss, A. J. Hannaford, P. W. G. Smith and A. R. Tatchell, Vogel's textbook of practical organic chemistry, *John Wiley and Sons*, New York, 5th edition, **1989**, 1076

33. S. Gillissen, "New Poly(arylene vinylene)derivatives via the sulphinyl precursor route", *Dissertation*, Hasselt University, **2002**

34. L. T. Scott, P. C. Cheng, M. M. Hashemi, M. S. Bratcher, D. T. Meyer and H. B. Warren, "Corannulene. A three-step synthesis", *Journal of the American Chemical Society*, 119, (45), **1997**, 10963-10968

35. J. Wouters, "Anionische en Radicalaire mechanismen in de Polymerisatie van MDMO-PPV", *Pre-PhD dissertation*, Hasselt University, **2006**

36. A. Palmaerts,"Synthesis of 7,10-bis(chloromethyl)fluoranthene", *intern report,* UHasselt, **2005**,

37. A. Henckens, I. Duyssens, L. Lutsen, D. Vanderzande and T. J. Cleij, "Synthesis of poly(p-phenylene vinylene) and derivatives via a new precursor route, the dithiocarbamate route", *Polymer*, 47, (1), **2006**, 123-131

38. D. W. Hawkins, B. Iddon, D. S. Longthorne and P. J. Rosyk, "Synthesis of Thieno-[2,3-B]-Thiophene, Thieno-[3,2-B]-Thiophene and Thieno-[3,4-B]-Thiophene and Thieno-[3',2'/4,5]-Thieno[3,2-D]Pyrimidin-7(6h)-One, Thieno-[2',3'/4,5]-Thieno[3,2-D]Pyrimidin-7(6h)-One and Thieno-[3',4'/4,5]-Thieno[3,2-D]Pyrimidin-7(6h)-One Starting from Thiophene", *Journal of the Chemical Society-Perkin Transactions 1*, (19), **1994**, 2735-2743

39. F. Mohanazadeh, M. Hosini and M. Tajbakhsh, "Sodium borohydride - ammonium carbonate: An effective reducing system for aldehydes and ketones", *Monatshefte Fur Chemie*, 136, (12), **2005**, 2041-2043

40. D. Vanderzande, *Dissertation thesis*,

41. F. T. Luo and A. Jeevanandam, "Simple transformation of nitrile into ester by the use of chlorotrimethylsilane", *Tetrahedron Letters*, 39, (51), **1998**, 9455-9456

Chapter Three

3. Exploring the Dithiocarbamate Route as an Entry Toward Plain Quinoxaline Phenylene

3.1 Introduction

Since the discovery of electro luminescence (EL) in conjugated polymers by Jeremy Burroughes and co-workers in 1990 a lot of research is being done on poly (*para*-phenylene vinylene) PPV and their related polymers.[1] PPV type materials have also become very interesting due to their wide variety of application in photovoltaic devices.[2] However, a general drawback of these conjugated polymers is that they are in principle insoluble and difficult to process. Therefore, the use of a precursor route is one of the solutions to the problem. Hereby, the soluble precursor polymer can be cast into film and thermally converted into the corresponding conjugated form. The precursor route which is suitable and used in this work is the Dithiocarbamate Precursor Route. Two issues are of great importance for the application of PPV-type conjugated polymers in photovoltaic application: the purity of the conjugated system and the ability to adapt their chemical and physical properties. This chapter will focus on both for the polymerisation of a novel conjugated polymer poly (*p*-quinoxaline vinylene) PQV. This polymer shows promising characteristics in use for organic solar cells.

As mentioned in chapter one, in organic solar cells, the exciton dissociation process only occurs at the donor/ acceptor interface. Hereby, the exciton diffusion lengths are small (1-10 nm)[3] and this limits the effective light-harvesting layer. Therefore, controlling the structure of the active layer (morphology) is crucial to obtain efficient devices. So far, most promising bulk heterojunctions were made of

a mixture of conjugated p-type and n-type materials or a mixture of conjugated polymer as p-type and fullerene derivatives as n-type material, Figure 3.26.[4]

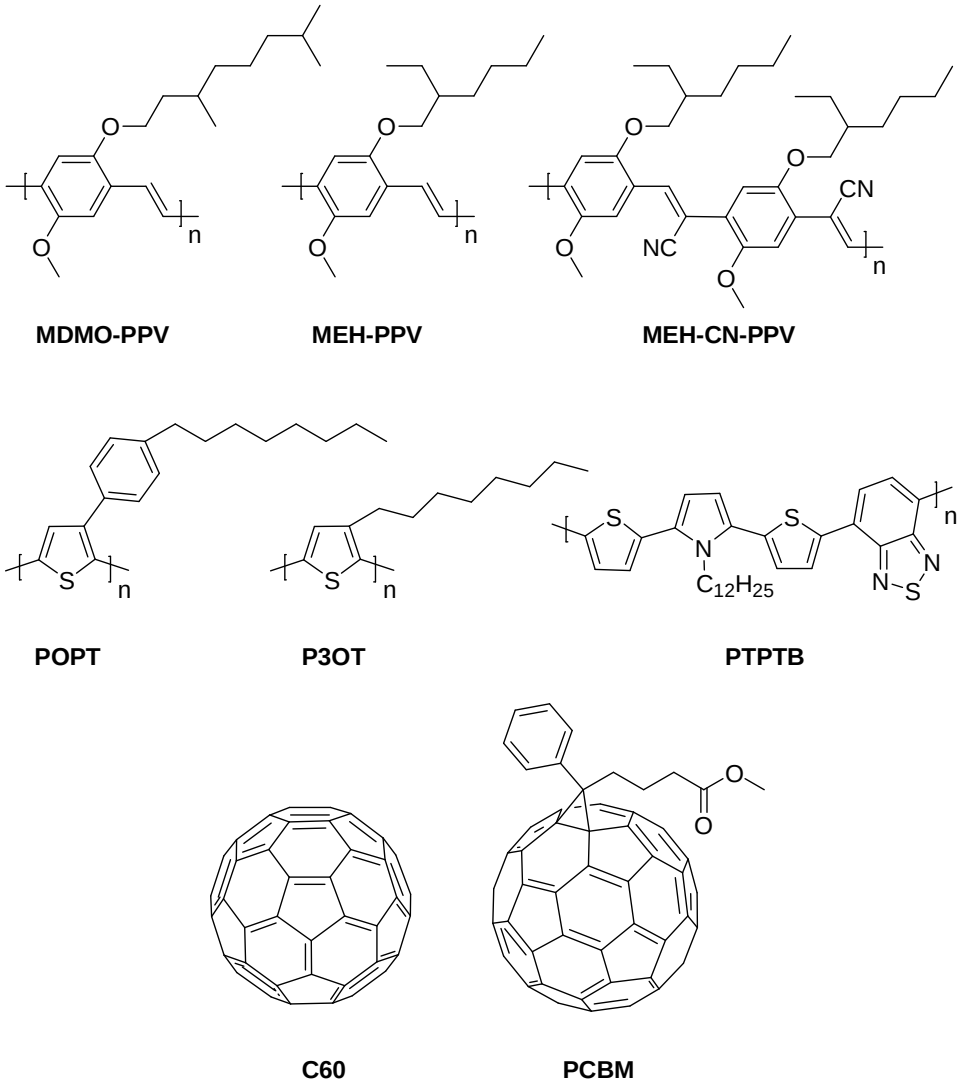

Figure 3.26: Structure of common conjugated polymers as p-type material (**MDMO**, **MEH-PPV**, **MEH-CN-PPV**, **POPT**, **P3OT** and **PTPTB**) and fullerene derivatives as n-type type material (**C60** and **PCBM**).

The last few years there is a lot of interest in the synthesis of polyquinoxaline derivatives. According to Takashi Fukuda and co-workers polyquinoxaline

derivatives **PQx** can be an excellent electron injecting material (n-type) for photovoltaic devices because it has many advantageous properties, such as high electron affinity, good thermal stability and good processability, Figure 3.27.[5]

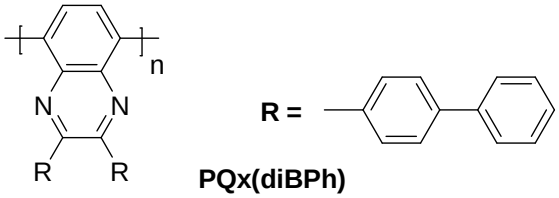

PQx(diBPh)

Figure 3.27: Chemical structure of poly(2,3-disubstituted Quinoxaline-5.8-diyl) **PQx**

Electron accepting materials should show four typical characteristics: they should have a very low LUMO (i); stabilised electrons (ii); high electron mobility (iii) and good solubility (iv). In general, there are also four known approaches in order to get an n-type material.

Approach one: Building a strong electron withdrawing group in the backbone of the polymer, such as cyano groups in poly (*para*-phenylene vinylene), Figure 3.28.

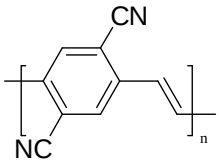

Figure 3.28: poly (*para*-dicyanophenylene-vinylene) (CN-PPV)

Approach two: building of a non-alternating polyaromatic group, such as poly (*para*-fluorantheen-vinyleen) (PFV). In the fluoranthene structure a fragment of C60 can be recognised, see Figure 3.29.

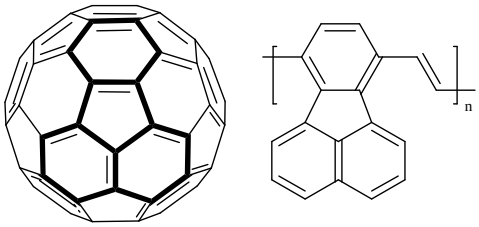

Figure 3.29: C60 and poly(*p*-fluorantheen-vinyleen) (PFV)

Approach three: building of polyaromatic systems, such as the structure of poly (perilynene-vinylene), Figure 3.30.

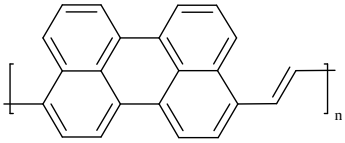

Figure 3.30: poly (perilynene-vinylene)

Approach four: building of aromatic structures, by replacing carbon atoms by electronegative elements (N), Figure 3.31.

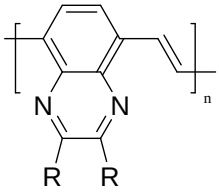

Figure 3.31: poly (*p*-quinoxaline vinylene) PQV

As mentioned before, polyquinoxaline derivatives with their high electron affinity belong to the class of n-type materials and can be assigned to the fourth approach mentioned above. There are different routes leading to the preparation of polyquinoxalines. According to literature polyquinoxaline derivatives are a well-established class of high-performance thermoplastics with high chemical and thermal stability[6, 7]. However, they have not found wide-spread use primarily due to the high cost of the tetraamines and tetraketones used in their synthesis. In fact, tetraketones are not commercially available. The polymerisations are also run via the Friedlander Reaction in an undesirable solvent (e.g. *m*-cresol), Scheme 3.37.

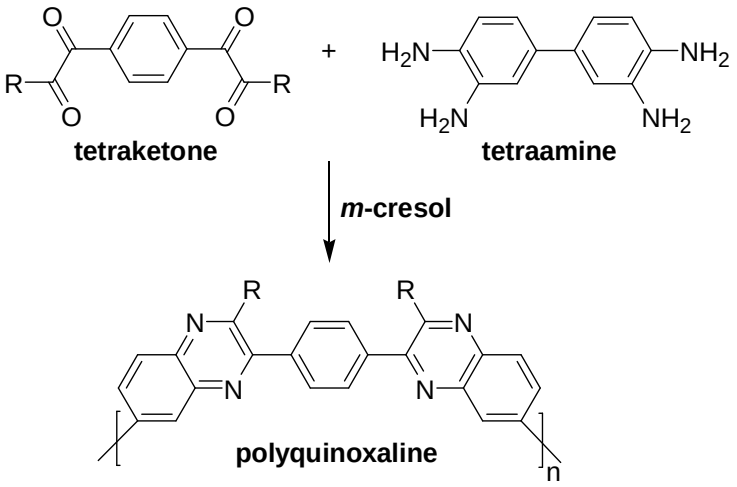

Scheme 3.37: Thermally Stable Polymers via the Friedlander Reaction

In 1989, Harris and Korleski were the first ones that polymerised the self-polymerisable monomer mixture of 2-(4-hydroxyphenyl)-3-phenyl-6-fluoroquinoxaline (**a**) and 3-(4-hydroxyphenyl)-2-phenyl-6-fluoroquinoxaline (**b**) in the presence of potassium carbonate into poly(aryl ether phenylquinoxaline) PPQ – a polyquinoxaline derivative - in an overall yield of 11%, Scheme 3.38.[8] Later, this route was optimised by Kim and co-workers. They obtained high glass transition temperature (Tgs) of 250-252°C and high mechanical properties which is an excellent combination for a high performance application[9].

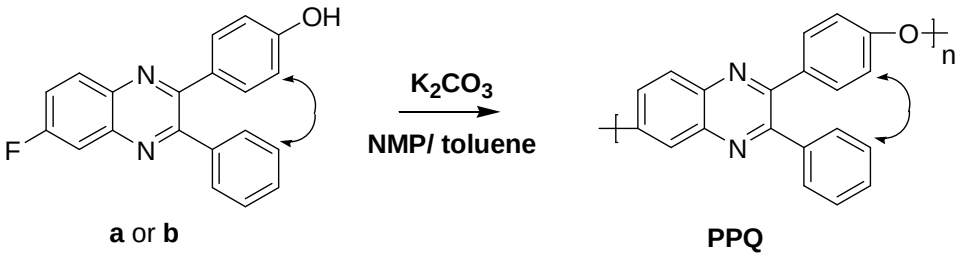

Scheme 3.38: Self-polymerisation of monomer mixture 2-(4-hydroxyphenyl)-3-phenyl-6-fluoroquinoxaline (**a**) and 3-(4-hydroxyphenyl)-2-phenyl-6-fluoroquinoxaline (**b**) into poly(aryl ether phenylquinoxaline) **PPQ**.

The same Tg (252°C) was obtained by the group of Klein and co-workers. They prepared the self-polymerisable monomer mixture of 2-(4-hydroxyphenyl)-3-phenyl-6-chloroquinoxaline (**c**) and 3-(4-hydroxyphenyl)-2-phenyl-6-chloroquinoxaline (**d**) and polymerised this in the presence of potassium carbonate and freshly prepared copper(I)chloride/quinoline catalyst mixture under Ullman ether coupling conditions in high yield, Scheme 3.39.[10]

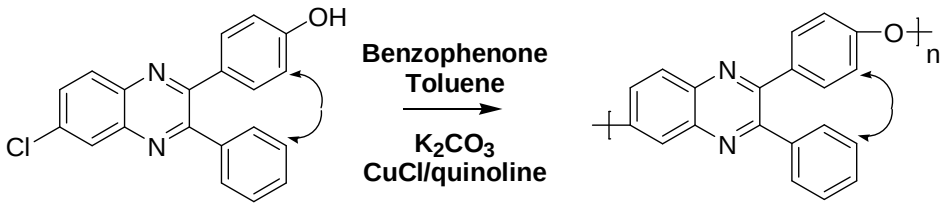

c or **d** **PPQ**

Scheme 3.39: Self-polymerisation of monomer mixture 2-(4-hydroxyphenyl)-3-phenyl-6-chloroquinoxaline (**c**) and 3-(4-hydroxyphenyl)-2-phenyl-6-chloroquinoxaline (**d**) into poly(aryl ether phenylquinoxaline) **PPQ**.

Also palladium- catalysed cross-coupling reactions were applied for the polymerisation of Quinoxalines via cross-coupling reactions, such as Stille reaction [11, 12], Sonogashira reaction [13], Suzuki reaction[14] and Heck[15] reactions. Although the polymers showed high fluorescence only oligomers were obtained using these palladium- catalysed cross-coupling routes. Few examples are depicted in Scheme 3.40 and Scheme 3.41.

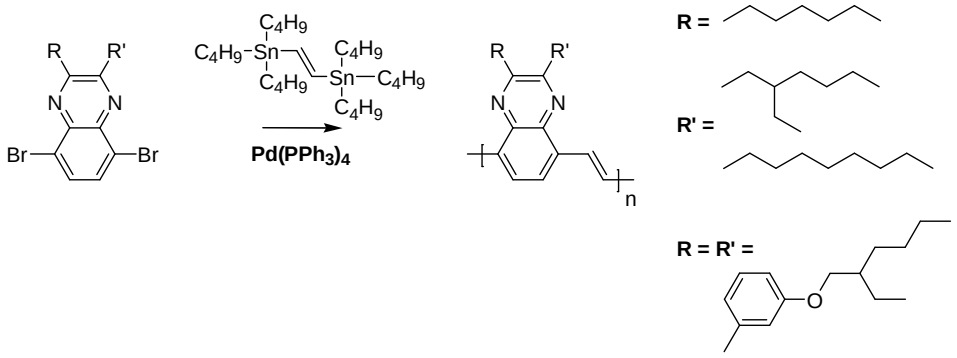

Scheme 3.40: Poly(quinoxaline vinylene)s synthesised via Stille cross-coupling.

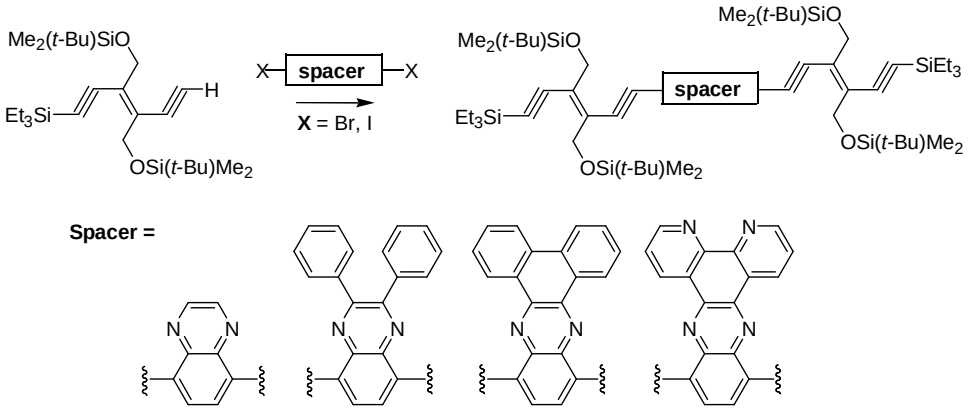

Scheme 3.41: Synthesis of hybrid oligomers of poly(quinoxaline)s via Sonogashira cross-coupling.

Baek and Chien obtained polymers with fluorescence maxima in the range of 431-449 nm with relatively narrow peak widths. This indicated that they had pure and intense fluorescence in both solution and solid states. The polymers obtained (Scheme 3.42) had thermal stability up to 350°C making them good candidates for the fabrication of optoelectronic devices emitting blue light[16].

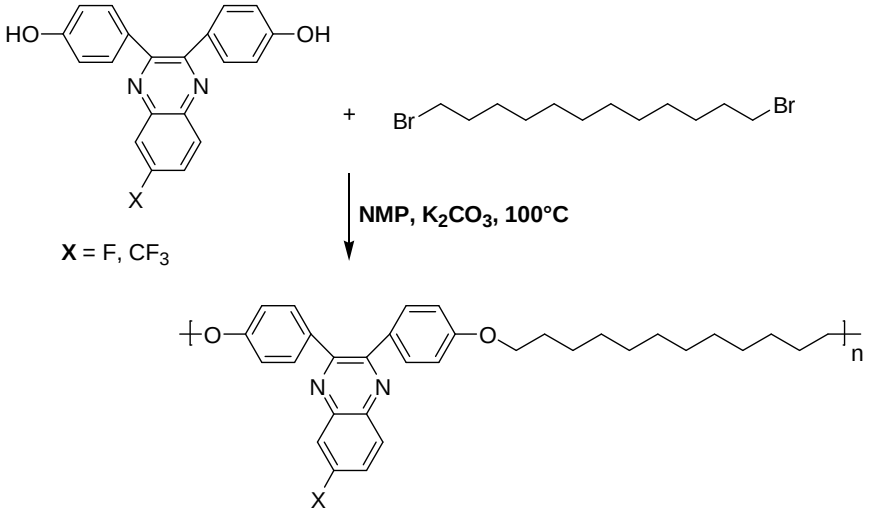

Scheme 3.42: Synthesis of the linear hyperbranched polyether containing phenylquinoxaline units with flexible aliphatic spacers.

In 2005 Gubbelmans and co-workers published an article on poly(phenylquinoxalines) for second-order nonlinear optical applications[17]. They synthesised new soluble chromophore-functionalised polymers with an average molecular weight between 5.500-31.000 g/mol by cyclopolycondensation of the respective bis(1,2-diketone)chromophore monomers with tetramine in *m*-cresol, Figure 3.32. The polymer exhibit high Tg (187-260°C) which makes them a good candidate for device application in the field of electro-optics and photonics.

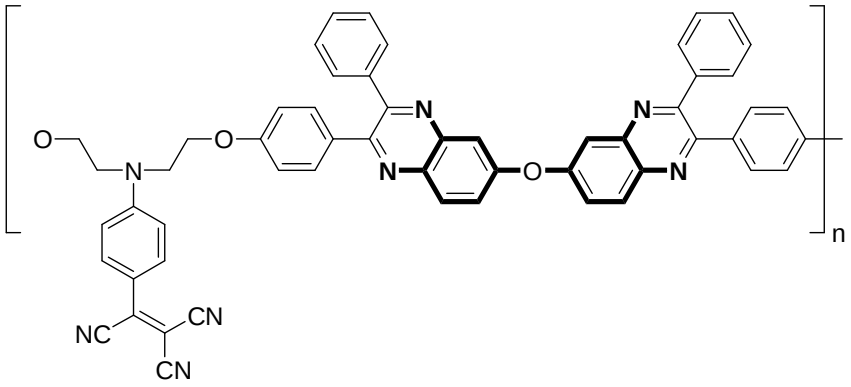

Figure 3.32: Structure of non-linear optical poly(phenylquinoxaline) prepared from by reaction of bis(1,2-diketone) chromophore monomer and tetramine (in bold) at room temperature.

Among the polyquinoxaline derivatives, poly (*p*-quinoxaline vinylene) PQV is the one which will be discussed in detail in this chapter. In this chapter efforts are made to present results concerning the synthesis and characterisation of PQV. In this work, the monomers were polymerised to their soluble precursor polymers via the Dithiocarbamate Precursor Route in high purity and high average molecular weights.

The conversion step, which leads to the final conjugated polymer, can be divided into two consecutive steps, the elimination and the evaporation of the polarizer, which was studied in detail by Margreet de Kok (in 1999) and Els Kesters (in 2002) in the case of sulphinyl precursor route[18, 19]. This conversion step can be monitored by several *in situ* techniques such as UV-Vis, FT-IR and ^{1}H-NMR.

3.2 Polymerisation

The bis-dithiocarbamate quinoxaline monomer **1** was synthesised in good yield and purity as described in chapter two. The monomer was purified by column chromatography with hexane/ $CHCl_3$ (9/1) as eluent. The polymerisation of the bis-dithiocarbamate quinoxaline monomer **1** is depicted in Scheme 3.43. The polymerisation was performed in a three-necked flask. The monomer was dissolved in dried THF and degassed by passing through a continuous nitrogen stream. A solution of base (2 M LDA solution in THF/n-hexane or, 1 M LHMDS solution in THF) was added in one go through a septum. Then, the reaction was stirred at a given temperature for 90 minutes under nitrogen atmosphere. After this time, the mixture was poured out in ice water in order to stop the reaction. The crude product was dissolved again in chloroform, and afterwards precipitated in methanol at 0 °C, then collected and dried in vacuo.

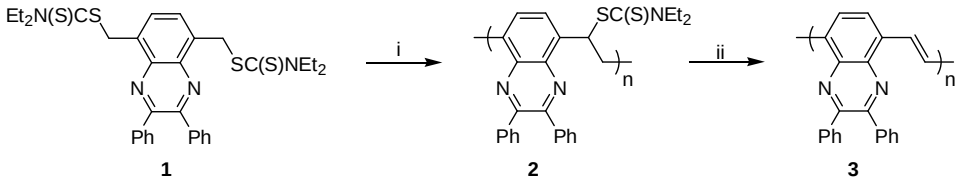

Scheme 3.43: Synthesis of the dithiocarbamate precursor polymer **2** and poly (*p*-quinoxaline vinylene) **PQV 3**: i) LDA or LHMDS, THF; ii) ΔT

The polymerisation results are presented in Table 3.2 , Table 3.4 and Table 3.5. The average molecular weights were determined by size exclusion chromatography (SEC) with dimethylformamide (DMF) as eluent against polystyrene standards. The M_w values reported in the table are average values between experiments done in duplo. The experiments done in the same conditions showed a very good reproducibility.

Polymer	Entry	LDA (eq.)	T (°C)	Mw (g/mol)	PD	Yield (%)
2	**1**	1	0	4000[a]	1.1	64
	2	2	0	4000[a]	1.2	82
	3	4	0	4000[a]	1.1	98
	4	1	0	4000[b]	1.2	74
	5	2	0	5000[b]	1.2	99
	6	4	0	4000[b]	1.1	72

[a] monomer concentration (0.2 M), [b] monomer concentration (0.4 M)

Table 3.2: Polymerisation results for 2 with the use of LDA as the base

Using different equivalent of LDA (1 or 2 equivalent) with different monomer concentration (0.2 or 0.4 M) at 0°C the polymerisation of **1** led only to the formation of oligomers – low average molecular weight (M_w ± 4000 g/mol). Therefore there was no use in deriving the λ_{max} values from *in situ* UV-Vis measurements. The precursor polymers were analysed by ^{1}H-NMR, the residual fraction showed only the presence of unreacted monomer and their chemical shifts are listed in Table 3.3.

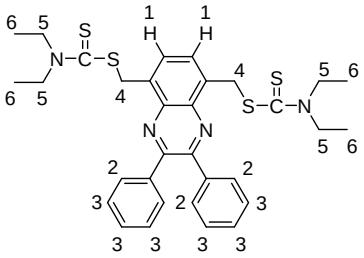

Proton	1H δ (ppm)
1; 2H, s	7.91
2; 4H, dt	7.60
3; 6H, m	7.34
4; 4H, t	5.28
5; 8H, dq	4.05/ 3.71
6; 12H, m	1,28

Table 3.3: 1H-NMR chemical shift values of 1

In the course of this work the use of an alternative base, *e.g.* Lithium Bis(trimethylsilyl)amide (LHMDS)[20] was suggested. Preliminary studies showed that the use of LHMDS (Table 3.4) instead of LDA yielded the precursor polymer **2** into excellent yield and reasonable high average molecular weight M_w especially at 0 °C. The λ_{max} values were derived from *in situ* UV-Vis measurements and give an indication on the quality of the materials made. The absorption value is directly correlated to the effective conjugation length of the polymer. The Mw values depicted in the table are average values between experiments done in duplo. The experiments done in the same conditions showed a very good reproducibility.

Polymer	Entry	LHMDS (eq.)	T (°C)	Mw (g/mol)	PD	Yield (%)
2	7	1	30	7000[a]	1.7	74
	8	1	30	6000[b]	1.5	84
	9	2	30	9000[a]	1.6	84
	10	1	0	9000[a]	2.0	84
	11	1	-15	8000[a]	2.1	58
	12	1	0	23000[a]	2.6	92
	13	1	0	44000[c]	2.6	99
	14	2	0	21000[a]	2.2	99
	15	2	0	21000[c]	2.4	99
	16	4	0	18000[a]	2.0	99
	17	4	0	19000[c]	2.1	99

[a] monomer concentration (0.2 M), [b] monomer concentration (0.3 M), [c] monomer concentration (0.4 M)

Table 3.4: Polymerisation results for **2** with the use of LHMDS as the base and less pure monomer **1**.

These data demonstrate that: using different monomer concentrations (0.2; 0.3 or 0.4 M) has no effect on the yield and average molecular weight of the polymer. As example compare entries 14 and 15, hereby similar average molecular weight and yields are obtained. Comparing the results on Table 3.4 it is clear that also the

equivalent of the base and the temperature are not significant for the polymerisation.

More important, the main significant parameter in these polymerisations is the type of base. Using LDA as base (Table 3.2) results in the formation of oligomers, while using LHMDS as base (Table 3.4) results mainly in the formation of polymers with good average molecular weights. These materials may be good candidates for further applications. According to Banishoeib the main advantage of using LHMDS instead of LDA relate to the opportunity to increase the reaction temperature from -78 °C to 0 °C, which is very important for a possible industrial application of this route[20]. It has to be noticed that the values of polydispersity (PD) are mainly constant using different parameter conditions. Only the λ_{max} of entry 7 till 11 (Table 3.4) was determined by *in situ* UV-Vis which was equal to 536, 557, 545, 552 and 562 nm respectively. As mainly oligomers were formed, further physical characterisation of these oligomers and polymers was not determined.

It has to be noticed that after the preparation of the bis-dithiocarbamate quinoxaline monomer **1** it cost a lot of effort to purify the monomer. From the analysis of **1** by thin layer chromatography (TLC) on silica plate in different mixtures of solvents the presence of two products with very close relative retention factor (R_f) values could be clearly observed. One product is the actual monomer **1** and the other one is a possible contamination of the monomer. Among the presence of other extra peaks in the aliphatic area from ^{1}H-NMR analysis, this is also clear from the appearance of an extra peak around 5.34 ppm (Figure 3.33).

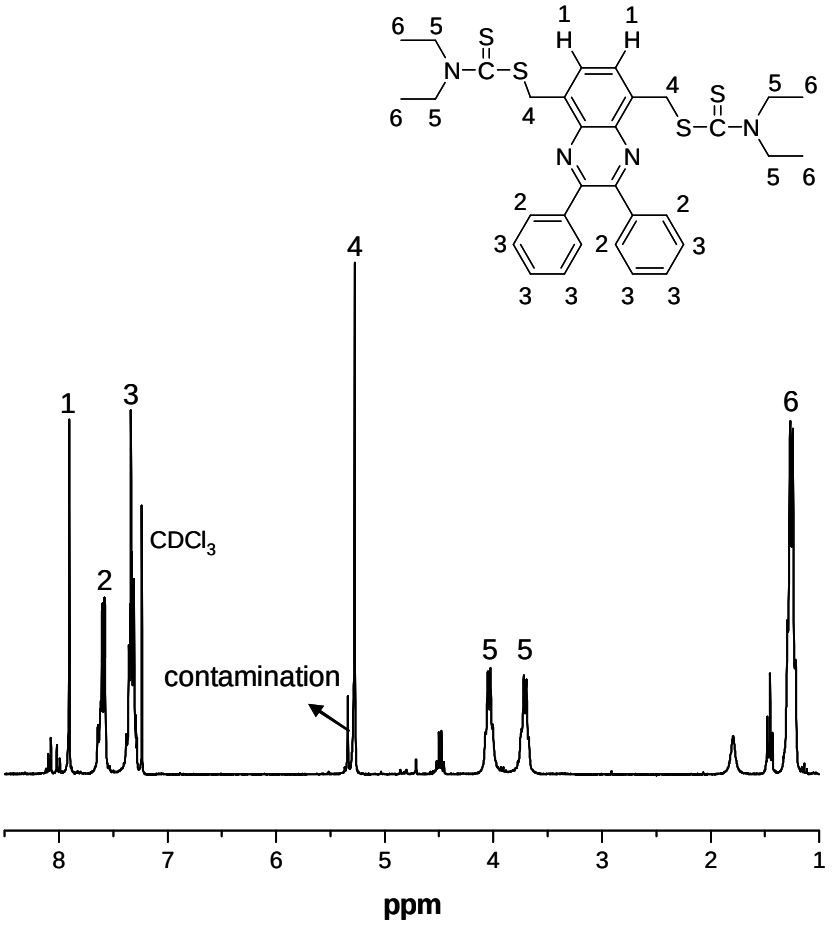

Figure 3.33: ^{1}H-NMR of the impure monomer **1**

In order to get higher average molecular weights for PQV different parameters were evaluated. Unfortunately the analysed residual fraction showed mainly the remaining monomer which is depicted in Figure 3.34. Possible explanation for the low average molecular weight is the presence of a contamination in the monomer. Therefore, the monomer was purified several times by crystallisation from a mixture of hexane/ $CHCl_3$ (7/3). Hereby pure crystals were obtained which can also be observed from the ^{1}H-NMR analysis of this fraction (Figure 3.35).

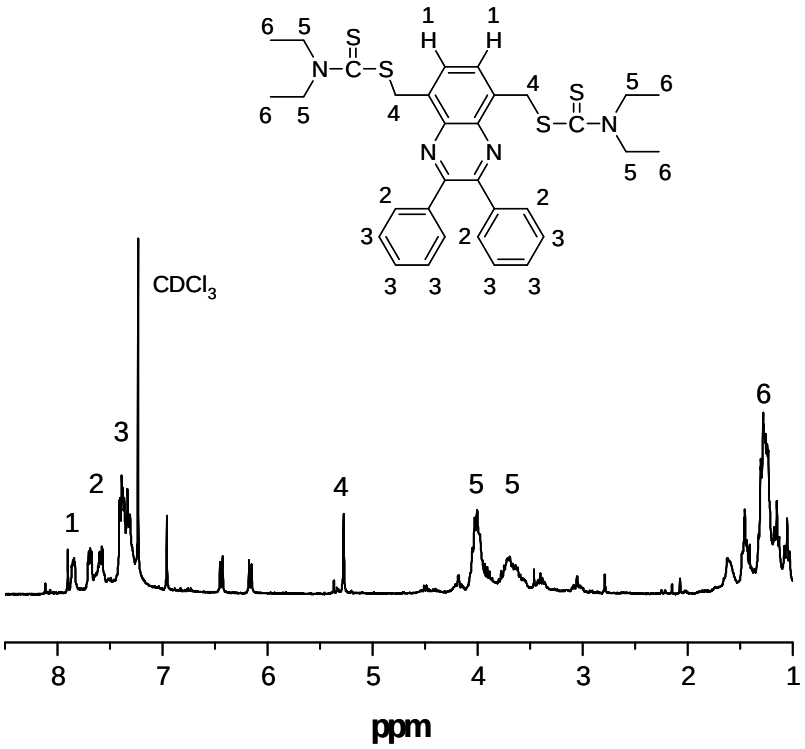

Figure 3.34: ^{1}H-NMR of the residual fraction after polymerisation of PQV with impure monomer

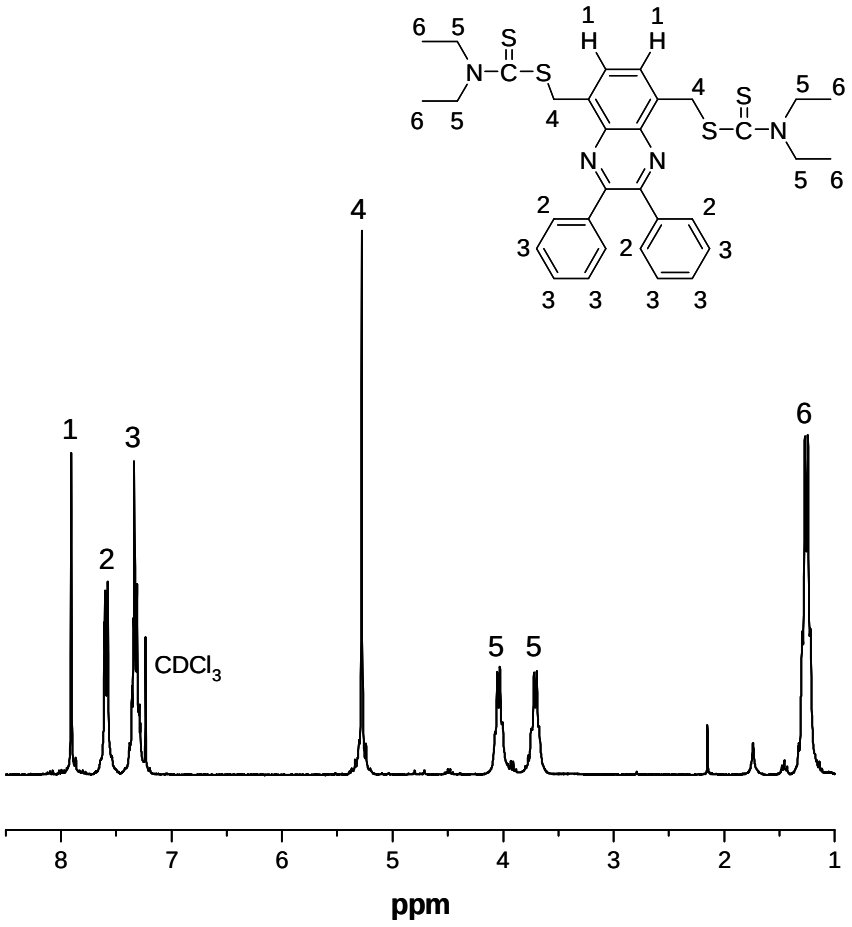

Figure 3.35: ^{1}H-NMR of the pure monomer **1**

The pure monomer **1** that was obtained was used for the polymerisation of the precursor polymer **2** with high yield in high average molecular weight that can be depicted in Table 3.5. The analysed residual fraction of these polymerisations showed only a small fraction of the remaining monomer. As a comparison also the ^{1}H-NMR spectrum of this residual fraction is reported, Figure 3.36.

Polymer	Entry	LHMDS (eq.)	T (°C)	Mw (g/mol)	PD	Yield (%)
2	18	1	0	56000[a]	3.4	84
	19	1	40	34000[a]	2.5	96
	20	1	0	50000[b]	3.3	82
	21	1	-30	42000[a]	3.4	76
	22	2	0	45000[a]	3.2	90
	23	2	0	42000[b]	3.2	84
	24	4	0	41000[a]	3.2	88
	25	4	0	44000[b]	3.3	87

[a] monomer concentration (0.2 M), [b] monomer concentration (0.4 M)

Table 3.5: Polymerisation results for **2** with the use of LHMDS as the base and pure monomer

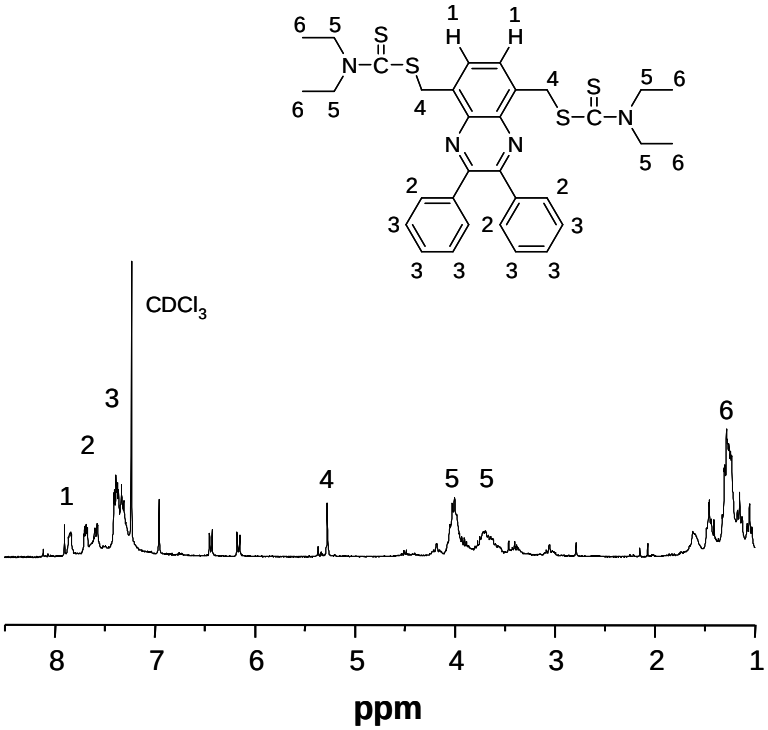

Figure 3.36: ^{1}H-NMR of the residual fraction after polymerisation of **PQV** with pure monomer

From these data it can be noticed that the change in monomer concentration (0.2 or 0.4 M) has no effect on the average molecular weight and yield of the precursor polymer (see entry 18 and 23). Concerning the base LHMDS, different equivalents were used for the polymerisation leading to comparable results as shown on Table 3.5 (entries 20, 22 and 25). The temperature can have a small significant effect on the polymerisation as working at 0°C seems to give slightly better results compared to other temperature conditions (see entry 18, 19 and 21). The λ_{max} was determined only for the entries 18 and 19 (Table 3.5) due to lack of time which was 532 and 534 nm respectively.

The additional purification step on the monomer leads to a big effect on the average molecular weight M_w of the polymer. Hereby, the average molecular weight of the polymers effectively doubles in reproducible manner. Also from the GPC chromatogram (Figure 3.37) it can be clearly seen that using an impure monomer leads mainly to oligomers while using a pure monomer leads mainly to high M_w polymers.

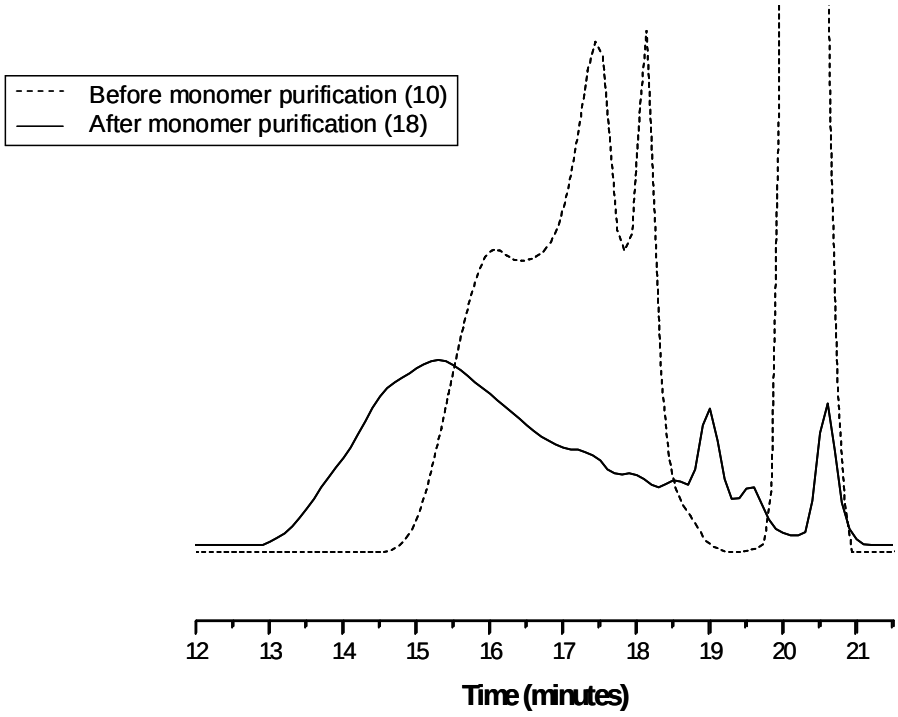

Figure 3.37: GPC chromatogram before and after purification of the monomer.

The results above are at odds with previous observations. In general most of the polymerisation reactions of the *p*-quinodimethane *p*-QM systems proceed via a self initiated radical polymerisation. Such radical polymerisations are rather insensitive to the presence of small amounts of impurities[21]. However, some earlier polymerisations via the dithiocarbamate precursor route carried out in our research group by Banishoeib, showed the possibility for the presence of an anionic mechanism next to the radical one[20]. Banishoeib observed in such cases a bimodal distribution for the precursor polymer of poly (2,5-thienylene vinylene) PTV, which according to her could be explained by the presence of two mechanisms taking place simultaneously. Moreover, according to her this bimodal behaviour from a radical polymerisation mechanism giving the high molecular weight fraction and

anionic mechanism giving the low molecular weight fraction. However, in our case in GPC only monomodal behaviour was observed, Figure 3.37.

Furthermore, the molecular weight obtained seems to be quite sensitive for the presence of impurities. This seems more consistent with the occurrence of a purely anionic polymerisation mechanism. Also the lack of sensitivity of the molecular weight toward monomer concentration seems to point in this direction. However, further elaboration of this hypothesis is part of future work.

3.3 Characterisation

3.3.1 Thermal conversion of the precursor polymer into the conjugated structure

To finalise the polymerisation one last step needs to be carried out which is the thermal conversion of the precursor polymer **2** to the conjugated polymer **3** (Scheme 3.44). Hereby, the thermal elimination of the polarizer group, i.e. the dithiocarbamate group takes place.

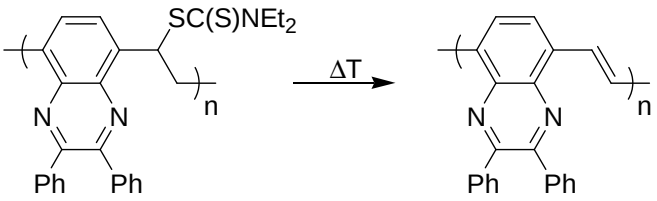

2 **3**

Scheme 3.44: Conversion step of the precursor polymer 2 to the conjugated polymer **3.**

The thermal conversion to the conjugated structure has been studied by means of *in situ* UV-Vis and *in situ* FT-IR spectroscopy, during which the spin-coated precursor polymer is heated at 2 °C/ minute from ambient temperature to 350 °C

under a continuous flow of nitrogen. The temperature dependant UV-Vis spectrum and profiles of the conversion process of the precursor polymer **2** for entry 10 (Table 3.4) - that was prepared from the less pure monomer - using *in situ* UV-Vis spectroscopy are plotted in Figure 3.38 and Figure 3.39.

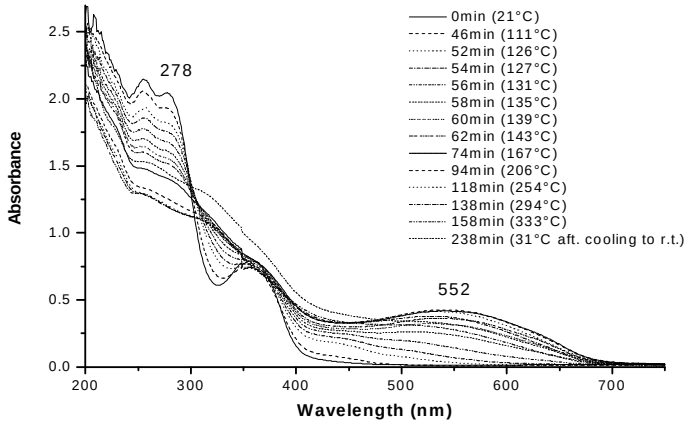

Figure 3.38: UV-VIS spectrum when ramping from RT to 350 °C and back for precursor polymer **2** (entry **10**).

The absorption maximum (λ_{max}) of PQV prepared via the dithiocarbamate precursor route is 545 nm at 333°C and 552 nm at ambient temperature, Figure 3.38. The absorbance of the absorption maximum of both the dithiocarbamate precursor polymer **2** (entry **10**) and PQV **3** are plotted as a function of increasing temperature in Figure 3.39. From this figure it can be observed, that the elimination of the dithiocarbamate groups of the precursor polymer (entry **10**) starts at 108°C and is completed at around 182°C under these heating conditions.

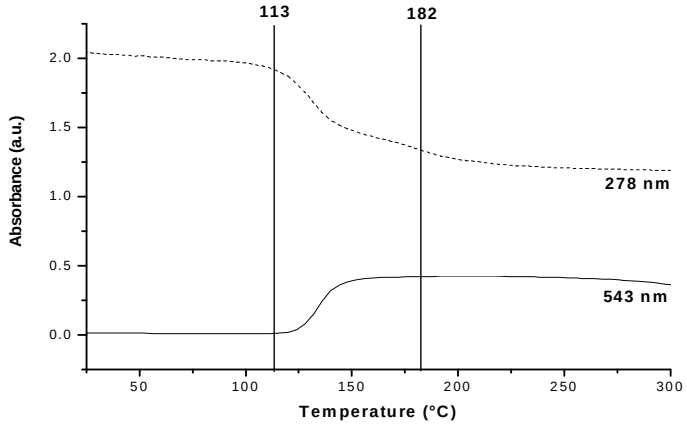

Figure 3.39: UV-Vis absorbance profiles at 278 nm and 543 nm as a function of temperature for the precursor polymer **2** (entry **10**).

In situ FT-IR spectroscopy measurements were also carried out. In Figure 3.40 and Figure 3.41 the temperature dependant IR spectra and profiles of the conversion process of the precursor polymer **2** (entry **10**) are plotted. The strong vibrations that are visible at 1484, 1416, 1268 and 1206 cm^{-1} are from the dithiocarbamate leaving group. The elimination of these the dithiocarbamate leaving group is vaguely visible by the disappearance of the mentioned vibrations after heating the precursor polymer **2**. Also it is clearly visible that a new vibration does not appear around 970-960 cm^{-1} which corresponds to the formation of the *trans*-vinylene double bond. This is also clear from the plotted profiles in Figure 3.41. Due to the use of less pure monomer for the polymerisation, low M_w polymer **2** (entry **10**) was formed which according to these *in situ* spectroscopy measurements did not result in the desired conjugated polymer **3**.

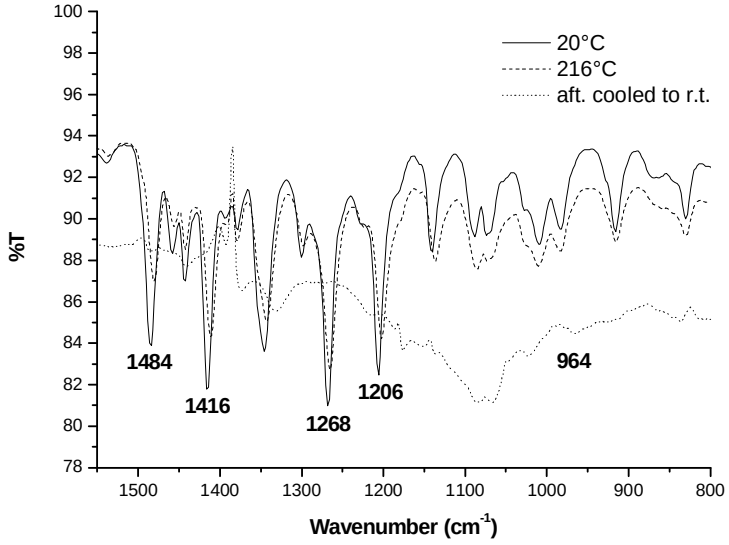

Figure 3.40: IR spectrum when ramping from RT to 350 °C and back for precursor polymer **2** (entry **10)**.

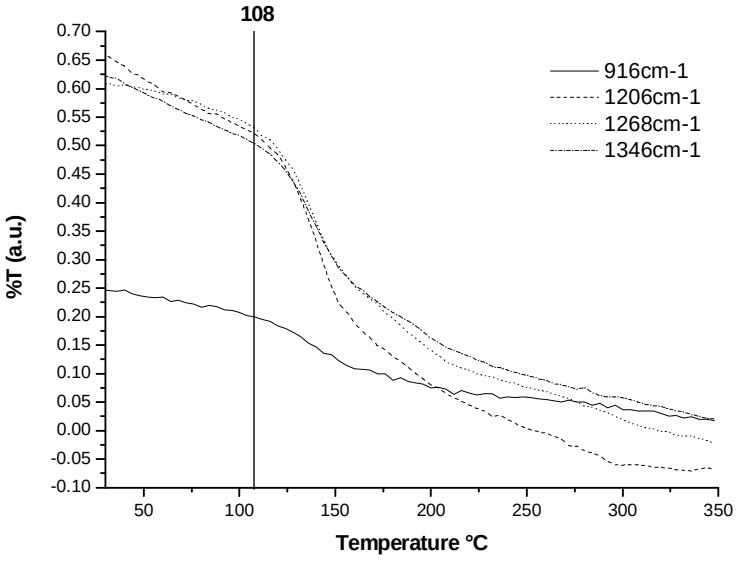

Figure 3.41: FT-IR absorbance profiles as a function of temperature for the precursor polymer **2** (entry **10)**.

Also the thermal conversion of the high M_w precursor polymer that was prepared from the pure monomer **2** (entry **18**, Table 3.5) was analysed by means of *in situ* UV-Vis and *in situ* FT-IR spectroscopy. The temperature dependant UV-Vis spectrum and profiles of the conversion process of the precursor polymer **2** (entry **18**) using *in situ* UV-Vis spectroscopy are plotted in Figure 3.42 and Figure 3.43. The absorption maximum (λ_{max}) of PQV is 531 nm at 309°C and 532 nm at ambient temperature, Figure 3.42. This λ_{max} is shifted to longer wavelength (lower energy) compared to the value of 435 nm obtained by the oligomers via the Sonogashira Cross-Coupling.[13] This is an indication of a significantly improved conjugation of the π-electron system.

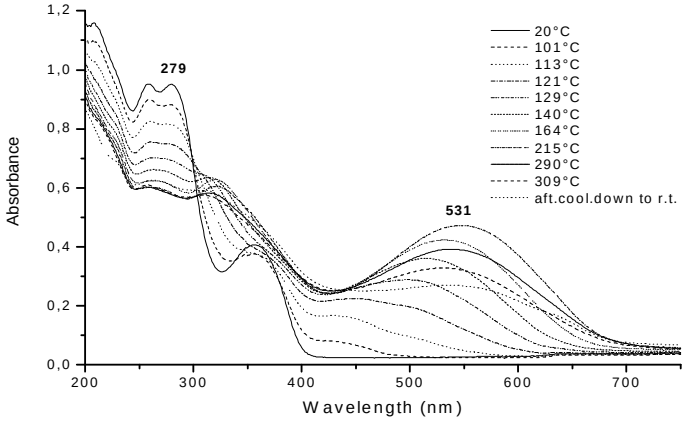

Figure 3.42: UV-VIS spectrum when ramping from RT to 350 °C and back for precursor polymer **2** (entry **18**).

It has to be noted that the optical properties of PQV are scarcely known in the literature. Still, the optical properties obtained using the dithiocarbamate precursor route are much better than those obtained using most other synthetic routes. Besides the λ_{max} also the optical band gap of PQV was determined from the UV-Vis spectroscopy data. An optical band gap of 1.81 eV was determined from the lowest energy edge of the π-π* absorption band.

The absorbance of the absorption maximum of both the dithiocarbamate precursor polymer **2** (entry **18**) and PQV **3** are plotted as a function of increasing temperature in Figure 3.43. It has to be noted, that the elimination of the dithiocarbamate groups of the precursor polymer **2** (entry **18**) starts at 109°C and it is completed at around 214°C under these heating conditions.

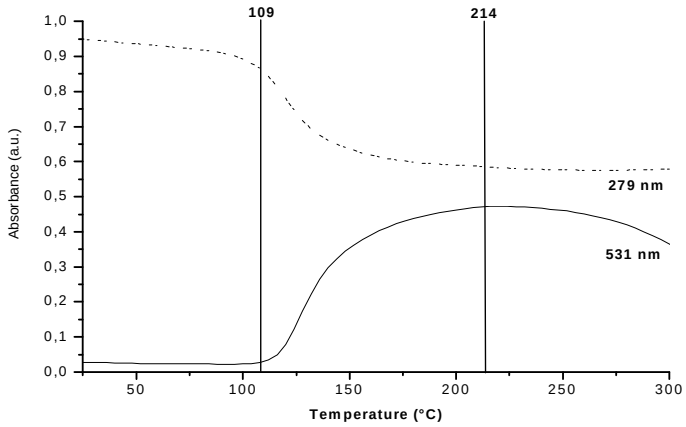

Figure 3.43: UV-Vis absorbance profiles at 279 nm and 531 nm as a function of temperature for the precursor polymer **2** (entry **18**).

The temperature dependant IR spectra and profiles of the conversion process of the precursor polymer **2** (entry **18**) using *in situ* FT-IR spectroscopy are plotted in Figure 3.44 and Figure 3.45. In the IR spectrum of **2** (entry **18**) strong vibrations arising from the dithiocarbamate leaving groups are visible at 1484, 1412, 1264 and 1206 cm^{-1} (Figure 3.44). The elimination of these the dithiocarbamate leaving groups is visible by the disappearance of the mentioned vibrations after heating the precursor polymer **2** (entry **18**). Hereby, a new vibration appears at 968 cm^{-1} which corresponds to the formation of the *trans*-vinylene double bond.

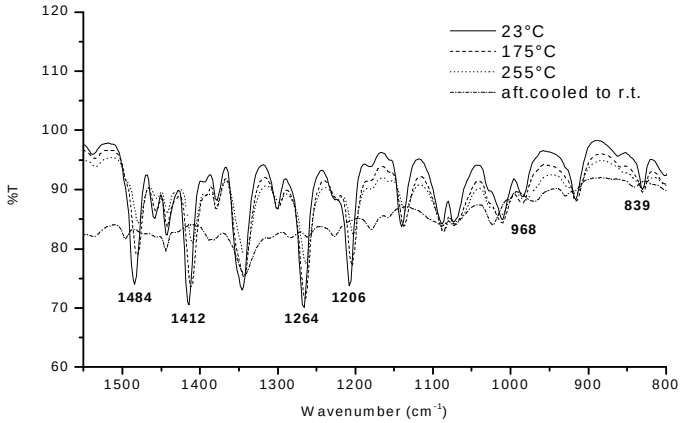

Figure 3.44: IR spectrum when ramping from RT to 350 °C and back for precursor polymer **2** (entry **18**).

Also the vibration at 839 cm^{-1} increases during the elimination process due to the *p*-phenylene C-H out-of-plane deformation. Both the decrease in the dithiocarbamate absorption and the increase in the double bond absorption start around 102°C and end around 213°C as can be seen in Figure 3.45.

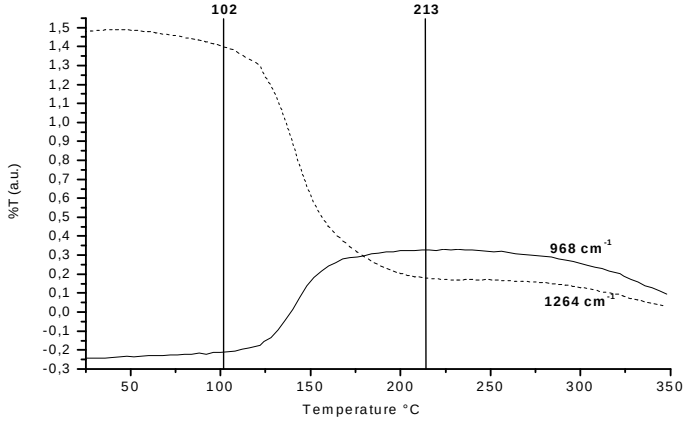

Figure 3.45: FT-IR absorbance profiles at 968 cm^{-1} and 1264 cm^{-1} as a function of temperature for the precursor polymer **2** (entry **18**).

As the functionality of a conjugated polymer depends on the stability of the conjugated system, thermal stability of the polymer is defined by the thermal stability of the chromophore. This can be directly measured by the *in situ* UV-Vis and *in situ* FT-IR measurements. From these measurements it can be noticed that PQV is thermally stable until 278°C. Once a breakdown of conjugation occurs, the conjugated polymer will not be suitable for opto-electronic applications.

3.3.2 Cyclic voltammetry

Cyclic voltammetry (CV) was applied on a PQV sample to investigate the electrochemical – Redox - behaviour of the polymers and to estimate the energy level of the highest occupied molecular orbital (HOMO) and lowest unoccupied molecular orbital (LUMO) energy levels. The electrochemical experiments were carried out in a conventional three-electrode cell using 0.1 M tetrabutylammoniumhexafluorophosphate (TBAPF6) in anhydrous acetonitrile as supporting electrolyte. The conversion was done with a temperature of 260°C under nitrogen atmosphere. The working electrode was an Indium-Tin-Oxide (ITO) coated glass substrate. The counter electrode was a platinum wire, which was placed in a separate compartment with a semi-porous frit. As a reference electrode, a silver wire in a 0.1 M AgNO3 containing electrolyte solution was used. After each measurement the reference electrode was calibrated with ferrocene (which under standard condition has an E° in the range 0.03 – 0.07 V *vs*. Ag/AgNO3). The oxidation process corresponds to the removal of electrons from the highest occupied molecular orbital (HOMO) and, it is associated with the ionisation potential (IP). Whereas, the reduction cycle corresponds to the filling by electrons of the lowest unoccupied molecular orbital (LUMO) (electron affinity EA). The onset oxidation and reduction potentials are closely related to the energies of the HOMO and LUMO levels of an organic molecule and thus can provide important information regarding the magnitude of the energy gap. The oxidation and reduction onset potentials are determined from a cyclic voltamogram. For the conversion from the oxidation and reduction potentials in Volt to an energy level in eV a large variety of calculation methods can be found in literature[22]. The energy

parameters IP (HOMO) and EA (LUMO) are related to the measured redox potentials by the equations:

$$IP = E_{HOMO} = - (E_{OX} + 4.44)eV$$

$$EA= E_{LUMO} = - (E_{RED} + 4.44)eV$$

Where the E_{OX} and E_{RED} are the oxidation and reduction potentials in volt *versus* the NHE (Normal Hydrogen Electrode) potential. The reduction potential of the reference electrode SCE (Saturated Calomel Electrode) is 0.24 V *vs*. NHE.

The Cyclic voltammogram of PQV is depicted in Figure 3.46. For PQV, the reduction peak is seen at -1.69 V *vs.* $Ag/AgNO_3$ and the re-oxidation peak is seen at -1.52 V *vs.* $Ag/AgNO_3$. The reduction process is quasi-reversible and can be repeated many times without any large degradation being noticed. The oxidation of PQV is irreversible. The onset potentials for the oxidation and the reduction are 0.42 V Ag/AgNO3 and -1.28 V *vs.* $Ag/AgNO_3$, respectively, which corresponds to a HOMO energy level of -5.35 eV and a LUMO energy level of -3.65 eV. The electrochemical band gap calculated from the onset reduction and oxidation potential is 1.70 eV, which is slightly lower than the optical band gap (1.78 eV). This is possibly due to the low accuracy of the calculated HOMO level, since this is an irreversible oxidation peak. According to these electrochemical results, it can be concluded that the LUMO of PQV (-3.65 eV) is lower in energy than that of the other conjugated polymers studied before in our group (PPV: -3.1 eV, 2,5-substituted di-alkoxy-PPV: -2.8 to -3.0 eV, PNV: -3.4 eV and PFV: -3.1 eV)[22]. That means that the electron affinity of PQV is higher than the conjugated polymers mentioned, as was anticipated based on the introduction of the quinoxaline units. This result is important for the application of PQV as an acceptor material in optoelectronic devices.

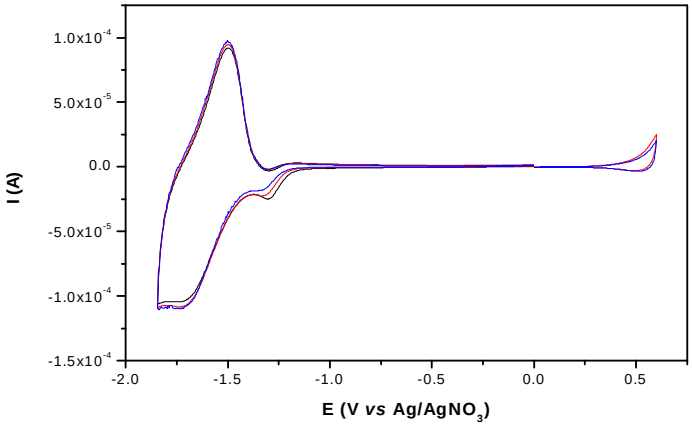

Figure 3.46: Cyclic voltammogram of PQV

3.4 *p*-Quinodimethane formation; observation of the potential intermediate

As it was mentioned in chapter 1, the actual monomer present in precursor routes is a *p*-quinodimethane *p*-QM system, which is formed on reaction of the premonomer with the base, Scheme 3.45. As the formation of *p*-QM system involves an elimination reaction, the possible reaction pathways will be shortly discussed in this section.

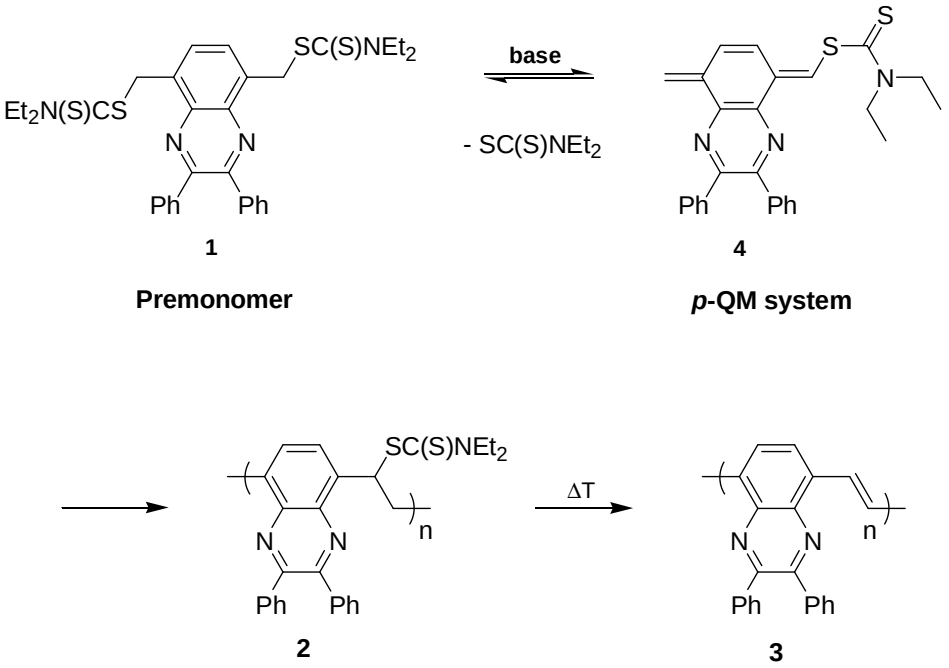

Scheme 3.45: The dithiocarbamate precursor route; formation of the actual monomer – the ***p*-QM system –** of **PQV**.

In general there are four different type of 1,6-elimination reactions known, Scheme 3.46. They only differ one from another in the order of reaction and the kind of intermediate or transition state. In Scheme 3.46 both the leaving group (L) and the polarizer (P) are a d*ithiocarbamate* ($SC(S)NR_2$) group.

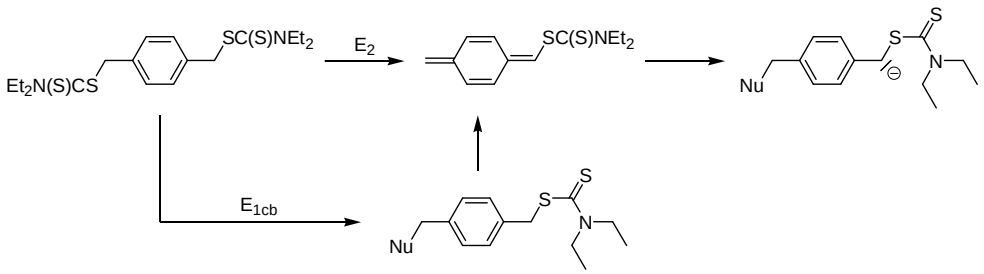

Scheme 3.46: General reaction scheme for *p*-quinodimethane formation through the dithiocarbamate precursor route.

E_1 reaction: This is a first order elimination reaction. In the first step a well-established carbenium ion is formed by expulsion of the leaving group. In the second step a proton is abstracted to yield the double bond. Hereby, the rate determing step **R.D.S.** is the formation of the carbenium ion. Since the reaction includes formation of a cathion, the reaction is very unlikely to occur under the basic conditions present in the precursor route. An E_1 mechanism would imply a spontaneous formation of the quinodimethane system which has never been observed for any precursor route.

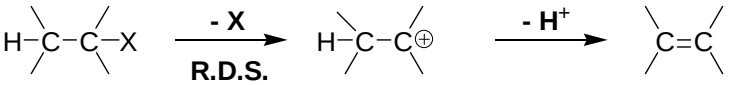

$(E_{1cb})_{rev}$ reaction: This is an elimination reaction where the formation of a carbanion is involved. If the anion is formed from the starting product in a rapid equilibrium and the leaving group departs in a subsequent slow step the mechanism involved is called the $(E_{1cb})_{rev}$ (reversible first order elimination reaction of the conjugated base). The rate determing step is the expulsion of the leaving group to yield the double bond. The energy diagram is depicted in Figure 3.47.

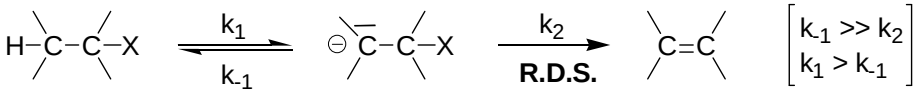

$(E_{1cb})_{irr}$ reaction: Also here the formation of a carbanion is involved. If the leaving group expulsion from the carbanion formed from the starting product is so fast that proton abstraction becomes rate determing the elimination mechanism is called $(E_{1cb})_{irr}$ ir(reversible first order elimination reaction of the conjugated base). The reaction rate is dependant on the base concentration in a proportional way. The energy diagram is depicted in Figure 3.47.

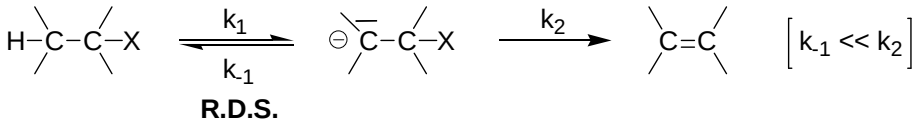

E_2 reaction: In this elimination reaction neither a cationic nor an anionic intermediate is involved. Expulsion of the leaving group and proton abstraction occurs at the same moment in a concerted way. Here a rate increase of the reaction will occur when an atom or group with better nucleofugal properties replaces the leaving group. The energy diagram is depicted in Figure 3.47.

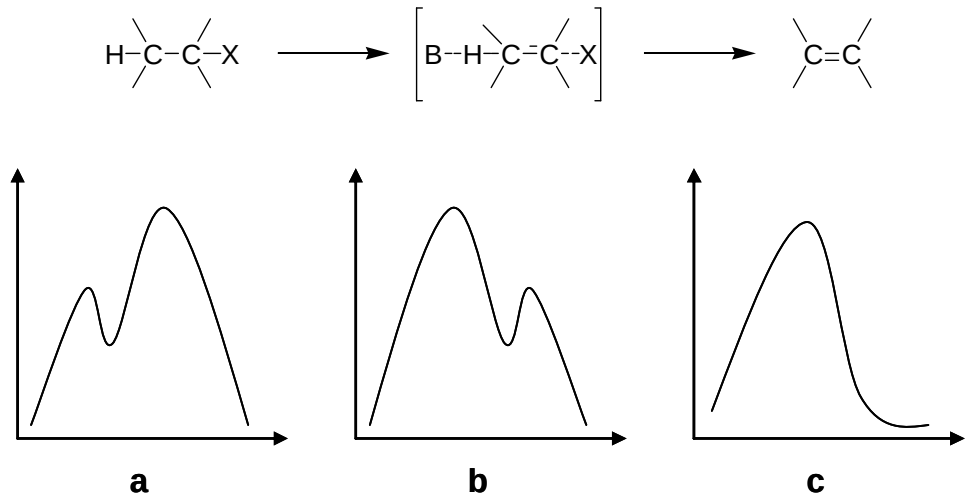

Figure 3.47: Energy diagram of a: $(E_{1cb})_{rev}$; b: $(E_{1cb})_{irr}$ and c: E_2 elimination reactions.

Also in Table 3.6 an overview is given about the mechanistic features of the last three elimination mechanisms[23].

Mechanism	β-proton exchange faster than elimination	Electron withdrawal at C_β	Leaving group effect
$(E_{1cb})_{rev}$	Yes	Small rate increase	Substantial
$(E_{1cb})_{irr}$	No	Rate increase	Small to negligible
E_2	No	Rate increase	Substantial

Table 3.6: Overview of the mechanisms of base induced elimination reactions

To find out more about the formation of *p*-QM system, it is important to obtain kinetic data from a mechanistic study on this *p*-QM system. As the *p*-QM intermediate has a strong absorbance in the UV-Vis spectrum, the formation of the actual monomer can be monitored by *in situ* UV-Vis spectroscopy. Therefore, the UV-Vis spectroscopy studies on the *p*-QM formation towards PQV from the **diBr-monomer** and **dithio-monomer** (Figure 3.48) have been carried out in subsequently *sec*-butanol and dry THF.

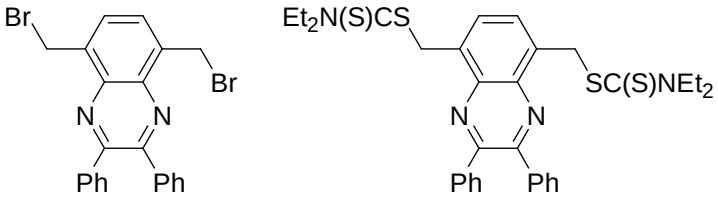

diBr-monomer **dithio-monomer**

Figure 3.48: diBr-monomer and dithio-monomer towards **PQV**.

A large excess of base (subsequently Na*t*BuO and LHMDS) is used to guarantee fast and complete formation of the *p*-QM system. The monomer concentrations used in these UV-Vis measurements are too low ($1x10^{-4}$) to perform self-initiate polymerisation. Therefore, the decrease in *p*-QM absorption only occurs by solvent-substitution on the quinoid structure to yield the solvent-substituted monomer, Scheme 3.47.

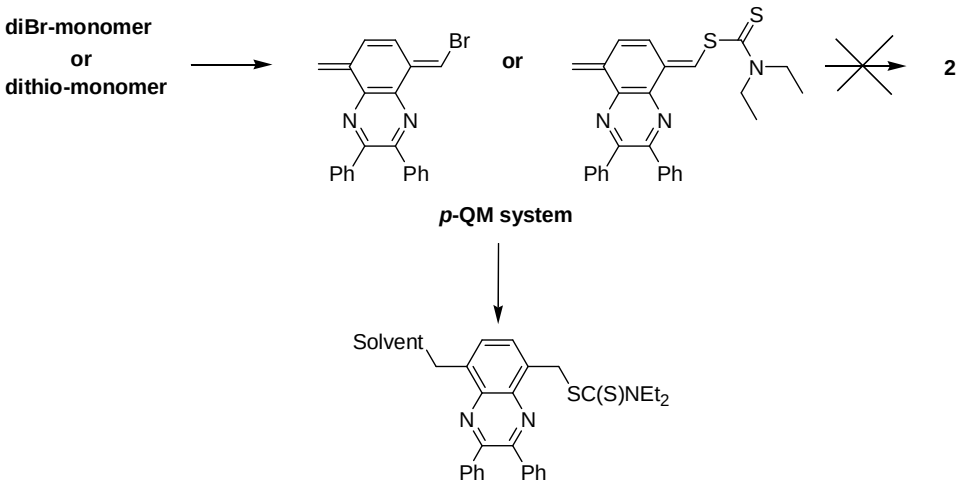

Scheme 3.47: Reaction scheme of the the ***p*-QM formation** and solvent-substitution.

For carrying out the measurements on the kinetics of the *p*-QM system in solution and obtaining the rate constants of the *p*-QM formation towards PQV, a $1 \cdot 10^{-4}$ M solution of the diBr-monomer in *sec*-BuOH is placed in a quarts cuvet. The base in excess, NatBuO ($4 \cdot 10^{-3}$ M) dissolved in *sec*-BuOH added at once and the UV-Vis detection starts within a few milliseconds. The same was carried out for the dithiocarbamate monomer **1** ($1 \cdot 10^{-4}$ M) in dry THF with LHMDS ($8 \cdot 10^{-3}$ M) as the base dissolved in dry THF.

When an excess of base is added to a diluted solution of a monomer, a typical plot can be observed in the UV-Vis spectrum. Here, three signals can be visible. The first signal corresponds to the premonomer, which decreases in time. The second signal corresponds to the solvent-substituted premonomer, which only increased in time as the reaction progresses. The third signal is assigned to the *p*-QM system, which first increases rapidly then subsequently decreases in time (Figure 3.49).

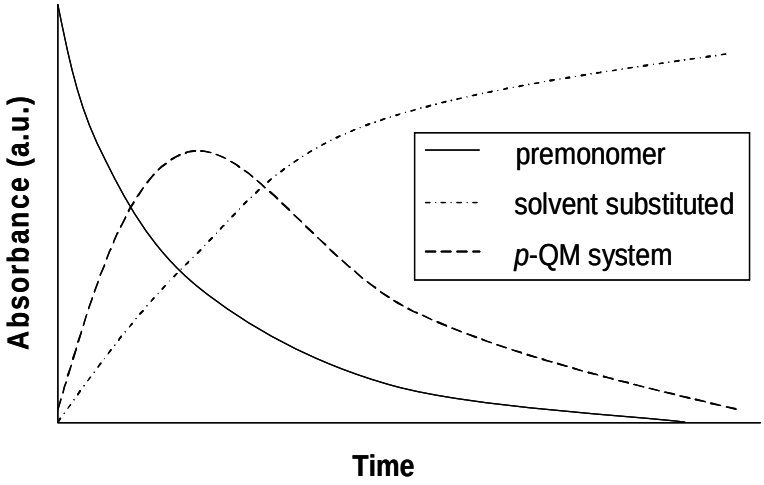

Figure 3.49: Typical UV-Vis spectrum of the ***p*-QM system** formation.

Unfortunately the performed experiments on the monomers could not indicate any prove for the formation of *p*-QM system. During the measurements it could be observed that there is a strong influence of the solvent peak on the monomers, especially in the case of THF which starts around 261 nm. The dithiocarbamate monomer **1** (before and after the addition of the base LHMDS) has a strong peak between 266 and 296 nm. There might be some kind of overlap between absorption spectra of the solvent and the monomer mixture. Important to note that from the absorption spectra it could be observed that there was neither a decrease of the premonomer peak nor an rapid increase of the *p*-QM signal, Figure 3.50. The same counts for the diBr monomer (before and after the addition of the base Na*t*BuO) in *sec*-BuOH. Neither an increase nor decrease of the peaks could be observed, Figure 3.51. More experiments need to be carried out in order to understand the mechanism involved for the *p*-QM formation via *in situ* UV-Vis spectroscopy.

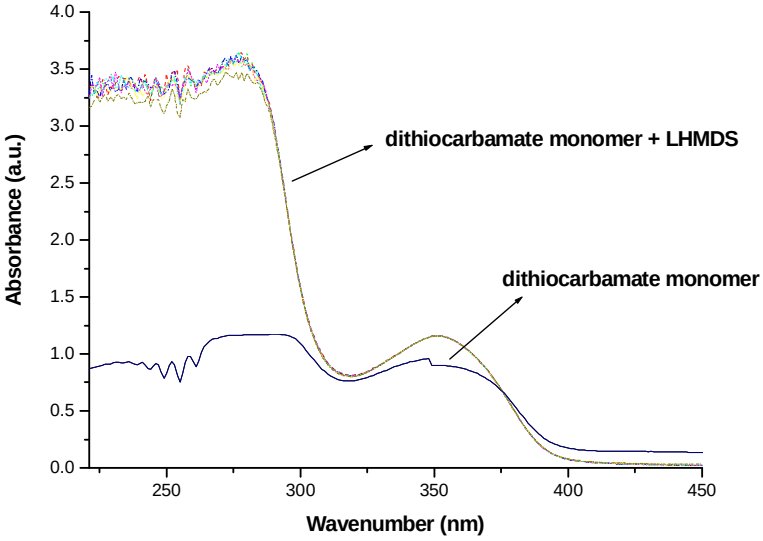

Figure 3.50: UV-Vis spectrum of the ***p*-QM formation** for the dithiocarbamate-monomer with and without LHMDS.

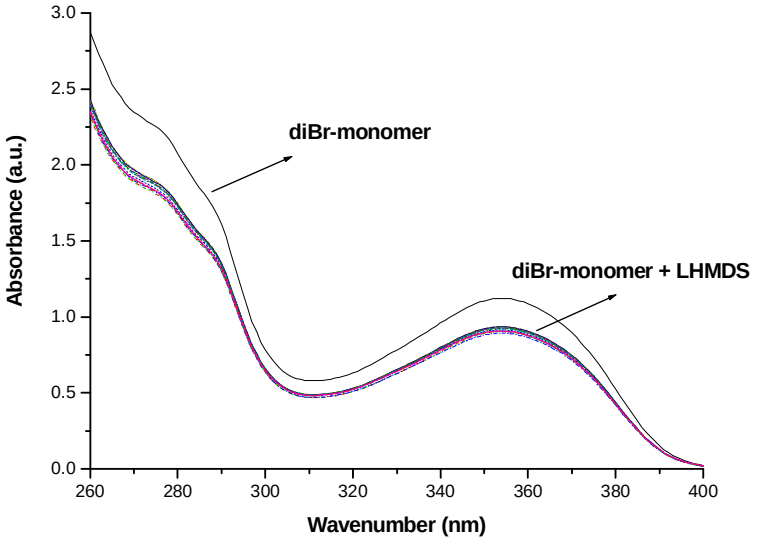

Figure 3.51: UV-Vis spectrum of the ***p*-QM formation** for diBr-monomer with and without Na*t*BuO.

A second effort to find a prove for the formation of the *p*-QM system was based on NMR experiments. In order to find a reliable prove for the formation of this *p*-QM system as a potential intermediate a simple experiment has been carried out. **1** was used as the standard starting material in the experiment with Lithium Bis(trimethylsilyl)amide **LHMDS** as the base and THF-d_8 as the solvent. Before the reaction started both the monomer **1** and the base were dissolved in THF-d_8 in separate vials prior to the reaction and cooled to -78°C. The reaction was carried out in NMR tube placed in an NMR spectrometer which was pre-cooled to -50°C. After complete addition of the base – annealing – a series of ^{1}H-NMR spectra was recorded. A representative selection of these spectra is shown in Figure 3.52.

Additionally, the crude product obtained after this *in situ* ^{1}H-NMR measurement was analysed by GPC in THF without further purification. The resulted polymer had an M_w of $42 \cdot 10^3$, M_n of $2 \cdot 10^3$ and polydisperisty of 2.07, which was much better than all the polymers measured before.

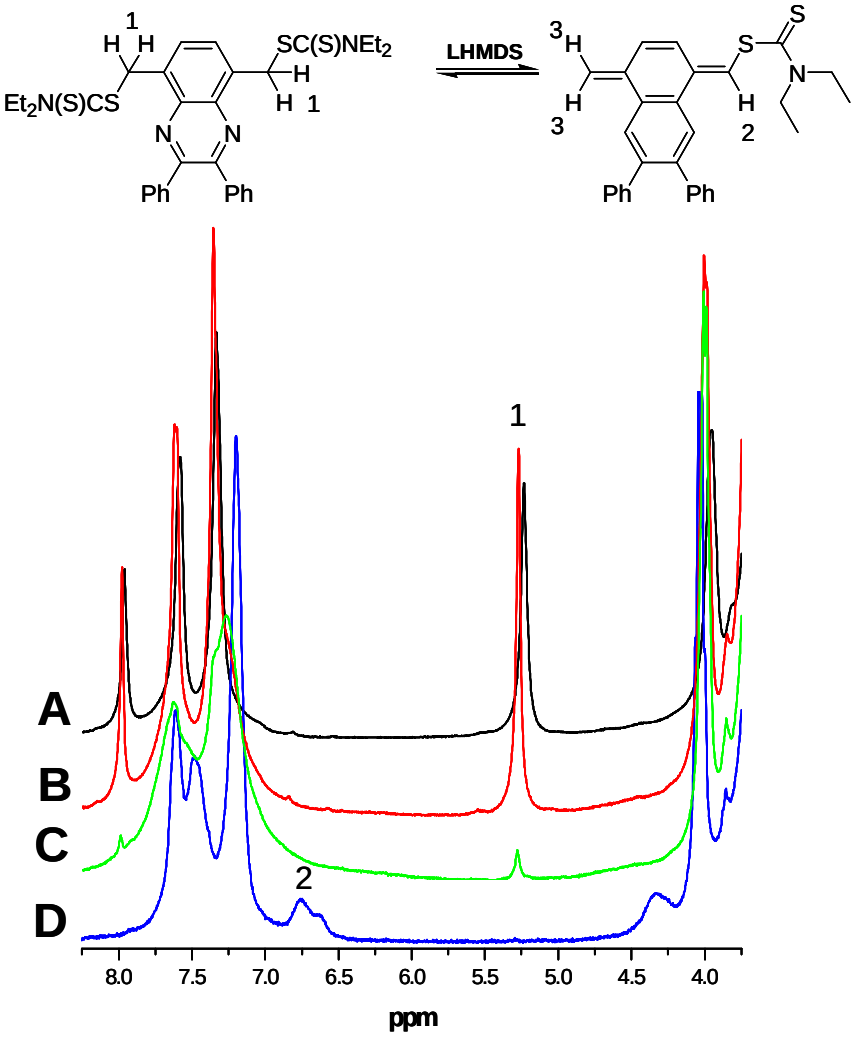

Figure 3.52: 1H-NMR spectra (section) of a dithiocarbamate precursor reaction carried out with 1 as the starting material, LHMDS as the base and THD-d_8 as the solvent. Spectra were recorded (A) at -50°C directly after annealing, (B) at -35°C after 40 min, (C) at -33°C after 3h 45 min and (D) at 30°C after 5h 45 min.

From the figure it can be seen that there is clear evidence that the consumption of the dithiocarbamate monomer **1** is drastically slowed down at these very low temperatures. Spectrum A, which was recorded immediately after the annealing procedure was finished, is dominated by the sharp and intense absorptions of the

starting material **1** at δ ≈ 5.24 ppm. The signal assignment on subsequently spectra B and C shows that there is approximately 35% and 99% of the starting material **1** converted. From these spectra it can be observed that the peaks are broadening in function of time and temperature. These broadening maybe the result of the decreased mobility of the molecules at very low temperature used.

Although the peak observable between δ ≈ 6.5 and 7.0 ppm (spectrum D) can be an indication for the formation of the Quinodimethane system **4** (between δ ≈ 5-7 ppm)[24] but unfortunately from the observed spectra it is not clear whether the Quinodimethane system **4** was formed or not. This peak together with the shoulder observed around δ ≈ 4.2 and 4.5 ppm can be an indication for the formation of the end group, consisting of proton or a dithiocarbamate group.
Also a schematic representation of the intensity of the protons as function of time and temperature are given in Figure 3.53.

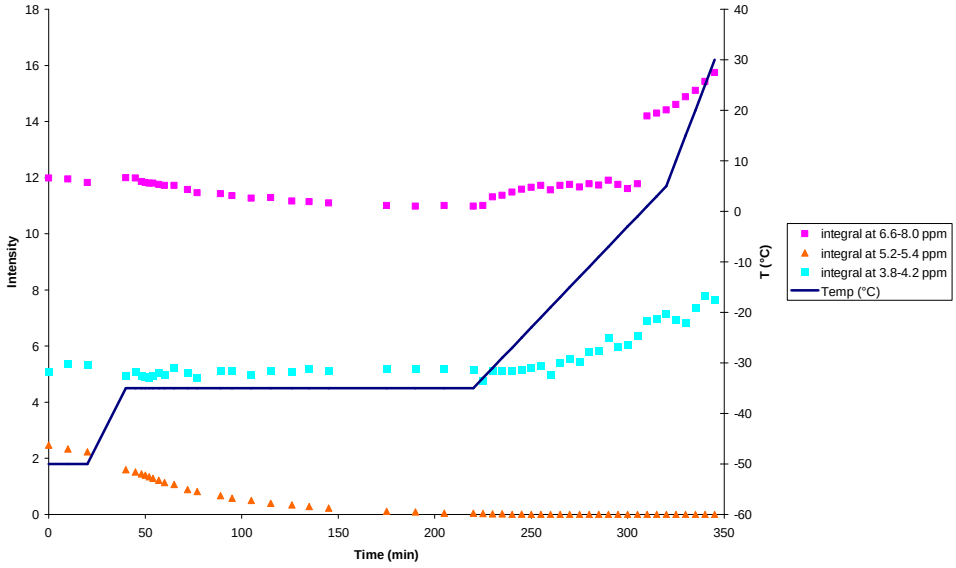

Figure 3.53: Schematic representation of the increase/ decrease of protons in function of time and temperature for 50 scans from -50°C to 30°C for monomer **1**.

From Figure 3.53 it can be observed that on the one hand the starting material is disappearing in function of time and temperature ($\delta \approx$ 5.2-5.4 ppm). On the other hand, the shoulders around $\delta \approx$ 3.8-4.2 ppm and 6.6-8-0 ppm are increasing. Therefore, on the basis of these results no conclusion can be drawn concerning the mechanism and the possible formation of the *p*-QM system. However, from the results of these experiments we can mention that the polymerisation has taken place at once and there is no indication for the presence of a possible intermediate (i.e. *p*-QM system).

3.5 Conclusion

In this chapter the main attention was paid on the polymerisation towards plain poly (*p*-quinoxaline vinylene) PQV as this polymer shows promising characteristics as n-type material in use for possible organic solar cells. The precursor route which was suitable and used in this work was the Dithiocarbamate Precursor Route. The polymerisations were carried out with either LDA or LHMDS as the base in different concentrations and at different temperatures.

The use of LDA led only to the formation of oligomers ($M_w \pm$ 4000 g/mol). The analysis by ^{1}H-NMR of the residual fraction showed only the presence of unreacted monomer. Polymerisation with LHMDS as the base instead of LDA yielded precursor polymer **2** with reasonable average molecular weights (M_w 6000-23000 g/mol). The precursor polymers, mainly considered as oligomers, had λ_{max} around 552 nm. In order to get higher average molecular weights for the precursor polymers a detailed study was done on the monomer. The ^{1}H-NMR analysis of the "impure monomer" showed a possible contamination of the monomer around 5.34 ppm. Therefore the monomer was purified several times by crystallisation, which yielded pure crystals of the monomer.

The polymerisations of the "pure monomer" lead to a substantial effect on the average molecular weight of the precursor polymers with M_w between 34000-

56000 g/mol and λ_{max} around 532 nm. From the GPC chromatogram two conclusions can be made: First of all, using impure monomer leads mainly to oligomers while using a pure monomer leads mainly to high M_w polymers. Second, in our case only a monomodal behaviour is observed.

In order to investigate the existence of the "real monomer" the *p*-QM sysyem some experiments were carried out on the monomer **1** with *in situ* UV-Vis and *in situ* ^{1}H-NMR techniques. Concerning the *in situ* UV-Vis measurements, neither an increase nor decrease of the peaks could be observed. Moreover, on the basis of *in situ* ^{1}H-NMR results, no conclusion can be drawn concerning the mechanism and the possible formation of the *p*-QM system. However, from the results of these experiments we can mention that the polymerisation has taken place at once and there is no indication for the presence of a possible intermediate (i.e. *p*-QM system).

As far as the mechanism of the polymerisation concerns, mostly in the case of the polymerisation of the *p*-QM systems a self initiating radical mechanism is observed. For such polymerisations the reaction is known to be less sensitive toward impurities. Given these observations a hypothesis can be put forward that the polymerisation follows the pure anionic mechanism.

3.6 Experimental section

3.6.1 Materials

All solvents used in the synthesis were distilled before use. Tetrahydrofuran (THF) was refluxed under nitrogen with sodium metal and benzophenone until a blue colour persisted and was then distilled. Lithium Bis(trimethylsilyl)amide **LHMDS** and Lithium diisopropyl amide **LDA** were purchased from Aldrich and used without further purification. THF-d_8 was purchased from Deutero GmbH, Kastellaun, Germany, and used as purchased. All the commercially available products were purchased from Acros or Aldrich.

3.6.2 Characterisation

Nuclear magnetic resonance (NMR) spectra were recorded on a Varian Inova 300 spectrometer at 300 MHz for ^{1}H-NMR and at 75 MHz for ^{13}C-NMR using a 5 mm probe.

***In situ* ^{1}H-NMR Instrumentation**

The monomer diethyl-dithiocarbamic acid 8-diethylthiocarbamoylsulfanylmethyl-2,3-diphenyl-quinoxalin-5-ylmethyl ester **1** (97 mg, 0.16 mmol) was dissolved in THF-d_8 (0.5 mL) and transferred into an NMR tube. The base Lithium Bis(trimethylsilyl)amide **LHMDS** (0.16 mL, 0.16 mmol) was dissolved in THF-d_8 (0.3 mL) and put into a 10 mL vial. The solution of base LHMDS in the solvent THF was cooled to -78°C. The NMR tube was cooled to -78°C, and the solution of LHMDS was injected into the cooled monomer solution using a syringe. After shaking, the reaction mixture was frozen in liquid nitrogen and transferred into an NMR spectrometer cooled to -50°C where measurements took place.

Gas chromatography/mass spectrometry (GC/MS) analyses were carried out with TSQ – 70 or Voyager mass spectrometers (Thermoquest); the capillary column was a Chrompack Cpsil5CB or Cpsil8CB.

Fourier Transform Infra Red spectroscopy (FT-IR) was performed on a Perkin Elmer Spectrum One FT-IR spectrometer (nominal resolution 4 cm-1, summation of 16 scans). Samples for the FT-IR characterisation were prepared by spin-coating the compounds from a chloroform solution (6 mg/ml) onto NaCl disks (diameter 25 mm and thickness 1 mm) at 500 rpm. The NaCl disks were heated in a Harrick oven high temperature cell (purchased from Safir), which was positioned in the beam of the FT-IR to allow *in situ* measurements. The temperature of the sample and the heating source were controlled by a Watlow temperature controller. The heating source was in direct contact with the NaCl disk. Spectra were taken continuously and the heating rate was 2 °C/min from room temperature up to 350 °C. The atmosphere in the temperature cell could be varied from a continuous flow

of nitrogen to vacuum (15 mmHg). Timebase software was used to investigate regions of interest.

Ultraviolet visible spectroscopy (UV-VIS) was performed on a VARIAN CARY 500 UV-VIS-NIR spectrophotometer (interval: 1 nm, scan rate: 600 nm/min, continuous run from 200 to 700 nm). The precursor polymer was spin-coated from a chloroform solution (6 mg/ml) onto quartz glass (diameter 25 mm and thickness 3 mm) at 700 rpm. The quartz glass was heated in the same Harrick oven high temperature cell as was used in the FT-IR measurements. The cell was placed in the beam of the UV-Vis spectrophotometer and spectra were taken continuously. The heating rate was 2 °C/min up to 350 °C. All measurements were performed under a continuous flow of nitrogen. Scanning kinetics software was used to investigate the regions of interest.

Thin Layer Chromatography (TLC) analyses were made on Merck aluminium sheets, 20 x 20 cm, covered with silica gel 60 F_{254}.

Cyclic Voltammetry (CV) was performed with an Autolab PGSTAT 20 potentiostat from Eco Chemie B.V., which was equipped with General Purpose Electrochemical System (GPES) software (version 4.9 for windows), in an electrolytic solution of 0.1M $TBAPF_6$ in anhydrous acetonitrile as supporting electrolyte and a conventional three-electrode cell. The cyclic voltammograms were recorded at a scan rate of 50 mV s^{-1}, at room temperature and under pressure of dry nitrogen. A platinum disc (area = 1.6 mm2) with a thin drop-cast film was used as the working electrode, and a platinum wire was used as the counter electrode. All potentials were relative to the Ag/AgCl reference electrode.

3.6.3 Synthesis

Polymerisation of monomer 1; precursor polymer (2)

All polymerisations were carried out in dry THF at different temperatures, with different bases (LDA or LHMDS) and different concentrations of the base and the

monomer. To a flame dried flask a solution of monomer **1** (300 mg) in dry THF at –78 °C (or -30, -15, 0, R.T., 40°C) was brought and degassed by passing through a continuous nitrogen flow. An equimolar LDA solution (a 2 M solution in THF/n-hexane) or LHMDS (Lithium Bis(trimethylsilyl)amide, 1 M solution in THF) was added in one go to the stirred monomer solution. The mixture was kept at –78 °C (or -30, -15, 0, R.T., 40°C) for 90 minutes under continuous nitrogen flow. After completion, the polymer was precipitated in ice water (100 mL), after which it was neutralised with HCl (1N) and extracted with chloroform (3 x 50 mL). The solvent of the combined organic layers was evaporated under reduced pressure and a second precipitation was performed in methanol (100 mL) at 0 °C. The polymer was collected and dried in vacuo. ^{1}H-NMR ($CDCl_3$) of precursor polymer **2** (entry **10**): 7.74-6.95 (br m, 12H), 3.94-3.91 (br q, 2H), 3.78-3.75 (br q, 2H), 3.41-3.36 (br t, 1H), 1.99 (br s, 2H), 1.33-0.83 (br d, 6H). ^{1}H-NMR ($CDCl_3$) of precursor polymer **2** (entry **18**): 7.59-7.19 (br m, 12H), 3.94-3.91 (br q, 2H), 3.78-3.73 (br q, 2H), 1.99 (br s, 2H), 1.34-1.28 (br dt, 6H).

Thermal conversion of the precursor polymer to the conjugated polymer in solution (3)

The precursor polymer **2** (180 mg) dissolved in 1,2-dichlorobenzene (45 ml) was refluxed at 190°C under stirring for 24 hours or at 120°C for 96 hours. After cooling down to ambient temperature, the solvent was evaporated and, the slurry obtained was precipitated in methanol and filtered. The purple coloured product was analysed by ^{1}H-NMR with no indication of the product, only the solvent 1,2-dichlorobenzene.

3.7 References

1. J. H. Burroughes, D. D. C. Bradley, A. R. Brown, R. N. Marks, K. Mackay, R. H. Friend and P. L. Burn, *Nature*, 347, **1990**, 539

2. N. S. Sariciftci, L. Smilowitz, A. J. Heeger and F. Wudl, *Science*, 258, **1992**, 1474

3. S. Glenis, G. Tourillon and F. Garnier, *Thin Solid Films*, 139, (3), **1986**, 221

4. C. J. Brabec, N. S. Sariciftci and J. C. Hummelen, "Plastic solar cells", *Advanced Functional Materials*, 11, (1), **2001**, 15-26

5. T. Fukuda, T. Kanbara, T. Yamamoto, K. Ishikawa, H. Takezoe and A. Fukuda, "Polyquinoxaline as an excellent electron injecting material for electroluminescent device", *Applied Physics Letters*, 68, (17), **1996**, 2346-2348

6. P. M. Hergenrother, *Polymer Science Engineering*, 16, (5), **1976**, 303

7. P. M. Hergenrother, *Journal of Macromolecular Science Reviews Macromolecular Chemistry*, C6, (1), **1971**, 1

8. F. W. Harris and J. E. Korleski, *Polym. Mat. Sci. Eng. Proc.*, 61, **1989**, 870

9. B. S. Kim, J. E. Korleski, Y. Zhang, D. J. Klein and F. W. Harris, "Development of a new poly(phenylquinoxaline) for adhesive and composite applications", *Polymer*, 40, (16), **1999**, 4553-4562

10. D. J. Klein, B. S. Kim and F. W. Harris, "Synthesis of poly(aryl ether phenylquinoxaline) via Ullmann ether condensation of chlorine-substituted A-B quinoxaline monomers", *Polymer Bulletin*, 47, (3-4), **2001**, 217-221

11. M. Jonforsen, T. Johansson, L. Spjuth, O. Inganas and M. R. Andersson, "Synthesis and characterization of poly(quinoxaline vinylene)s and poly(pyridopyrazine vinylene)s with phenyl substituted side-groups", *Synthetic Metals*, 131, (1-3), **2002**, 53-59

12. M. Jonforsen, Johansson, T., Inganäs, O., Andersson, M.R., "Synthesis and Characterisation of Soluble and n-Dopable Poly(quinoxaline vinylene)s and Poly(pyridopyrazine vinylene)s with Relatively Small Gap", *Macromolecules*, 35, **2002**, 1638-1643

13. M. J. Edelmann, J. M. Raimundo, N. F. Utesch, F. Diederich, C. Boudon, J. P. Gisselbrecht and M. Gross, "Dramatically enhanced fluorescence of

heteroaromatic chromophores upon insertion as spacers into oligo(triacetylene)s", *Helvetica Chimica Acta*, 85, (7), **2002**, 2195-2213

14. Q. Sun, X. Zhan, C. Yang, Y. Liu, Y. Li and D. Zhu, "Photo- and electroluminescence properties of fluorene-based copolymers containing electron- or hole-transporting unit", *Thin Solid Films*, 440,, **2003**, 247-254

15. A. P. Kulkarni, Jenekhe, S.A., "Blue Light-Emitting Diodes with Good Spectral Stability Based on Blends of Poly(9,9-dioctylfluorene): Interplay between Morphology, Photophysics, and Device Performance", *Macromolecules*, 36,, **2003**, 5285-5296

16. J. B. Baek and L. C. Chien, "Synthesis and photoluminescence of linear and hyperbranched polyethers containing phenylquinoxaline units and flexible aliphatic spacers", *Journal of Polymer Science Part a-Polymer Chemistry*, 42, (14), **2004**, 3587-3603

17. E. Gubbelmans, T. Verbiest, I. Picard, A. Persoons and C. Samyn, "Poly(phenylquinoxalines) for second-order nonlinear optical applications", *Polymer*, 46, (6), **2005**, 1784-1795

18. M. d. Kok, "Chemical Modification of Sulphinyl Precursor Polymers Towards PPV", *Ph.D. Dissertation*, Hasselt University,

19. E. Kesters, *Ph.D. Dissertation*, Hasselt University, **2002**

20. F. Banishoeib, "Study of the Dithiocarbamate Route as a viable synthetic route towards Poly(Thienylene Vinylene) Derivatives", *Dissertation*, Hasselt University, **2007**

21. L. Hontis, V. Vrindts, D. Vanderzande and L. Lutsen, "Verification of radical and anionic polymerization mechanisms in the sulfinyl and the Gilch route", *Macromolecules*, 36, (9), **2003**, 3035-3044

22. S. Fourier, "Spectroscopy, electrochemistry and spectro-electrochemistry of PPV and PTV Derivatives; the effect of backbone structure and side chain polarity on the optoelectronic properties of conjugated polymers", *Dissertation*, Hasselt University, **2007**

23. F. Motmans, "Synthesis and Characterisation of Polar PPV derivatives through the Sulphinyl Precursor Route", *Dissertation*, Hasselt University, **2004**

24. J. Wiesecke and M. Rehahn, "Direct Observasion of alpha-Chloro-*p*-quinodimethane as the Real Monomer in the Gilch Polymerization Leading to

Poly(*p*-phenylene vinylene)", *Macromolecular Rapid Communications*, 28, **2007**, 188-193

Chapter Four

4. Different Approaches to Introduce Side Chains; Soluble Derivatives of Poly (*para*-Quinoxaline Vinylene) PQV

4.1 Introduction

Natural and synthetic polymers have been in use for many years. Among them, conjugated polymers are at a point of development that their application as e.g. sensors[1-3], organic field effect transistors (OFETs)[4-7], light-emitting diodes (LED's)[8, 9], photovoltaic cells[10-17] and organic solar cells[14, 18-21] becomes even more attractive. Conjugated polymers date back to the end of 1970s, when the first "conducting" conjugated polymer (polyacetylene, see Figure 1.4) was discovered by Shirakawa, Heeger and MacDiarmid[22].

As it was mentioned in chapter one, there are different approaches towards the synthesis of conjugated polymer materials (e.g. oxidative or reductive coupling). Unfortunately, often the mentioned synthetic routes lead to insoluble and infusible materials with low molecular weight (oligomers).[23-29]

This problem makes the conjugated polymers less interesting for application. A solution to this problem is the synthesis of conjugated polymers with long flexible alkyl or alkoxy side chains.

So far most of the conjugated polymers that are synthesised are p-type materials. However n-type conjugated polymers are up till now not much known.

As an alternative to C60 derivatives, the synthesis and characterisation of a n-type conjugated polymer, poly (*p*-quinoxaline vinylene) (**PQV**) (see Figure 3.31) was presented in chapter three. This conjugated polymer (PQV) shows characteristics of an n-type material but said materials may also be interesting to act as electron-donor material in an active layer of an organic solar cell.

The quinoxaline structure was introduced as a combination of an electron donor and electron acceptor copolymer by Lee and co-workers[30]. By using Stille cross-coupling reaction they prepared in high yield π-conjugated copolymers with thiophene as electron donating material and diheptyl-quinoxaline as strong electron withdrawing material, Scheme 4.48. Unfortunately, due to lack of suited solvent they could not perform the GPC analysis in order to determine the mean average molecular weights $\mathbf{M_w}$ of the copolymer. However, in 2004, after further research they patented their results with the statement of high solubility in common organic solvent and stability in air.

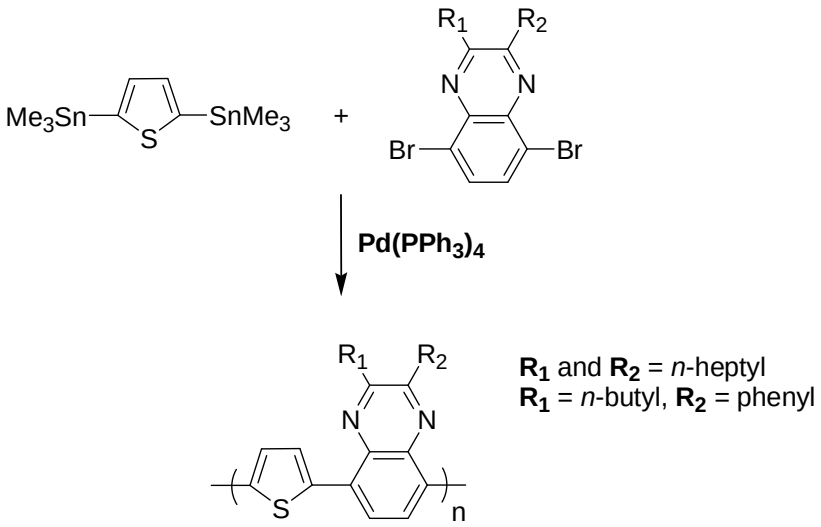

Scheme 4.48: Synthesis of alternating electron donor (thiophene) and electron acceptor (quinoxaline) copolymer by Stille cross-coupling reaction.

In 2002, Maria Jonforsen[31] published an article using the same Stille cross-coupling reaction to prepare poly(quinoxaline vinylene)s with soluble linear and

branched aliphatic side chains, Scheme 4.49. Unfortunately, these polymers (mainly oligomers) had poor stability. A possible explanation was the presence of the sensitive hydrogen group at the α position on the side chain.

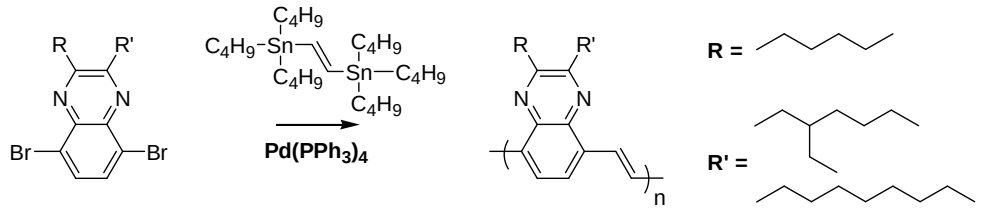

Scheme 4.49: Synthesis of poly(quinoxaline vinylene)s with soluble linear and branched aliphatic side chains via Stille cross-coupling reaction.

A year after, Jonforsen published another article[32] on the preparation of poly(quinoxaline vinylene)s with phenyl substituted side groups, Scheme 4.50. According to her results this polymer is even a better candidate as n-type material since the polymer does not have α hydrogen on the side chain and therefore expected to be more stable.

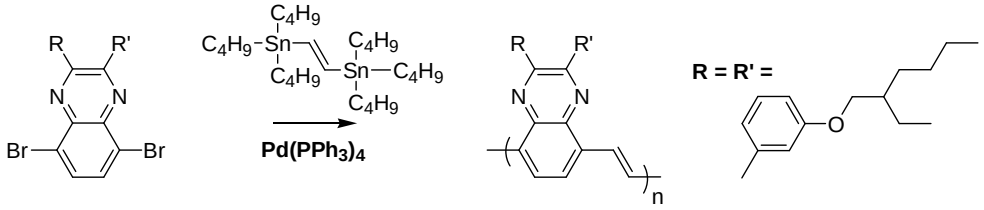

Scheme 4.50: Synthesis of poly(quinoxaline vinylene)s with soluble phenyl substituted side groups via Stille cross-coupling reaction.

An interesting study was done by Jong-Beom Baek[33] on blue fluorescent linear and hyperbranched quinoxaline polyethers, Scheme 4.51. The polyethers were prepared by self-polymerisable AB_2 monomers and they had very high mean average molecular weights (M_w 1,445,000-1,507,000 g/mol). Moreover, the polymers were soluble in most common organic solvents and they were thermally stable up to 350^0C making them interesting candidate for the fabrication of optoelectronic devices emitting blue light.

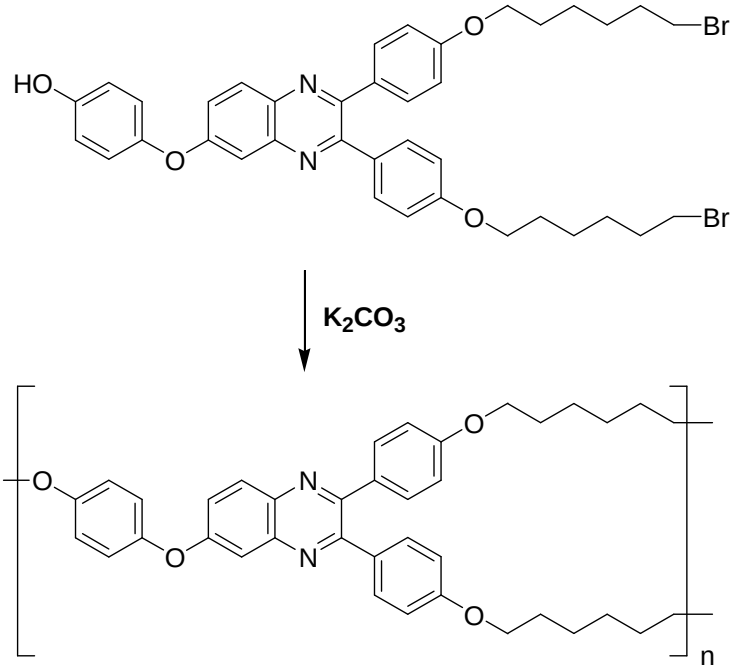

Scheme 4.51: Synthesis of the linear polymers prepared by self-polymerisable AB_2 monomers.

Argiri Tsami and co-workers studied the synthesis of alternating quinoxaline/oligothiophene copolymers with *n*-octyl and 4-*n*-octylbiphenyl-1-yl side chains via heteroaryl-heteroaryl cross-coupling after Stille[34]. The copolymers containing alternating 2,5-thienylene (x = 1) or two thiophenes (x = 2) units with alkyl on the quinoxaline moiety were soluble in chloroform and chlorobenzene, therefore their GPC analysis was possible. They obtained mean average molecular weights M_w of 18 200-62 700 g/mol. The copolymers containing three (x = 3) or four (x = 4) thiophene units with the in-plane alkyl substituents on the quinoxaline moiety were not soluble and therefore they could not be analysed. Interesting is the shift of wavelength absorption band towards lower energies which is not dependent on the length of oligothiphene units, Scheme 4.52.

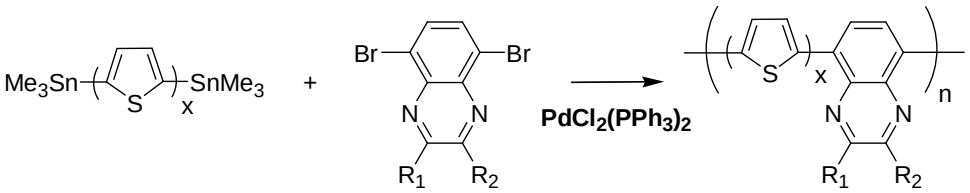

R_1 = **R_2** = *n*-octyl
R_1 = **R_2** = 4-*n*-octylbiphenyl-1-yl

Scheme 4.52: Synthesis of alternating quinoxaline/oligothiophene copolymers containing 2,5-thienylene, bithiophene (x = 2), trithiophene and tetratiophene units with R = *n*-octyl and 4-*n*-octylbiphenyl-1-yl side chains via heteroaryl-heteroaryl cross-coupling after Stille.

In 2007, Mammo[35] and co-workers published their results on the synthesis and characterisation of polyfluorene quinoxaline copolymers for use in plastic solar cells. They incorporated fluorene with alternating electron withdrawing groups (branched quinoxaline) and electron donating groups (thiophene) in order to lower the band gap, Figure 4.54. They mention that due to the side chains on these groups the polymers exhibit both high solubility and high molecular weight.

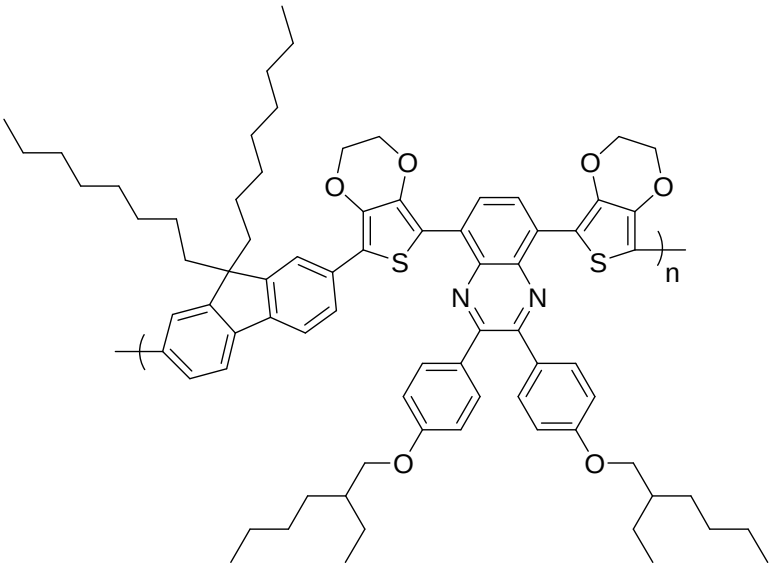

Figure 4.54: Chemical structures of fluorene with alternating electron withdrawing groups (branched quinoxaline) and electron donating groups (thiophene).

From the literature mentioned above, it is clear that alkyl or alkoxy side chains seem to play an important role for good solubility and processability of conjugated polymers in order to use them as semi-conducting material for photovoltaic application. Therefore, in this chapter efforts will be made to synthesise soluble derivatives of PQV via the dithiocarbamate precursor route, which is developed in our lab, in order to improve the processability and solubility of the conjugated polymers. The synthesised intermediary and compounds were analysed by ^{1}H-NMR, ^{13}C-NMR, GC-MS and FT-IR.

4.2 Introduction of side chains; synthesis towards soluble derivatives of PQV

The *n*-hexyl quinoxaline can be obtained starting from the commercially available 2-oxooctanenitrile and the commercially available 2,1,3-benzothiadiazole **1** towards **7a**. The 3-hexyl-acenaphto quinoxaline can be obtained starting from the previously prepared 5-Hexyl-acenaphthylene-1,2-dione[36-39] and the commercially available 2,1,3-benzothiadiazole **1** towards **7b**. The octyl substituted quinoxalines can be obtained starting from the commercially available 1-bromo-4-octyl-benzene and 2,1,3-Benzothiadiazole **1** towards **7c**. The octyloxy substituted quinoxalines can be obtained starting from the commercially available 4-bromophenol, 1-bromooctane and 2,1,3-benzothiadiazole **1** towards **7d**. The synthetic route is depicted in Scheme 4.53.

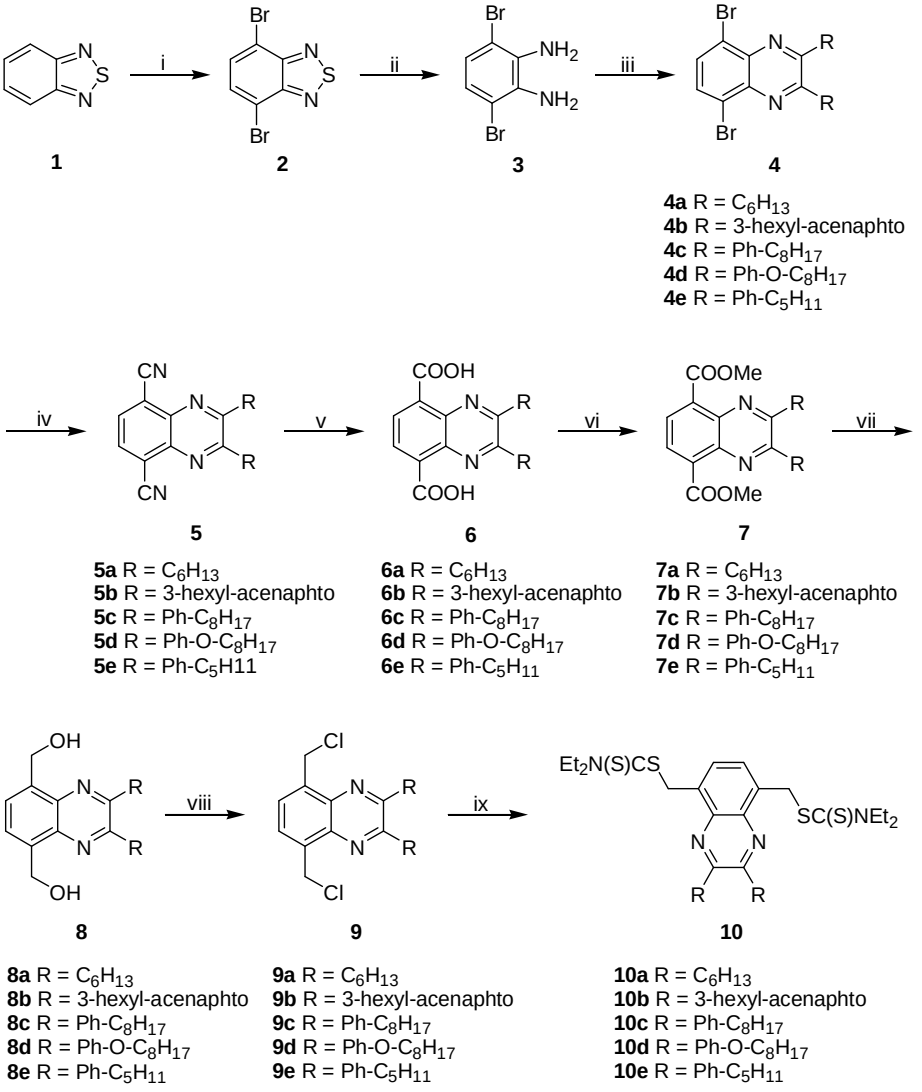

Scheme 4.53: Synthesis towards soluble alkyl, alkoxy and 3-hexyl-acenaphto substituted derivative of quinoxaline. Dithiocarbamate monomer **10** synthesis via the Benzothiadiazole route: i) **1**, Br_2, HBr, 130°C, 5h, RT, 20h; ii) **2**, $NaBH_4$, EtOH, 5h, 0°C, RT, 20h, inert atmosphere; iii) **3**, **11** (a, b, c, d or e), EtOH, ΔT, 27h; iv) **4** (**a**, **b**, **c**, **d** or **e**) CuCN, DMF, 164°C, 4h, $FeCl_3$, HCl, H_2O, 65°C, 0.5h; v) **5** (**a**, **b**, **c**, **d** or **e**) NaOH (10%), H_2O, EtOH, 110°C, 24h, HCl; vi) **6** (**a**, **b**, **c**, **d** or **e**), MeOH, H_2SO_4 (1%), inert atmosphere, 80°C, 20h; vii) **7 (a, b, c, d or e)**, $NaBH_4$, EtOH, inert atmosphere, refluxed, 5h, NH_4Cl, RT, 24h; viii) **8** (**a**, **b**, **c**, **d** or **e**), $SOCl_2$, RT, 24h; ix) **9** (**a**, **b**, **c**, **d** or **e**), $NaSC(S)NEt_2$, diethyl ether, 72h.

The reaction steps for the preparation of soluble derivatives of PQV are analogues to the ones described for the synthesis of plain PQV (chapter 2). The only difference is the synthesis of the **1,2-diketone** instead of commercially available benzil for the preparation of **4** which will be discussed in detail.

There are a number of methods for introducing alkyl groups into organic compounds (e.g. Grignard, Wittig, organolithium) but unfortunately most of them lead to the formation of many side products or need very reactive reagents[39]. A facile route is the synthesis of 1,2-diketone by coupling of *keto cyanide*[40] which is depicted in Scheme 4.54. The commercially available keto cyanide **12** was added slowly to ZnI_2 dissolved in dry THF and the mixture was stirred under nitrogen atmosphere at room temperature. After 1.5 hours diluted HCl was added and the reaction mixture was worked up and analysed.

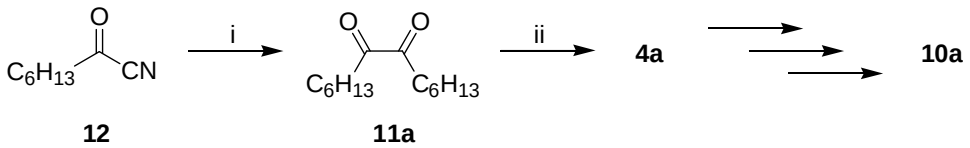

12 **11a**

Scheme 4.54: i) **12**, ZnI_2, dry THF, room temperature, 1.5 hours; ii) **3**, **11a**, EtOH, ΔT, 27h.

Baruah and co-workers suggested a possible mechanism involved for the synthesis of **11a**. Although the detail of the mechanism involved is not clear, they propose that it is likely the reaction starts by an electron transfer from ZnI_2 to $C_5H_{11}COCN$. The radical anion $(C_5H_{11}COCN)^{\bullet -}$ formed could be cleaved into $C_5H_{11}CO^{\bullet}$ and CN^- . The radical $C_5H_{11}CO^{\bullet}$ can dimerise into 1,2-diketone **11a** or it can be reduced into an acyl anion species, which on acylation can give the corresponding 1,2-diketone **11a** in 78% yield. Unfortunately this is not the case in here. The experiment was carried out several times and all of them resulted in qualitative formation of the side product heptanoic acid **13**, Figure 4.55.

A possible mechanism involved could be the acidic hydrolysis of the ketocyanide group (COCN)[41]. Although nitriles do not contain a carbonyl group, they are usually

considered to be derivatives of carboxylic acids because in the presence of an acid complete hydrolysis of a nitrile could produce a carboxylic acid. In this case when the diluted solution of HCl is used the side product **13** was formed. This was also determined by ^{1}H-NMR and ^{13}C-NMR analysis, Table 4.7.

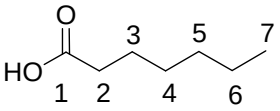

13

Figure 4.55: Heptanoic acid as major side product in the synthesis of 1,2-diketone.

δ

Proton	1H δ (ppm)	Carbon	13C δ (ppm)
1; 1H, s (COOH)	11.56	1; 1C	180.51
2; 2H, t	2.32-2.25	2; 1C	34.04
3; 2H, m	1.61-1.53	3; 1C	31.24
4; 6H, m	1.35-1.18	4; 1C	28.54
5; 6H, m	1.35-1.18	5; 1C	24.46
6; 6H, m	1.35-1.18	6; 1C	22.26
7; 3H, t	0.88-0.82	7; 1C	13.77

Table 4.7: ^{1}H-NMR and ^{13}C-NMR chemical shift values of **13**.

Acenaphthylene-1,2-dione was one of the starting materials used by Palmaerts in order to prepare poly(*p*-fluoranthene vinylene) **PFV** (Figure 4.56). PFV is a promising candidate for application as strong electron acceptor – n-type material - in organic solar cells[42]. There are two advantages in applying this fluoranthene unit into quinoxaline unit; on one hand, by adding another n-type material to quinoxaline unit, there is a possiblity in making the material even more electron withdrawing leading to lowering the band gap. On the other hand, by adding alkyl side chains, soluble derivatives can be obtained which will be easy to process for photovoltaic application.

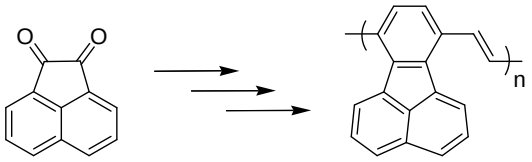

Acenaphthylene-**1,2-dione** Poly(*p*-Fluoranthene Vinylene) **PFV**

Figure 4.56: The overall scheme for preparation of poly(*p*-fluoranthene vinylene) PFV.

The 1,2-diketone **11b** used in this work was also prepared by Palmaerts in two steps[36-39]. Hereby, the commercially available 1-bromonaphthalene **14** was converted to **15** by Grignard reaction with $C_6H_{13}MgBr$, followed by Friedel-Crafts acylation with oxalyl chloride to 1,2-diketone **11b**. The follow-up reaction steps are analogues to the ones described for the synthesis of Plain PQV (chapter 2). The reaction for the synthesis of **11b** is depicted in Scheme 4.55.

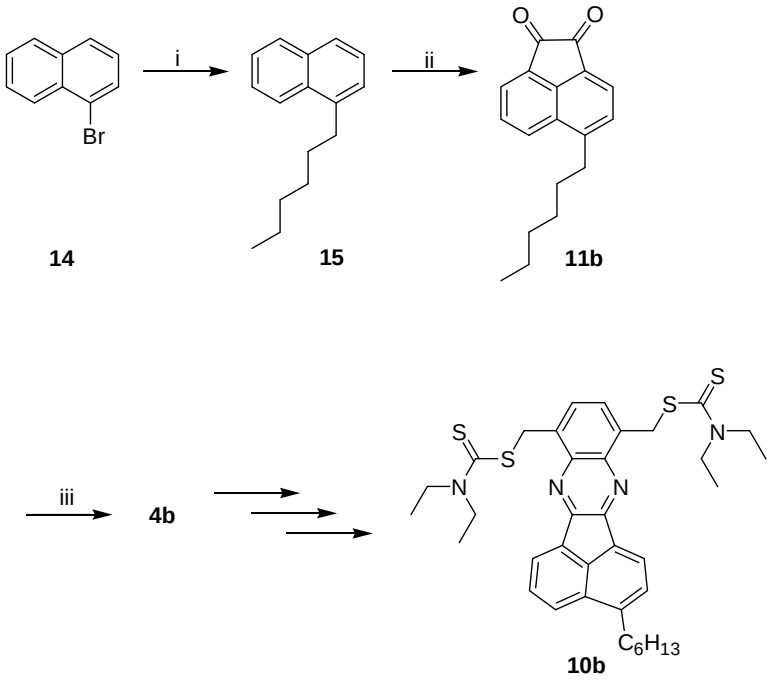

Scheme 4.55: i) 1-bromonaphthalene **14**, $C_6H_{13}MgBr$, $Ni(dppp)Cl_2$, diethyl ether, 0°C,24h, HCl; ii) **15**, $AlCl_3$, oxalylchloride, 1,2-dichloroethane, 0°C, 6 hour; iii) **3**, **11b**, EtOH, ΔT, 27h.

For the intermediary products **4b**, **5b**, **6b** and **7b** good yield and purity was obtained. The intermediary product **8b** resulted in very impure product which was used in the next step without further purification. Unfortunately the synthesis of **9b** failed. Probably due to the formation of many side products that were impossible to be separated by chromatography. As it can be seen in Scheme 4.56, a short cut towards the dithiocarbamate monomer **10b** has been applied. This has been done in order to improve the synthesis procedure towards quinoxalines and their derivatives. Hereby the four step procedure from the intermediary products **4b** to **8b** via the Benzothiadiazole route (chapter two) can be replaced by the simple two step procedure of **4b** to **8b** via **17a**. From TLC and ^{1}H-NMR analysis we could see that the product **17a** was formed but the purification of **17a** by column chromatography did not lead to pure product. Therefore **17a** was used in the next step without further purification. Unfortunately the synthesis of **8b** from the dialdehyde **17a** did not lead to the right product. The crude compound obtained after the reaction was not soluble in any common organic solvents, therefore the analysis of the compound could not take place.

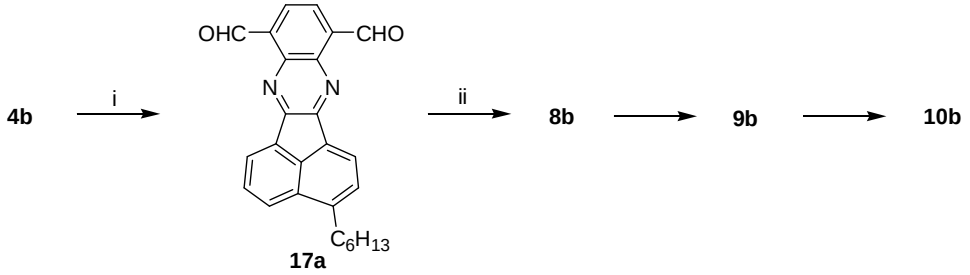

Scheme 4.56: i) **4b**, THF, 1.6M *n*-BuLi, –78°C, formylpiperidine, N_2, 12h; ii) **17a**, reduction, EtOH, $NaBH_4$.

As it was mentioned in chapter one, since the first report on π-conjugated polymers as semi-conductor, a number of these polymers have been intensively investigated in order to fabricate devices for industrial applications[43, 44]. In order to study their potential applications many PPV type conjugated polymers have been studied so far as they have attracted much attention because of their strong electroluminescent properties[45]. PQV type materials has not been studied much in

the literature, still they seem to be very promising material for application as n-type semi-conductor in organic solar cells[30, 46]. However, the intrinsic insolubility of the conjugated structure restricts further development of PQV as semi-conductor for application. In order to improve its solubility efforts have been made to introduce phenyl alkyl (Ph-C_5H_{11} and Ph-C_8H_{17}) and phenyl alkoxy (Ph-OC_8H_{17}) side chains into the PQV structure as it can be depicted in Scheme 4.57.

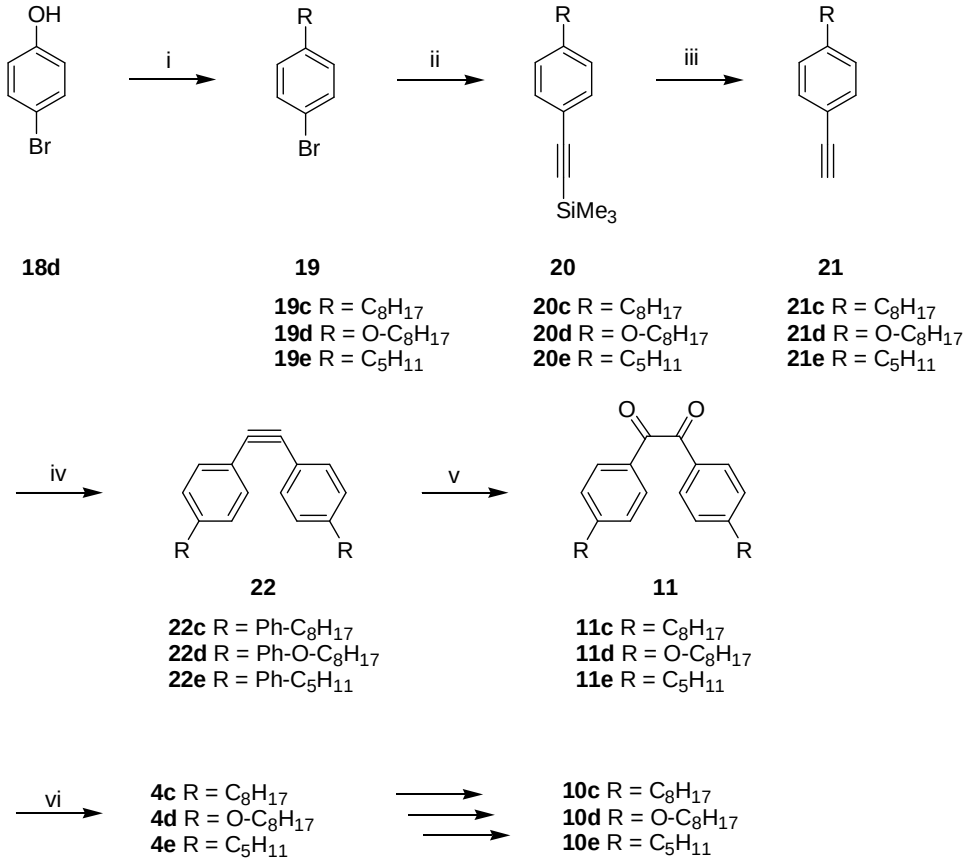

Scheme 4.57: i) **18d**, Na*t*BuO, 1-bromooctane, NaI (cat.), EtOH, ΔT, 4h; ii) **19** (**c** or **d**), trimethylsilylacetylene, $P(Ph)_3$, CuI, $PdCl_2[P(Ph)_3]_2$, piperidine, 80 °C, 24 h; iii) **20** (**c** or **d**), KF, DMF, room temperature, 3h; iv) **19** (**c**, **d**, **e**), **21** (**c**, **d**, **e**), $P(Ph)_3$, CuI, $PdCl_2[P(Ph)_3]_2$, piperidine, 80 °C, 24 h; v) **22** (**c**, **d**, **e**), $KMnO_4$, room temeperature, 4 h; vi) 3, **11** (**c**, **d**, **e**), I_2, EtOH, room temperature, ((c, 3h), (d, 96h), (e, 1h)).

The intermediary product 5,8-dibromo-2,3-bis-(4-octyl-phenyl)-quinoxaline **4c** was prepared in a five step reaction sequence according to Scheme 4.57. Starting from the commercially available 1-Bromo-4-octyl-benzene **19c** the reaction steps are analogues to the ones described for the synthesis of **4d**. After many efforts to purify the product it was used in the next step without further purification.

The intermediary product 5,8-dibromo-2,3-bis-(4-octyloxy-phenyl)-quinoxaline **4d** was prepared in a six step reaction sequence according to Scheme 4.57. Starting from the commercially available 4-bromo-phenol **18d** and commercially available 1-bromooctane, a Williamson etherification gives 1-bromo-4-octyloxy-benzene **19d** in high yield[47]. Subsequently, **19d** is converted to **22d** by a sequence of Sonogashira cross-coupling reactions[48]. The catalytic cycle for Sonogashira cross-coupling reaction is depicted in Figure 4.57. The three characteristic steps in the catalytic cycle are: *Oxidative addition* (**O.A.**)*, transmetallation* and *reductive elimination* (**R.E.**). The transmetallation step is the slowest step in the catalytic cycle and it is believed to be the *rate-determing step* (**R.D.S.**). For cross-coupling involving carbon-carbon bond formation, the ligand substitution is a transmetallation reaction[49,50]. First, 1-bromo-4-octyloxy-benzene **19d** was coupled with trimethylsilylacetylene to give **20d** in high yield. After quantitative deprotection of the triple bond with potassium fluoride in DMF, the 1-ethynyl-4-octyloxy-benzene **21d** was coupled with **19d** resulting in 1,2-dioctyloxy benzene ethylene **22d**. Oxidation of **22d** with $KMnO_4$ in acetone/ water, at room temperature for 4 hours resulted in the formation of very impure 1,2.diketone **11d**.[45]

Since after many efforts the purification by crystallisation of either **11c** or **11d** failed due to inefficient solvent, the product was not possible to be analysed and it was used in the next step without further purification. This resulted in very impure formation of the products **4c** and **4d**. In the process of purifying these products a lot of the product was lost which was not enough in order to continue the experiment.

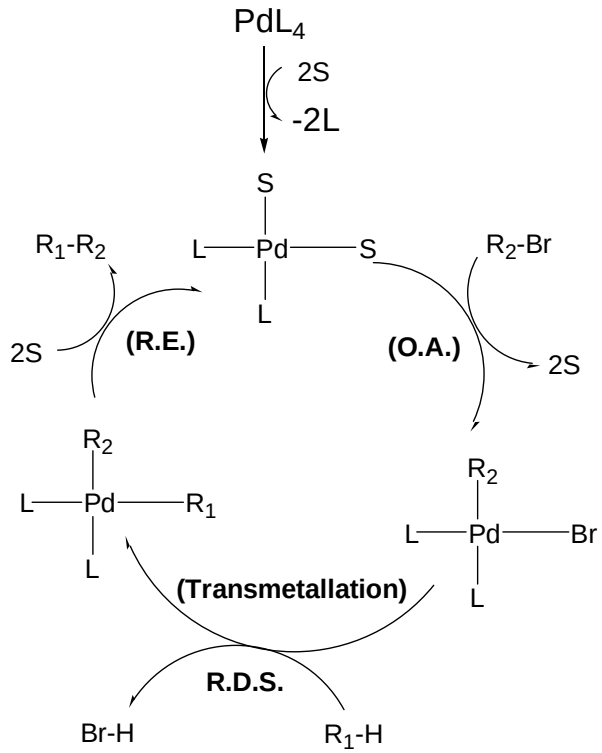

Figure 4.57: The catalytic cycle for Sonogashira Cross-Coupling reaction.

The products **4c** and **4d** could not be separated from the formed side products which could be depicted on ^{1}H-NMR and ^{13}C-NMR. Therefore, it was difficult to continue with very low and impure yield of these materials. One major reason for the low yield could be the presence of a steric hindrance. Therefore, on one hand for shortening the reaction steps and on the other hand for preparing a soluble derivative of PQV, the synthesis of quinoxaline with pentyl phenyl side chains was chosen.

The intermediary 5,8-dibromo-2,3-bis-(4-pentyl-phenyl)-quinoxaline **10e** was prepared in nine step reaction sequence according to Scheme 4.57. Starting from the commercially available 1-ethynyl-4-pentyl benzene **21e** and commercially available 1-bromo-4-pentyl benzene **19e**, the reaction steps are analogues to the ones described for the synthesis of **4d**. The follow-up reaction steps are analogues to the ones described for the synthesis of Plain PQV (chapter 2).

As can be seen in Scheme 4.58, a short cut towards the dithiocarbamate monomer **10e** has been applied. This has been done in order to improve the synthesis procedure towards quinoxalines and their derivatives. Hereby the four step procedure from the intermediary products **4e** to **8e** via Benzothiadiazole route (chapter two) can be replaced by the simple two step procedure of **4e** to **8e** via **17b**. The purification of **17b** by column chromatography did not lead to pure product. According to NMR and GC-MS analysis, besides the product, many side products were formed as well, from which some possible structure are depicted in Figure 4.58. Therefore **17b** was used in the next step without further purification. Unfortunately the synthesis of **8e** failed. The main reason could be the presence of many side products. More experiments need to be carried out in order to create a better, optimised and shorter reaction route.

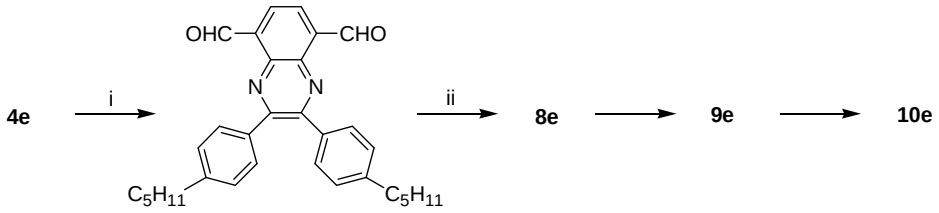

Scheme 4.58: i) **4b**, THF, 1.6M *n*-BuLi, –78°C, 1-formylpiperidine, N_2, 12h; ii) **17b**, reduction, EtOH, $NaBH_4$.

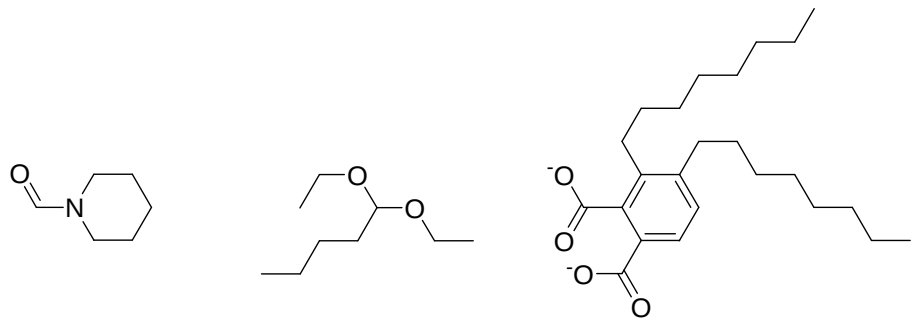

formylpiperidine **1,1-diethoxypentane** **di-octylphthalate**

Figure 4.58: Possible presence of side products formed during the synthesis of **17b**.

4.3 Conclusion

The main aim of this chapter was to prepare and analyse soluble derivatives of PQV by introduction of long flexible alkyl or alkoxy side chains. The preparation of quinoxaline monomer **10a** with *n*-hexyl side chains failed. In order to obtain one of the starting materials 1,2-diketon **11a**, the experiment was carried out several times and all of them resulted in quantitative formation of the side product heptanoic acid **13**. A possible mechanism involved could be the acidic hydrolysis of the nitrile group (CN) in the presence of diluted solution of hydrochloric acid which was determined by ^{1}H-NMR and ^{13}C-NMR analysis as well.

Concerning the quinoxaline monomer **10b** with 3-hexyl-acenaphto units, the intermediary products **4b** up to **7b** were obtained in good yield and purity. They were further analysed by ^{1}H-NMR, ^{13}C-NMR and GC-MS. The intermediary product **8b** and **9b** were synthesised with the formation of many side products that were impossible to be separated by purification. Therefore, a solution was the use of an alternative route via **17a** towards the synthesis of the dithiocarbamate monomer **10b**. Unfortunately the synthesis failed due to the insolubility of the intermediary products in any common organic solvents. Therefore, the analysis of the intermediary products could not take place as well.

For the synthesis of quinoxaline with dioctyl-diphenyl and dioctyloxy-diphenyl side chains, many steps are required which is time consuming. Among the reactions a sequence of Sonogashira cross-coupling reactions was applied in order to prepare the intermediary products. The intermediary products **20c** up to **22c** and **19d** up to **22d** were obtained in good yield. Many efforts were done for the synthesis and purification of the 1,2-diketones **11c** and **11d**. Since the purification by crystallisation was not successful due to inefficient solvent, the analysis of the compounds could not be carried out. Therefore, the 1,2-diketones **11c** and **11d** were used in the next step without further purification. This resulted in very impure formation of the products **4c** and **4d** which were lost quantitatively in the process of purifying these products. One of the reasons for this low yield could be the presence of sterric hindrance due to the long alkyl side chains. Regrettably, due to lack of time and loss of product the experiments could not be continued.

In order to synthesise soluble derivatives of quinoxaline in short time, an effort was made to prepare penthyl-diphenyl quinoxaline **10e**. It was chosen for penthyl in order to get a possible better solubily of the intermediary products in common organic solvents. The synthesis of **10e** was carried out in a nine step reaction sequence which was analogues to the synthesis mentioned earlier. Also here an alternative route was applied via **17b** towards the dithiocarbamate monomer **10e**.
The purification of **17b** by column chromatography did not lead to pure product. According to ^{1}H-NMR, ^{13}C-NMR and GC-MS analysis, besides the product, many side products were formed as well. Therefore the synthesis of **8e** failed and the synthesis of the final product could not be carried out.
The purification of many products, especially the final monomers was not possible. Some of the intermediary products were not soluble in common organic solvents. Therefore, a pure monomer could not be obtained. Without pure monomer, the polymerisation would not be successful. As we were running out of time, the possibility for repeating the entire procedure was not there.

4.4 Experimental section

4.4.1 Materials

All solvents used in the synthesis were distilled before use. Tetrahydrofuran (THF) was refluxed under nitrogen with sodium metal and benzophenone until a blue colour persisted and was then distilled. All the commercially available products were purchased from Acros or Aldrich. 2,1,3-benzothiadiazole **1**, 5-hexyl-acenaphthylene-1,2-dione **11b** was prepared by Palmaerts[36-39], 2-oxooctanenitrile **12**, 4-bromophenol **18d**, bromine, ZnI_2, 1-bromooctane , 1-bromo-4-octyl-benzene **19c**, 1-bromo-4-pentyl benzene **19^{e}**, 1-ethynyl-4-pentyl benzene **21e**, , NaI, CuI, trimethylsilylacetylene, triphenylphosphine, *trans*-dichlorobis(triphenylphosphine)palladium(II), tetrakis triphenylphosphine palladium, KF, formylpiperidine, *n*-BuLi (1.6M in hexane) and $KMnO_4$ were purchased from

Acros or Aldrich and used without further purification. ZnI_2 was flashed with nitrogen prior to use and used at once.

4.4.2 Characterisation

Nuclear magnetic resonance (NMR) spectra were recorded on a Varian Inova 300 spectrometer at 300 MHz for ^{1}H-NMR and at 75 MHz for ^{13}C-NMR using a 5 mm probe.

Gas chromatography/mass spectrometry (GC/MS) analyses were carried out with TSQ – 70 or Voyager mass spectrometers (Thermoquest); the capillary column was a Chrompack Cpsil5CB or Cpsil8CB.

Fourier Transform Infra Red spectroscopy (FT-IR) was performed on a Perkin Elmer Spectrum One FT-IR spectrometer (nominal resolution 4 cm-1, summation of 16 scans). Samples for the FT-IR characterisation were prepared by spin-coating the compounds from a chloroform solution (6 mg/mL) onto NaCl disks (diameter 25 mm and thickness 1 mm) at 500 rpm.

TLC analyses were made on Merck aluminium sheets, 20 x 20 cm, covered with silica gel 60 F254.

4.4.3 Synthesis

4,7-dibromo-benzo[1,2,5]thiadiazole (2)

The synthesis of this product is similar to the synthesis of **15** (chapter 2).

3,6-dibromo-benzene-1,2-diamine (3)

The synthesis of this product is similar to the synthesis of **16** (chapter 2).

8,11-dibromo-3-hexyl-acenaphtho[1,2-b]quinoxaline (4b)

To a 100 mL round-bottomed flask equipped with a large magnetic stirring bar, a reflux condenser, a heating mantel and electronic thermometer was added **3** (1 g, 0.0038 mol) and **11b** (1 g, 0.0038 mol) dissolved in ethanol (60 mL). The reaction mixture was stirred and refluxed for 27 hours. The reaction mixture was cooled to ambient temperature overnight. The precipitate was filtered off, washed with cold ethanol and air-dried. The product was obtained as milk-coffee coloured solid (1.42 g, 76% yield). ^{1}H-NMR ($CDCl_3$): 8.41-8.38 (d, 1H), 8.32-8.29 (d, 1H), 8.17-8.14 (d, 1H), 7-83 (d, 2H), 7.78-7.72 (m, 1H), 7.56-7.53 (d, 1H), 3.14-3.09 (t, 2H), 1.81-1.73 (m, 2H), 1.45-1.31 (m, 6H), 0.91-0.86 (t, 3H); ^{13}C-NMR ($CDCl_3$): 154.81-154.62 (2C), 144.54 (2C), 139.79-139.55 (2C), 137.38-128.86 (3C), 128.85-127.03 (4C), 124.20-124.09 (2C), 123.22 (1C), 122.65 (2C), 32.56 (1C), 31.53-31.39 (2C), 29.29 (1C), 22.48 (1C), 13.95 (1C); GC-MS: 496 (M^+), 425 (M^+-C_5H_{11}), 346 (M^+-C_5H_{11}-Br), 265 (M^+-C_5H_{11}-Br-Br), 238 (M^+-C_5H_{11}-Br-Br-CH=CH), 213 (M^+-C_5H_{11}-Br-Br-CH=CH-2C), 138 (M^+-C_5H_{11}-Br-Br-CH=CH-2C-C_4N_2), 100 (M^+-C_5H_{11}-Br-Br-CH=CH-2C-C_4N_2-C_3H_3), 74 (M^+-C_5H_{11}-Br-Br-CH=CH-2C-C_4N_2-C_3H_3-C_2H_2).

5,8-dibromo-2,3-bis-(4-octyl-phenyl)-quinoxaline (4c)

To a 100 mL round-bottomed flask equipped with a large magnetic stirring bar, a mixture of **3** (2.90 g, 0.011 mol) and **11c** (4.82 g, 0.011 mol) dissolved in ethanol (58 mL). To this was added iodine (cat., 0.28 g, 0.0011 mol) and the reaction mixture was stirred at room temperature for 3 hours. After completion of the reaction, the reaction mixture was poured onto crushed ice and stirred for 10-15 min.

The solid which separated was filtered, washed with aqueous sodium thiosulfate solution (3 x 50 mL) to remove iodine and subsequently with water, then crystallised from ethanol to afford the brown coloured product (3.54 g, 48%). ^{1}H-NMR ($CDCl_3$): 7.86 (s, 2H), 7.57-7.47 (d, 4H), 7.15-7.12 (d, 4H), 2.63-2.58 (t, 4H), 1.60-1.53 (m, 4H), 1.28-1.25 (m, 20H), 0.89-0.84 (t, 6H); ^{13}C-NMR ($CDCl_3$): 154.11 (2C), 144.64-131.12 (8C), 130.02-128.31 (8C), 123.50 (2C), 35.69 (2C), 31.77-29.16 (10C), 22.56 (2C), 14.00 (2C).

5,8-Dibromo-2,3-bis-(4-octyloxy-phenyl)-quinoxaline (4d)

The synthesis of **4d** is analogous to the synthesis of **4c** with exception of the compounds **3** and **11d** as the starting materials. Only a very small amount of brown-green coloured product was obtained. ^{1}H-NMR ($CDCl_3$): 7.42-7.39 (s, 2H), 6.84-6.81 (d, 4H), 3.96-3.91 (t, 4H), 1.76-1.73 (m, 4H), 1.43 (m, 4H), 1.29-1.26 (m, 16H), 0.87-0.84 (t, 6H); ^{13}C-NMR ($CDCl_3$): 158.94 (2C), 135.46-114.46 (18C), 68-04 (2C), 31.80-22.64 (24C), 14.10 (2C).

5,8-dibromo-2,3-bis-(4-pentyl-phenyl)-quinoxaline (4e)

The synthesis of **4e** is analogous to the synthesis of **4c** with exception of the compounds **3** and **11e** as the starting materials resulting in 5.49 g product (41%). ^{1}H-NMR ($CDCl_3$): 7.86 (s, 2H), 7.58-7.54 (dt, 4H), 2.63-2.58 (t, 4H), 1.63-1.55 (m, 4H), 1.33-1.26 (m, 8H), 0.90-0.85 (t, 6H); ^{13}C-NMR ($CDCl_3$): 154.19 (2C), 144.72 (2C), 139.17 (2C), 135.35 (2C), 132.74 (2C), 130.10 (4C), 128.40 (4C), 123.56 (2C), 35.73 (2C), 31.40-30.85 (2C), 22.49 (2C), 14.02 (2C); 580 (M^+), 509 (M^+-C_5H_{11}), 438 (M^+-$2C_5H_{11}$), 362 (M^+-$2C_5H_{11}$-Ph), 326 (M^+-$2C_5H_{11}$-Ph-C=N), 234 (M^+-$2C_5H_{11}$-2Ph-C=N), 154 (M^+-$2C_5H_{11}$-2Ph-C=N-Br), 130 (M^+-$2C_5H_{11}$-2Ph-C=N-Br-C=C), 116 (M^+-$2C_5H_{11}$-2Ph-C=N-Br-C=C-CH).

3-Hexyl-acenaphtho[1,2-b]quinoxaline-8,11-dicarbonitrile (5b)

In a flask **4b** (1.35 g, 0.0027 mol) and CuCN (0.56 g, 0.0063 mol) were dissolved in 10 mL DMF. The reaction mixture was stirred and refluxed under an inert atmosphere at 164°C for 4 hours. After the reaction mixture was cooled down, it was poured into a solution of $FeCl_3$ (3.5 g), HCl (conc., 0.69 mL) and water (5.21 mL) and stirred at 65°C for 30 minutes. The aqueous solution was filtered through a path of celite and extracted with $CHCl_3$ (5 x 50 mL). The organic layer was washed with subsequently 5 mL HCl (1:1) and 5 mL 15% NaOH (aq.). To neutralise the combined organic layers they were washed twice with H_2O (100 mL). They were also washed with NaCl (sat., 100 mL) and finally dried over $MgSO_4$. After filtration and evaporation the product was precipitated in *n*-hexane. Finally, filtration resulted in the formation of a yellow coloured product (0.86 g, 82% yield). ^{1}H-NMR ($CDCl_3$): 8.24-7.23 (m, 7H), 3.14-2.92 (d, 2H), 2.15-0.88 (m, 11H).

2,3-Bis-(4-pentyl-phenyl)-quinoxaline-5,8-dicarbonitrile (5e)

The synthesis of **5e** is analogous to the synthesis of **5b** with exception of the compound **4e** as the starting material. The crude product was purified by a short Column Chromatography (*n*-hexane: ethyl acetate) resulting in 2.97 g pure product (88%). ^{1}H-NMR ($CDCl_3$): 8.10 (s, 2H), 7.61-7.57 (d, 4H), 7.18-7.14 (d, 4H), 2.65.2.59 (t, 4H), 1.64-1.57 (m, 4H), 1.32-1.30 (m, 8H), 0.91-0.86 (t, 6H); ^{13}C-NMR ($CDCl_3$): 156.41 (2C), 145.69 (2C), 140.04 (2C), 134.45 (2C), 133.55 (2C), 130.01 (2C), 128.43-128.18 (4C), 116.82 (2C), 114.89 (2C), 35.62 (2C), 31.25-30.62 (4C), 22.34 (2C), 13.87 (2C)); GC-MS: 473 (M^+), 402 (M^+-C_5H_{11}), 331 (M^+-$2C_5H_{11}$), 243 (M^+-$2C_5H_{11}$-Ph-C), 215 (M^+-$2C_5H_{11}$-Ph-C-2N), 117 (M^+-$2C_5H_{11}$-Ph-C-2N-C-Ph-C), 89 (M^+-$2C_5H_{11}$-Ph-C-2N-C-Ph-C-2N).

3-Hexyl-acenaphtho[1,2-b]quinoxaline-8,11-dicarboxylic acid (6b)

To **5b** (0.86 g, 0.0022 mol) suspended in 20 mL NaOH (10%) was added absolute ethanol (10 mL) and heated overnight (100°C). After completion of the reaction the condenser was detached and the solution was refluxed for a few minutes in the open flask to remove dissolved ammonia and some of the ethanol. The suspension was cooled and filtered. To the filtrate hydrochloric acid (conc.) was added until the precipitation of the product was complete. The crude yellow coloured product was filtered off, washed subsequently with toulene, $CHCl_3$, EtOAc and aceton (bad solubility) and dried over $MgSO_4$. Finally, after filtration and evaporation the pale brown product obtained (0.28 g, 29% yield) was used in the next step without additional analysis.

2,3-Bis-(4-pentyl-phenyl)-quinoxaline-5,8-dicarboxylic acid (6e)

The synthesis of **6e** is analogous to the synthesis of **6b** with exception of the compound **5e** as the starting material. The crude product was crystallised from toluene resulting in pure pale brown crystals (2.07 g, 68%). ^{1}H-NMR ($CDCl_3$): 8.89 (br s, 2H), 7.45 (br s, 4H), 7.24 (br s, 4H), 2.66 (br s, 4H), 1.64 (br s, 4H), 1.32 (br s, 8H), 0.89 (br s, 6H); ^{13}C-NMR ($CDCl_3$): 164.33 (2C), 153.82 (2C), 137.99 (2C), 132.88 (2C), 129.59 (2C), 35.63 (4C), 31.27 (2C), 22.32 (2C), 13.89 (2C).

3-Hexyl-acenaphtho[1,2-b]quinoxaline-8,11-dicarboxylic acid dimethyl ester (7b)

0.44 g of **6b** (0.001 mol) was added to a mixture of MeOH (20 mL) and H_2SO_4 (2 mL, 70%) and refluxed at 80°C under inert conditions overnight. After completion of the reaction, the condenser was detached and the reaction mixture was cooled. The reaction mixture was extracted with CH_2Cl_2 (3 x 50 mL). The combined organic layers were washed with water and dried over $MgSO_4$. After filtration and evaporation a pale brown compound as impure product was obtained which was used in the next step without further purification.

[8-methoxycarbonylmethyl-2,3-bis-(4-pentyl-phenyl)-quinoxalin-5-yl]-acetic acid methyl ester (7e)

The synthesis of **7e** is analogous to the synthesis of **7b** with exception of the compound **6e** as the starting material. Purification of the product did not help resulting in an impure product. ^{1}H-NMR ($CDCl_3$): 8.07 (s, 2H), 7.60-7.56 (d, 4H), 7.14-7.11 (d, 4H), 4.06-4-05 (d, 6H), 2.67-2.57 (m, 4H), 1.65-1.54 (m, 4H), 1.35-1.23 (m, 8H), 0.91-0.83 (m, 6H); ^{13}C-NMR ($CDCl_3$): 166.05 (2C), 152.95 (2C), 137.98 (2C), 133.26 (2C), 129.98 (2C), 52.59 (2C), 31.25 (4C), 30.70 (2C), 22.35 (2C), 13.87 (2C).

(8-Hydroxymethyl-2,3-diphenyl-quinoxalin-5-yl)-methanol (8b)

From diester: To the diester **7b** (0.58 g, 0.0013 mo) suspended in 30 mL absolute ethanol was added $NaBH_4$ (1.06 g, 0.028 mol) in one portion. The reaction mixture was refluxed under inert atmosphere overnight. After cooling down a saturated NH_4Cl solution (30 mL) was added and the solution was stirred overnight. The solvent was evaporated and the precipitated solids were dissolved by addition of the minimum necessary amount of water. The resulting solution was extracted with ethyl acetate (5 x 50 mL) and the combined organic layers were dried over $MgSO_4$. After filtration and evaporation the crude brown compound that was obtained was analysed not leading to the right product.

From dialdehyde: To a 50 mL three-necked round-bottomed flask equipped with a condenser, was added the **17a** (360 mg, 0.92 mmol) dissolved in ethanol (36

mL). To this solution was added $NaBH_4$ (34.8 mg, 0.92 mmol) and $(NH_4)_2CO_3$ (88.4 mg, 0.92 mmol) and the reaction mixture was stirred at room temperature for 1 hour. The reaction progress was monitored by TLC. After completion of the reaction the mixture was filtered through a path of celite and the filtrate was concentrated under reduced pressure to obtain a compound that after analysis proved not to be the right product.

[8-hydroxymethyl-2,3-bis-(4-pentyl-phenyl)-quinoxalin-5-yl]-methanol (8e)

The synthesis of **8e** from diester is analogous to the synthesis of **8b** with exception of the compound **7e** as the starting material. The crude mixture was purified by column chromatography (n-hexane: ethyl acetate = 7:3) leading to a yellow oil (1.80 g, 57%). ^{1}H-NMR ($CDCl_3$): 7.54 (s, 2H), 7.44-7.39 (dd, 4H), 7.20-7.11 (dd, 4H), 5.20 (s, 4H), 2.60-2.58 (m, 4H), 1.66-1.56 (m, 4H), 1.36-1.21 (m, 8H), 0.91-0.82 (m, 6H); ^{13}C-NMR ($CDCl_3$): 151.86 (2C), 139.66 (2C), 137.54 (2C), 127.41 (2C), 63.60 (2C), 31.28 (4C), 30.71 (2C), 22.35 (2C), 13.89 (2C).

The synthesis of **8e** from dialdehyde is analogous to the synthesis of **8b** with exception of the compound **17b** as the starting material. The crude mixture was not soluble in common organic solvents. Still, an effort was made to crystallise it from $CHCl_3$, not leading to the right product.

5,8-Bis-chloromethyl-2,3-bis-(4-pentyl-phenyl)-quinoxaline (9e)

In a one-necked round-bottomed flask (100 mL) equipped with a magnetic stirring bar the diol **8e** (0.95 g, 0.0020 mol) was dissolved in thionyl chloride (9.5 mL). The reaction mixture was stirred at room temperature under inert atmosphere overnight. After completion *Very Slowly* pH was brought to 7 by saturated/ concentrated $NaHCO_3$, extracted with CH_2Cl_2 (3 x 50 mL) and the combined organic layers (brown oil) were washed with water and dried over $MgSO_4$. Finally, after filtration and evaporation the crude yellow/brown compound that was obtained was analysed and used in the next step. ^{1}H-NMR ($CDCl_3$): 7.83 (s, 2H), 7.53-7.49 (d, 4H), 7.16-7.11 (d, 4H), 5.34-5.32 (d, 4H), 2.65-2.58 (m, 4H), 1.68-1.58 (m 4H), 1.37-1.24 (m, 8H), 0.92-0.87 (m, 6H); ^{13}C-NMR ($CDCl_3$): 153.10 (2C), 139.25 (2C), 130.01 (2C), 129.29 (2C), 41.17 (4C), 31.31 (2C), 30.73 (2C), 22.38 (2C), 13.90

(2C); GC-MS: 520 (M^+), 484 (M^+-Cl), 449 (M^+-2Cl), 377 (M^+-2Cl-C_5H_{11}), 307 (M^+-2Cl-2C_5H_{11}), 218 (M^+-2Cl-2C_5H_{11}-C_7H_4), 166 (M^+-2Cl-2C_5H_{11}-C_7H_4-C_4H_4), 102 (M^+-2Cl-2C_5H_{11}-C_7H_4-C_4H_4-N=C-C=N-C), 76 (M^+-2Cl-2C_5H_{11}-C_7H_4-C_4H_4-N=C-C=N-C-2C).

Diethyl-dithiocarbamic acid 8-diethylthiocarbamoylsulfanylmethyl-2,3-bis-(4-pentyl-phenyl)-quinoxalin-5-ylmethyl ester (10e)

In a one-necked round-bottomed flask (100 mL) equipped with a magnetic stirring bar was added the impure diCl-dipentyl-compound **9e** (1 g, 0.0019 mol) and sodiumdithiosalt (1.31 g, 0.0058 mol). To this was added 20 mL of ether and the reaction mixture was stirred at room temperature till completion of the reaction and monitored by TLC. The reaction was stopped by the addition of water (20 mL) and stirred for a while. The reaction mixture was extracted with ether (3 x 50 mL), and dried over $MgSO_4$. Finally, after filtration and evaporation an impure compound (brown foam) was obtained, which was purified by a short Column Chromatography (*n*-hexane: $CHCl_3$ = 9:1) followed by crystallisation from *n*-hexane: $CHCl_3$ = 7:3 not leading to the right product.

1,2-diketones; Tetradecane-7,8-dione (11a)

To a three-necked round-bottomed flask (50 mL) equipped with a magnetic stirring bar, was added the dry ZnI_2 (1.01 g, 3.16 mmol) dissolved in dry THF (51 mL). To this solution was added slowly 2-oxooctanenitrile (0.5 mL, 3.16 mmol). The mixture was stirred under nitrogen atmosphere at room temperature for 1.5 hours and monitored by TLC. After 1.5 hours, diluted HCl was added and the reaction mixture was extracted with diethyl ether (3 x 25 mL). The ether extract was washed with $NaHCO_3$ solution (3 x 25 mL), dried over sodium sulphate, and concentrated under reduced pressure which after analysis did not afford the right product.

1,2-Bis-(4-octyloxy-phenyl)-ethane-1,2-dione (11c)

To a 1 L three-necked round-bottomed flask equipped with a magnet was added 1,2-dioctyl benzene ethylene **22c** (8.3 g, 0.021 mol), acetone (415 mL) and distilled water (145 mL). $KMnO_4$ (16.6 g, 0.105 mol) was slowly added and the reaction mixture was stirred at room temperature for 4 hours. After the reaction was

completed, black MnO_2 solids were removed by filtration over a path of Celite. After evaporation the concentrated filtrate was extracted with ethyl acetate (3 x 200 mL) and dried over $MgSO_4$. After evaporation of the solvent under reduces pressure, an effort was made to purify the product by crystallisation from subsequently MeOH, $CHCl_3$ and acetone without resulting to the right product.

1,2-Bis-(4-octyloxy-phenyl)-ethane-1,2-dione (11d)

The synthesis of **11d** is analogous to the synthesis of **11c** with exception of the compound **22d** as the starting material. The crude mixture was not soluble in common organic solvents. Still, an effort was made to crystallise it from MeOH and $CHCl_3$, not resulting to the right product.

1,2-Bis-(4-pentyl-phenyl)-ethane-1,2-dione (11e)

The synthesis of **11e** is analogous to the synthesis of **11c** with exception of the compound **22e** as the starting material. The crude mixture was crystallised from MeOH by which the product as yellow oil was obtained (31.1 g, 70%). ^{1}H-NMR ($CDCl_3$): 7.88-7.85 (d, 4H), 7.30-7.27 (d, 4H), 2.68-2.62 (t, 4H), 1.66-1.53 (m, 4H), 1.37-1.28 (m, 8H), 0.93-0.84 (t, 6H); ^{13}C-NMR ($CDCl_3$): 194.53 (2C), 150.95 (2C), 131.21-128.40 (10C), 36.16 (2C), 31.35-30.66 (4C), 22.44 (2C), 13.95 (2C); GC-MS: 350 (M^+), 279 (M^+-C_5H_{11}), 175 (M^+-C_5H_{11}-Ph-CO), 88 (M^+-C_5H_{11}-Ph-CO-C_5H_{11}-O), 76 (M^+-C_5H_{11}-Ph-CO-C_5H_{11}-CO).

3-Hexyl-acenaphtho[1,2-b]quinoxaline-8,11-dicarbaldehyde (17a)

To a three-necked round bottomed flask of 50mL the diBromophenyl quinoxaline **4b** (1 g, 0.0020 mol) was dissolved in dry THF (12.5 mL). *n*-BuLi (1.6M, 0.0044 mol, 2.75 mL) was added SLOWLY with syringe to the solution from above and stirred at –78°C for 30 minutes. Hereby N_2 was bubbled through the solution. Then, the solution was quenched with formylpiperidine (0.49 mL, 0.0044 mol), and after the mixture was stirred for 12 hours at 25°C. For the work up 30 mL of HCl 2M was added and the reaction mixture was extracted with $CHCl_3$ (3 x 10 mL). The organic layer was dried over $MgSO_4$ and the solvent was evaporated under reduced pressure. The crude product as red oil was purified by column chromatography (*n*-

hexane: ethyl acetate = 9:1). The analysis showed strong presence of 1-formylpiperidine.

2,3-Bis-(4-pentyl-phenyl)-quinoxaline-5,8-dicarbaldehyde (17b)

The synthesis of **17b** is analogous to the synthesis of **17a** with exception of the compound **4e** as the starting material. After purification by column chromatography an effort was made to purify the product by low pressure flash chromatography obtaining 22% product. Unfortunately the analysis showed strong presence of the starting material.

1-bromo-4-octyloxy-benzene (19d)

To a three-necked round-bottomed flask (100 mL) a mixture of 4-bromophenol **18d** (5 g, 28.9 mmol), Na*t*BuO (3.33 g, 34.7 mmol) and EtOH (30 mL) was stirred at room temperature under N_2 atmosphere for 1hour. After which 1-bromooctane (6.1 mL, 34.7 mmol) and NaI (0.13 g, 0.88 mmol) were added. The resulting solution was stirred for 4 hours at reflux temperature. The reaction was quenched with water (30 mL), and extracted with CH_2Cl_2 (3 x 10 mL). The combined organic extracts were dried over anhydrous $MgSO_4$. Evaporation of the solvent under reduced pressure gave the crude yellow coloured oil, which was purified by column chromatography (*n*-hexane) to yield a colourless oil (7.98 g, 97%). ^{1}H-NMR ($CDCl_3$): 7.38-7.32 (dt, 2H), 6.79-6.73 (dt, 4H), 3.93-3.84 (t, 2H), 1.87-1.71 (m, 2H), 1.47-1.29 (m, 10H), 0.95-0.86 (t, 6H); ^{13}C-NMR ($CDCl_3$): 158.14 (1C), 132.02 (2C), 116.09 (2C), 112.38 (1C), 68.02 (1C), 32.78 (1C), 31.77 (3C), 28.13 (1C), 22.62 (1C), 14.04 (1C); GC-MS: 285 (M^+), 172 (M^+-C_8H_{17}), 93 (M^+-C_8H_{17}-Br), 76 (C_8H_{17}-Br-O).

Trimethyl-(4-octyl-phenylethynyl)-silane (20c)

To a 500 mL round-bottomed flask equipped with a large magnetic stirring bar and oil bath was added 1-bromo-4-octyl-benzene **19c** (5 g, 19 mmol) and trimethylsilylacetylene (5.3 mL, 37 mmol) in *n*-propylamine. $Pd[P(Ph)_3]_4$ (5.24 g, 4.6 mmol) was added and the resulting mixture was refluxed under nitrogen atmosphere overnight. After cooling to ambient temperature, the solvent was evaporated and the crude product was purified by chromatography (*n*-hexane then

slowly increasing the polarity with ethyl acetate) to afford the product as yellow oil (4.72 g, 87%). ^{1}H-NMR ($CDCl_3$): 7.40-7.37 (dd, 2H), 7.12-7.02 (dd, 2H), 2.61-2.52 (dt, 2H), 1.61-1.56 (m, 2H), 1.28 (br s, 10H), 0.92-0.87 (t, 6H), 0.27-0.24 (s, 9H); GC-MS: 287 (M^+), 272 (M^+-CH_3), 186 (M^+-CH_3-$SiMe_3$-C), 175 (M^+-CH_3-$SiMe_3$-2C), 91 (M^+-CH_3-$SiMe_3$-2C-C_6H_{12}).

Trimethyl-(4-octyloxy-phenylethynyl)-silane (20d)

To a 250 mL round-bottomed flask equipped with a large magnetic stirring bar and oil bath was added 1-bromo-4-octyloxy-benzene **19d** (5 g, 18 mmol), $P(Ph)_3$ (0.46 g, 1.8 mmol), CuI (0.34 g, 1.8 mmol), and $PdCl_2[P(Ph)_3]_2$ (0.63 g, 0.9 mmol) dissolved in piperidine (100 mL) and heated at 50 °C. Trimethylsilylacetylene (5 mL, 35 mmol) was added drop wise and the resulting mixture was stirred at 80 °C for 24 h under nitrogen atmosphere. The reaction mixture was poured into a saturated NH_4Cl solution (100 mL) and extracted with CH_2Cl_2 (3 x 50 mL). The organic phase was washed with subsequently saturated NH_4Cl (3 x 50 mL) and water (3 x 50 mL). After removing the solvent under reduced pressure the residue was purified by filtration on silica gel (*n*-hexane then *n*-hexane:EtOAc = 75:25) to afford the pure product (4.01 g, 74%). ^{1}H-NMR ($CDCl_3$): 7.40-7.35 (d, 2H), 6.81-6.76 (d, 2H), 3.94-3.89 (t, 2H), 1.80-1.70 (m, 2H), 1.45-1.28 (m, 10H), 0.91-0.86 (t, 3H), 0.26-0.21 (m, 9H); GC-MS: 303 (M^+), 287 (M^+-CH_3), 190 (M^+-CH_3-$SiMe_3$-CC), 176 (M^+-CH_3-$SiMe_3$-CC-CH_2), 91 (M^+-CH_3-$SiMe_3$-CC-CH_2-C_6H_{12}).

1-Ethynyl-4-octyl-benzene (21c)

To a 500 mL round-bottomed flask equipped with a magnetic stirring bar was added trimethyl-(4-octyl-phenylethynyl)-silane **20c** (10.3 g, 0.036 mol) dissolved in DMF (286 mL). To this was added a solution of potassium fluoride (4.18 g, 0.072 mol) in 20 mL water and the mixture was stirred at room temperature for 3 hours. After completion the reaction mixture was poured into water (200 mL) and extracted with toluene (3 x 150 mL). The organic phase was washed with water (3 x 150 mL) and dried over $MgSO_4$.Then, the solvent was concentrated under reduced pressure to obtaind brown oil. This oil was purified by column chromatography (petroleum ether) to obtain the product in good yield (8.06 g, 83%). ^{1}H-NMR ($CDCl_3$): 7.48-7.43 (dt, 2H), 7.18-7.14 (dt, 2H), 3.06 (s, 1H), 2.66-

2.60 (t, 2H), 1.67-1.62 (m, 2H), 1.35 (br m, 10H), 0.99-0.94 (t, 3H); ^{13}C-NMR ($CDCl_3$): 143.81 (1C), 132.47-132.09 (2C), 128.40 (2C), 119.49-119.36 (1C), 83.91 (1C), 77.65-76.61 (1C), 35.99 (1C), 35.44-32.03 (2C), 31.35 (1C), 29.61-29.41 (2C), 22.81 (1C), 14.21 (1C); GC-MS: 214 (M^+), 185 (M^+-C_2H_5), 171 (M^+-C_3H_7), 157 (M^+-C_4H_9), 143 (M^+-C_5H_{11}), 129 (M^+-C_6H_{13}), 115 (M^+-C_7H_{15}), 102 (M^+-C_8H_{17}), 89 (M^+-C_8H_{17}-CH), 77 (M^+-C_8H_{17}-CH-C).

1-Ethynyl-4-octyloxy-benzene (21d)

The synthesis of **21d** is analogous to the synthesis of **21c** with exception of the compound **20d** as the starting material. After purification by column chromatography (petroleum ether) the product was obtained in good yield (2.91 g, 97%).

^{1}H-NMR ($CDCl_3$): 7.45-7.39 (dt, 2H), 6.85-6.80 (dt, 2H), 3.95-3.90 (t, 2H), 3.00 (s, 1H), 1.82-1.72 (m, 2H), 1.47-1.30 (br m, 10H), 0.93-0.88 (t, 3H); ^{13}C-NMR ($CDCl_3$): 159.52 (1C), 133.84-131.89 (2C), 114.40-113.91 (3C), 83.76 (1C), 75.76 (1C), 67.98 (1C), 31.84 (1C), 29.38-29.19 (3C), 26.04 (1C), 22.69 (1C), 14.12 (1C); GC-MS: 230 (M^+), 201 (M^+-C_2H_5), 145 (M^+-C_6H_{13}), 131 (M^+-C_7H_{15}), 101 (M^+-C_8H_{17}-O), 89 (M^+-C_8H_{17}-O-C), 76 (M^+-C_8H_{17}-O-CH-C).

1,2-dioctyl benzene ethynene (22c)

To a 250 mL round-bottomed flask equipped with a large magnetic stirring bar and oil bath was added 1-bromo-4-octyl-benzene **19c** (4.31 g, 16.6 mmol), $P(Ph)_3$ (0.44 g, 1.66 mmol), CuI (0.32 g, 1.66 mmol), and $PdCl_2[P(Ph)_3]_2$ (0.58 g, 0.83 mmol) dissolved in piperidine (87 mL) and heated at 50 °C. 1-Ethynyl-4-octyl-benzene **21c** (6.67 g, 31.1 mmol) was added drop wise and the resulting mixture was stirred at 80 °C for 24 h under nitrogen atmosphere. The reaction mixture was poured into a saturated NH_4Cl solution and extracted with CH_2Cl_2. The organic phase was washed with subsequently saturated NH_4Cl (3 x 30 mL) and water (3 x 30 mL). After removing the solvent the residue was purified by a short column chromatography (*n*-hexane: $CHCl_3$ = 1:1) to afford the product in good yield (8.3 g, 66%). ^{1}H-NMR ($CDCl_3$): 7.41-7.38 (d, 4H), 7.07-7.04 (d, 4H), 2.65-2.58 (t, 4H), 1.63-1.60 (m, 4H), 1.32-1.30 (br m, 20H), 0.93-0.89 (t, 6H); ^{13}C-NMR ($CDCl_3$): 141.81 (2C), 131.46-131.24 (4C), 130.16-128.41 (4C), 119.27 (2C), 88.95 (2C),

35.93 (2C), 31.92-31.31 (4C), 29.51-29-30 (6C), 22.71 (2C), 14.14 (2C); GC-MS: 402 (M^+), 303 (M^+-C_7H_{15}), 204 (M^+-$2C_7H_{15}$), 190 (M^+-C_7H_{15}-C_8H_{17}), 165 (M^+-C_7H_{15}-C_8H_{17}-C-CH).

1,2-dioctyloxy benzene ethynene (22d)

The synthesis of **22d** is analogous to the synthesis of **22c** with exception of the compounds **19d** and **21d** as the starting materials. 33% Product was obtained (1.66 g). 7.35-7.31 (d, 4H), 6.76-6.73 (d, 4H), 3.96-3.91 (t, 4H), 1.80-1.71 (m, 4H), 1.54-1.26 (br m, 20H), 0.89-0.84 (t, 6H); ^{13}C-NMR ($CDCl_3$): 158.92-158.20 (2C), 132.79-132.13 (4C), 113.60 (6C), 87.90 (2C), 72.83 (2C), 31.77 (2C), 29.29-29.19 (6C), 29.96 (2C), 22.62 (2C), 14.07 (2C).

1,2-dipentylbenzene ethynene (22e)

The synthesis of **22e** is analogous to the synthesis of **22c** with exception of the compounds **19e** and **21e** as the starting materials. The impure product was purified by column chromatography (petroleum ether), to afford the pure product in good yield (17.9 g, 89%).

7.44-7.41 (d, 4H), 7.15-7.12 (d, 4H), 2.62-2.57 (t, 4H), 1.65-1.55 (m, 4H), 1.36-1.26 (m, 8H), 0.91-0.85 (t, 6H); ^{13}C-NMR ($CDCl_3$): 143.20 (2C), 131.43 (4C), 128.42 (4C), 120.57 (2C), 88.89 (2C), 35.85 (2C), 31.42-30.93 (4C), 22.52 (2C), 14.02 (2C); GC-MS: 318 (M^+), 261 (M^+-C_4H_9), 204 (M^+-$2C_4H_9$), 190 (M^+-C_4H_9-C_5H_{11}), 165 (M^+-C_4H_9-C_5H_{11}-C-CH_2).

4.5 References

1. M. Gerard, A. Chaubey and B. D. Malhotra, *Biosensors & Bioelectronics*, 17, **2002**, 345

2. P. S. Heeger and A. J. Heeger, *PNAS*, 96, (22), **1999**, 12219

3. P. Cooreman, R. Thoelen, J. Manca, M. v. d. Ven, V. Vermeeren, L. Michiels, M. Ameloot and P. Wagner, *Biosensors & Bioelectronics*, 20, **2005**, 2151

4. A. R. Brown, A. Pomp, C. M. Hart and D. M. d. Leeuw, *Science*, 270, **1995**, 972

5. C. D. D. Dimitrakopoulos and P. R. L. Malenfant, *Advanced Materials*, 14, **2002**, 99

6. C. Reese, M. Roberts and M. L. Bao, *Materialstoday*, **2004**, 20

7. L. L. Chua, J. Zaumseil, J. F. Chang, E. C. W. Ou, P. K. H. Ho, H. Sirringhaus and R. H. Friend, "General observation of n-type field-effect behaviour in organic semiconductors", *Nature*, 434, (7030), **2005**, 194-199

8. D. D. C. Bradley, *Synthetic Metals*, 54, **1993**, 401

9. A. Kraft, A. C. Grimsdale and A. B. Holmes, "Electroluminescent conjugated polymers - Seeing polymers in a new light", *Angewandte Chemie-International Edition*, 37, (4), **1998**, 402-428

10. H. Hoppe and N. S. Sariciftci, "Organic Solar cells: An overview", *Journal of Materials Research*, 19, (7), **2004**, 1924

11. H. Spanggaard and F. C. Krebs, "A brief history of the development of organic and polymeric photovoltaics", *Solar Energy Materials and Solar Cells*, 83, (2-3), **2004**, 125

12. N. S. Sariciftci, L. Smilowitz, A. J. Heeger and F. Wudl, *Science*, 258, **1992**, 1474

13. D. Meissner, *Photon*, **1999**,

14. C. J. Brabec, N. S. Sariciftci and J. C. Hummelen, "Plastic solar cells", *Advanced Functional Materials*, 11, (1), **2001**, 15-26

15. J. Johnson, *C & EN*, **2004**, 25

16. G. Dennler and N. S. Sariciftci, *Proceedings of IEEE*, 93, (8), **2005**, 1429

17. M. Reyes-Reyes, K. Kim and D. L. Carroll, "High-efficiency photovoltaic devices based on annealed poly(3-hexylthiophene) and 1-(3-methoxycarbonyl)-propyl-1-phenyl-(6,6)C-61 blends", *Applied Physical Letters*, 87, (8), **2005**, 083506

18. J. J. M. Halls, C. A. Walsh, N. C. Greenham, E. A. Marseglia and R. H. Friend, *Nature*, 376, **1995**, 498

19. S. E. Shaheen, C. J. Brabec, N. S. Sariciftci, F. Padinger, T. Fromherz and J. C. Hummelen, "2.5% efficient organic plastic solar cells", *Applied Physics Letters*, 78, (6), **2001**, 841-843

20. F. Padinger, R. S. Rittberger and N. S. Sariciftci, "Effects of postproduction treatment on plastic solar cells", *Advanced Functional Materials*, 13, (1), **2003**, 85-88

21. G. Yu, J. Gao, J. C. Hummelen, F. Wudl and A. J. Heeger, "Polymer Photovoltaic Cells - Enhanced Efficiencies Via a Network of Internal Donor - Acceptor Heterojunctions", *Science*, 270, (5243), **1995**, 1789

22. H. Shirakawa, E. J. Louis, A. G. MacDiarmid, C. K. Chiang and A. H. Heeger, *J. Chem. Soc. Chem. Comm.*, **1977**, 578

23. W. Heitz, W. Brügging, L. Freund, M. Gailberger, A. Greiner, H. Jung, U. Kampschulte, N. Niesser, F. Osan, H. W. Schmidt and M. Wicker, *Macromol. Chem.*, 189, **1988**, 119-127

24. H. Martelock, A. Greiner and W. Heitz, *Macromol. Chem.*, 192, **1991**, 967-979

25. A. Greiner, H. Martelock, A. Noll, N. Siegfried and W. Heitz, *Polymer*, 32, (10), **1991**, 1857-1861

26. M. Remmers, M. Schultze and G. Wagner, *Macromol. Rapid Communication*, 17, **1996**, 239-252

27. A. W. Cooke and K. B. Wagener, *Macromolecules*, 24, **1990**, 1404

28. M. Rehahn and A.-D. Schlüter, *Chem. Letters*, 11, **1987**, 375

29. M. Hanack, J. L. Segura and H. S. Spreitzer, *Advanced Materials*, 8, **1996**, 663

30. B.-L. Lee, Yamamoto, T., "Syntheses of New Alternating CT-Type Copolymers of Thiophene and Pyrido[3,4-b]pyrazine Units: Their Optical and Electrochemical Properties in Comparison with Similar CT Copolymers of Thiophene with Pyridine and Quinoxaline", *Macromolecules*, 32,, **1999**, 1375-1382

31. M. Jonforsen, Johansson, T., Inganäs, O., Andersson, M.R., "Synthesis and Characterisation of Soluble and n-Dopable Poly(quinoxaline vinylene)s and

Poly(pyridopyrazine vinylene)s with Relatively Small Gap", *Macromolecules*, 35, **2002**, 1638-1643

32. M. Jonforsen, T. Johansson, L. Spjuth, O. Inganas and M. R. Andersson, "Synthesis and characterization of poly(quinoxaline vinylene)s and poly(pyridopyrazine vinylene)s with phenyl substituted side-groups", *Synthetic Metals*, 131, (1-3), **2002**, 53-59

33. J. B. Baek and L. C. Chien, "Synthesis and photoluminescence of linear and hyperbranched polyethers containing phenylquinoxaline units and flexible aliphatic spacers", *Journal of Polymer Science Part a-Polymer Chemistry*, 42, (14), **2004**, 3587-3603

34. A. Tsami, T. W. Bunnagel, T. Farrell, M. Scharber, S. A. Choulis, C. J. Brabec and U. Scherf, "Alternating quinoxaline/oligothiophene copolymers - synthesis and unexpected absorption properties", *Journal of Materials Chemistry*, 17, (14), **2007**, 1353-1355

35. W. Mammo, S. Admassie, A. Gadisa, F. L. Zhang, O. Inganas and M. R. Andersson, "New low band gap alternating polyfluorene copolymer-based photovoltaic cells", *Solar Energy Materials and Solar Cells*, 91, (11), **2007**, 1010-1018

36. A. Sygula and P. W. Rabideau, "Non-pyrolytic syntheses of buckybowls: Corannulene, cyclopentacorannulene, and a semibuckminsterfullerene", *Journal of American Chemical Society*, 121, **1999**, 7800-7803

37. A. Palmaerts,"Synthesis of 7,10-bis(chloromethyl)fluoranthene", *intern report,* UHasselt, **2005**,

38. A. Palmaerts,"Synthesis of 1-Heptyl-naphthalene", *intern report,* UHasselt, **2005**,

39. K. Tamao, S. Kodama, I. Nakajima, M. Kumada, A. Minato and K. Suzuki, "Nickel-Phosphine Complex-Catalyzed Grignard Coupling .2. Grignard Coupling of Heterocyclic-Compounds", *Tetrahedron*, 38, (22), **1982**, 3347-3354

40. B. Baruah, A. Boruah, D. Prajapati and J. S. Sandhu, "Sm or Zn-induced coupling reactions. A facile route to 1,2-diketones", *Tetrahedron Letters*, 38, (43), **1997**, 7603-7604

41. T. W. Solomons, "Hydrolysis of nitriles", Fundamentals Of Organic Chemistry, *John Wiley & Sons, Inc.*, University of South Florida, Fifth edition, **1997**, 772-774

42. A. Palmaerts, M. v. Haren, L. Lutsen, T. J. Cleij and D. Vanderzande, "Synthesis and properties of poly(p-fluoranthene vinylene): A novel conjugated polymer with nonalternant repeating units", *Macromolecules*, 39, (7), **2006**, 2438-2440

43. J. H. Burroughes, D. D. C. Bradley, A. R. Brown, R. N. Marks, K. Mackay, R. H. Friend and P. L. Burn, *Nature*, 347, **1990**, 539

44. Z. Peng, Bao, Z., Galvin, M.E., "Oxadiazole-Containing Conjugated Polymers for Light-Emitting Diodes", *Adv. Mater.*, 10, (No. 9), **1998**, 680-684

45. K. B. Chen, H. C. Li, C. K. Chen, S. H. Yang, B. R. Hsieh and C. S. Hsu, "Novel poly(2,3-biphenyl-1,4-phenylenevinylene) derivatives containing long branched alkoxy and fluorenyl substituents: Synthesis, characterization, and their applications for polymer light-emitting diodes", *Macromolecules*, 38, (21), **2005**, 8617-8624

46. B. L. Lee, *European Patent Application*, EP 1 542 294 A1, **2004**, 1-18

47. I. Van Severen, F. Motmans, L. Lutsen, T. J. Cleij and D. Vanderzande, "Poly(p-phenylene vinylene) derivatives with ester- and carboxy-functionalized substituents: a versatile platform towards polar functionalized conjugated polymers", *Polymer*, 46, (15), **2005**, 5466-5475

48. S. Ito, M. Wehmeier, J. D. Brand, C. Kübel, R. Epsch, J. P. Rabe and K. Müllen, "Synthesis ans Self-Assembly of Functionalized Hexa-*peri*-hexabenzocoronenes", *Chemical European Journal*, 6, (23), **2000**, 4327-4342

49. Z. Olomi, "Introduction of aromatic and heteroaromatic groups in the 2-and 8-positions of the Troger's base core via Suzuki, Stille and Negishi cross-coupling", *Master's degree Dissertation*, Lund, **2003**

50. C. Solano, D. Svensson, Z. Olomi, J. Jensen, O. F. Wendt and K. Warnmark, "Introduction of aromatic and heteroaromatic groups in the 2-and 8-positions of the Troger's base core by Suzuki, Stille and Negishi cross-coupling reactions - A comparative study", *European Journal of Organic Chemistry*, (16), **2005**, 3510-3517

Chapter Five

5. Physical Characterisation and Device Towards Organic Solar Cells

5.1 Introduction

Long ago Nicolaus Copernicus (1473 — 1543) discovered that everything goes around the Sun and not around the earth! The Sun, in the core of our solar system, is an ultimate source of energy and indeed life on Earth is fully dependent on that source.

As it was mentioned in chapter one; the concern for global warming is increasing every year. The general public becomes more and more aware of the limitations one is facing concerning the stability of future supply of today's main energy sources (i.e. oil, coal, gas, uranium) and their long-term effects on the natural balance on our planet. Therefore, we are urged to develop renewable energy sources.

In order to use the sun as an energy source, photovoltaic cells that convert this sunlight into electricity have been with us for decades[1]. Although sunlight is free, the commercial use of traditional silicon-based solar cells has been limited due to its high production costs. However, to prevent this problem, solar cells based on organic materials (e.g. conjugated polymeric materials) are extensively studied as an alternative during the last few years.

In this chapter efforts are made to present the results concerning the physical characterisation and device application of plain poly (*p*-quinoxaline vinylene) **PQV** (Figure 5.59) towards solar cells; not only as n-type material but also as p-type

material depending on the opposite material in the active layer of the solar cell device.

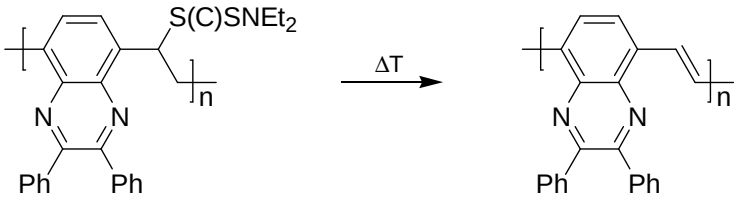

Precursor Polymer **PQV**

Figure 5.59: poly (*p*-quinoxaline vinylene) **PQV**.

In this work, the precursor polymers were analysed by photoluminescence and EPR measurements leading to surprising results. Also, solar cells were prepared from the corresponding precursor polymers with High Tg-PPV and PCBM showing promising characteristics. Furthermore, AFM measurements were performed on the polymer blend.

5.2 Photoluminescence (PL) and Electron Pulsed Resonance (EPR)

The charge transfer efficiency in blends with PQV was investigated by Aranzazu Aguirre and Griet Janssen from the group of Etienne Goovaerts at University of Antwerp.

The samples for PL measurements were prepared from spin-coated films with High Tg-PPV/PQV blends from chlorobenzene in 1:1 ratio and with pure PQV and PQV/PCBM blends from chloroform 1:2 ratio. The samples for EPR measurements were prepared from dried drop cast films of the corresponding solutions which were finally converted to the conjugated polymer[2,3,4,5,6,7].

The acceptor behaviour of PQV was examined by blending the polymer with high Tg-PPV (Tg = 150°C) as donor-material[8]. The PL spectra of the spin coated film,

shows a decrease of the High Tg-PPV emission by a factor of 4 (estimated at 585 nm and relative to the unconverted film), in comparison with pure PQV (Figure 5.60)[9]. As it was shown that the pure High Tg-PPV emission is hardly changing even under prolonged thermal treatment, the decrease of its PL intensity in the blend is a possible indication for efficient charge transfer. This is confirmed by the decrease of its decay time in the blend with PQV (Figure 5.61)[8].

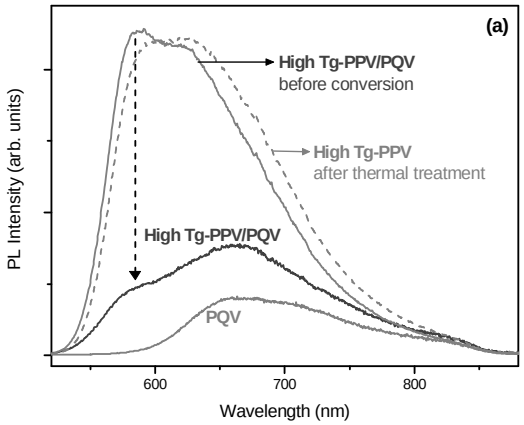

Figure 5.60: PL spectra of a High Tg-PPV/PQV.

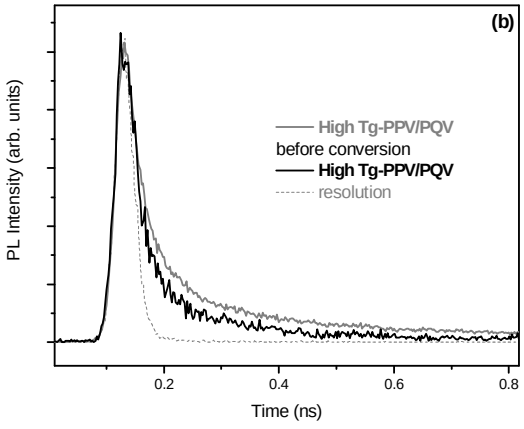

Figure 5.61: PL decay time of the High Tg-PPV/PQV film.

The interpretation of the EPR results was hampered by a relatively strong radical signal from the PQV, which is, in addition, light-sensitive. Moreover, the EPR signals from pure PQV (not shown) and from the polaron in High Tg-PPV (Figure 5.62, dashed line) are overlapping, making it difficult to allocate the origin of the light-induced signal of the High Tg-PPV/PQV EPR spectrum. Still, the light-induced changes in the spectrum of High Tg-PPV/PQV are more pronounced than those for pure PQV, and in combination with the optical results, we can assign the changes to the occurrence of charge transfer from the High Tg polymer to PQV. The light-induced changes are therefore assigned to the polaron in High Tg-PPV, which has an pseudo-axial symmetry with $g_{\perp} = 2.0021$ and $g_{//} = 2.0032$.

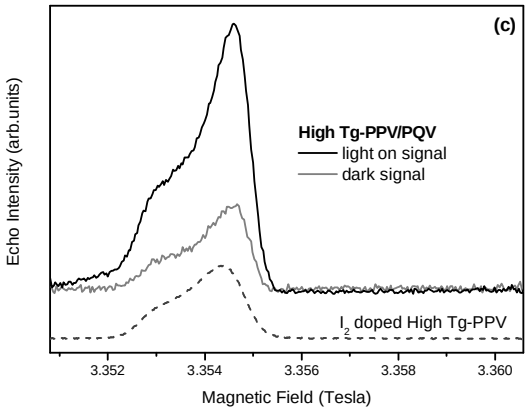

Figure 5.62: Pulsed W-band EPR spectrum of High Tg-PPV/PQV.

Also the donor behaviour of PQV was examined by blending the polymer with PCBM as as acceptor-material. This is illustrated by the nearly complete PL-quenching of the PQV emission (Figure 5.63) and by the decrease of PQV decay time when blended with PCBM (Figure 5.64). It should be noted that in this case the remaining signals in the Time Resolved PL measurements are only marginal and part of the remaining spectrum ($\lambda > 690$ nm) originates from PCBM.

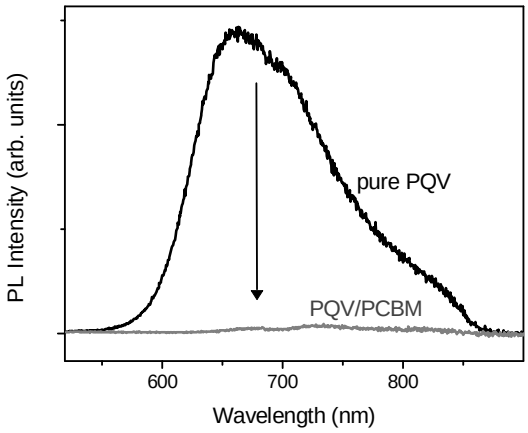

Figure 5.63: PL spectra of a pure PQV film compared to a PQV/PCBM blended film.

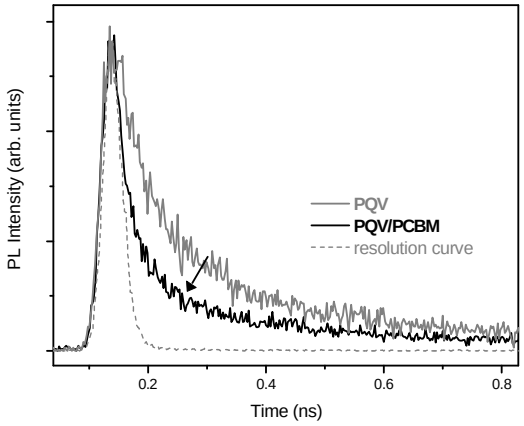

Figure 5.64: Decay curves from pure and PCBM blended PQV films.

The EPR spectrum from PQV/PCBM (Figure 5.65) clearly shows 2 radical signals: the PQV polaron is expected around 3.354 T and the PCBM- radical spectrum with main line at 3.358 T (g = 1.999)[10]. Compared to the relatively strong radical signal from plain PQV observed in EPR, no strong conclusions can be drawn as to the origin of the light-induced signal at 3.354 T in the PQV/PCBM spectrum. However,

the strong increase of the well-defined $PCBM^-$ radical spectrum gives unambiguous proof for an efficient charge transfer.

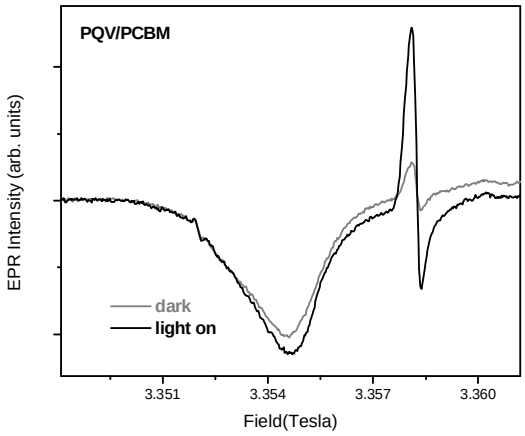

Figure 5.65: W-band CW EPR spectrum, obtained at 100 K of PQV/PCBM.

To complete the picture, beside PL and EPR measurements, also UV-Vis spectra of plain PQV, PQV/ PCBM and High-Tg-PPV/ PQV were determined as depicted in Figure 5.66.

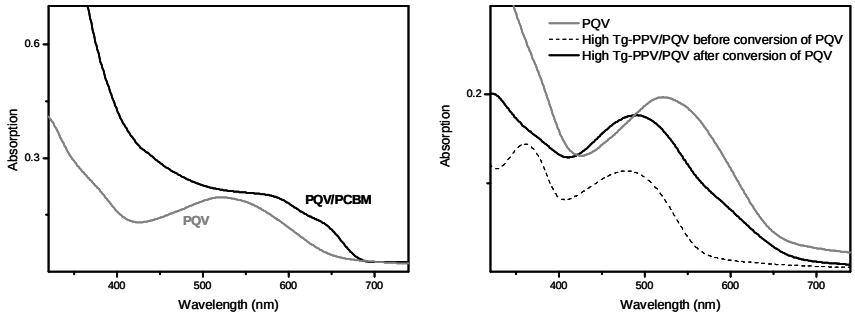

Figure 5.66: shows the UV-Vis absorption spectra of PQV compared to PQV/PCBM, and of PQV compared to High Tg-PPV/PQV.

5.3 Solar cell device and Atomic Forse Microscopy (AFM)

Solar simulation and AFM measurements were performed by Tom Aernouts and Claudio Girotto from the group of Jef Poortmans at IMEC Leuven.

In order to further investigate the molecular organisation present in PQV material, the UV-Vis spectra of films prepared from very diluted solutions in chlorobenzene were evaluated. The solutions were heated from room temperature to 250°C at 5°C/ minutes and slowly cooled down back to room temperature. UV-Vis spectra of the polymers in solution at room temperature were taken, Figure 5.67 (see also chapter three).

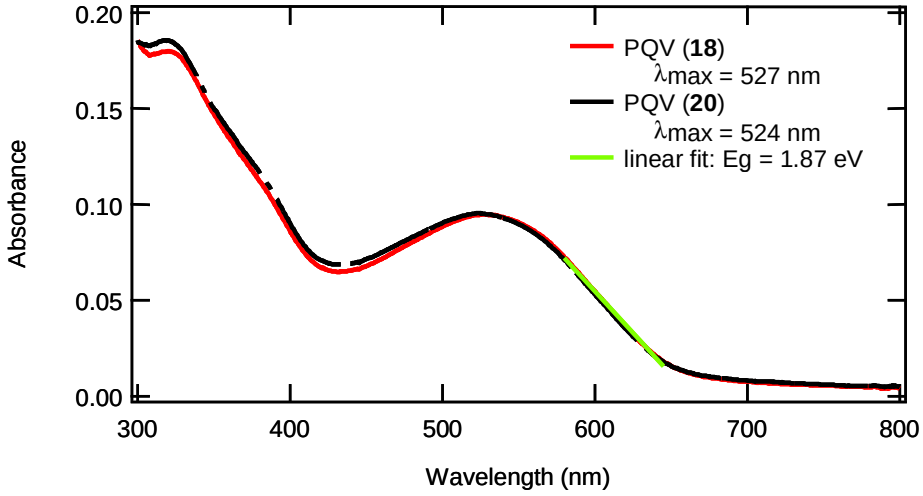

Figure 5.67: UV-Vis spectrum for PQV **2** (entry **18** and entry **20**).

With the aim to further investigate the microstructure, a PQV based solar cell with PCBM (1:1) was blended and spincoated from chlorobenzene (0.05% solution in chlorobenzene). The sample was prepared from glass/ ITO/ PEDOT/ PQV/ PCBM / Al top contact. The current voltage characteristics of this substrate was analysed (Figure 5.68) leading to large shunting behaviour.

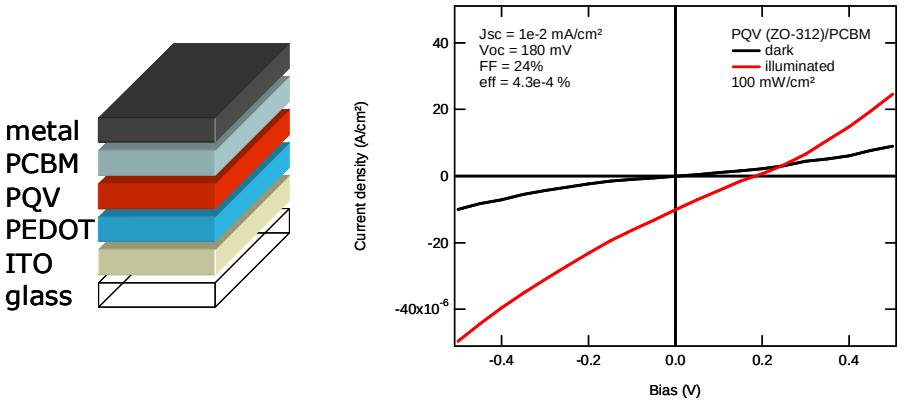

Figure 5.68: I-V curve of the planar construction PQV/ PCBM blend (1:1) spincoated from chlorobenzene.

An effort was made to prepare a bulkheterojunction based solar cell between PQV and PCBM (1:4) blended and spincoated from chlorobenzene (0.05% solution in chlorobenzene)[11,12]. The sample was prepared from glass/ ITO/ PEDOT/ PQV:PCBM / Al top contact. The current voltage characteristics of this substrate was analysed (Figure 5.69 and Figure 5.70) leading to low performance.

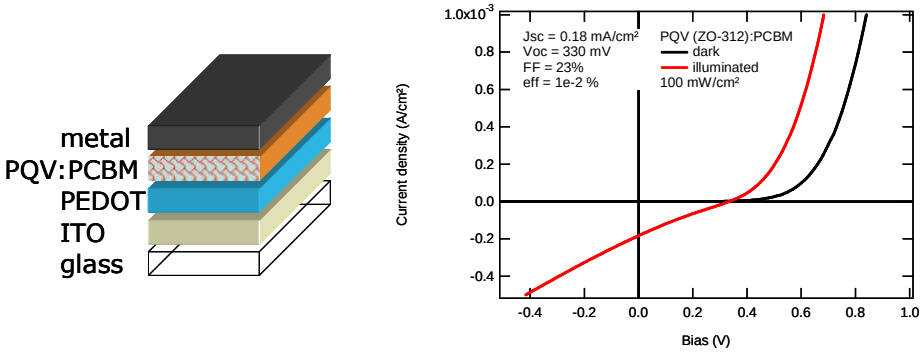

Figure 5.69: I-V curve of the bulk heterojunction PQV:PCBM blend (1:4) spincoated from chlorobenzene.

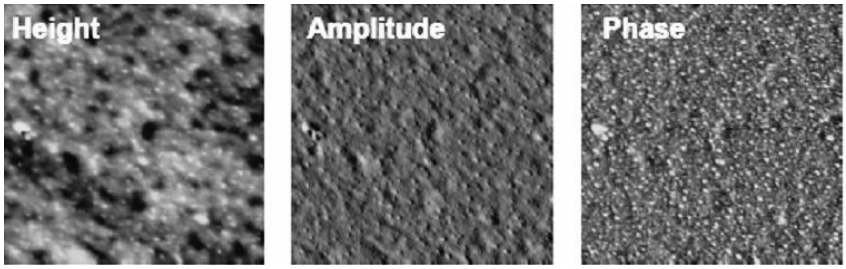

Figure 5.70: AFM image for PQV (0.05% in chlorobenzene) 1 x 1 μm^2 subsequently from left right height, amplitude and face.

From the AFM analysis two main observations were made concerning the low performance of the device. First, the planar construction shows large shunting behaviour. This can be due to an unfavourable morphology, whereby there is a small interconnection between the electrodes. This shunting behaviour can result in low performance, especially in low Voc and FF. Second, the low Jsc could be related to limited charge carrier mobility in the polymer. However, more measurements need to be carried out in order to have reproducible results for application of PQV in photovoltaic devices.

Solar cell devices were also studied by Koen Vandewal from the group of Prof. Jean Manca at IMO division, University of Hasselt.

PQV precursor was dissolved in chlorobenzene (1 wt% solution). The solution was heated for 12 hours at 120 °C to allow the partial conversion of the PQV precursor in chlorobenzen. After 12 hours the conversion was stopped by cooling down to room temperature, and PCBM was added in a 1:1 ratio. Organic devices with an active layer of PQV:PCBM blends were constructed, for which the sample was prepared from glass/ ITO/ PEDOT/ PQV:PCBM / Al top contact. This substrate was analysed by solar simulation using J-V and EQE measurements (Figure 5.71 and Figure 5.72).

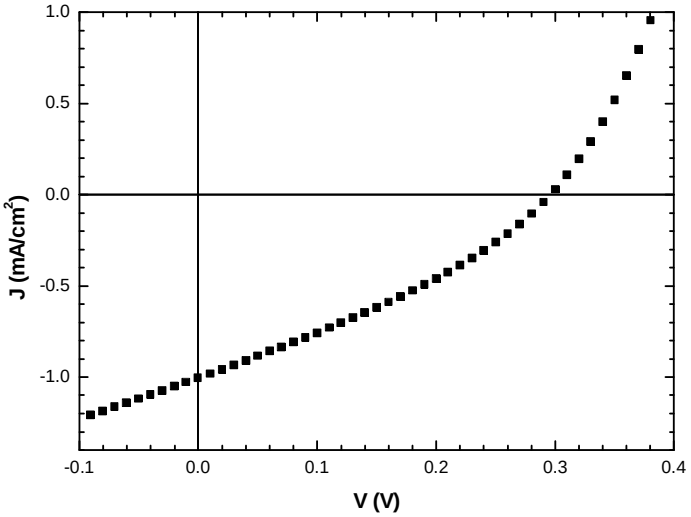

Figure 5.71: J-V measurement of PQV in chlorobenzene.

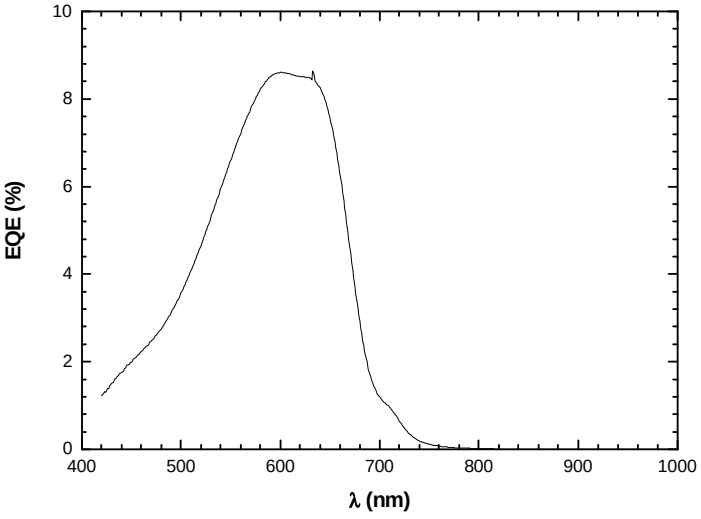

Figure 5.72: J-V measurement of PQV in chlororbenzene.

From Figure 5.71 and Figure 5.72 it can be determined that the Short-Circuit Current I_{sc} caused by the illumination of the solar cell simulator is around -1.0

mA/cm^2 for a Voltage of V = 0 V. This value is rather high for a non optimised solar cell compared to optimised values for e.g. MDMO-PPV (3 mA/cm^2) and P3HT (8-10 mA/cm^2)[13, 14]. The same comparison can be made with the optimised values for Open-Circuit Voltage V_{oc} which is around 0.3 V for I = 0. This is a quite low value compared to the values for MDMO-PPV (0.8 V) and P3HT (0.6 V)[13, 14]. This low value can possibly be the result of the holes in the film, which is caused either by the elimination process from the precursor polymer to the conjugated polymer or by impurities (not converted material) present in the film. The expected value for Voc can be determined from the HOMO-LUMO diagram which might be approximately 1 V. The Fill Factor FF is 0.32 which is rather low compared to MDMO-PPV and P3HT having a value of 0.5. This can be probably caused by pinholes in the film. The total power efficiency = $V_{oc} \cdot I_{sc} \cdot FF$ = 0.1% is quite low but it has to be taken into account that this value is not optimised. Therefore, higher values for Voc and FF can be obtained on condition that high quality films are obtained. For now it can be concluded that PQV in combination with PCBM could be a very promising p-type material.

5.4 Conclusion

Concerning the PL and EPR measurements; the conversion of the PQV –although always performed with the same procedure- was clearly influenced when blended with other compounds: depending on the compound, different absorption spectra of the PQV were found. This might indicate that the conversion was not always complete.

Such a difference was observed with the blend with PCBM, and also in the blends with High-Tg PPV, the conversion does not lead to the same absorption spectra. In the latter, although the same ratio for PQV and High-Tg PPV was used in the film, the absorption of the PQV was much less. This may point to a lower absorption coefficient. One might think that the incomplete charge transfer could be due to an incomplete conversion of the PQV in this case. However, longer heating or using

higher temperatures for the conversion was avoided to not damage the properties of the donor material.
About the PL intensities in the spectra: for the same reason as described above, it is difficult to compare the emission intensity of the pure PQV with that of the High Tg/PQV film. It was however very clear that the PL intensity of PQV is weak compared to other polymers.

Concerning the AFM measurements; the conversion conditions in film are tested. Several solar cell device constructions have been examined, with best performance for a PQV:PCBM blended active layer. Hereby, performance is still limited in J_{sc}, V_{oc} with a reduced value for FF which can be due to shunting. However, more experiments need to be carried out concerning the shunting behavior.

Furthermore it can be said that the not optimised values for J_{sc} and V_{oc} are quite good compared to optimised values for MDMO-PPV and P3HT. One thing is clear that PQV is a promising p-type material when it is applied in combination with PCBM.

The conjugated polymers obtained after conversion reveals interesting results from optical absorption measurements. From the AFM, PL and EPR measurements it can be concluded that the PQV polymer reveals an n-type behaviour when blending the polymer with a donor material like High Tg-PPV. Still, the charge transfer process observed in blends of PQV with an acceptor material like PCBM demonstrates also its donor character. PQV can be an interesting material for use in photovoltaic application. However, up till now, only certain steps are tested. Therefore, more experiments need to be carried out.

5.5 Experimental section

5.5.1 Photoluminescence (PL) and Electron Paramagnetic Resonance (EPR)

The photoluminescence (PL) measurements on spin-coated films were performed with a Varian Cary Eclipse fluorometer (excitation wavelength of 503 nm). Time-resolved PL spectra were obtained by streak camera detection after excitation with 400 nm laser pulses (1.5 kHz, <2 ps) from the frequency-doubled output of a Ti-sapphire laser amplifier (Spectra Physics Spitfire). W-band (95 GHz) light-induced electron paramagnetic resonance (LI-EPR) was performed with a Bruker ELEXSYS E680 spectrometer in conjunction with a split-coil 6-T superconducting magnet (Oxford Instruments). These measurements were performed using an Oxford flow cryostat and with a Bruker cylindrical cavity and probehead. Optical excitation was performed with 10 mW of the 514.5 nm line of an Ar^+ ion laser. Pulsed EPR experiments were performed at 15 K to obtain the spectra of the High Tg-PPV/PQV (field-swept electron spin echo (ESE) after a 2-pulse sequence $\pi/2$=180ns, τ=720ns, π=360ns). The PQV/PCBM spectra were obtained with continuous wave (CW) EPR at 100 K (microwave power of 70 μW, modulation frequency 10 kHz, modulation amplitude 1 G). In all cases, the EPR spectra were rescaled to a microwave frequency of 94.00 GHz.

Samples were prepared from chlorobenzene (High Tg-PPV/PQV, 1:1 ratio) or chloroform (pure PQV and PQV/PCBM blends, 1:2 ratio) solutions. For the optical measurements, spin-coated films were prepared; the samples for EPR were prepared from dried drop cast films of the corresponding solutions. The final PQV samples for both the optical and the EPR measurements were obtained after converting respectively the spin-coated or drop-casted blended films on a hot plate during 13 minutes at 150°C under N_2 atmosphere.

5.5.2 Solar cell device and AFM at IMEC

Solar cell devices are fabricated on glass substrates (1.25 x 1.25 cm²) covered with indium tin oxide (ITO) (Merck Display Technologies, sheet resistance < 20 Ω/□) which was patterned by standard UV-photolithography. Afterwards, the substrates were thoroughly cleaned by ultrasonication in subsequent detergent and acetone baths for 10 minutes. The cleaning cycle was finished by submerging them in hot isopropylalcohol (IPA), washing in de-ionized water and drying under nitrogen flow. Prior to depositing a poly(3,4-ethylenedioxythiophene):poly(stryrenesulfonate) (PEDOT:PSS) (Baytron P AI4083, HC Starck) layer by spin coating, an oxygen plasma treatment (100W, 10 minutes) was carried out on the substrates. Drying of the PEDOT:PSS layer was done on a hotplate at 120 °C for 10 min in air.

The active layer resulted from a solution spin coated on the substrate in an inert N2 atmosphere. Afterwards, the samples were loaded into a vacuum evaporation set-up (pressure below 10^{-6} Torr) to deposit Al backside electrodes (100 nm) through a shadow mask. In this way, on one substrate several solar cell devices with active areas ~0.03 cm² are fabricated.

Current-density versus voltage (J–V) characterization has been performed in the dark and under simulated illumination using an Agilent 4156C parameter analyzer and a LOT-Oriel 1000-W xenon arc lamp with AM 1.5D filters. Calibration was performed by a KG3 band pass filter and a calibrated silicon photodetector.

5.5.3 Solar cell device at IMO

Solution preparation; PQV precursor was dissolved in chlorobenzene in a 1 wt% solution. The solution was heated for 12 hours at 120 °C to allow the partial conversion of the PQV precursor in chlorobenzene. After 12 hours the conversion was stopped by cooling down to room temperature, and PCBM was added in a 1:1 ratio.

Device construction; Organic devices with an active layer of PQV:PCBM blends were constructed using a standard procedure in N_2 atmosphere. First, a 40 nm thick poly(3,4-ethylenedioxythiophene-polystyrenesulfonate (PEDOT-PSS, Bayer) layer was spincoated from an aqueous solution onto indium tin oxide (ITO, 100 nm) coated glass. These substrates were dried for 20 min on a hotplate at 120 °C. Subsequently the active layers of the blended materials were spincoated from a chlorobenzene solution on top of the PEDOT-PSS layer. Finally, 20 nm of Ca and 60 nm of Al were evaporated through a shadow mask as top electrode. All devices have an active area of 25 cm^2.

Device measurement; All measurements were performed in N2 atmosphere. The IV-characteristics were measured under illumination with an Oriel solar simulator equipped with a Xenon Short Arc lamp with a power of 150W, using a home build setup with a Keithley 2004 current voltage source meter.

5.6 References

1. J. Manuel, "Organic Solar Cells", *Environmental Health Perspectives*, 113, (5), **2005**, A 301

2. N. S. Sariciftci, L. Smilowitz, A. J. Heeger and F. Wudl, *Science*, 258, **1992**, 1474

3. V. Dyakonov, G. Zoriniants, M. Scharber, C. J. Brabec, R. A. J. Janssen, J. C. Hummelen and N. S. Sariciftci, *Physics Review B*, 59, **1999**, 8019

4. J. d. Ceuster, E. Goovaerts, A. Bouwen, J. C. Hummelen and V. Dyakonov, *Physics Review B*, 64, **2001**, 195-206

5. M. Al-Ibrahim, H. K. Roth, M. Schroedner, A. Konkin, U. Zhokhavets, G. Gobsch, P. Scharff and S. Sensfuss, *Organic Electronics*, 6, **2005**, 65

6. H. Hoppe and N. S. Sariciftci, *Journal of Materials Chemistry*, 16, **2006**, 45

7. K. Colladet, S. Fourier and T. J. Cleij, *Macromolecules*, 40, **2007**, 65

8. S. Bertho, W. Moons, G. Janssen, I. Haeldermans, A. Swinnen, L. Lutsen, J. D'Haen, E. Goovaerts, J. Manca and D. Vanderzande, *accepted by Organic and Nanoparticle Hybrid Photovoltaic Devices (Mater. Res. Soc. Symp. Proc. Volume 1013E,*
Warrendale, PA), **2007**,

9. "The intensity of the pure PQV emission is only indicative, mainly because of an uncertainty on the film thickness",

10. "In the dark spectrum a residual PCBM signal is observed probably resulting from illumination at room temperature during sample handling",

11. C. J. Brabec, A. Cravino, D. Meissner, N. S. Sariciftci, T. Fromherz, M. T. Rispens, L. Sanchez and J. C. Hummelen, "Origin of the open circuit voltage of plastic solar cells", *Advanced Functional Materials*, 11, (5), **2001**, 374-380

12. A. Gadisa, M. Svensson, M. R. Andersson and O. Inganäs, *Applied Physics Letters*, 84, **2002**, 1609

13. P. Vanlaeke, A. Swinnen, I. Haeldermans, G. Vanhoyland, T. Aernouts, D. Cheyns, C. Deibel, J. D'Haen, P. Heremans, J. Poortmans and J. V. Manca, "P3HT/PCBM bulk heterojunction solar cells: Relation between morphology and

electro-optical characteristics", *Solar Energy Materials & Solar Cells*, 90, **2006**, 2150–2158

14. T. Munters, T. Martens, L. Goris, V. Vrindts, J. Manca, L. Lutsen, W. De Ceuninck, D. Vanderzande, L. De Schepper, J. Gelan, N. S. Sariciftci and C. J. Brabec, "A comparison between state-of-the-art 'gilch' and 'sulphinyl' synthesised MDMO-PPV/PCBM bulk hetero-junction solar cells", *Thin Solid Films*, 403, **2002**, 247-251

Chapter Six

6. Summary

6.1 Introduction

In this dissertation the main attention was paid to exploring the synthesis and characterisation of Quinoxaline Based conjugated polymers towards solar cells. The dithiocarbamate precursor route which was developed in our research group was used for the synthesis of the polymers[1].

The Dithiocarbamate precursor route opens a wide range of possibilities to prepare materials for device application. This way, the disadvantages (instable precursor polymers with gel formation, premature elimination etc.) can be limited and a wide range of conjugated polymers (e.g. poly(quinoxaline vinylene)) can be synthesised that were otherwise not possible via other routes. In this thesis, the results on the synthesis and characterisation of PQV show that this polymer is an interesting material for photovoltaic application. Since there is not much known in the literature, much work can be done to have better insight in the preparation and characterisation of this polymer for solar cell application.

6.2 Synthetic approaches towards Quinoxaline Core – Monomer synthesis

The aim of the research done in this dissertation is the synthesis and characterisation of conjugated polymers; in particular Quinoxaline based conjugated polymers towards solar cells, Figure 6.73.

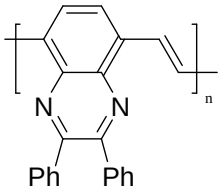

poly (p-quinoxaline vinylene)
PQV

Figure 6.73: Quinoxaline based conjugated polymer; poly (*p*-quinoxaline vinylene) PQV

Prior to polymerisation, our major goal was the synthesis and optimisation of the dithiocarbamate quinoxaline monomer. First, efforts were made to prepare the dithiocarbamate quinoxaline monomer via the Immino-oxime cyclisation route (Scheme 6.59). Unfortunately, the cyclisation of α-arylimino oxime appeared to be irreproducible. Also the bromination of 5,8-dimethyl-2,3-diphenylquinoxaline was not efficient and productive to produce the desired monomer.

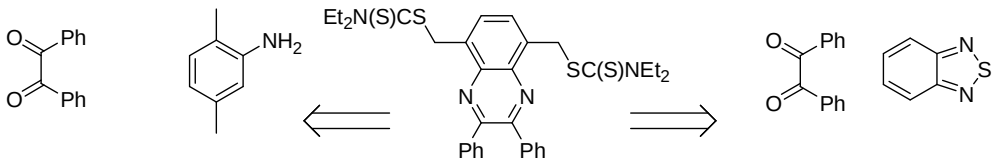

Immino-oxime cyclisation route

dithiocarbamate quinoxaline monomer

Benzothiadiazole route

Scheme 6.59: Overview of the Immino-oxime cyclisation route (left) and the Benzothiadiazole route (right) toward the dithiocarbamate quinoxaline monomer

A better procedure was found to be the Benzothiadiazole route (Scheme 6.59), by which good yields and reproducible products were obtained. For optimising the procedure and improving the yield and purity of the intermediary products an extensive study on the influence of different reaction conditions was carried out. In order to succeed in this goal, modifications for the synthesis of 5,8-dibromo-2,3-diphenyl-quinoxaline was carried out leading to high and pure product. Then, some alternative routes were applied to shorten the reaction time for the synthesis of (8-

hydroxymethyl-2,3-diphenyl-quinoxalin-5-yl)-methanol via 2,3-diphenyl-quinoxaline-5,8-dicarboxylic acid diethyl ester or via 2,3-diphenyl-quinoxaline-5,8-dicarbaldehyde. The synthesis of (8-Hydroxymethyl-2,3-diphenyl-quinoxalin-5-yl)-methanol by reduction of 2,3-Diphenyl-quinoxaline-5,8-dicarbaldehyde was not successful when the reduction is carried out with $LiAlH_4$ since many impurities were formed. However, from our experience, concerning the quinoxaline intermediary products, the reduction is promising when carried out with $NaBH_4$ as the reducing agent. Finally, alternative procedures were applied to improve the reaction rate for the chlorination step toward the synthesis of 5,8-bis chloromethyl-2,3-diphenyl-quinoxaline. In order to achieve this goal, 8-hydroxymethyl quinoline and hydroxymethyl pyridine were chosen as reference samples. The use of these procedures helped us improve the chlorination step toward 5,8-bis chloromethyl-2,3-diphenyl-quinoxaline leading to good results for our prepared dithiocarbamate quinoxaline monomer.

6.3 Exploring Polymerisation towards Plain PQV

In this section, efforts were made to carry out the polymerisation of the dithiocarbamate quinoxaline monomer for the preparation of a novel conjugated polymer poly (*p*-quinoxaline vinylene) PQV via dithiocarbamate precursor route (Scheme 6.60), which shows promising characteristics in use for organic solar cells.

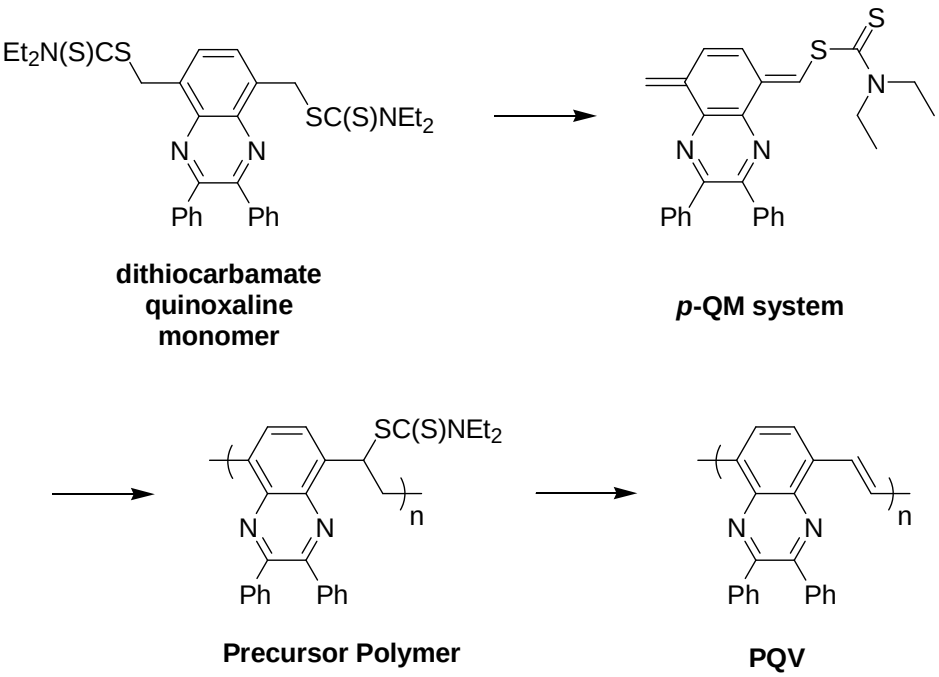

Scheme 6.60: General scheme for the polymerization of PQV via dithiocarbamate precursor route

Two issues are of great importance for the application of PPV-type conjugated polymers in photovoltaic application: the purity of the conjugated system and the ability to adapt their chemical and physical properties. In this work we have focussed on both by carrying out an extensive study on the influence of different reaction conditions on the polymerization of PQV. Two different bases (e.g. LDA and LHMDS) with different monomer concentrations and different temperatures were used for the mentioned polymerisation.

The polymerisation with LDA as the base let only to the formation of oligomers. Hereby, the analysis by ^{1}H-NMR of the residual fraction confirmed only the presence of unreacted monomer. On the other hand, the use of LHMDS as the base yielded precursor polymer with reasonable average molecular weights (i.e. oligomers). These precursor polymers were prepared from at that time not known "impure monomer", which was also confirmed by ^{1}H-NMR analysis. Therefore the monomer was purified by crystallisation, leading to substantially higher average

molecular weight of the precursor polymers. The effect of using “impure” and “pure” monomer was also clear on the GPC chromatogram of the precursor polymers; impure monomer leads mainly to oligomers while pure monomer leads mainly to high M_w polymers.

An additional study was done on the monomer to investigate the existence of the “real monomer” the *p*-QM system (Scheme 6.60) with *in situ* UV-Vis and *in situ* ^{1}H-NMR techniques. The *in situ* UV-Vis measurements did not lead to any substantial result as neither an increase nor a decrease of the peaks could be observed. Also on the basis of *in situ* ^{1}H-NMR results, no conclusion can be drawn concerning the mechanism and the possible formation of the *p*-QM system. However, what we did understand from the results obtained is that the polymerisation has taken place at once and there is no indication for the presence of a possible intermediate (i.e. *p*-QM system). Generally, concerning the mechanism for the precursor routes the polymerisation is mainly initiated by a radical mechanism which is known to be less sensitive for impurities[2]. On the other hand, the existence of the anionic mechanism (which is very sensitive toward impurities) should not be excluded as well[3]. In our case, taking this into account an hypothesis can be put forward that the polymerisation follows the pure anionic mechanism, which is remarkable.

6.4 Different approaches to introduce side chains; soluble derivatives of PQV

As the mentioned synthetic routes from chapter one lead mainly to insoluble and infusible conjugated polymers[4, 5], it makes them less interesting for application as photovoltaic materials[6]. In order to prepare soluble conjugated polymers, a solution to this problem is the synthesis of conjugated polymers with long flexible alkyl or alkoxy side chains. Therefore, in this work efforts were made to introduce different side chains (Figure 6.74) into diphenyl quinoxaline units in order to produce soluble derivatives of PQV.

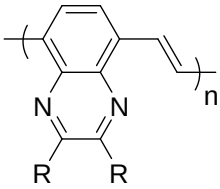

$R_1 = C_6H_{13}$
R_2 = 3-hexyl-acenaphto
$R_3 = Ph\text{-}C_8H_{17}$
$R_4 = Ph\text{-}O\text{-}C_8H_{17}$
$R_5 = Ph\text{-}C_5H_{11}$

Figure 6.74: PQV with different side chains.

Efforts were made to prepare the dithiocarbamate quinoxaline monomer with *n*-hexyl (C_6H_{13}) side chains. Unfortunately the reaction fails because the 1,2-diketon tetradecane-7,8-dione needed for this step could not be isolated. Instead, the side product heptanoic acid was formed in large extend, which was confirmed by ^{1}H-NMR and ^{13}C-NMR analysis. A possible mechanism involved could be the acidic hydrolysis of the ketocyanide group (COCN) in the presence of diluted solution of hydrochloric acid.

An effort was made to synthesise the dithiocarbamate quinoxaline monomer with 3-hexyl-acenaphto units. Some of the intermediary products at start of the synthesis were obtained with good purity and good yield. Unfortunately, (8-hydroxymethyl-2,3-diphenyl-quinoxalin-5-yl)-methanol was prepared with the formation of many side products that were impossible to be separated by purification. Also an alternative route via the synthesis of 3-hexyl-acenaphtho[1,2-b]quinoxaline-8,11-dicarbaldehyde towards the desired dithiocarbamate monomer failed due to the insolubility of the intermediary products in any common organic solvents.

Concerning the synthesis of the dithiocarbamate quinoxaline monomer with dioctyl-diphenyl or dioctyloxy-diphenyl side chains, many steps are required including a sequence of Sonogashira cross-coupling reactions. Also here some of the intermediary products at start of the synthesis were obtained with good purity and good yield. Efforts to prepare the 1,2-diketones 1,2-Bis-(4-octyloxy-phenyl)-ethane-1,2-dione and 1,2-Bis-(4-octyloxy-phenyl)-ethane-1,2-dione respectively was not successful.

Also an effort was made to prepare the dithiocarbamate quinoxaline monomer with dipenthyl-diphenyl side chains. Besides the used Benzothidiazole route, also an alternative route was applied by trying to prepare the intermediary product 2,3-Bis-(4-pentyl-phenyl)-quinoxaline-5,8-dicarbaldehyde. Unfortunately the purification of this dialdehyde by column chromatography did not lead to pure product. ^{1}H-NMR, ^{13}C-NMR and GC-MS analysis showed the existence of many side products. Therefore the synthesis toward the dithiocarbamate quinoxaline monomer with dipenthyl-diphenyl side chains could not be continued. Unfortunately, due to lack of time, the possibility for repeating the entire procedure was not there. If there is a possibility to modify the reaction route, the synthesis of derivatives of PQV seems promising.

6.5 Physical characterisation and device towards Solar Cells

As the concern for global warming is increasing every year the urge for developing renewable energy sources is increasing as well. On that account, the sun is a good alternative as energy source for converting its light into electricity. Photovoltaic cells that convert this sunlight into electricity have been with us for decades[7]. As the traditional silicon-based solar cells has been limited due to its high production costs, solar cells based on organic materials (e.g. conjugated polymeric materials) as an alternative have become very interesting the last few decades.

In this work efforts were made to analyse the precursor polymers of PQV by photoluminescence PL and EPR measurements leading to surprising results. Different absorption spectra of the PQV were found when the polymer was blended with different type of compounds (e.g. High-Tg PPV, PCBM). The reason could be that the conversion was not always complete or for some reason the spectrum can have changed on its own. Therefore, it is difficult to compare the emission intensity of the pure PQV with other polymers as the EPR and PL intensity of PQV is weak compared to other polymers.

Also some AFM measurements were carried out on the precursor polymers by testing some solar cell device constructions. The best performance was obtained for PQV:PCBM blended active layer. Moreover, the performance is still limited in both J_{sc} and V_{oc}. The reduced value for FF can be due to shunting. However, more experiments need to be carried out concerning the shunting behavior.

Furthermore, it can be said that the not optimised values for J_{sc} and V_{oc} are quite good compared to optimised values for MDMO-PPV and P3HT. One thing is clear that PQV is a promising p-type material when it is applied in combination with PCBM.

The conjugated polymers obtained after conversion reveals interesting results from optical absorption measurements. From the AFM, PL and EPR measurements it can be concluded that the PQV polymer reveals an n-type behaviour when blended with a donor material like High Tg-PPV. Still, the charge transfer process observed in blends of PQV with an acceptor material like PCBM demonstrates its donor character. PQV can be an interesting material for use in photovoltaic application.

However, up till now, only certain steps are tested toward PQV type materials. Therefore, more experiments are needed to be carried out in order to improve the scope and limitations of PQV as semi-conducting material towards Solar Cells.

6.6 References

1. A. Henckens, K. Colladet, S. Fourier, T. J. Cleij, L. Lutsen, J. Gelan and D. Vanderzande, "Synthesis of 3,4-diphenyl-substituted poly(thienylene vinylene) low-band-gap polymers via the dithiocarbamate route", *Macromolecules*, 38, (1), **2005**, 19-26

2. L. Hontis, V. Vrindts, D. Vanderzande and L. Lutsen, "Verification of radical and anionic polymerization mechanisms in the sulfinyl and the Gilch route", *Macromolecules*, 36, (9), **2003**, 3035-3044

3. F. Banishoeib, "Study of the Dithiocarbamate Route as a viable synthetic route towards Poly(Thienylene Vinylene) Derivatives", *Dissertation*, Hasselt University, **2007**

4. A. Greiner and W. Heitz, *Macromol. Chem. Rapid Commun.*, 9, **1988**, 581

5. R. N. McDonald and T. W. Cambell, *Journal of American Chemical Society*, 82, **1960**, 4669

6. W. Heitz, W. Brügging, L. Freund, M. Gailberger, A. Greiner, H. Jung, U. Kampschulte, N. Niesser, F. Osan, H. W. Schmidt and M. Wicker, *Macromol. Chem.*, 189, **1988**, 119-127

7. J. Manuel, "Organic Solar Cells", *Environmental Health Perspectives*, 113, (5), **2005**, A 301

Samenvatting

De laatste paar jaar is de bezorgdheid over de opwarming van de aarde (*global warming*) en daardoor de noodzaak voor niet vervuilende energiebronnen enorm toegenomen. Aangezien de energievoorziening van de aarde voornamelijk afkomstig is van de zon, is dit ook een goed alternatief in plaats van het verbranden van fossiele branstoffen.

Fotovoltaïsche cellen zijn gemaakt van halfgeleiders, welke zonlicht om zetten naar elektriciteit (bijv. zonnecellen) bestaan al tientallen jaren. Aangezien de traditioneel solicium gebasserde zonnecellen duur zijn en derhalve voor massa procuctie ongeschikt zijn, worden alternatief zonnecellen gebaseerd op geconjugeerde organische materialen (bijv. poly (*para*-fenyleen vinyleen) PPV) steeds interessanter. Dergelijke zonnecellen zijn niet alleen goedkoop, maar zijn ook licht in gewicht en flexibel in gebruik. Vandaar dat het doel van het onderzoek beschreven in dit proefschrift de synthese en karakterisering van geconjugeerde polymeren is; Meer specifiek is gekeken naar op Quinoxalin gebaseerde geconjugeerde polymeren voor gebruik in zonnecellen. De bereiding van de polymeren heeft plaatsgevonden via de vakgroep ontwikkelde dithiocarbamaat precursor route. Hierbij wordt een oplosbaar niet geconjugeerde polymeer omgezet naar zijn onoplosbare geconjugeerde vorm. Aangezien er over dit quinoxaline polymeer niet veel bekend is in de literatuur, is veel werk uitgevoerd om een beter inzicht te krijgen in de bereiding en de analyse van dit polymeer voor toepassingen in organische zonnecellen.

In **hoofdstuk één** wordt achtergrond informatie gegeven over het ontstaan en de geschiedenis van geconjugeerde polymeren. Tevens wordt hun bereiding via verschillende precursor routes besproken. Daarnaast wordt er ook gekeken naar hun eigenschappen als halfgeleider en de relatie tussen hun chemische en eletronische eigenschappen (band gap). Tenslotte wordt een overzicht gegeven van de werking in een zonnecel.

In **hoofdstuk twee** wordt de bereiding van de dithiocarbamaat quinoxalin monomeer besproken. Allereerst wordt er gestreefd om het dithiocarbamaat quinoxaline monomeer via de Imino-oxime cyclisatie route te bereiden. Aangezien via deze route de cyclisatie van α-arylimino oxime niet reproduceerbaar blijkt te zijn en de brominering van 5,8-dimethyl-2,3-difenylquinoxalin niet doeltreffend is, is de Benzothiadiazol route voorgesteld als een betere procedure (ik zou hier schrijven "blijkt de Benzothiadiazol route een betere procedure". Er worden hoge opbrengsten en goede reproduceerbaarheden bereikt. Door de reaktieomstandigheden te bestuderen kan de procedure worden geoptimaliseerd en een verbeterde opbrengsten en zuiverheiden van de verschillende tussenproducten worden verkregen. Door modificaties en alternatieve routes toe te passen worden de reaktiesnelheden van enkele essentiele stappen ter bereiding van de dithiocarbamaat quinoxalin monomer verkort .

De polymerisatie van het dithiocarbamaat quinoxalin monomeer wordt in **hoofdstuk drie** besproken. Dit polymeer kan mogelijk gebruikt worden in nieuwe organische zonnecel toepassingen. Om de polymerisatie succesvol uit te voeren zijn verschillende reactieomstandigheden bestudeerd, Naast de zuiverheid van het geconjugeerde systeem is ook het veranderen van hun chemische en fysische eigenschappen bekeken. Daarnaast zijn de polymerisaties ook uitgevoerd met verschillende monomeerconcentraties en temperaturen en met LDA en LHMDS als basen. De polymerisatie met LDA als base heeft slechts tot oligomeren geleid. Deze conclusie is getrokken doordat niet gereageerde monomeer pieken in het ^{1}H-NMR spectrum van de rest fractie aanwezig waren. De polymerisatie met LHMDS als de base en met het op dat moment niet bekend "onzuivere" monomeer heeft geleid tot precursor polymeren met iets hogere gemiddelde molmassa's gewichten welk ook werden gekarakteriseerd met ^{1}H-NMR. Uiteindelijk, na meerdere zuiveringen van het monomeer, blijken precursor polymeren met verrassend hoge gemiddelde molmassa's verkregen te worden. Daarnaast is in dit hoofdstuk een onafhankelijke onderzoek uitgevoerd op het monomeer om het bestaan van de "echte monomeer" het *p*-QM systeem te onderzoeken door toepassing van *in situ* UV-Vis en *in situ* ^{1}H-NMR technieken. Uit de resultaten kunnen twee conclusies worden getrokken, namelijk dat de polymerisatie onmiddelijk plaatsvindt en dat er

met de genoemde technieken niet leiden tot een concrete bewijs voor het bestaan van een mogelijke intermediair (*p*-QM systeem). Wat betreft het mechanisme voor de precursor routes, is het algemeen bekend dat de polymerisatie grotendeels geïnitieerd wordt door een radicaal mechanisme welk bekend is minder gevoelig te zijn voor onzuiverheden. Echter, het bestaan van een anionische mechanisme (welk zeer gevoellig is voor onzuiverheden) moet ook niet worden uitgesloten. In het geval van PQV kan een mogelijke hypothese zijn dat de polymerisatie verrassend genoeg wordt uitgevoerd door een uitsluitend anionisch.mechanisme.

Om oplosbare derivaten van difenyl quinoxalin te produceren, wordt in **hoofdstuk vier** gekeken om verschillende zijketens in het geconjugeerde systeem te bouwen. Hierbij is grote aandacht besteed aan de bereiding van het dithiocarbamaat quinoxalin monomeer met *n*-hexyl (C_6H_{13}) of 3-hexyl-acenaphto als zijketens. Dit resulteert echter in het ontstaan van meerdere bijproducten welk onoplosbaar zijn in algemeen bekende organische oplosmiddellen en maakt het onmogelijk om deze intermediare producten te isoleren met zuiveringstechnieken. In dit hoofdstuk wordt tevens aandacht besteed aan de bereiding van het dithiocarbamaat quinoxalin monomeer met dioctyl-difenyl of dioctyloxy-difenyl als zijketens. Voor de synthese van deze producten zijn meerdere reactiestappen nodig, waarbij ook enkele Sonogashira cross-coupling reacties worden uitgevoerd. Tijdens de eerste stappen worden tussenproducten met hoge opbrengst en zuiverheid verkregen. Uiteindelijk blijkt dat door niet efficiente oplosmiddel de zuivering van enkele tussenproducten onmogelijk is, waardoor ze verloren zijn gegaan en de vervolg experimenten niet konden worden uitgevoerd. Echter, op het einde van het project, nam de noodzaak voor de bereiding van de oplosbare derivaten van PQV toe. Derhalve is tijdens een laatste experiment gepoogd om deze derivaten te synthetiseren door de introductie van dipentyl-difenyl als zijketen. Echter, ook hier komt het probleem van de onoplosbaarheid van de tussenproducten in algemeen bekende oplosmiddellen. Het is daarom tijdens dit onderzoek onmogelijk gebleken om de tussenproduten te zuiveren en vervolgens te analyseren. Niettemin, als er mogelijkheden zijn om deze route te verbeteren, lijkt de bereiding van PQV derivaten de manier om veelbelovende polymeren te maken voor toepassing in zonnecel industrie.

Tenslotte wordt in **hoofdstuk vijf** de meest belangrijke resultaten, de fysische karakterisering van PQV en materialen voor toepassing in de zonnecel industrie besproken. Hierbij wordt de precursor polymeer van PQV geblend met verschillende materialen (High-Tg PPV, PCBM) en geanalyseerd met PL en EPR technieken, welk leiden tot verschillende absorptie spectra voor PQV. Een verklaring voor deze gevarieerde absorptie spectra voor PQV kan zijn dat de omzetting naar de geconjugeerde systeem niet volledig is uitgevoerd. Daardoor, wordt het moeilijk om de emissie intensiteit van zuivere PQV te vergelijken met andere polymeren aangezien de EPR en PL intensiteit van PQV zwak is vergeleken met andere polymeren. Naast de toepassing van PL en EPR technieken, zijn er ook AFM technieken toegepast om deze precursor polymeren te analyseren, welke leiden tot de beste performance voor een blend van PQV:PCBM als aktieve laag voor een zonnecel. Hoewel de prestatie beperkt blijft voor de niet geoptimalieerde waarden voor J_{sc}, V_{oc} en FF, zijn de waarden niet slecht vergeleken met de uitgaande geoptimaliseerde waarden voor MDMO-PPV en P3HT vanuit de literatuur. Echter, meer experimenten dienen te worden uitgevoerd voordat een duidelijke conclusie kan worden getrokken wat betreft de waarden voor J_{sc}, V_{oc} en FF voor PQV. In ieder geval kan naar aanleding van de in dit hoofdstuk verkregen resultaten met optische absorptie technieken, de conclusie worden getrokken dat na omzetting van de precursor het polymeer het gevormde PQV bevat. Verder tonen de AFM, PL en EPR meetingen van PQV polymeer aan het bestaan van een n-type eigenschap wanneer de PQV polymeer geblend is met een donor type materiaal zoals High Tg-PPV. Echter, de ladingoverdracht welk is waargenomen in PQV geblend met een acceptor materiaal zoals PCBM laat het bestaan van een p-type eigenschap zien. Derhalve kan PQV een zeer interessant materiaal zijn voor het gebruik in fotovoltaïsche cellen.

Tot slot zijn, wat PQV betreft, tot nu toe slechts enkele stappen zijn getest. Echter, meer experimenten en studies dienen te worden uitgevoerd om PQV als halfgeleidend materiaal te kunnen toepassen in de zonnecel industrie.

List of abbreviations

ACN	acetonitrile
Ac_2O	acetic anhydride
AFM	atomic force microscopy
Ag	wire Silver wire electrode
Ag/AgCl	Silver/Silver Chloride electrode
Al	Aluminium
AM	Air mass
Bp	boiling point
BuLi	butyl lithium
c	speed of light ($3\ 10^8\ ms^{-1}$)
CB	conduction band
$CHCl_3$	chloroform
CH_2Cl_2	dichloromethane
CI	chemical ionisation
CS_2	carbon disulfide
CV	cyclic voltammetry
cw	continuous wave
DIP-MS	direct insert probe mass spectrometry
DMF	N,N-dimethylformamide
DP	degree of polymerization
PD	Poly Dispersity
DTC	dithiocarbamate
E	Energy (in J)
E1	Elimination
EA	electron affinity
EI	electron impact
EL	electroluminescence
EtOAc	ethyl acetate
Et_2O	diethyl ether

E_g	band gap
eV	electronvolt
Fc	ferrocene
FF	field factor
FET	field effect transistor
FT-IR	Fourier transform infrared
GC/MS	gas chromatography/mass spectrometry
GPC	gel permeation chromatography
h	Planck constant ($6.626\ 10^{-34}$ Js)
HCl	hydrogen chloride
HOMO	highest occupied molecular orbital
H_2O_2	hydrogen peroxide
IP	ionisation potential
ITO	indium tin oxide
J_{sc}	short circuit current
LBG	low band gap
LDA	lithium diisopropyl amide
LED	light emitting diodes
LHMDS	lithium hexamethyl disilazide
Li-EPR	light Electron Paramagnetic Resonance
LiF	lithium fluoride
LUMO	lowest unoccupied molecular orbital
KOH	potassium hydroxide
MeOH	methanol
M_n	number-average molecular weight
M_w	weight-average molecular weight
NaH	Sodium Hydride
NBS	N-bromosuccinimide
n-doping	reduction
NHE	Normal Hydrogen Electrode
$NiCl_2$(dppp)	dichloro[1,3-bis(diphenylphosphino)propane]nickel(II)
NMR	nuclear magnetic resonance
OFET	organic field-effect transistor

PA	poly(acetylene)
PCBM	[6,6]-phenyl–C_{61}–butyric acid methyl ester
PCE	power conversion efficiency
PD	polydispersity (Mw/Mn)
p-doping	oxidation
PEDOT/PSS	poly(3,4-ethylene dioxythiophene) poly(styrene) sulphonate
PITN	poly(isothianaphthene)
PL	photoluminescence
PLED	polymer light-emitting diode
PPP	poly(p-phenylene)
PPV	poly(p-phenylene vinylene)
PPy	poly(pyrrole)
PS	poly(styrene)
P_3HT	poly(3-hexylthiophene)
PT	poly(thiophene)
Pt	platinum
p-TsOH	para-toluenesulphonic acid
PTV	poly(2,5-thienylene vinylene)
p-QM	para-quinodimethane
ROH	alcohol
R.T.	room temperature
SCE	Saturated Calomel Electrode
SEC	size exclusion chromatography
S_N1	substitution
$SOCl_2$	thionyl chloride
$TBAPF_6$	Tetra Butyl Ammonium hexaFluoro Phosphate
TeO_2	Telluriumoxide
TFT	thin film transistor
TEMPO	tetramethylpiperinoxyl
TGA	thermogravimetric analysis
THF	tetrahydrofuran
THT	tetrahydrothiophene
TLC	thin-layer chromatography

T_1	spin-lattice relaxation time
T_2	spin-spin relaxation time
TTC	trithiocarbonate
UV-Vis	ultraviolet visible
VB	valence band
V_{oc}	open circuit voltage
XRD	X-ray diffraction
XTC	xanthate
ν	frequency
λ_{max}	maximum absorption wavelength

List of publications

Exploring Quinoxaline Based Cunjugated Polymers Towards Organic Solar Cells – Zarina OLOMI, P. Adriaensens, T.J. Cleij, L. Lutsen, D. Vanderzande, Aranzazu Aguirre and Griet Janssen, Etienne Goovaerts, 2007, *in preparation*.

Acknowledgement

Thinking this will be the easiest part of my thesis, I wanted to write this part after I have finished writing the rest of the thesis. To be honest… it is not the easiest part for me because each one of you contributed to this thesis in your own special way and I want to thank all of you in my own special way. First of all, my great gratitude goes to my mentor, professor Dirk Vanderzande, my co-mentor, dr. Peter Adriaensens and the Department of Organic and Polymer Chemistry (SBG/OS) of Hasselt University for giving me the opportunity to do my Ph.D and the necessary research work.

I would like to thank Koen Vandewal from the group of Prof. Jean Manca at our IMO division for performing the Mobility measurements on solar cell devices. I thank Tom Aernouts and Claudio Girotto from the group of Jef Poortmans at IMEC Leuven for performing the needed Solar simulation and AFM measurements. Many thanks to our collaborators, Aranzazu Aguirre and Griet Janssen from the group of Etienne Goovaerts at University of Antwerp for investigating the charge transfer efficiency of my samples. It was always educational and fun working with all the members from the NANOSOLAR project.

I also want to thank Huguette Penxten for performing FT-IR and UV-Vis measurements. Professor Thomas Cleij… thank you for your good advices which were always useful to me. Sofie, my gratitude goes to you, not only for performing CV measurements but also for being a good colleague. Raoul …whenever I wanted a NMR measurement on my samples you were there to take care of that, therefore Thank you very much. I also want to express my gratitude to dr. Ynze Mengerink, who got interested in my work and took the time to review my thesis.

I shouldn't forget mentioning other colleagues for their collaboration; Iris and Veerle, you were always there for me for performing GPC measurements. My gratitude goes out to both of you. Veerle, whenever any of us needed some

advice, you were there to help us. You have become a good friend to me and I cherish that friendship a lot. The same counts for Ine, it was always fun working with you side by side sharing the same bench. Thank you Inetje for becoming a dear friend and I wish you and Michael lots of luck with the preparations for The Day☺. Kristof and Lien, or better said "the A Team" thanks to both of you I had many pleasant moments. I can never forget Kristof being the joke maker and Lien being the sunshine of the office. I thank you for those wonderful moments.

Whenever I had problems with my PC I knew whom to contact → Jimmy! I think you are the kind of person that never says "no" to help someone. I thank you for all your support and patience. Wibren (double-U), Jan, Bert, Arny the Palmy, Hanne, Fré and Joke thank you for being a good support during those few years at the university. Those of you that have started writing their thesis or will start soon, the best of luck! Also my gratitude goes to Jérôme, who has been a great guide in the world of chemistry; I thank you and wish you the best of luck!

I shouldn't forget the help of my former students Lize Yaspers and Tim Verheyen that helped me a lot with performing some experiments for me. Michael (Mr. van Haren Jr.), it has been ten years that we know each other and you have been not only a non-stop dear friend to me but whenever I needed explanation about chemistry you were there to help me with pleasure. I thank you for everything and wish you the Best of Luck ☺…I shouldn't forget mentioning another special friend…we have come from two different countries with different backgrounds but the bond was formed at once. Faty…a person like you I have never seen before, you are unique indeed and I am proud to be called as one of your friends.

Finally, I would like to thank my family; mom and dad… I know it was not easy to raise me, especially in the years that we lived in war in Afghanistan. Both of you never asked me anything except to be a good person and work hard. My gratutute to both of you is endless, still I hope you accept this thesis as a way of my gratitude to both of you. Palo, I can never forget your continuous support, not only during my study but for any decision at any time in my life…Thank you P! Zaki, my younger but Taller bro, although you are much younger than me but your objective

advices were always welcome to me…thank you from the bottom of my heart. Last but not the least, Sed, I can not imagine my life without you. Thank you for being there, for your patience and enormous support, especially when I was writing my thesis. My thesis would not be the same without your support.

I learnt a lot thanks to all of you, and I wish all of you the best of luck and happiness in the world!

زرینه